

**THE ROLE AND REGULATION OF EXTRACELLULAR VESICLES RELEASED BY B
CELLS IN RESPONSE TO CD24**

By

Hong Dien Phan

A Thesis Submitted to the School of Graduate Studies

in Partial Fulfilment of the

Requirements for the Degree of

Doctor of Philosophy

Department of Biochemistry

Memorial University of Newfoundland

October 2024

St. John's, Newfoundland and Labrador

Abstract

Extracellular vesicles (EVs) are membrane-encapsulated nanosized particles that carry bioactive cargo, including proteins, nucleic acids, and lipids. EVs are secreted by most living cells, including B lymphocytes (B cells). B cells are antibody-producing immune cells that develop in the bone marrow, where different cell surface receptors regulate their maturation. One of the earliest surface proteins expressed in developing B cells is called CD24, a glycosylphosphatidylinositol (GPI)-linked protein localized to lipid rafts on the cell plasma membrane. Past research in the Christian lab showed that engagement of CD24 on the immature murine WEHI-231 B lymphoma cell line could cause the release of bioactive EVs. Following in the footsteps of the first discovery, this work employed a model system where donor cells expressing palmitoylated GFP (WEHI-231-GFP) were co-cultured, after stimulation, with recipient cells lacking either IgM (WEHI-303 murine B cells) or CD24 (CD24 knock-out mouse bone marrow B cells). The study found that EVs traffic lipid and membrane proteins between B cells in response to stimulation of either CD24 or IgM on the donor cells. Importantly, this study found that EV-mediated transfer of CD24 or BCR may affect B cell development by inducing apoptosis in recipient bystander cells. The following study aimed to determine how CD24 regulates the release of EVs. Bioinformatic analysis showed that CD24 expression is linked to the PI3K/AKT and mTOR signaling pathways. Using chemical and genetic inhibition, I found that an aSMase/PI3K/mTORC2/ROCK/actin pathway regulates EV release. Lastly, through live cell imaging, the study confirmed that ROCK is required for inducing the membrane dynamics required for EV release, presumably by regulating tethering of the actin cytoskeleton to the plasma membrane. The information obtained from this study and other research indicate that EVs induced by CD24 stimulation are ectosomes that budded off from the plasma membrane rather than exosomes that originated from multivesicular bodies. Significantly, these data have

uncovered a novel pathway regulating ectosome release that has not been reported in any cell types. This research topic provides a window into the diverse function of CD24 as well as increasing our knowledge of how CD24 regulates EV release in cell-to-cell communication.

Acknowledgements

First and foremost, my heartfelt appreciation goes to my thesis supervisor, Dr. Sherri Christian. Her patience, and unwavering support have been the cornerstone of my academic journey. Thank you for your valuable advice, both scientifically and personally, and thank you for giving me the opportunity to present my work at several conferences. I learnt a lot through the level of detail she has while writing or while designing an experiment. I would like to express my deep gratitude for her encouragement and enthusiasm which cultivated in me the virtues of rigorous scientist and an effective communicator.

I am thankful to my committee members, Dr. Craig S. Moore and Dr. Pavan Kakumani for their invaluable and constructive inputs on my research. Specially, to Dr. Martin Mulligan, you supported me throughout my PhD process, and while you will not be able to witness my success in person. Your strength lives on in me.

I would also like thank the old and current students I had the chance to meet during my thesis: Modeline Longjohn, Nikitha K. Pallegar, Reilly H. Smith, Delania J.B. Gormley, Willow R. Squires, Veronica Castro, Kaitlyn E. Mayne, Grant R. Kelly, and Rashid Jafardoust.

I would like to thank Nicole C. Smith at the Cold-ocean Deep-water Research Facility, and Stephanie Tucker and Chris Corkum at the Medical Laboratory Facilities, for expert assistance with flow cytometry. I thank the staff in Animal Care Services, for their excellent assistance.

I am grateful to the Biochemistry staff and faculty for providing the support through my research.

I am thankful to my funding agencies, VIED, Mitacs, the Beatrice Hunter Cancer Research Institute and the Terry Fox Research Institute for supporting through my training and research.

Finally, I would like to thank my parents for their endless love and support. They may not have understood pretty much everything I was doing but they were always there for me.

Table of Contents

Abstract	i
Acknowledgements	iii
Table of Contents	iv
List of Tables	viii
List of Figures	ix
List of Abbreviations	x
List of Supplemental Figures	xiii
Chapter 1: Introduction	1
1.1. The immune cells	1
1.2. B cells	3
1.2.1. Development of B cells	3
1.2.2. Markers expression in B cell development stages	7
1.3. Extracellular vesicles	10
1.3.1. Historical background	10
1.3.2. Nomenclature and classification	11
1.3.3. Biogenesis	14
1.3.4. EV composition	17
1.4. B cell-derived EVs	24
1.4.1. B cell-derived EV cargo	24
1.4.2. B cell-derived EVs crosstalk with the immune system	25
1.5. CD24	27

1.6. Research objectives of the thesis.....	30
1.6.1. Objective 1: Determine if CD24 induces transfer of functional protein to recipient cells via EVs.....	31
1.6.2. Objective 2: Determine if other receptors stimulate EV-mediated transfer of functional proteins.....	31
1.6.3. Objective 3: Elucidate the mechanism of CD24-mediated EV release.....	31
1.7. Publications arising from this thesis.....	34
1.8. References	36
Chapter 2: CD24 and IgM stimulation of B cells triggers transfer of functional B cell receptor to B cell recipients via extracellular vesicles.....	62
2.1. Abstract.....	62
2.2. Graphical abstract.....	63
2.3. Introduction	64
2.4. Materials and Methods	67
2.4.1. Animal care	67
2.4.2. Cell culture and transfection.....	67
2.4.3. Primary bone marrow B cell isolation.....	68
2.4.4. Cell stimulation.....	68
2.4.5. EV isolation by size exclusion chromatography (SEC)	70
2.4.6. Nanoparticle tracking analysis.....	71
2.4.7. EV isolation by Vn96 peptide-based affinity isolation	71
2.4.8. Western blot.....	71
2.4.9. IgM and CD24 detection by flow cytometry.....	72

2.4.10. Phospho-ERK detection by flow cytometry	72
2.4.11. Apoptosis assay by flow cytometry	73
2.4.12. Confocal microscopy.....	73
2.4.13. Statistical analysis.....	74
2.5. Results	74
2.5.1. EV trafficking of lipid and membrane proteins between murine B lymphoma cells in response to CD24 stimulation.	74
2.5.2. CD24 engagement on donor cells induces transfer of lipids and CD24 to recipient cells.....	83
2.5.3. CD24 engagement on donor cells induces transfer of signaling-competent IgM and CD24 to recipient cells.....	86
2.5.4. IgM stimulation of donor cells induces transfer of lipids and CD24 to recipient cells	89
2.5.5. IgM stimulation of donor cells induces transfer of signaling-competent IgM to recipient cells.....	91
2.6. Discussion	94
2.7. Acknowledgments	99
2.8. References	100
2.9. Supplemental figures.....	107
Chapter 3: CD24 regulates extracellular vesicle release via an aSMase/PI3K/mTORC2/ROCK/actin pathway in B lymphocytes.....	115
3.1. Abstract.....	115
3.2. Graphical abstract.....	116
3.3. Introduction	117

3.4. Materials and Methods	121
3.4.1. Cell culture	121
3.4.2. Bioinformatics	122
3.4.3. Phosphatidylinositol (3,4,5)-trisphosphate (PIP ₃) Quantification	123
3.4.4. Analysis of cell surface IgM and lipid transfer by flow cytometry	123
3.4.5. Immunoblotting.....	124
3.4.6. Live cell imaging.....	125
3.4.7. Statistical analysis	126
3.5. Results	126
3.6. Discussion	145
3.7. References	150
3.8. Supplemental figures.....	161
4. Chapter 4: Discussion	167
4.1. Summary of results.....	167
4.2. Discussion and Question Arising	168
4.3. Conclusion.....	173
4.4. References	174
Appendix	180

List of Tables

Table 1.1. Markers expression in B cell development stages.

9

List of Figures

Figure 1.1. Diagram of B cell development in the bone marrow.	4
Figure 1.2. The biogenesis, compositions and uptake of extracellular vesicles (EVs).	13
Figure 1.3. Diagram of the research objectives.	33
Figure 2.1. CD24 stimulation of donor cells causes transfer of GFP-labeled membrane and IgM to recipient cells.	78
Figure 2.2. EV-dependent transfer of GFP and IgM by EVs.	80
Figure 2.3. CD24 stimulation of donor cells causes transfer of GFP-labeled membrane and CD24 to recipient cells.	85
Figure 2.4. CD24 stimulation causes transfer of functional IgM and CD24 from donor to recipient cells.	88
Figure 2.5. IgM stimulation of donor cells causes transfer of GFP-labeled membrane and CD24 to recipient cells.	90
Figure 2.6. IgM stimulation of donor cells causes transfer of functional IgM to recipient cells.	93
Figure 3.1. CD24 expression is associated with the PI3K-Akt signaling and mTOR pathways.	128
Figure 3.2. CD24-mediated EV release is regulated by PI3K.	131
Figure 3.3. CD24-mediated EV release is dependent on Akt and mTOR signaling pathways.	134
Figure 3.4. CD24-mediated EV secretion is dependent on ROCK.	137
Figure 3.5. CD24-mediated EV release is controlled by actin cytoskeleton re-organization.	140
Figure 3.6. CD24-mediated EV release is controlled by aSMase activity.	141
Figure 3.7. Representative images of WEHI-231-GFP cells show EV release and cell activation.	144

List of Abbreviations

APCs	Antigen-presenting cells
MHC	Major histocompatibility complex
HSC	Hematopoietic stem cells
ST-HSC	Short term hematopoietic stem cells
MPP	Multipotent progenitor
CLP	Common lymphoid progenitor
CMP	Common myeloid progenitor
IL7R	Interleukin-7 receptor
DCs	Dendritic cells
BLP	B lymphocyte progenitor
Ig	Immunoglobulin
H	Heavy
L	Light
BCR	B cell receptor
GC	Germinal center
EV	Extracellular vesicles
ILVs	Intraluminal vesicles
MVBs	Multivesicular bodies
mRNA	Messenger ribonucleic acid
miR	microRNAs
JEV	Journal of Extracellular Vesicles

ISEV	The International Society for Extracellular Vesicles
CanSEV	The Canadian Society for EVs
MVs	Microvesicles
ESCRTs	Endosomal Sorting Complex Required for Transports
nSMase	Neutral sphingomyelinase
PS	Phosphatidylserine
PE	Phosphatidylethanolamine
PC	Phosphatidylcholine
SM	Acid sphingomyelin
PIP ₂	Phosphatidylinositol 4,5-bisphosphate
PIP ₃	Phosphatidylinositol (3,4,5)-trisphosphate
PLC	Phospholipase C
PLD	Phospholipase D
PI3K	Phosphoinositide 3-kinase
ARF6	ADP-ribosylation factor 6
ROCK	Rho-associated kinase
SM	Sphingomyelin
PI	Phosphatidylinositol
MPP	Matrix metalloproteinases
DNA	Deoxyribonucleic acid
CD	Cluster of different
GPI	Glycosyl-phosphatidylinositol
TLR	Toll-like receptor

DAMP	Danger associated molecular pattern
MAPK	Mitogen activated protein kinase
RRMS	Relapsing-remitting multiple sclerosis
Th1	T helper 1
SN	Supernatant
cSN	Cleared SN
RT	Room temperature
EGFR	Epidermal growth factor receptor
siRNA	Small interfering RNA
aSMase	Acid sphingomyelinase
C1P	Ceramide-1-phosphate
S1P	Sphingosine-1-phosphate
MSC	Mesenchymal stromal cell
IFN	Interferon
PRRs	Pattern recognition receptors

List of Supplemental Figures

Supplemental Figure 2.1. Cell characterization and gating strategies.	108
Supplemental Figure 2.2. CD24 stimulation causes transfer of functional IgM and CD24 from donor to recipient cells.	110
Supplemental Figure 2.3. Characterization of EVs isolated from cell culture..	111
Supplemental Figure 2.4. CD24 stimulation of donor cells did not induce GFP or BCR transfer to recipient cells through a transwell system.	112
Supplemental Figure 2.5. CD40 induces transfer of IgM but not lipid while CD48 induces transfer of lipid but not IgM.	113
Supplemental Figure 3.1. Pre-treatment with inhibitor on donor WEHI-231-GFP cells inhibits the transfer of GFP and IgM from donor to recipient cells in response to CD24.	162
Supplemental Figure 3.2. nSMase has no effect on EV release regulation.	163
Supplemental Figure 3.3. Inhibition of CD24-mediated EV release by PI3K/Akt/mTORC2/ROCK signaling pathways.	164
Supplemental Figure 3.4. Calcium has no influence on the regulating of EV release.	165

Chapter 1: Introduction

1.1. The immune cells

The immune system is a complex network of organs, cells and proteins that defend the body against infection and disease. There are two subsystems that make up the immune system: the innate immune system and the adaptive immune system. The innate immune system is the first to respond to early pathogens, characterized by rapid and generally non-specific response. On the other hand, the adaptive immune system is slower to respond but is highly specific to a particular antigen and can provide long-lasting immunological memory¹.

The innate immune response involves many different types of cells. For instance, mast cells, basophils and eosinophils produce cytokines, granules, and enzymes to combat microbes immediately on infection². Natural killer cells play a major role in the rejection of tumor and the elimination of infected cells through the release of perforins and granzymes³. Neutrophils and macrophages are the two primary cell types that comprise phagocytes⁴. The roles of the two cell types are similar in that they both ingest and kill bacteria via various bactericidal mechanisms. Neutrophils also have granules and enzyme pathways that eliminate pathogenic microbes. Neutrophils are short-lived cells, while macrophages are long-lived cells that not only play a role in phagocytosis but are also involved in antigen presentation to T cells⁵. Dendritic cells (DCs) also phagocytose and function as antigen-presenting cells (APCs) that act as essential messengers between innate and adaptive immunity⁶. Moreover, emerging evidence also demonstrated that DCs and macrophages express a variety of pattern recognition receptors (PRRs) important for microbe recognition⁷. PRRs-activated macrophages and DCs can influence the fate of B cells during normal inflammatory response⁸.

Moreover, trained immunity is a concept that describes how certain innate immune cells can undergo long-lasting changes after an initial encounter with a pathogen or vaccination⁹. This training enhances their response to subsequent infections, providing a more robust and effective defense. Trained immunity involves epigenetic and metabolic reprogramming of innate immune cells, allowing them to respond more faster and stronger to similar challenges in the future¹⁰. For instance, the functional reprogramming of DCs also shows immune memory response. In this regard, DCs isolated from *Cryptococcus neoformans* vaccinated mice displayed strong interferon (IFN)- γ production and enhanced proinflammatory cytokine following secondary challenge¹¹. In addition, monocytes or macrophages that encounter fungi like *Candida albicans* can mount trained immune response. This training can lead to improved phagocytosis and increased production of inflammatory mediators upon re-exposure¹². There is evidence that the bacillus Calmette-Guerin vaccine for tuberculosis, can induce trained immunity in monocytes and macrophages. After vaccination, these cells exhibit a heightened ability to respond to other pathogens, even cancer, not just *Mycobacterium tuberculosis*, demonstrating a broader protective effect¹³. NK cells can be trained by exposure to cytomegalovirus^{14,15}. Following initial infection, NK cells can respond more robustly to subsequent infections, demonstrating enhanced cytotoxic activity and increased production of cytokines like IFN- γ , resulting in a more protective immune response against cytomegalovirus^{14,15}. The duration of trained immunity has been proven to persist at least three months and up to a year, although heterologous protection against infections induced by live vaccinations can extend up to five years¹⁶. However, it is generally considered to be shorter-lived than adaptive immunological memory¹⁷.

Adaptive immunity is the part of the immune system that can be concomitantly induced¹. It involves the activation of DCs, and specialized B cells and T cells, which recognize and remember specific antigens. This memory allows the body to mount a faster and stronger

response upon subsequent encounters with the same pathogen¹⁸. T cells originate in the bone marrow and, following migration, mature in the thymus¹⁹. T cells require the action of APCs to recognize a specific antigen. The surface of APCs expresses a group of proteins known as the major histocompatibility complex class I (MHC-I) and MHC-II. Class I and II MHC proteins have crucial roles in presenting foreign protein antigens to cytotoxic and T helper (Th) cells²⁰. The interaction of the Th cells with the MHC class II region on the B lymphocytes assist in the immunologic activation of B cells²¹. Once activated the B cells will differentiate to mature plasma cells. Plasma cells can produce up to thousands of antibody molecules per second per cell²².

1.2. B cells

1.2.1. Development of B cells

B lymphocytes are essential components of the adaptive immune system and have a major role in humoral immune reactions due to their ability to produce antibodies against foreign antigens. B cells originate from hematopoietic stem cells (HSC) in the bone marrow, which is seeded by HSC developing in the fetal liver during embryonic life. The initial stages of B cell development are differentiation steps of HSC into the various hematopoietic lineages. HSC were first described a half-century ago by Till, McCulloch, and colleagues, who reported that these cells can self-renew in lethally irradiated mice, and colony-forming cells appearing in the spleen were discovered^{23,24}. Figure 1.1 depicts hematopoiesis and highlights some of the factors involved in B cell differentiation.

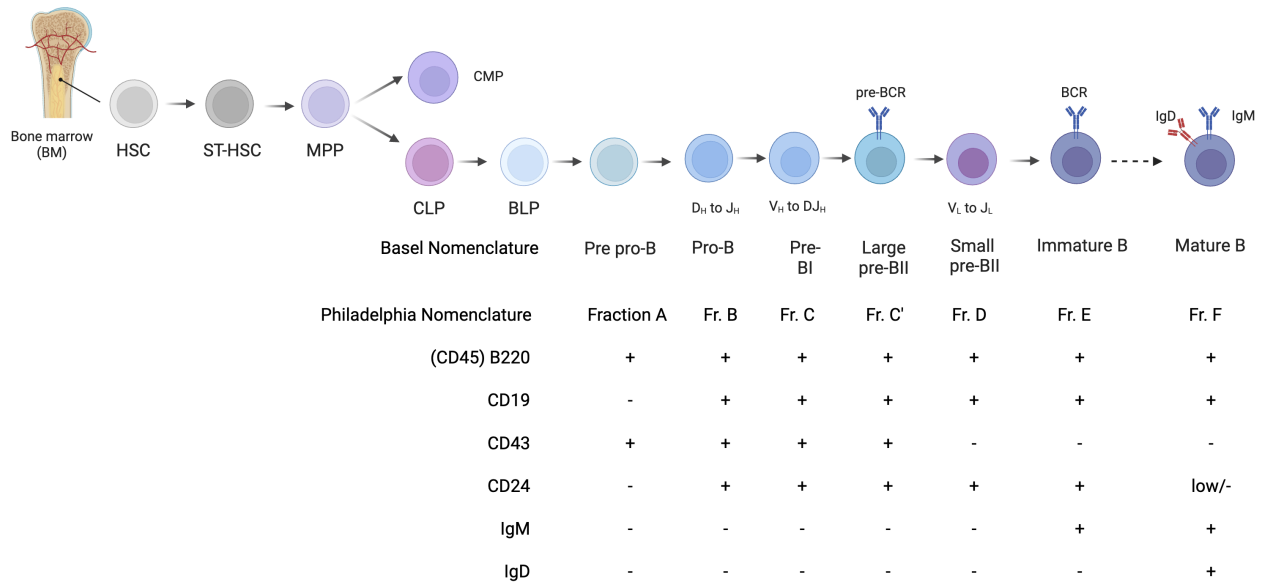


Figure 1.1. Diagram of B cell development in the bone marrow. Schematic representation of the different B cell differentiation stages with their denomination according to the Basel and Philadelphia nomenclatures. The pattern of expression of the main markers used to characterize each subset is shown with positive or negative. VDJ_H and VJ_L rearrangements are indicated. HSC: hematopoietic stem cell; ST-HSC: short term HSC; MPP: multipotent progenitor; CMP: common myeloid progenitor; CLP: common lymphoid progenitor; BLP: B lymphocyte progenitor. Created with BioRender.com.

The phenotypic characterization of murine HSCs demonstrated that they lack expression of mature blood cell markers and are thus called lineage-negative (Lin^-) and express the surface epitopes c-kit, Sca-1 and Thy-1.1²⁵. It was then shown that the $\text{Lin}^- \text{c-kit}^+ \text{Sca-1}^+$ fraction retained multilineage repopulation potential, and further differentiation of the long-term HSC into short-term (ST) HSC is marked by the gain of CD34 expression²⁶. Progression from ST-HSC to the multipotent progenitor (MPP) subset is observed in the presence of CD135 (Flk-2/ Flt-3)²⁷. MPP cells then differentiate into a common lymphoid progenitor (CLP) and a common myeloid progenitor (CMP) by interleukin-7 receptor (IL7R) upregulation²⁸. CMP can give rise to various myeloid lineage cells, while CLP marks the entry into the lymphoid lineage, such as T, B, and natural killer (NK) cells. B lymphocyte progenitor (BLP) cells gain this multilineage developmental potential upon conditional promotion of Ly6D²⁹. Thus, murine BLPs are characterized by the cell-surface expression of $\text{Lin}^- \text{CD117/c-kit}^- \text{Sca-1}^- \text{Ly6D}^+ \text{IL-7R}^+ \text{Flk-2}^+$.

Beginning with BLPs, B cell progression in the bone marrow proceeds through distinct stages of development culminating in final immature B cells. Hardy and Rolink established the standards for the phenotypic characteristics of the various B cell stages, which are now known as the Philadelphia and Basel nomenclatures, respectively^{30,31}. The stages of B cell development in the bone marrow are antigen-independent and involve generating several intermediary precursor cells that rise from BLPs. The BLPs create the entry in the earliest pre-pro B cell stages as indicated by B220 expression but not CD19 expression. The subsequent stages of B cell differentiation have a specific and crucial role in developing the functional rearrangement process of the immunoglobulin (Ig) gene segments, which is identified based on how the heavy (IgH) chain and light (IgL) chain gene segments are rearranged. The rearrangements of genes encoding the IgH chain are first seen in pro-B cells between the D and J segments, followed by a second rearrangement joining an upstream V region to the complete VDJ_H recombination that takes place

at the pre-BI stage. The functional rearrangement of the μ -H chain gene segments marks the entry into the pre-B-cell stage. The pre-B cells undergo 1 or 2 cell divisions and contain the μ heavy chain bound to the surrogate light chain, composed of the invariant $\lambda 5$ and VpreB proteins, with the Ig α /Ig β signalling complex to form the pre-B cell receptor (BCR)³²⁻³⁴. The pre-BCR has two functions. The first task is to shut down the activities and expression of the enzyme machinery catalyzing the rearrangements of the H chain gene segments, a process termed allelic exclusion³⁵. This process prevents the expression of two H chains with two different specificities by the same cell. The second task is to initiate the rearrangement of the L chain genes. Upon expression of a functional IgL chain, the mature BCR is formed by association with the Ig μ chain at the immature B cell stage. Considering that the establishment of a signaling-competent cell surface form of the BCR depends on the interaction between Ig- α/β and IgM, this is critical for B cell development. While the Ig portion of the receptor serves as the antigen-binding subunit, the Ig- α/β is responsible for disseminating intracellular signals³⁶. BCR signaling is required for B cell maturation and survival, immature B cells are sensitive to antigen binding in that if they bind self-antigen in the bone marrow they die^{37,38}. To complete development, immature B cells leave the bone marrow and become mature naïve B cells. The BCR on mature cells contains membranes form of IgM and IgD associated with Ig- α/β ³⁶. While both IgM and IgD require Ig- α/β for generating intracellular signals, IgD, but not IgM, can travel to the cell surface in the absence of Ig- α/β ³⁹. Mature B cells migrate to the secondary lymphoid organs, such as the spleen and lymph nodes, where they complete their maturation in the periphery⁴⁰.

Following their development in the bone marrow, naïve B cells have a half-life of roughly six weeks, during which they enter the circulation and lymph node organs⁴¹. The time that naïve B cells will spend approximately 24 hours in lymphoid follicles unless they are exposed to

antigens derived from invading pathogens⁴². If activated by an antigen, naïve B cells migrate to the outer follicles, where they undergo proliferation⁴³. Some of the proliferating B cells differentiate into short-lived plasma cells in extrafollicular environments, and some B cells differentiate into germinal center-independent memory B cells⁴⁴. This memory B cell subsets have the capacity to produce cytokines, such as TNF- α , IFN- γ and IL-12 that impact several cell types of both the adaptive and the immune systems⁴⁵. Alternatively, the activated naïve B cells undergo rapid proliferation to form the germinal centre (GC), where affinity maturation takes place. The highest-affinity B cells exit the GC, either as memory B cells or as long-lived plasma cells that contribute to serological memory⁴⁶.

1.2.2. Markers expression in B cell development stages

Both Hardy and Rolink used B220 and CD19 as lineage markers, along with the surface expression of BCR as a maturity marker. However, Hardy and colleagues employed CD43, CD24, and BP1 expressions to further develop their classification⁴⁷. For instance, CD43 is expressed in the early pre-pro-B cell stage and disappears at the large pre-BII stage, while BP1 appears between the pre-BI and small pre-BII stages. Interestingly, CD24 expression is detectable on pro-B cells, with the highest expression seen in the large pre-BII stage, followed by a gradual decline in expression, as B cells mature and exit the bone marrow. On the other hand, Rolink and colleagues discovered CD117 and CD43 appearing in early pre-pro-B cells, followed by a gradual decline at pre-BI and large pre-BII stages, respectively. CD25 was found to appear suddenly between the large pre-BII stage and the small pre-BII stage⁴⁸. Thus, B cells develop through several well-characterized stages, ending with the expression of surface IgM and IgD class Ig molecules associated with Ig α and Ig β , forming the BCR, responsible for detection of

antigen⁴⁹. Further developmental growth and maturation in the periphery are constrained by positive and negative selection, mediated by BCR signaling, and aiming to produce a non-self-reactive, immune-competent repertoire of naïve B cells⁵⁰. Despite the ongoing generation of new cells in the bone marrow, the mature B cell count in an adult mouse does not change. An adult mouse is thought to produce $1-2 \times 10^7$ immature B cells daily⁵¹. These cells exit the bone marrow as immature transitional B cells, but only roughly 3% become mature B cells⁵². Several factors have been shown to contribute to cell death and restrict the growth of the peripheral B cell compartment, including self-reactivity⁵³, incomplete maturation⁵⁴, competition of follicular niches⁵⁵, and trophic mediators⁵⁶. As a result, the equilibrium between cell production and cell death keeps the size of the peripheral B cell compartment unchanged⁵⁷. Table 1.1 summarises the cell surface markers used to distinguish B cell subpopulations.

Table 1.1. Markers expression in B cell development stages.

Fraction	Cell type	Markers
A	Pre-pro B cell	B220 ⁺ CD19 ⁻ CD24 ^{low} CD25 ⁻ CD43 ⁺ CD93 ⁺ CD117 ⁺ IgM ⁻
B	Pro-B cell	B220 ⁺ CD19 ⁺ CD24 ⁺ CD25 ⁻ CD43 ⁺ CD117 ^{low} IgM ⁻
C	Pre-BI cell	B220 ⁺ CD19 ⁺ CD24 ⁺ CD25 ⁻ CD43 ⁺ CD117 ^{low} IgM ⁻
C'	Large pre-BII cell	B220 ⁺ CD19 ⁺ CD24 ⁺ CD25 ⁺ CD43 ^{low} IgM ⁻
D	Small pre-BII cell	B220 ⁺ CD19 ⁺ CD24 ⁺ CD25 ⁺ IgM ⁻
E	Immature B cell	B220 ⁺ CD19 ⁺ CD24 ^{high} IgM ⁺ IgD ⁻
F	Mature B cell	B220 ⁺ CD19 ⁺ CD23 ⁺ CD24 ^{low/-} CD25 ⁺ IgM ⁺ IgD ⁺

1.3. Extracellular vesicles

1.3.1. Historical background

The earliest evidence for the existence of extracellular vesicles (EVs) was initially published in 1946 by Chargaff and West⁵⁸. They reported the presence of a precipitable component in platelet-free plasma that can expedite the synthesis of thrombin. These findings demonstrated for the first time that components other than platelets were involved in blood coagulation. Afterwards, the phenomena of vesicle secretion by cells was documented in the late 1960s by Bonucci and Anderson, who observed that chondrocytes secreted vesicles that were approximately 100 nm in size^{59,60}. In the same timeframe, another study demonstrated that platelets can release tiny vesicles known as "platelet dust"⁶¹. Subsequently, Trams used the word "exosomes" in 1981 to characterize a broad array of vesicles produced from cultivated cells, with sizes varying from 40 nm to 1 μm ⁶². That was to change, though, in 1983 when the research teams of Stahl and Johnstone simultaneously announced that reticulocytes released transferrin receptors linked to 50 nm-sized vesicles into the extracellular space^{63,64}. Johnstone later found in 1987 that this type of release occurred via the endosomal pathway⁶⁵. This included the creation of intraluminal vesicles (ILVs) in the endosome, which were then released extracellularly when multivesicular bodies (MVBs) fused with the plasma membrane. This time, these ILVs were referred to as "exosomes," a name that Trams et al. first developed.

A breakthrough study by Raposo and colleagues showed in 1996 that B cells produce exosomes that display MHC class II⁶⁶. Importantly, the discovery that messenger ribonucleic acids (mRNAs) and microRNAs (miRNAs) could be found in exosomes isolated from human and murine mast cells, identifying them as mediators of cell-cell communication, sparked a renewed interest in EV research since 2007⁶⁷. The first gathering of scientists working on EVs took place in Montreal, Canada, in 2005. Six year later, in 2011, an international conference on

EVs was arranged at the Institute Curie in Paris, France. The phrase "extracellular vesicles" has been suggested to describe cell-generated particles encased in a lipid bilayer⁶⁸. At the same year, the Journal of Extracellular Vesicles (JEV) and the International Society for Extracellular Vesicles (ISEV, <https://www.isev.org/>) were founded with the goal of standardizing the discipline. The society now has more than 2000 members, and several national EV societies have also been established. The Canadian Society for EVs (CanSEV, <http://www.canvesicle.com>) held their first conference in 2022.

1.3.2. Nomenclature and classification

Since their initial description, the nomenclature for extracellular vesicles has gotten confusing over time. The gathered information demonstrates that, depending on the pathophysiological condition of the origin cell, the content, size, and membrane composition of the EVs are extremely complicated and varied. Vesicles that cells emit are referred to by a number of names. The cells or tissues from which they are discharged have given vesicles their names. Therefore, nomenclature such as oncosomes, for EVs released by cancer cells^{69,70}, prostasomes, for EVs produced by prostate epithelial cells^{71,72} or dexosomes, for EVs released by dendritic cells^{73,74} have been used.

On the other hand, words like calcifying matrix vesicles^{75,76}, tolerosomes^{77,78}, or argosomes⁷⁹ can be found based on their biological function. Although particular traits have been suggested for each subpopulation of EVs, there is currently no commonly recognized identification of each subgroup, and the issue is still up for discussion^{80,81}. Consequently, authors are advised to use the term "extracellular vesicle" to refer to any cell-secreted vesicle, unless they can identify reliable and noteworthy markers specific to their experimental system, as per the guidelines provided by ISEV in their Minimal Information for Studies of Extracellular Vesicles

(MISEV) guidelines⁸². Nonetheless, the two fundamental standards determining the most often used nomenclature are the biogenesis mode and the biochemical markers. EVs may then be precisely divided into two main groups: exosomes and microvesicles (MVs) also known as ectosomes, which differ in biogenesis (as shown in Figure 1.2). Exosomes, ranging in size from 30 nm to 150 nm, are released through exocytosis from MVBs^{83–85}. MVs or ectosomes are formed by outward budding from the cell's plasma membrane and are 100 nm to 1000 nm in size^{86,87}. The cargo of EVs contains the proteins, lipids, nucleic acids, and membrane receptors of the cells from which they originate^{88–90}. EVs released into the extracellular space can enter body fluids and potentially reach distant tissues. Once taken up by neighboring and/or distal cells, EVs can transfer functional cargo that may alter the biological functions of target cells, thereby contributing to both physiological and pathological processes⁹¹.

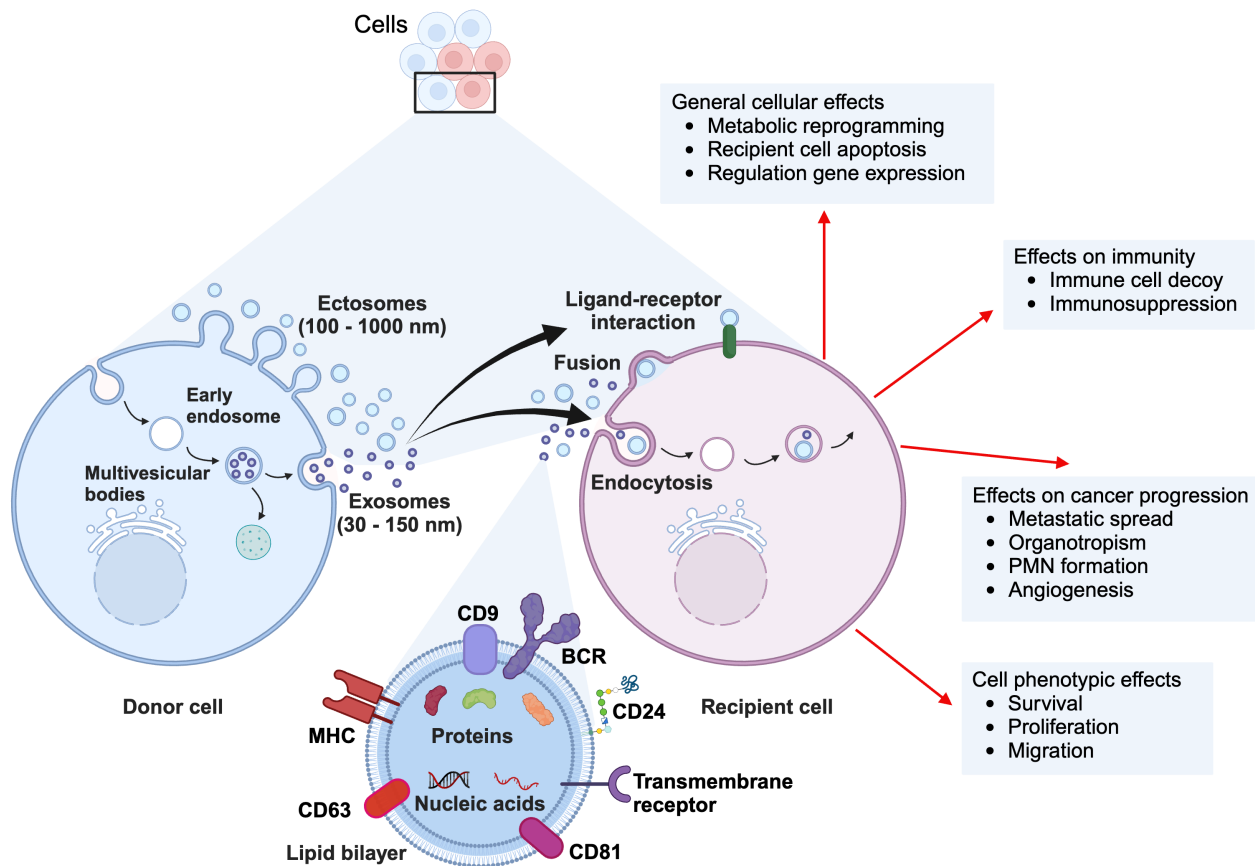


Figure 1.2. The biogenesis, compositions and uptake of extracellular vesicles (EVs). EVs are heterogeneous, phospholipid membrane-enclosed structures. Two main types of EV are distinguished based on their biogenesis, known as exosomes and ectosomes. Exosomes, ranging in size from 30 nm to 150 nm, are generated by the exocytosis of multivesicular bodies. By contrast, ectosomes (100 nm to 1000 nm) are released by plasma membrane budding and blebbing. EVs have spherical structures consisting of a lipid bilayer and contain complex contents, including lipid bilayer, proteins, surface proteins, and nucleic acids. The released EVs are taken up by recipient cells mainly through three ways, including endocytosis, membrane fusion, and ligand-receptor interaction. Once attached to a target cells, the contents of EVs can mediate intercellular communication that impacts a variety of cellular and tissue functions (red arrows). Created with BioRender.com.

1.3.3. Biogenesis

1.3.3.1. Biogenesis of exosomes

Exosomes are vesicles surrounded by a lipid bilayer, having a size from 30 nm to 150 nm^{92,93} and a density ranging from 1.10 to 1.21 g/ml⁹⁴. The formation of exosomes begins in endosomes, with inward budding of the limiting membranes of late endosomes to generate ILVs, causing formation of MVBs⁸³. MVBs may traffic to lysosomes for degradation or to the cell surface for fusion with the plasma membrane, where they are released into the extracellular space as exosomes⁹⁵. It appears that MVB cholesterol levels impact the fate of these multivesicular bodies. However, the exact causes are still unknown. Other research shows that the lysosome breaks down cholesterol-poor vesicles while secreting cholesterol-rich vesicles⁹⁶.

The ESCRT machinery (Endosomal Sorting Complex Required for Transport) is the most well-studied pathway for inducing the formation of ILVs and subsequently of MVBs^{97,98}. The ESCRTs comprise four complexes (ESCRT-0, -I, -II, and -III) and the accessory Vps4 complex, each comprising many subunits⁹⁷. The primary job of ESCRT 0-II is to sort cargo on endosomal membranes into functional microdomains. In contrast, Vps4 assists ESCRT-III in completing the budding and scission of these domains to produce ILVs⁹⁹. Recent evidence has revealed that TSG101 and ALIX are commonly seen as exosome constituent proteins and are components of the ESCRT complex^{100,101}. The ESCRT accessory protein ALIX interacts with ESCRT-III subunits to promote intraluminal vesicle budding and abscission¹⁰⁰. Moreover, Rab GTPases, the most abundant family of proteins in the Ras superfamily of GTPases, are essential for exosome secretion and play a crucial role in intracellular vesicle transport, including endosome recycling and MVB trafficking to lysosomes¹⁰². Research has revealed that many Rab proteins, including Rab27A/B, Rab7, Rab31, and Rab35, control exosome secretion¹⁰³. It has also been reported that Rab GTPases and SNARE proteins collaborate to cause the release of exosomes into the

extracellular space by fusion of late endosomes with the plasma membrane^{102,104}. Although the ESCRT pathway is the critical driver of exosome synthesis, other studies have demonstrated that exosomes can be released via an ESCRT-independent pathway. For instance, inhibition of the ESCRT-dependent pathway by depleting four ESCRTs did not eliminate MVB release¹⁰⁵.

The ESCRT-independent pathway of exosome biogenesis involves the formation of lipid rafts; sphingomyelinase converts sphingomyelin into ceramide. The study reported that the release of exosomes is reduced after inhibition of neutral sphingomyelinase (nSMase), a protein responsible for the production of ceramide, suggesting that the budding of ILVs requires ceramide, an essential component of lipid raft microdomains¹⁰⁶. In addition, ApoE and tetraspanin CD63 are recruited for ILV formation and subsequent exosome release without the requirement of ESCRT or ceramide^{107,108}. In addition to this method of exosome synthesis, "endosome like domains" on the plasma membrane can be directly budded to produce exosomes through enrichment in endosomal and exosomal proteins¹⁰⁹. On the other hand, it has been demonstrated that actin-myosin binding is involved in the production of exosomes and MVBs¹¹⁰. However, additional proof is required to validate exosome biogenesis from the plasma membrane.

1.3.3.2. Biogenesis of ectosomes

MVs, also known as ectosomes, are large lipid bilayer vesicles with varying sizes in a diameter range from 100 nm up to 1000 nm and a density of less than 1.10 g/ml¹¹¹. They result following reorganizing the actin-myosin cytoskeleton and occur by direct budding of the outer cellular membrane⁹³. MV release can be regulated via several pathways. For example, it has been shown that MV release can be stimulated through increased intracellular Ca²⁺ concentrations¹¹². At steady state, the anionic phospholipids, phosphatidylserine (PS) and

phosphatidylethanolamine (PE) localize to the inner leaflet of the plasma membrane. At the same time, phosphatidylcholine (PC) and sphingomyelin (SM) are found on the external membrane leaflet¹¹³. The physiological membrane asymmetry is maintained by five transmembrane enzymes: gelsolin, scramblase, flippase, translocase and calpain¹¹⁴. The increase in the cytoplasmic Ca^{2+} levels inhibits the aminophospholipid translocase and activates lipid scramblase at the same time^{115,116}. This process drives rearrangements in the asymmetry of the membrane phospholipids to expose PS from the inner leaflet to the cell surface. It then leads to the physical collapse of cell membrane asymmetry, which can promote MV release.

In addition to lipids, cytoskeletal elements and their regulators are required for MV formation¹¹². Reducing the levels of phosphatidylinositol 4,5-bisphosphate (PI(4,5)P₂), which participates in anchoring the membrane to the cortical cytoskeleton, can induce the disruption of the cortical cytoskeleton interaction with the plasma membrane^{117,118}, leading to increased MV biogenesis¹¹⁹. Reduction of PI(4,5)P₂ can occur via activation of phospholipase C (PLC)- γ , phospholipase D (PLD), phosphoinositide 3-kinases (PI3Ks), or phosphatidylinositol phosphatases¹²⁰. Rab22a and ARF6, members of the Ras GTPase family, also have essential roles in MV generation. Rab22A is directly involved in MV formation as evidenced by the fact that it colocalizes with budding vesicles and that vesicle release is prevented by Rab22A knockdown¹²¹. Importantly, ARF6 activity is required for subsequent phospholipase D activation, leading to localized myosin light chain kinase activity at the neck of budding vesicles¹²². Furthermore, ARF6-mediated activation of RhoA and Rho-associated kinase (ROCK) signaling have been implicated in MV formation^{122,123}. An additional study has shown that the antagonistic interaction between Rab35 and ARF6 also controls MV biogenesis¹²⁴. Furthermore, a key regulator in the formation of MVs, Ca^{2+} ions also contribute to the reorganization of the cytoskeleton through the

activation of cytosolic calpain protease¹²⁵. Calpain cleaves several cytoskeletal components such as actin, ankyrin, protein 4.1 and spectrin^{126,127}. Calpain-mediated cleavage of the cytoskeleton further disrupts the cortical cytoskeleton protein network, consequently allowing membrane budding. Lastly, similar to exosomes, ceramide production can increase MV release¹²⁸.

1.3.4. EV composition

Cells release EVs of different sizes and intracellular origin. EVs are heterogeneous, phospholipid membrane-enclosed structures that comprise a variety of soluble or membrane proteins, lipids, metabolites, and nucleic acids⁸⁸⁻⁹⁰. EV cargo can vary depending on the cell type, physiologic state, and biologic environment leading to differences in EV composition and subsequent function¹²⁹⁻¹³¹. Interestingly, EVs, which are released in greater density by cancer cells¹³², can promote tumor development and are involved in mediating intercellular communication within the tumor microenvironment¹³³. Indeed, medulloblastoma cells released 13,400-25,300 EVs per cell per 48 h, while normal fibroblast cells released 3,800-6,200 EVs per cell per 48 h¹³⁴. In addition, EV release also depends on a response to external stimuli such as inflammatory signals^{135,136}, ATP¹³⁷, heat stress¹³⁸, increased intracellular calcium levels¹³⁹, and hypoxia¹⁴⁰. Different cell culture platforms have also been shown to significantly impact to EV composition. It has been reported that mesenchymal stromal cell (MSC)-derived EVs carry a higher number of immunomodulatory cytokines when MSCs are grown in a 3D culture¹⁴¹. It has been demonstrated that decreased cell seeding density in culture flasks results in increased EV production¹⁴². Even the polarity of epithelial cells affects the release of different EV subpopulations. Basolaterally secreted EVs are enriched in TSG101, CD9, and CD81, whereas apically secreted EVs express CD63, HSP70, annexin A1, and flotillin-1. Due to the differences

in these markers, EV cargos probably should be classified into distinct EVs based on cell polarity¹⁴³.

1.3.4.1. Lipids

EVs are mainly composed of phosphatidylserine (PS), phosphatidyl-ethanolamine (PE), sphingomyelin (SM), phosphatidylinositol (PI), phosphatidylcholine (PC), cholesterol and ceramide^{144,145}. Several studies have shown that the lipid composition of EVs differs significantly compared to their parent cells. For instance, exosomes contain a higher quantities of PS, SM, cholesterol and PC (approximately 2-3 times) than their parent cells^{144,146}. Unlike exosomes, MVs contain lipids that are precisely like those of their parent cells¹⁴⁷. It is commonly known that exosomes exhibit greater rigidity than the plasma membranes of cells^{148,149}. This rigidity has been suggested to be a pH-dependent mechanism. The ILVs are generated in an acidic pH environment (pH 5.5) inside the MVBs, and they are released into a neutral pH environment to become exosomes. Indeed, the membrane rigidity of exosomes increase between pH 5 and 7¹⁴⁸. This discovery may clarify why EV cellular absorption is enhanced in environments with lower pH, such the tumor microenvironment¹⁴⁹. EV-bound cholesterol and sphingomyelin were found to contribute to their rigidity and stability^{72,150}. It reported that conical-shaped PS helps to build the curved vesicular shape of EVs and encourages the fusion and fission of EVs¹⁵¹. Moreover, prostaglandins, a group of lipids derived from arachidonic acid, contained in EVs that activate signaling pathways in rat basophil leukemia cells¹⁵². It has been consistently demonstrated that exosomes exhibit a higher degree of membrane lipid order than MVs when subjected to detergent treatments¹⁵³. Pancreatic tumor cells are less likely to survive when synthetic nanoparticles mimic the lipid composition of EVs¹⁵⁴. However, in a distinct human pancreatic tumoral cell line, these artificial exosome-like nanoparticles activated the survival pathway¹⁵⁵. When considered

collectively, these findings indicate that lipids participate in cellular signaling pathways and provide structural rigidity and stability to the vesicular membrane¹⁵⁶.

1.3.4.2. Proteins

Proteins are vital components of the EV payload. These common vesicular proteins are mainly involved in vesicle structure, biogenesis, and trafficking. EVs carry endosome-associated proteins, including cytoskeletal proteins (actin, myosin, and tubulin), proteins involved in transport and fusion (Rab11, Rab7, Rab2, and Annexins), ESCRT proteins (TSG-101 and Alix), chaperones (HSP70 and HSP90), and tetraspanin proteins (CD9, CD63, CD81, and CD82)^{157–159}. EVs contain specific cytoplasmic proteins from the cell of origin, such as GTP-binding protein, ADP-ribosylation factor 6 (ARF6), matrix metalloproteinases (MMPs), glycoproteins (e.g., GPIIb, GPIIb-IIIa), integrins, receptors (e.g., EGFRvIII), and cytoskeletal elements (e.g., β -actin and α -actinin-4)^{157,158}. Compared to proteins present in the nucleus and mitochondria, proteins found in the plasma membrane and cytoplasm are more commonly segregated into EVs^{160,161}.

EVs also contain cell-type specific proteins that serve for biomarker discovery. For instance, EVs from patients with melanoma carry the tumor-associated antigen, MART1¹⁶², while ovarian carcinoma cell-derived EVs contain epithelial cell adhesion molecule, EpCAM and CD24¹⁶³. Moreover, EVs contain glycosylated proteins that are essential for diagnostic purposes¹⁶⁴. Indeed, glypican-1 contained in pancreatic cancer cell-derived EVs may be a potential screening marker to detect early-stage pancreatic cancer¹⁶⁵. Tumor cell-derived EVs have been shown to carry the immunosuppressive factor PD-L1, and EV-PD-L1 serves as an early clinical benefit signal in melanoma¹⁶⁶. Tumor cell-derived EVs also contain a higher level of the “do not eat me” signal CD47 and a decreased level of the “eat me” signal PS than

heterogeneous EVs, providing possible reasons for the longer lifetime of tumor cell-derived EVs¹⁶⁷.

Apart from their role as biomarkers, EV-associated proteins are crucial for intercellular communication. It was demonstrated that EV-bound EGFRvIII isolated from glioblastoma patients induces the activation of MAPK and AKT signaling pathways and thus increases in anchorage-independent growth capacity¹⁶⁸. EVs from docetaxel-resistant cells transferred MDR-1/P, a P-glycoprotein, into the docetaxel-sensitive cells, significantly increasing resistance to docetaxel in recipient cells¹⁶⁹. It should be noted that B cell-derived EVs carry functional peptide MHC complexes and induce antigen-specific MHC-II-restricted T cell responses⁶⁶. Moreover, EVs may transport MHC class II that interacts with the T cell receptor and activates naïve CD4 T cells to initiate an immune response¹⁷⁰. Tumor cell-derived EVs carry immunosuppressive factors, such as FASL and PD-L1 and can induce directly the death of T cells and NK cells through the FAS/FASL and PD1/PD-L1 pathways¹⁷¹. Tumor cell-derived EVs also inhibit the maturation of DCs by causing the release of IL-6, suppress NK cell response by downregulating NKG2D expression on NK cells via EV-associated TGFβ1, and cause CD8⁺ T cells to undergo apoptosis through EV-associated FASL, TRAIL, or PD-L1¹⁷². Altogether, cells secrete EVs to communicate with other cells by delivering signals through their content and surface proteins.

1.3.4.3. Nucleic acids

Notable progress in the characterization of EVs has shown their capacity to transport RNA and DNA cargo. Depending on the kind of cell, EVs have different amounts of RNA. Some cancer-derived EVs contain more total RNA than those derived from healthy cells¹³⁴. EVs contain mRNA and miRNA that may potentially be useful as diagnostic markers for diseases¹⁷³.

For instance, moesin, an mRNA cargo linked to proliferation and epithelial integrity, was upregulated in amniotic fluid EVs from fetuses with fetal prenatal hydronephrosis and had more diagnostic potential than existing clinical indicators, such as ultrasound imaging¹⁷⁴. The expression of miRNAs, including miR-21, miR-141, miR-200a, miR-200b, miR-200c, miR-205, and miR-214, was significantly higher in EVs isolated from patients with ovarian cancer through blood tests¹⁷⁵. Notably, evidence of increased miR-30a-5p in the urine of ovarian serous adenocarcinoma patients might serve as a promising diagnostic and therapeutic target¹⁷⁶. Moreover, urinary exosomes from individuals with prostate cancer were used for RNA extraction analysis. The results showed significant downregulation of five specific miRNAs: miR-196a-5p, miR-34a-5p, miR-143-3p, miR-501-3p, and miR-92a-1-5p. In particular, miR-196a-5p and miR-501-3p show promise as prostate cancer indicators^{177,178}. Interestingly, plasma exosomal miR-1290 and miR-375 are promising prognostic biomarkers for castration-resistant prostate cancer¹⁷⁹. Serum exosomes from individuals with relapsing-remitting multiple sclerosis (RRMS) show decreased levels of two specific miRNAs, hsa-miR-122-5p and hsa-miR-196b-5p, which may be a useful biomarker for RRMS¹⁸⁰.

EV-contained mRNAs and miRNAs can also be delivered and functionally transferred to other cells^{181,182}. For instance, the functional transfer of small RNA via exosomes can regulate gene expression in recipient DCs when using viral miRNAs endogenously produced in Epstein-Barr virus (EBV)-infected B cells¹⁸³. Additionally, T regulatory cells transferred EV-associated miRNAs (such as miR-155, Let7b and Let7d) to Th1 cells, suppressing Th1 cell proliferation and cytokine secretion¹⁸⁴. Moreover, specific miRNAs (such as miR-150-5p and miR-142-3p) associated with T regulatory cell-derived EVs modulate the function of DCs, specifically their cytokine production and their phagocytic capacities¹⁸⁵. The melanoma-EVs-enriched miRNAs, including miR-122, miR-149, miR-3187-3p, miR-181a/b, and miR-498, reduce T-cell responses

and cytotoxic activity by decreasing TCR signaling, granzyme B and cytokine secretion¹⁸⁶. Interestingly, miR-19a-3p associated EVs produced from nucleophosmin-1 mutated acute myeloid leukemia cells could be transferred to CD8⁺ T cells, which directly downregulated the expression of solute-carrier family 6 member 8, which resulted in decreased creatine import and ATP production, leading to immunosuppression of T cells¹⁸⁷. In addition, epithelial ovarian cancer (EOC)-derived EV miR-181c-5p may upregulate HOXA10 by targeting KAT2B and activate the JAK1/STAT3 pathway to promote the M2 polarization of tumor-associated macrophages, ultimately promoting growth and metastasis of EOC cells *in vitro* and *in vivo*. It should be noted that exosomal miR-21 and miR-29a activate toll-like receptor (TLR)-7 and TLR8 receptors in immune cells, leading to lung cancer growth and metastasis^{188,189}. Similarly, neuroblastoma-derived EVs can deliver miR-21 that triggers TLR8 in monocytes, leading to upregulation of miR-155 in those cells¹⁹⁰. Recently, some RNA-binding proteins have been discovered to be essential for the selective sorting of miRNAs into exosomes¹⁹¹. A four-nucleotide motif, like GGAG and GGCU, has been found to be abundant in miRNAs in exosomes and an interaction between this motif and the ribonucleoprotein (hnRNPA2B1) appears to be facilitated in loading these miRNAs into MVBs¹⁹². For instance, a recent study has demonstrated that hnRNPA2B1 binds to miR-122-5p through the exosome sorting motif and may promote the selective sorting of miR-122-5p into lung cancer-derived exosomes¹⁹³. Importantly, they discovered that the delivery of lung cancer-derived EVs containing miR-122-5p liver cells in a distant microenvironment, which promotes the formation of a pre-metastasis microenvironment, leading to hepatic metastasis of lung cancer¹⁹³. Another work highlights that YBX1 binds specifically to RNA sorting motifs, including ACCAGCCU, CAGUGAGC and UAAUCCCA in exosomes derived from HEK293 cells¹⁹⁴. Moreover, YBX-1 is required for miR-223 abundance into exosomes released from HEK293T cells¹⁹⁵. YBX-1-mediated sorting of miR-

133 into human endothelial progenitor cell-derived exosomes caused by hypoxia/reoxygenation to promote fibroblast angiogenesis and mesenchymal-endothelial transition¹⁹⁶. However, the process of packaging RNA into EVs has not yet been fully clarified.

Apart from carrying RNA, EVs also contain genomic DNA, mitochondrial DNA, and short DNA sequences of retrotransposons. It was shown that over 90% of cell-free DNA is found in exosomes extracted directly from whole human blood plasma¹. The first study showed that mitochondrial DNA exists in EVs and may be transferred to other cells¹⁹⁸. It should be noted that genomic DNA from exosomes produced from pancreatic cancer cell lines and serum from patients with pancreatic cancer identified mutations in KRAS and p53¹⁹⁹. Moreover, EV-secreted DNA fragments contribute to cellular homeostasis by inhibiting the activation of cytoplasmic DNA sensors²⁰⁰. Interestingly, T cells can secrete EVs containing genomic and mitochondrial DNA that induce antiviral response in DCs via the cGAS-STING cytosolic DNA-sensing pathway²⁰¹. *In vitro*, it was discovered that EVs harboring mitochondrial DNA might trigger an inflammatory response in naïve pulmonary epithelial cells²⁰². Evidence suggested that EVs from human plasma are associated with mitochondrial DNA, which decreases with age²⁰³. However, the sorting mechanism of DNA into EVs remains unknown. Therefore, more investigation is needed to ascertain whether DNA is present in EVs and, if so, what its true importance is.

Generally, EVs play a role in intercellular communication and are involved in numerous physiological and pathological processes. The cargo of EVs can reflect the physical state of the originating cells, serving to propagate the pathological state and act as a potential biomarker of disease including neurological diseases, diabetes, and cancer²⁰⁴. Moreover, EVs exert their influence to interact with recipient cell and alter the phenotype of receiving cells. Tumor-derived EVs promote oncogenic progression such as angiogenesis, immune evasion and metastasis²⁰⁵. Considering their capacity to overcome biological barriers and transfer bioactive components,

EVs are showing great potential for therapeutic applications. Stem cell-derived EVs have capacity to accelerate tissue regeneration²⁰⁶ and stimulate cardiac repair²⁰⁷.

1.4. B cell-derived EVs

1.4.1. B cell-derived EV cargo

The investigation of B cell-derived EVs was initially described in 1996⁶⁶. B cells exhibited MVBs fusing with the plasma membrane, producing EVs that express MHC molecules. Mass spectrometry-based proteomic characterization demonstrated that EVs derived from B cells contain abundant MHC-I, MHC-II, CD45, chaperones (HSP70 and HSP90), integrins and other proteins¹⁵⁰. EVs were also concentrated in lipids that are normally enriched in detergent-resistant membranes, such as cholesterol, sphingomyelin, and ganglioside GM3¹⁵⁰. Additionally, the plasma MHC-II contained in B cell-derived EVs is incorporated with CD20, CD63, CD81, and other tetraspanin family members^{150,208,209}. It has been proposed that these proteins can be recruited at MVBs by the ESCRT machinery via the cytosolic adaptors syntenin and ALIX for incorporation into EVs^{210,211}.

It has been demonstrated that CD20 not only forms complexes with MHC-II and CD40²¹², but it can also cooperate with BCR to take part in signal transduction²¹³. CD20 also can stimulate B cells through calcium channels²¹⁴, which causes a significant amount of EVs to be released²¹⁵. The release of EVs produced from B cells might be impacted by environmental changes. In fact, in response to heat stress, B cells produced EVs with higher concentrations of HSPs, including HSP27, HSP70, HSC70, and HSP90 while other heat shock proteins, HSP60 and GP96, were excluded from EVs²¹⁶. B cell-derived EVs also include functional integrins, enabling high-affinity contact with other cells, such as cytokine-activated fibroblasts²¹⁷. Moreover, stimulation of CD40 or BCR and TLR9 in B cells releases an increased density of EVs containing human

leukocyte antigen through the classical NF- κ B pathway²¹⁸. It has also been demonstrated that B cell-derived EVs express high levels of MHC-I, MHC-II, CD45, BCR complex, and tetraspanins (CD9 and CD81) when B cells were stimulated through CD40 and IL-4 receptor²¹⁹. This investigation revealed that IgM and IgD present at the plasma membrane were incorporated into the EV release pathway, whereas other isotypes, primarily IgA, IgG₁, IgG₂, and IgG₃, were released as soluble forms unrelated to the membrane. Interestingly, IgG-mediated BCR cross-linking induces the release of EVs, but to a lesser degree as a result of TCR-plasma-MHC-II interaction²²⁰.

Apart from proteins, B cell-derived EVs transport miRNAs. Exosomes from EBV-infected B cells were found to contain EBV-encoded miRNAs that could be functionally transferred to noninfected DCs, possibly interfering with the development of adaptive immunity¹⁸³. Interestingly, B cell-derived EVs could deliver exogenous miR-155 to macrophages²²¹. After treatment with rituximab, a downregulation of miR-155 levels in B cell-derived EVs was observed²²². This work shows that miR-155 found in EVs could be developed into a useful biomarker for diagnosis or a target for treatment. Moreover, miR-330-3p from B plasma cell-derived EVs is a critical regulator of ovarian cancer stroma and promotes tumor metastasis through the JAM2 pathway²²³. According to this research, inhibiting the noncanonical exosomal miR-330-3p/JAM2 axis may be a useful therapeutic strategy for high-grade serous ovarian tumors.

1.4.2. B cell-derived EVs crosstalk with the immune system

B cell-derived EVs load MHC-I and -II molecules on their surface for antigen presentation, which, in turn, interact with other immune cells and influence their functionality. In this context,

EVs derived from B cells that contain abundant MHC-II molecules have been shown to stimulate antigen-specific CD4⁺ T cell responses *in vitro*⁶⁶. Some studies have shown that B cell-derived EVs can directly stimulate T lymphocytes activation^{170,218}. B cell-derived EVs were also enriched in MHC-I that was required for an antigen presentation to CD8⁺ T cell population^{219,224}. The activation of cytotoxic T lymphocytes (CTL) by B cell-derived EVs still required CD4⁺ T cells, CD8⁺ T cells, and NK cells to be present. The CTL response was completely lost without any of these immune cell types. Interestingly, host B cells, the BCR, and B-cell-secreted antibodies did not directly contribute to the CTL response triggered by exogenous B-cell-derived EVs, based on using mouse models with B cells depleted of membrane-bound and secreted antibodies²²⁵. Moreover, EVs from B cells can bind to follicular DCs as they contain $\alpha_4\beta_1$ integrins that interact with VCAM-1 on the surface of follicular DCs. Importantly, follicular DCs do not express MHC-II but instead, pick up peptide-loaded MHC-II molecules after binding B lymphocyte-derived EVs to follicular DCs. This molecule on the follicular DC surface is necessary to induce the affinity maturation phenomenon in B lymphocytes²²⁶.

Other receptors found on EVs produced from B cells have also been shown to affect various immune cell types. For instance, B cell-derived EVs carry CD38, an active glycoprotein enzyme, that associates with signaling complexes HSC-70, Lyn, and CD81. The presence of CD38 on the surface of EVs can potentially act as an intercellular messenger of T cell activation²²⁷. It has been observed that CD19⁺ EVs from B cells contain high CD39 and CD73, which are critical enzymes in the adenosine pathway that hydrolyze ATP released by chemotherapy-treated tumor cells into adenosine and attenuate chemotherapeutic efficacy by inhibiting antitumor CD8⁺ T cell responses²²⁸. Remarkably, B cell-derived EVs may also have MHC-II and FASL, which cause CD4⁺ T cells to undergo apoptosis through FAS and FASL

interaction²²⁹. Moreover, functional integrins and ICAM-1 are carried by B cell-derived EVs, which enable high-affinity interactions with extracellular matrix proteins and open the door for cargo delivery to T cells. ICAM-1 interacts with leukocyte function-associated antigen-1 molecules that are expressed on T cells to enhance the transfer of cargo. In some cases, B cell-derived EVs also express β_1 and β_2 integrins. By the expression of β_1 integrins, EVs can bind to pro-inflammatory cytokine-activated fibroblasts and collagen type I and fibronectin in the extracellular matrix²¹⁷. Another fascinating discovery is that B cell-derived EVs carry complement 3 (C3) fragments and BCR-antigen complexes²²⁰. Antigen-loaded B cells release C3-carrying EVs which then interact with G protein coupled receptors on T cells. This interaction promotes better T cell responses even when the presence of antigen concentration is suboptimal²³⁰.

1.5. CD24

Cluster of differentiation 24 (CD24), also referred to as heat-stable antigen, is a small, heavily glycosylated cell surface protein linked to lipid rafts on the plasma membrane via a glycosyl-phosphatidylinositol (GPI) anchor²³¹. CD24 was first discovered in 1978 and has been known to be specifically recognized by rat anti-mouse antibodies including M1/75.21, M1/22.54, M1/89.1, M1/9.47 and M1/69.16²³². Of these monoclonal antibodies, M1/69 was found to have the highest avidity for this newly identified antigen²³³. The protein core of CD24 comprises approximately 30 amino acids linked to the N- and/or O-glycosylation and P-selectin binding sites, which is considered as major function of CD24²³⁴. CD24 is located on chromosome 6q21, a polymorphic allele, of which, the protein has molecular weights ranging from 30 to 70kDa²³⁵. CD24 expression has been reported in many cell types²³⁶. These include hematopoietic cells

(immature B cells, T cells, granulocytes, dendritic cells, and macrophages) and non-immune cells (neural cells, regenerating muscle cells, and various epithelial cells, as well as tumors).

CD24 carries out diverse functions by interacting its incorporated glycans with various ligands. CD24 has fourteen-O and two N-glycosylation sites, which can bind with different signal transducers on lipid raft domains through engaging in cis (same cell) or trans (other cell) interactions^{237,238}. There are several ligands found to bind to CD24, including P-, L-, and E-selectin, Sialic-acid-binding immunoglobulin-like lectin (Siglec) G or Siglec 10, TAG-1 and contactin, L1 cell adhesion molecule and Neural cell adhesion molecule²³⁹. For instance, CD24 interacts in cis with a moderator of TLR signaling, Siglec-G, and in trans with the danger associated molecular pattern (DAMP) protein HMGB1^{240,241}. In this case, CD24 acts an adapter, binding both HMGB1 and Siglec-G, activating Siglec-G and ultimately inhibiting TLR-4 signaling.

CD24 is one of the molecules found the earliest on the surface of B cells during B cell development²⁴². Indeed, the expression of CD24 in human B cell development presents earlier than the expression of CD19²⁴³. CD24 is first expressed in Fraction B (pro-B cell stage), then it rises in pre-B cells and immature B cells, where it reaches its maximum levels. However, when B cells enter circulating B cell stage, CD24 expression declines, and continues to fall in subsequent Hardy fractions until it is expressed at low levels by the end of bone marrow development²⁴⁴.

CD24, as a GPI-anchored protein, lacks an intracellular domain, and it has to interact with other signal transducers through glycolipid-enriched membrane (GEM) domains, also called lipid rafts^{237,238}. The GEM domain is considered an important platform for signaling molecules, such as the Src family tyrosine kinases (SFK) and G-proteins^{245,246}. Several reports have shown that GPI-linked CD24 protein is associated with SFK, which consists of nine members, Blk, Fgr, Fyn,

Hck, Lck, Lyn, Src, Yes, and Yrk^{246,247}. An association between CD24 and either c-Fgr or Lyn was shown in SW2 and K562 erythroleukemia cell lines respectively²⁴⁸ while B cell lymphomas showed a signaling and physical association between CD24 and Lck, Hck, and Lyn, but not Fyn²⁴⁷. Moreover, an association between CD24 and Lyn was shown in Human Burkitt's lymphoma cells²⁴⁹, whereas the MTLy breast cancer cell line associates CD24 with Src²⁵⁰. Taken together, these investigations demonstrate that CD24 communicates via several Src family proteins.

It has been demonstrated that CD24 expression triggers the activation of several signaling pathways relevant to cancer. For instance, crosslinking between CD24 and Wnt signaling results in β -catenin activated by CD24 to interact with the Wnt pathway and to cause β -catenin to translocate into the nucleus^{251,252}. Also, it has been shown that Notch and Wnt/ β -catenin signaling pathways play important roles in the activation of liver cancer stem cells expressing CD24²⁵³. Several studies have demonstrated that Notch-related signaling pathways positively correlated with CD24 expression in cancer cells^{254–256}. Moreover, knockdown of CD24 led to decreased expression of Notch1, which inhibited proliferation and apoptosis in cancer stem cells²⁵⁷. MAPK cascades are shown to be involved in CD24-induced tumorigenesis in tumor cells. It is worth noting that CD24 activated cell proliferation was not only p38 MAPK-dependent but also ERK1/2-dependent^{258,259}. In addition, CD24 induces proliferation and invasiveness in cells through the activation of PI3K/Akt, NF- κ B and ERK^{260,261}. Another study demonstrated that CD24 controls STAT3 phosphorylation through the activation of SFK²⁶².

CD24 induces apoptosis in B cell precursors, including pro-B cells, pre-B cells and immature B cells²³¹. Stimulation with anti-CD24 monoclonal antibodies induces apoptosis in pre-B cells but not mature splenic B cells²⁶³. The treatment with anti-CD24 monoclonal antibodies

induced the activation of p38 MAPK and leads to the apoptosis of pre-B cells. Also, CD24 engagement activates several caspase proteins, including caspase-2, -3, -7 and -8, which are known to be involved in the induction of apoptosis²⁶⁴. Cross-linking CD24 on human B cells with monoclonal antibodies can transduce cytoplasmic calcium mobilization²⁶⁵. Moreover, Burkitt's lymphoma cells undergo apoptosis when antibody-mediated cross-linking of CD24 induces it through glycolipid-enriched membrane domains or lipid rafts²⁴⁹. This process is closely linked to the BCR-mediated apoptosis signal, which involves activating the SFK, and then initiating downstream signaling cascades.

Our laboratory has previously reported that antibody stimulation of CD24 induces apoptosis in the mouse WEHI-231 B cell line and mouse primary bone marrow-derived B cells²⁴². This finding found that cross-linking CD24 has been shown to up-regulated caspase-3/7 activity in WEHI-231 cells after anti-CD24 and second antibody stimulation. Furthermore, treatment with anti-CD24 monoclonal antibody promotes the generation of CD24-bearing plasma membrane-derived EVs²⁴². Recent work also indicates that CD24 induces compositional changes to the surface receptors of B cell MVs with variable effects on their RNA and protein cargo²⁶⁶. EVs play pivotal roles in cell-to-cell communication during different pathological and physiological processes. The passage of EVs between the donor and recipient cells is still unknown upon CD24 engagement. Therefore, understanding the role of CD24-mediated EVs and its cargo is my long-term goal.

1.6. Research objectives of the thesis

Given the current state of knowledge with CD24-mediated stimulation of B cells and EV generation, my research focused on three major objectives as described in Figure 1.3

1.6.1. Objective 1: Determine if CD24 induces transfer of functional protein to recipient cells via EVs.

Hypothesis: The transfer of EVs in response to CD24 engagement from donor to recipient cells alters recipient cell function.

Specific objectives:

- a. Determine if lipid and protein are transferred to recipient B cells in response to CD24 stimulation via EVs using flow cytometry.
- b. Determine if transferred protein are functional in the recipient cells using flow cytometry.

1.6.2. Objective 2: Determine if other receptors stimulate EV-mediated transfer of functional proteins.

Hypothesis: EVs induced by stimulation of B cells through anti-IgM or other receptors with common function or structure to CD24 can transfer cargo and alter function of recipient cells.

- a. Determine if surface proteins having common function or structure to CD24 are expressed on donor B cells using flow cytometry.
- b. Determine if lipid and protein are transferred to recipient B cells in response to other receptor stimulation via EVs using flow cytometry.
- c. Determine if transferred proteins are functional in the recipient cells using flow cytometry.

1.6.3. Objective 3: Elucidate the mechanism of CD24-mediated EV release

Hypothesis: EVs induced by CD24 stimulation are MVs budded off the plasma membrane via the PI3K/AKT/mTOR pathway, not exosomes derived from MVBs.

Specific objectives:

- a. Identify the relationship between CD24 gene expression and signaling pathways in B cells using bioinformatics.
- b. Determine if inhibition of downstream targets, PI3K/AKT, mTOR, and ROCK signaling pathway, inhibits lipids and proteins transfer to recipient cells in response to CD24 using flow cytometry.

Key Objectives

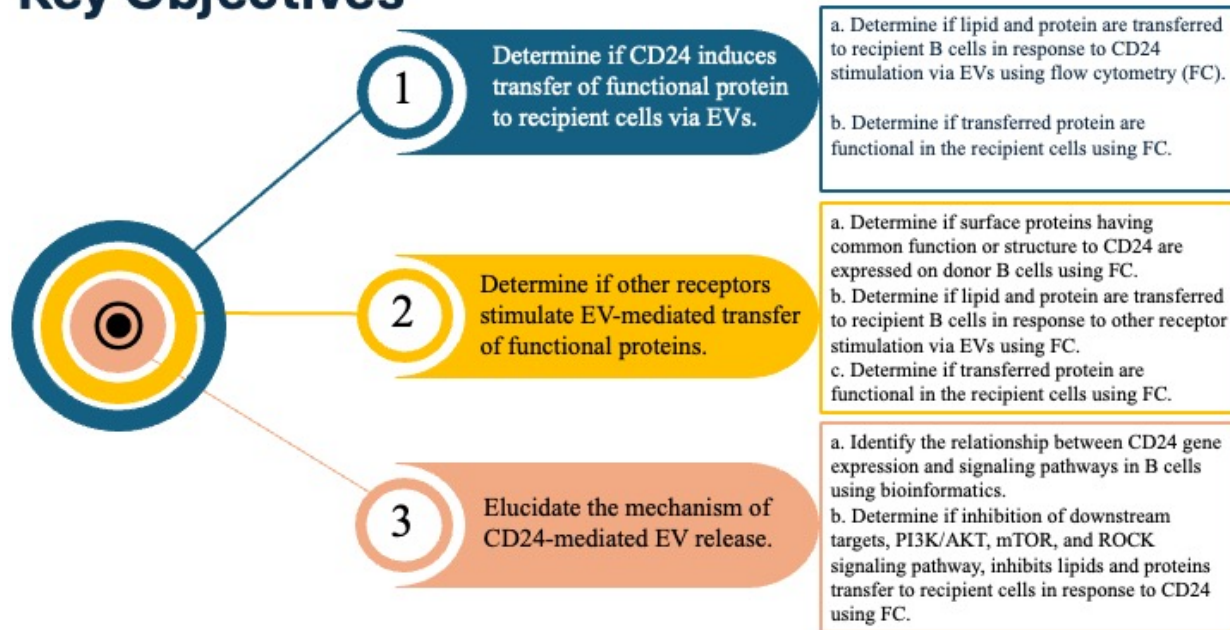


Figure 1.3. Diagram of the research objectives.

1.7. Publications arising from this thesis

The results presented in this thesis have all been published as follows:

Objectives 1 and 2

1. Hong-Dien Phan, Delania J.B. Gormley, Reilly H. Smith, Modeline N. Longjohn, May Dang-Lawson, Linda Matsuuchi, Micheal R. Gold, Sherri L. Christian. CD24 and IgM stimulation of B cells triggers transfer of functional CD24 and B cell receptor to B cell recipients via extracellular vesicles. 2021. *Journal of Immunology*, 207 (12): 3004-3015

Authors contributions: HDP and SLC conceived the idea and designed the experiments.

HDP performed FACS analysis of the transfer of EVs in response to CD24 and IgM stimulation, DG performed FACS analysis of the transfer of EVs in response to CD48 stimulation, RS performed FACS analysis of the transfer of EVs in response to CD40 stimulation, MNL performed analysis of EVs by NTA and Western blot, MDL generated transfected cells for a model co-cultured system, LM and MG reviewed the data. All authors approved the final manuscript.

Objective 3:

2. Hong-Dien Phan, Willow R.B. Squires, Kaitlyn E. Mayne, Grant R. Kelly, Rashid Jafardoust, Sherri L. Christian. CD24 regulates extracellular vesicle release via an aSMase/PI3K/mTORC2/ROCK/actin pathway in B lymphocytes. 2024. *Journal of Extracellular Vesicles* (submitted).

Authors contributions: HDP and SLC conceived the idea and designed the experiments.

HDP performed FACS analysis, Western blot and transfected siRNA cells, WS performed

bioinformatic and FACS analysis, KM, GK, RS performed evaluation of live cell imaging.

All authors approved the final manuscript.

Other:

3. Modeline N. Longjohn, Hong-Dien Phan, Sherri L. Christian. Chapter 2: Culturing suspension cancer cell lines. 2022. Springer Nature. Cancer cell Biology: Methods and Protocols, Methods in Molecular Biology, Vol. 2508.

Authors contributions: HDP wrote a draft manuscript, MNL wrote the final manuscript,

SLC reviewed and edited the manuscript. All authors approved the final manuscript.

1.8. References

1. Bonilla, F. A. & Oettgen, H. C. Adaptive immunity. *J. Allergy Clin. Immunol.* 125, S33–S40 (2010).
2. Stone, K. D., Prussin, C. & Metcalfe, D. D. IgE, mast cells, basophils, and eosinophils. *J. Allergy Clin. Immunol.* 125, S73–S80 (2010).
3. Kucuksezer, U. C. et al. The Role of Natural Killer Cells in Autoimmune Diseases. *Front. Immunol.* 12, 622306 (2021).
4. Silva, M. T. & Correia-Neves, M. Neutrophils and Macrophages: the Main Partners of Phagocyte Cell Systems. *Front. Immunol.* 3, 174 (2012).
5. Su, Y., Gao, J., Kaur, P. & Wang, Z. Neutrophils and Macrophages as Targets for Development of Nanotherapeutics in Inflammatory Diseases. *Pharmaceutics* 12, 1222 (2020).
6. Gardner, A., Pulido, Á. de M. & Ruffell, B. Dendritic Cells and Their Role in Immunotherapy. *Front. Immunol.* 11, 924 (2020).
7. Akira, S., Uematsu, S. & Takeuchi, O. Pathogen Recognition and Innate Immunity. *Cell* 124, 783–801 (2006).
8. Kawai, T. & Akira, S. Toll-like receptor and RIG-I-like receptor signaling. *Ann. N. Y. Acad. Sci.* 1143, 1–20 (2008).
9. Ochando, J., Mulder, W., J. M., Madsen, J. C., Netea, M. G. & Duivenvoorden, R. Trained immunity — basic concepts and contributions to immunopathology | Nature Reviews Nephrology. *Nat. Rev. Nephrol.* 19, 23–37 (2022).
10. Divangahi, M. et al. Trained immunity, tolerance, priming and differentiation: distinct immunological processes. *Nat. Immunol.* 22, 2–6 (2021).

11. Hole, C. R. et al. Induction of memory-like dendritic cell responses in vivo. *Nat. Commun.* 10, 2955 (2019).
12. Quintin, J. et al. *Candida albicans* Infection Affords Protection against Reinfection via Functional Reprogramming of Monocytes. *Cell Host Microbe* 12, 223–232 (2012).
13. Buffen, K. et al. Autophagy Controls BCG-Induced Trained Immunity and the Response to Intravesical BCG Therapy for Bladder Cancer. *PLoS Pathog.* 10, e1004485 (2014).
14. Sun, J. C., Beilke, J. N. & Lanier, L. L. Adaptive immune features of natural killer cells. *Nature* 457, 557–561 (2009).
15. Min-Oo, G. & Lanier, L. L. Cytomegalovirus generates long-lived antigen-specific NK cells with diminished bystander activation to heterologous infection. *J. Exp. Med.* 211, 2669 (2014).
16. Nankabirwa, V. et al. Child survival and BCG vaccination: a community based prospective cohort study in Uganda. *BMC Public Health* 15, 175 (2015).
17. Dominguez-Andres, J. & Netea, M. G. Long-term reprogramming of the innate immune system. *J. Leukoc. Biol.* 105, 329–338 (2019).
18. Inoue, T. & Kurosaki, T. Memory B cells. *Nat. Rev. Immunol.* 24, 5–17 (2024).
19. Kumar, B. V., Connors, T. & Farber, D. L. Human T cell development, localization, and function throughout life. *Immunity* 48, 202–213 (2018).
20. Primorac, D. et al. Adaptive Immune Responses and Immunity to SARS-CoV-2. *Front. Immunol.* 13, (2022).
21. Akkaya, M., Kwak, K. & Pierce, S. K. B cell memory: building two walls of protection against pathogens. *Nat. Rev. Immunol.* 20, 229–238 (2020).
22. Khodadadi, L., Cheng, Q., Radbruch, A. & Hiepe, F. The Maintenance of Memory Plasma Cells. *Front. Immunol.* 10, 721 (2019).

23. Till, J. E. & McCulloch, E. A. A Direct Measurement of the Radiation Sensitivity of Normal Mouse Bone Marrow Cells. *Radiat. Res.* 14, 213–222 (1961).
24. Siminovitch, L., McCulloch, E. A. & Till, J. E. The distribution of colony-forming cells among spleen colonies. *J. Cell. Comp. Physiol.* 62, 327–336 (1963).
25. Spangrude, G. J., Heimfeld, S. & Weissman, I. Purification and characterization of mouse hematopoietic stem cells. *Science* 241, 58–63 (1988).
26. Wilson, A. et al. Hematopoietic Stem Cells Reversibly Switch from Dormancy to Self-Renewal during Homeostasis and Repair. *Cell* 135, 1118–1129 (2008).
27. Liu, L. et al. Homing and Long-Term Engraftment of Long- and Short-Term Renewal Hematopoietic Stem Cells. *PLOS ONE* 7, e31300 (2012).
28. Kondo, M., Weissman, I. L. & Akashi, K. Identification of Clonogenic Common Lymphoid Progenitors in Mouse Bone Marrow. *Cell* 91, 661–672 (1997).
29. Inlay, M. A. et al. Ly6d marks the earliest stage of B-cell specification and identifies the branchpoint between B-cell and T-cell development. *Genes Dev.* 23, 2376–2381 (2009).
30. Rolink, A. & Melchers, F. B-cell development in the mouse. *Immunol. Lett.* 54, 157–161 (1996).
31. Hardy, R. R. & Hayakawa, K. B cell development pathways. *Annu. Rev. Immunol.* 19, 595–621 (2001).
32. Sakaguchi, N. & Melchers, F. Lambda 5, a new light-chain-related locus selectively expressed in pre-B lymphocytes. *Nature* 324, 579–582 (1986).
33. Kudo, A. & Melchers, F. A second gene, VpreB in the lambda 5 locus of the mouse, which appears to be selectively expressed in pre-B lymphocytes. *EMBO J.* 6, 2267–2272 (1987).

34. Karasuyama, H., Kudo, A. & Melchers, F. The proteins encoded by the VpreB and lambda 5 pre-B cell-specific genes can associate with each other and with mu heavy chain. *J. Exp. Med.* 172, 969–972 (1990).
35. Ten Boekel, E., Melchers, F. & Rolink, A. G. Precursor B cells showing H chain allelic inclusion display allelic exclusion at the level of pre-B cell receptor surface expression. *Immunity* 8, 199–207 (1998).
36. Reth, M. Antigen receptors on B lymphocytes. *Annu. Rev. Immunol.* 10, 97–121 (1992).
37. Srinivasan, L. et al. PI3 kinase signals BCR-dependent mature B cell survival. *Cell* 139, 573–586 (2009).
38. Schweighoffer, E. & Tybulewicz, V. L. Signalling for B cell survival. *Curr. Opin. Cell Biol.* 51, 8–14 (2018).
39. Venkitaraman, A. R., Williams, G. T., Dariavach, P. & Neuberger, M. S. The B-cell antigen receptor of the five immunoglobulin classes. *Nature* 352, 777–781 (1991).
40. Nemazee, D. Mechanisms of central tolerance for B cells. *Nat. Rev. Immunol.* 17, 281–294 (2017).
41. Lee, D. S. W., Rojas, O. L. & Gommerman, J. L. B cell depletion therapies in autoimmune disease: advances and mechanistic insights. *Nat. Rev. Drug Discov.* 20, 179–199 (2021).
42. Tomura, M. et al. Monitoring cellular movement in vivo with photoconvertible fluorescence protein “Kaede” transgenic mice. *Proc. Natl. Acad. Sci.* 105, 10871–10876 (2008).
43. Morgan, D. & Tergaonkar, V. Unraveling B cell trajectories at single cell resolution. *Trends Immunol.* 43, 210–229 (2022).
44. Kurosaki, T., Kometani, K. & Ise, W. Memory B cells. *Nat. Rev. Immunol.* 15, 149–159 (2015).

45. Tsay, G. J. & Zouali, M. The Interplay Between Innate-Like B Cells and Other Cell Types in Autoimmunity. *Front. Immunol.* 9, (2018).
46. Inoue, T. Memory B cell differentiation from germinal centers. *Int. Immunol.* 35, 565–570 (2023).
47. Hardy, R. R., Carmack, C. E., Shinton, S. A., Kemp, J. D. & Hayakawa, K. Resolution and characterization of pro-B and pre-pro-B cell stages in normal mouse bone marrow. *J. Exp. Med.* 173, 1213–1225 (1991).
48. Rolink, A., Grawunder, U., Winkler, T. H., Karasuyama, H. & Melchers, F. IL-2 receptor alpha chain (CD25, TAC) expression defines a crucial stage in pre-B cell development. *Int. Immunol.* 6, 1257–1264 (1994).
49. Vale, A. M., Kearney, J. F., Nobrega, A. & Schroeder, H. W. Chapter 7 - Development and Function of B Cell Subsets. in *Molecular Biology of B Cells (Second Edition)* (eds. Alt, F. W., Honjo, T., Radbruch, A. & Reth, M.) 99–119 (Academic Press, London, 2015).
doi:10.1016/B978-0-12-397933-9.00007-2.
50. Edry, E. & Melamed, D. Receptor editing in positive and negative selection of B lymphopoiesis. *J. Immunol. Baltim. Md 1950* 173, 4265–4271 (2004).
51. Carsetti, R., Köhler, G. & Lamers, M. C. Transitional B cells are the target of negative selection in the B cell compartment. *J. Exp. Med.* 181, 2129–2140 (1995).
52. Osmond, D. G. Proliferation kinetics and the lifespan of B cells in central and peripheral lymphoid organs. *Curr. Opin. Immunol.* 3, 179–185 (1991).
53. Nossal, G. J. V. Negative selection of lymphocytes. *Cell* 76, 229–239 (1994).
54. Shvitiel, S., Leider, N., Sadeh, O., Kraiem, Z. & Melamed, D. Impaired Light Chain Allelic Exclusion and Lack of Positive Selection in Immature B Cells Expressing Incompetent Receptor Deficient of CD191. *J. Immunol.* 168, 5596–5604 (2002).

55. Cyster, J. G. & Goodnow, C. C. Antigen-induced exclusion from follicles and anergy are separate and complementary processes that influence peripheral B cell fate. *Immunity* 3, 691–701 (1995).
56. Scholz, J. L. et al. BlyS inhibition eliminates primary B cells but leaves natural and acquired humoral immunity intact. *Proc. Natl. Acad. Sci. U. S. A.* 105, 15517 (2008).
57. Crowley, J. E. et al. Homeostatic control of B lymphocyte subsets. *Immunol. Res.* 42, 75–83 (2008).
58. Chargaff, E. & West, R. The biological significance of the thromboplastic protein of blood. *J. Biol. Chem.* 166, 189–197 (1946).
59. Anderson, H. C. Vesicles associated with calcification in the matrix of epiphyseal cartilage. *J. Cell Biol.* 41, 59–72 (1969).
60. Bonucci, E. Fine structure and histochemistry of ‘calcifying globules’ in epiphyseal cartilage. *Z. Zellforsch. Mikrosk. Anat. Vienna Austria* 1948 103, 192–217 (1970).
61. Wolf, P. The Nature and Significance of Platelet Products in Human Plasma. *Br. J. Haematol.* 13, 269–288 (1967).
62. Trams, E. G., Lauter, C. J., Salem, N. & Heine, U. Exfoliation of membrane ecto-enzymes in the form of micro-vesicles. *Biochim. Biophys. Acta* 645, 63–70 (1981).
63. Harding, C., Heuser, J. & Stahl, P. Receptor-mediated endocytosis of transferrin and recycling of the transferrin receptor in rat reticulocytes. *J. Cell Biol.* 97, 329–339 (1983).
64. Pan, B.-T. & Johnstone, R. M. Fate of the transferrin receptor during maturation of sheep reticulocytes in vitro: Selective externalization of the receptor. *Cell* 33, 967–978 (1983).
65. Johnstone, R. M., Adam, M., Hammond, J. R., Orr, L. & Turbide, C. Vesicle formation during reticulocyte maturation. Association of plasma membrane activities with released vesicles (exosomes). *J. Biol. Chem.* 262, 9412–9420 (1987).

66. Raposo, G. et al. B lymphocytes secrete antigen-presenting vesicles. *J. Exp. Med.* 183, 1161–1172 (1996).
67. Valadi, H. et al. Exosome-mediated transfer of mRNAs and microRNAs is a novel mechanism of genetic exchange between cells. *Nat. Cell Biol.* 9, 654–659 (2007).
68. György, B. et al. Membrane vesicles, current state-of-the-art: emerging role of extracellular vesicles. *Cell. Mol. Life Sci. CMLS* 68, 2667–2688 (2011).
69. Di Vizio, D. et al. Large oncosomes in human prostate cancer tissues and in the circulation of mice with metastatic disease. *Am. J. Pathol.* 181, 1573–1584 (2012).
70. Meehan, B., Rak, J. & Di Vizio, D. Oncosomes - large and small: what are they, where they came from? *J. Extracell. Vesicles* 5, 33109 (2016).
71. Gunnar, R. Prostatosomes are Pluripotent and Well–Organized Organelles in Human Semen. *EJIFCC* 11, 1–5 (1999).
72. Brouwers, J. F. et al. Distinct lipid compositions of two types of human prostatosomes. *Proteomics* 13, 1660–1666 (2013).
73. Le Pecq, J.-B. Dexosomes as a therapeutic cancer vaccine: From bench to bedside. *Blood Cells. Mol. Dis.* 35, 129–135 (2005).
74. Nikfarjam, S., Rezaie, J., Kashanchi, F. & Jafari, R. Dexosomes as a cell-free vaccine for cancer immunotherapy. *J. Exp. Clin. Cancer Res.* 39, 258 (2020).
75. Anderson, H. C. Matrix vesicles and calcification. *Curr. Rheumatol. Rep.* 5, 222–226 (2003).
76. Ansari, S. et al. Matrix Vesicles: Role in Bone Mineralization and Potential Use as Therapeutics. *Pharmaceuticals* 14, 289 (2021).
77. Karlsson, M. et al. ‘Tolerosomes’ are produced by intestinal epithelial cells. *Eur. J. Immunol.* 31, 2892–2900 (2001).

78. Östman, S., Taube, M. & Telemo, E. Tolerosome-induced oral tolerance is MHC dependent. *Immunology* 116, 464–476 (2005).
79. Christian, J. L. Argosomes: intracellular transport vehicles for intercellular signals? *Sci. STKE Signal Transduct. Knowl. Environ.* 2002, pe13 (2002).
80. Van der Pol, E., Böing, A. N., Gool, E. L. & Nieuwland, R. Recent developments in the nomenclature, presence, isolation, detection and clinical impact of extracellular vesicles. *J. Thromb. Haemost.* 14, 48–56 (2016).
81. Witwer, K. W. & Théry, C. Extracellular vesicles or exosomes? On primacy, precision, and popularity influencing a choice of nomenclature. *J. Extracell. Vesicles* 8, 1648167 (2019).
82. Théry, C. et al. Minimal information for studies of extracellular vesicles 2018 (MISEV2018): a position statement of the International Society for Extracellular Vesicles and update of the MISEV2014 guidelines. *J. Extracell. Vesicles* 7, 1535750 (2018).
83. Jeppesen, D. K., Zhang, Q., Franklin, J. L. & Coffey, R. J. Extracellular vesicles and nanoparticles: emerging complexities. *Trends Cell Biol.* 33, 667–681 (2023).
84. Brodeur, A. et al. Apoptotic exosome-like vesicles transfer specific and functional mRNAs to endothelial cells by phosphatidylserine-dependent macropinocytosis. *Cell Death Dis.* 14, 449 (2023).
85. Van Niel, G. et al. Challenges and directions in studying cell-cell communication by extracellular vesicles. *Nat. Rev. Mol. Cell Biol.* 23, 369–382 (2022).
86. Crompot, E. et al. Extracellular vesicles of bone marrow stromal cells rescue chronic lymphocytic leukemia B cells from apoptosis, enhance their migration and induce gene expression modifications. *Haematologica* 102, 1594–1604 (2017).
87. Witwer, K. W. et al. Standardization of sample collection, isolation and analysis methods in extracellular vesicle research. *J. Extracell. Vesicles* 2, 20360 (2013).

88. Tkach, M. & Théry, C. Communication by Extracellular Vesicles: Where We Are and Where We Need to Go. *Cell* 164, 1226–1232 (2016).
89. Raposo, G. et al. B lymphocytes secrete antigen-presenting vesicles. *J. Exp. Med.* 183, 1161–72 (1996).
90. Teo, B. H. D. & Wong, S. H. MHC class II-associated invariant chain (Ii) modulates dendritic cells-derived microvesicles (DCMV)-mediated activation of microglia. *Biochem. Biophys. Res. Commun.* 400, 673–678 (2010).
91. Longjohn, M. N. et al. Deciphering the messages carried by extracellular vesicles in hematological malignancies. *Blood Rev.* 46, 100734 (2021).
92. Raposo, G. & Stoorvogel, W. Extracellular vesicles: Exosomes, microvesicles, and friends. *J. Cell Biol.* 200, 373–383 (2013).
93. Doyle, L. M. & Wang, M. Z. Overview of Extracellular Vesicles, Their Origin, Composition, Purpose, and Methods for Exosome Isolation and Analysis. *Cells* 8, 727 (2019).
94. New, S. E. P. & Aikawa, E. Role of Extracellular Vesicles in De Novo Mineralization. *Arterioscler. Thromb. Vasc. Biol.* 33, 1753–1758 (2013).
95. Hessvik, N. P. & Llorente, A. Current knowledge on exosome biogenesis and release. *Cell. Mol. Life Sci. CMLS* 75, 193–208 (2018).
96. Möbius, W. et al. Immunoelectron microscopic localization of cholesterol using biotinylated and non-cytolytic perfringolysin O. *J. Histochem. Cytochem. Off. J. Histochem. Soc.* 50, 43–55 (2002).
97. Henne, W. M., Buchkovich, N. J. & Emr, S. D. The ESCRT Pathway. *Dev. Cell* 21, 77–91 (2011).
98. Hurley, J. H. ESCRTs are everywhere. *EMBO J.* 34, 2398 (2015).

99. Henne, W. M., Stenmark, H. & Emr, S. D. Molecular Mechanisms of the Membrane Sculpting ESCRT Pathway. *Cold Spring Harb. Perspect. Biol.* 5, a016766 (2013).
100. Zhang, Y., Liu, Y., Liu, H. & Tang, W. H. Exosomes: biogenesis, biologic function and clinical potential. *Cell Biosci.* 9, 19 (2019).
101. Larios, J., Mercier, V., Roux, A. & Gruenberg, J. ALIX- and ESCRT-III–dependent sorting of tetraspanins to exosomes. *J. Cell Biol.* 219, (2020).
102. Blanc, L. & Vidal, M. New insights into the function of Rab GTPases in the context of exosomal secretion. *Small GTPases* 9, 95–106 (2017).
103. Jin, Y. et al. Extracellular signals regulate the biogenesis of extracellular vesicles. *Biol. Res.* 55, 35 (2022).
104. Liu, C. et al. Identification of the SNARE complex that mediates the fusion of multivesicular bodies with the plasma membrane in exosome secretion. *J. Extracell. Vesicles* 12, 12356 (2023).
105. Stuffers, S., Sem Wegner, C., Stenmark, H. & Brech, A. Multivesicular endosome biogenesis in the absence of ESCRTs. *Traffic Cph. Den.* 10, 925–937 (2009).
106. Trajkovic, K. et al. Ceramide triggers budding of exosome vesicles into multivesicular endosomes. *Science* 319, 1244–1247 (2008).
107. Van Niel, G. et al. Apolipoprotein E Regulates Amyloid Formation within Endosomes of Pigment Cells. *Cell Rep.* 13, 43–51 (2015).
108. Van Niel, G. et al. The tetraspanin CD63 regulates ESCRT-independent and dependent endosomal sorting during melanogenesis. *Dev. Cell* 21, 708–721 (2011).
109. Booth, A. M. et al. Exosomes and HIV Gag bud from endosome-like domains of the T cell plasma membrane. *J. Cell Biol.* 172, 923–935 (2006).

110. Piper, R. C. & Katzmann, D. J. Biogenesis and Function of Multivesicular Bodies. *Annu. Rev. Cell Dev. Biol.* 23, 519–547 (2007).
111. Yáñez-Mó, M. et al. Biological properties of extracellular vesicles and their physiological functions. *J. Extracell. Vesicles* 4, 10.3402/jev.v4.27066 (2015).
112. Pap, E., Pállinger, E., Pásztói, M. & Falus, A. Highlights of a new type of intercellular communication: microvesicle-based information transfer. *Inflamm. Res. Off. J. Eur. Histamine Res. Soc. AI* 58, 1–8 (2009).
113. Bretscher, M. S. Asymmetrical lipid bilayer structure for biological membranes. *Nature. New Biol.* 236, 11–12 (1972).
114. Piccin, A., Murphy, W. G. & Smith, O. P. Circulating microparticles: pathophysiology and clinical implications. *Blood Rev.* 21, 157–171 (2007).
115. Hankins, H. M., Baldrige, R. D., Xu, P. & Graham, T. R. Role of flippases, scramblases, and transfer proteins in phosphatidylserine subcellular distribution. *Traffic Cph. Den.* 16, 35–47 (2015).
116. Nagata, S., Suzuki, J., Segawa, K. & Fujii, T. Exposure of phosphatidylserine on the cell surface. *Cell Death Differ.* 23, 952–961 (2016).
117. Raucher, D. et al. Phosphatidylinositol 4,5-Bisphosphate Functions as a Second Messenger that Regulates Cytoskeleton–Plasma Membrane Adhesion. *Cell* 100, 221–228 (2000).
118. Niebuhr, K. et al. Conversion of PtdIns(4,5)P₂ into PtdIns(5)P by the *S. flexneri* effector IpgD reorganizes host cell morphology. *EMBO J.* 21, 5069–5078 (2002).
119. Flaumenhaft, R. Formation and fate of platelet microparticles. *Blood Cells. Mol. Dis.* 36, 182–187 (2006).
120. Nebl, T., Oh, S. W. & Luna, E. J. Membrane cytoskeleton: PIP₂ pulls the strings. *Curr. Biol.* 10, R351–R354 (2000).

121. Wang, T. et al. Hypoxia-inducible factors and RAB22A mediate formation of microvesicles that stimulate breast cancer invasion and metastasis. *Proc. Natl. Acad. Sci. U. S. A.* 111, E3234–E3242 (2014).
122. Muralidharan-Chari, V. et al. ARF6-regulated shedding of tumor cell-derived plasma membrane microvesicles. *Curr. Biol.* CB 19, 1875–1885 (2009).
123. Sedgwick, A. E., Clancy, J. W., Olivia Balmert, M. & D'Souza-Schorey, C. Extracellular microvesicles and invadopodia mediate non-overlapping modes of tumor cell invasion. *Sci. Rep.* 5, 14748 (2015).
124. Li, B., Antonyak, M. A., Zhang, J. & Cerione, R. A. RhoA triggers a specific signaling pathway that generates transforming microvesicles in cancer cells. *Oncogene* 31, 4740–4749 (2012).
125. Taylor, J., Azimi, I., Monteith, G. & Bebawy, M. Ca²⁺ mediates extracellular vesicle biogenesis through alternate pathways in malignancy. *J. Extracell. Vesicles* 9, 1734326 (2020).
126. Perrin, B. J., Amann, K. J. & Huttenlocher, A. Proteolysis of cortactin by calpain regulates membrane protrusion during cell migration. *Mol. Biol. Cell* 17, 239–250 (2006).
127. Storr, S. J., Carragher, N. O., Frame, M. C., Parr, T. & Martin, S. G. The calpain system and cancer. *Nat. Rev. Cancer* 11, 364–374 (2011).
128. Crivelli, S. M. et al. Function of ceramide transfer protein for biogenesis and sphingolipid composition of extracellular vesicles. *J. Extracell. Vesicles* 11, e12233 (2022).
129. Kowal, J. et al. Proteomic comparison defines novel markers to characterize heterogeneous populations of extracellular vesicle subtypes. *Proc. Natl. Acad. Sci.* 113, E968–E977 (2016).

130. Crescitelli, R. et al. Distinct RNA profiles in subpopulations of extracellular vesicles: apoptotic bodies, microvesicles and exosomes. *J. Extracell. Vesicles* 2, 10.3402/jev.v2i0.20677 (2013).
131. Chen, S. et al. Lipidomic characterization of extracellular vesicles in human serum. *J. Circ. Biomark.* 8, 1849454419879848 (2019).
132. Logozzi, M. et al. High levels of exosomes expressing CD63 and caveolin-1 in plasma of melanoma patients. *PloS One* 4, e5219 (2009).
133. Kharaziha, P., Ceder, S., Li, Q. & Panaretakis, T. Tumor cell-derived exosomes: a message in a bottle. *Biochim. Biophys. Acta* 1826, 103–111 (2012).
134. Balaj, L. et al. Tumour microvesicles contain retrotransposon elements and amplified oncogene sequences. *Nat. Commun.* 2, 180 (2011).
135. Jong, O. G. de et al. Cellular stress conditions are reflected in the protein and RNA content of endothelial cell-derived exosomes. *J. Extracell. Vesicles* 1, 10.3402/jev.v1i0.18396 (2012).
136. Kilpinen, L. et al. Extracellular membrane vesicles from umbilical cord blood-derived MSC protect against ischemic acute kidney injury, a feature that is lost after inflammatory conditioning. *J. Extracell. Vesicles* 2, 10.3402/jev.v2i0.21927 (2013).
137. Wang, J., Pendurthi, U. R. & Rao, L. V. M. Sphingomyelin encrypts tissue factor: ATP-induced activation of A-SMase leads to tissue factor decryption and microvesicle shedding. *Blood Adv.* 1, 849–862 (2017).
138. Chen, T., Guo, J., Yang, M., Zhu, X. & Cao, X. Chemokine-Containing Exosomes Are Released from Heat-Stressed Tumor Cells via Lipid Raft-Dependent Pathway and Act as Efficient Tumor Vaccine. *J. Immunol.* 186, 2219–2228 (2011).

139. Montecalvo, A. et al. Mechanism of transfer of functional microRNAs between mouse dendritic cells via exosomes. *Blood* 119, 756 (2011).
140. Park, J. E. et al. Hypoxic Tumor Cell Modulates Its Microenvironment to Enhance Angiogenic and Metastatic Potential by Secretion of Proteins and Exosomes. *Mol. Cell. Proteomics MCP* 9, 1085 (2010).
141. Kim, D. et al. EV-Ident: Identifying Tumor-Specific Extracellular Vesicles by Size Fractionation and Single-Vesicle Analysis. *Anal. Chem.* 92, 6010–6018 (2020).
142. Patel, D. B. et al. Impact of cell culture parameters on production and vascularization bioactivity of mesenchymal stem cell-derived extracellular vesicles. *Bioeng. Transl. Med.* 2, 170–179 (2017).
143. Chen, Q., Takada, R., Noda, C., Kobayashi, S. & Takada, S. Different populations of Wnt-containing vesicles are individually released from polarized epithelial cells. *Sci. Rep.* 6, 35562 (2016).
144. Skotland, T., Sandvig, K. & Llorente, A. Lipids in exosomes: Current knowledge and the way forward. *Prog. Lipid Res.* 66, 30–41 (2017).
145. Skotland, T., Sagini, K., Sandvig, K. & Llorente, A. An emerging focus on lipids in extracellular vesicles. *Adv. Drug Deliv. Rev.* 159, 308–321 (2020).
146. Subra, C., Laulagnier, K., Perret, B. & Record, M. Exosome lipidomics unravels lipid sorting at the level of multivesicular bodies. *Biochimie* 89, 205–212 (2007).
147. Fitzner, D. et al. Selective transfer of exosomes from oligodendrocytes to microglia by macropinocytosis. *J. Cell Sci.* 124, 447–458 (2011).
148. Laulagnier, K. et al. Mast cell- and dendritic cell-derived exosomes display a specific lipid composition and an unusual membrane organization. *Biochem. J.* 380, 161–171 (2004).

149. Parolini, I. et al. Microenvironmental pH is a key factor for exosome traffic in tumor cells. *J. Biol. Chem.* 284, 34211–34222 (2009).
150. Wubbolts, R. et al. Proteomic and biochemical analyses of human B cell-derived exosomes. Potential implications for their function and multivesicular body formation. *J. Biol. Chem.* 278, 10963–10972 (2003).
151. Chernomordik, L. V. & Kozlov, M. M. Protein-lipid interplay in fusion and fission of biological membranes. *Annu. Rev. Biochem.* 72, 175–207 (2003).
152. Subra, C. et al. Exosomes account for vesicle-mediated transcellular transport of activatable phospholipases and prostaglandins. *J. Lipid Res.* 51, 2105–2120 (2010).
153. Osteikoetxea, X. et al. Differential detergent sensitivity of extracellular vesicle subpopulations. *Org. Biomol. Chem.* 13, 9775–9782 (2015).
154. Beloribi, S. et al. Exosomal Lipids Impact Notch Signaling and Induce Death of Human Pancreatic Tumoral SOJ-6 Cells. *PLOS ONE* 7, e47480 (2012).
155. Beloribi-Djefafia, S., Siret, C. & Lombardo, D. Exosomal lipids induce human pancreatic tumoral MiaPaCa-2 cells resistance through the CXCR4-SDF-1 α signaling axis. *Oncoscience* 2, 15–30 (2014).
156. Record, M., Silvente-Poirot, S., Poirot, M. & Wakelam, M. J. O. Extracellular vesicles: lipids as key components of their biogenesis and functions. *J. Lipid Res.* 59, 1316–1324 (2018).
157. Van Niel, G., D’Angelo, G. & Raposo, G. Shedding light on the cell biology of extracellular vesicles. *Nat. Rev. Mol. Cell Biol.* 19, 213–228 (2018).
158. Maas, S. L. N., Breakefield, X. O. & Weaver, A. M. Extracellular Vesicles: Unique Intercellular Delivery Vehicles. *Trends Cell Biol.* 27, 172–188 (2017).

159. Colombo, M. et al. Analysis of ESCRT functions in exosome biogenesis, composition and secretion highlights the heterogeneity of extracellular vesicles. *J. Cell Sci.* 126, 5553–5565 (2013).
160. Raimondo, F., Morosi, L., Chinello, C., Magni, F. & Pitto, M. Advances in membranous vesicle and exosome proteomics improving biological understanding and biomarker discovery. *Proteomics* 11, 709–720 (2011).
161. Choi, D.-S. et al. The protein interaction network of extracellular vesicles derived from human colorectal cancer cells. *J. Proteome Res.* 11, 1144–1151 (2012).
162. Andre, F. et al. Malignant effusions and immunogenic tumour-derived exosomes. *Lancet Lond. Engl.* 360, 295–305 (2002).
163. Runz, S. et al. Malignant ascites-derived exosomes of ovarian carcinoma patients contain CD24 and EpCAM. *Gynecol. Oncol.* 107, 563–571 (2007).
164. Williams, C. et al. Glycosylation of extracellular vesicles: current knowledge, tools and clinical perspectives. *J. Extracell. Vesicles* 7, 1442985 (2018).
165. Melo, S. A. et al. Glypican-1 identifies cancer exosomes and detects early pancreatic cancer. *Nature* 523, 177–182 (2015).
166. Chen, G. et al. Exosomal PD-L1 contributes to immunosuppression and is associated with anti-PD-1 response. *Nature* 560, 382–386 (2018).
167. Yu, Z. et al. Untouched isolation enables targeted functional analysis of tumour-cell-derived extracellular vesicles from tumour tissues. *J. Extracell. Vesicles* 11, e12214 (2022).
168. Al-Nedawi, K. et al. Intercellular transfer of the oncogenic receptor EGFRvIII by microvesicles derived from tumour cells. *Nat. Cell Biol.* 10, 619–624 (2008).

169. Corcoran, C. et al. Docetaxel-Resistance in Prostate Cancer: Evaluating Associated Phenotypic Changes and Potential for Resistance Transfer via Exosomes. *PLOS ONE* 7, e50999 (2012).
170. Muntasell, A., Berger, A. C. & Roche, P. A. T cell-induced secretion of MHC class II-peptide complexes on B cell exosomes. *EMBO J.* 26, 4263–4272 (2007).
171. Reale, A., Khong, T. & Spencer, A. Extracellular Vesicles and Their Roles in the Tumor Immune Microenvironment. *J. Clin. Med.* 11, 6892 (2022).
172. Buzas, E. I. The roles of extracellular vesicles in the immune system. *Nat. Rev. Immunol.* 23, 236–250 (2023).
173. O’Brien, K., Breyne, K., Ughetto, S., Laurent, L. C. & Breakefield, X. O. RNA delivery by extracellular vesicles in mammalian cells and its applications. *Nat. Rev. Mol. Cell Biol.* 21, 585–606 (2020).
174. Li, J. et al. Multiomics-based study of amniotic fluid small extracellular vesicles identified Moesin as a biomarker for antenatal hydronephrosis. *Clin. Transl. Med.* 13, e1360 (2023).
175. Taylor, D. D. & Gercel-Taylor, C. MicroRNA signatures of tumor-derived exosomes as diagnostic biomarkers of ovarian cancer. *Gynecol. Oncol.* 110, 13–21 (2008).
176. Zhou, J. et al. Urinary microRNA-30a-5p is a potential biomarker for ovarian serous adenocarcinoma. *Oncol. Rep.* 33, 2915–2923 (2015).
177. Rodríguez, M. et al. Identification of non-invasive miRNAs biomarkers for prostate cancer by deep sequencing analysis of urinary exosomes. *Mol. Cancer* 16, 156 (2017).
178. Bryant, R. J. et al. Changes in circulating microRNA levels associated with prostate cancer. *Br. J. Cancer* 106, 768–774 (2012).
179. Huang, X. et al. Exosomal miR-1290 and miR-375 as prognostic markers in castration-resistant prostate cancer. *Eur. Urol.* 67, 33–41 (2015).

180. Selmaj, I. et al. Global exosome transcriptome profiling reveals biomarkers for multiple sclerosis. *Ann. Neurol.* 81, 703–717 (2017).
181. Camussi, G., Deregibus, M. C., Bruno, S., Cantaluppi, V. & Biancone, L. Exosomes/microvesicles as a mechanism of cell-to-cell communication. *Kidney Int.* 78, 838–848 (2010).
182. Kosaka, N. et al. Secretory mechanisms and intercellular transfer of microRNAs in living cells. *J. Biol. Chem.* 285, 17442–17452 (2010).
183. Pegtel, D. M. et al. Functional delivery of viral miRNAs via exosomes. *Proc. Natl. Acad. Sci. U. S. A.* 107, 6328–6333 (2010).
184. Okoye, I. S. et al. MicroRNA-Containing T-Regulatory-Cell-Derived Exosomes Suppress Pathogenic T Helper 1 Cells. *Immunity* 41, 89–103 (2014).
185. Tung, S. L. et al. Regulatory T cell-derived extracellular vesicles modify dendritic cell function. *Sci. Rep.* 8, 6065 (2018).
186. Vignard, V. et al. MicroRNAs in Tumor Exosomes Drive Immune Escape in Melanoma. *Cancer Immunol. Res.* 8, 255–267 (2020).
187. Peng, M. et al. Tumour-derived small extracellular vesicles suppress CD8⁺ T cell immune function by inhibiting SLC6A8-mediated creatine import in NPM1-mutated acute myeloid leukaemia. *J. Extracell. Vesicles* 10, e12168 (2021).
188. Fabbri, M. et al. MicroRNAs bind to Toll-like receptors to induce prometastatic inflammatory response. *Proc. Natl. Acad. Sci. U. S. A.* 109, E2110-2116 (2012).
189. Lehmann, S. M. et al. An unconventional role for miRNA: let-7 activates Toll-like receptor 7 and causes neurodegeneration. *Nat. Neurosci.* 15, 827–835 (2012).
190. Kb, C. et al. Exosome-mediated transfer of microRNAs within the tumor microenvironment and neuroblastoma resistance to chemotherapy. *J. Natl. Cancer Inst.* 107, (2015).

191. Fabbiano, F. et al. RNA packaging into extracellular vesicles: An orchestra of RNA-binding proteins? *J. Extracell. Vesicles* 10, e12043 (2020).
192. Villarroya-Beltri, C. et al. Sumoylated hnRNPA2B1 controls the sorting of miRNAs into exosomes through binding to specific motifs. *Nat. Commun.* 4, 2980 (2013).
193. Li, C. et al. hnRNPA2B1-Mediated Extracellular Vesicles Sorting of miR-122-5p Potentially Promotes Lung Cancer Progression. *Int. J. Mol. Sci.* 22, 12866 (2021).
194. Kossinova, O. A. et al. Cytosolic YB-1 and NSUN2 are the only proteins recognizing specific motifs present in mRNAs enriched in exosomes. *Biochim. Biophys. Acta BBA - Proteins Proteomics* 1865, 664–673 (2017).
195. Shurtleff, M. J. et al. Broad role for YBX1 in defining the small noncoding RNA composition of exosomes. *Proc. Natl. Acad. Sci. U. S. A.* 114, E8987 (2017).
196. Lin, F. et al. YBX-1 mediated sorting of miR-133 into hypoxia/reoxygenation-induced EPC-derived exosomes to increase fibroblast angiogenesis and MEndoT. *Stem Cell Res. Ther.* 10, 263 (2019).
197. Fernando, M. R., Jiang, C., Krzyzanowski, G. D. & Ryan, W. L. New evidence that a large proportion of human blood plasma cell-free DNA is localized in exosomes. *PloS One* 12, e0183915 (2017).
198. Guescini, M., Genedani, S., Stocchi, V. & Agnati, L. F. Astrocytes and Glioblastoma cells release exosomes carrying mtDNA. *J. Neural Transm.* 117, 1–4 (2010).
199. Kahlert, C. et al. Identification of Double-stranded Genomic DNA Spanning All Chromosomes with Mutated KRAS and p53 DNA in the Serum Exosomes of Patients with Pancreatic Cancer. *J. Biol. Chem.* 289, 3869–3875 (2014).
200. Takahashi, A. et al. Exosomes maintain cellular homeostasis by excreting harmful DNA from cells. *Nat. Commun.* 8, 15287 (2017).

201. Torralba, D. et al. Priming of dendritic cells by DNA-containing extracellular vesicles from activated T cells through antigen-driven contacts. *Nat. Commun.* 9, 2658 (2018).
202. Szczesny, B. et al. Mitochondrial DNA damage and subsequent activation of Z-DNA binding protein 1 links oxidative stress to inflammation in epithelial cells. *Sci. Rep.* 8, 914 (2018).
203. Lazo, S. et al. Mitochondrial DNA in extracellular vesicles declines with age. *Aging Cell* 20, e13283 (2021).
204. Shetty, A. K. & Upadhyya, R. Extracellular Vesicles in Health and Disease. *Aging Dis.* 12, 1358 (2021).
205. Bebelman, M. P., Janssen, E., Pegtel, D. M. & Crudden, C. The forces driving cancer extracellular vesicle secretion. *Neoplasia N. Y. N* 23, 149 (2020).
206. Kirkham, A. M. et al. MSC-Derived Extracellular Vesicles in Preclinical Animal Models of Bone Injury: A Systematic Review and Meta-Analysis. *Stem Cell Rev. Rep.* 18, 1054–1066 (2022).
207. Maring, J. A. et al. Cardiac Progenitor Cell–Derived Extracellular Vesicles Reduce Infarct Size and Associate with Increased Cardiovascular Cell Proliferation. *J Cardiovasc. Transl. Res.* 12, 5 (2018).
208. Escola, J. M. et al. Selective enrichment of tetraspan proteins on the internal vesicles of multivesicular endosomes and on exosomes secreted by human B-lymphocytes. *J. Biol. Chem.* 273, 20121–20127 (1998).
209. Buschow, S. I. et al. MHC class II-associated proteins in B-cell exosomes and potential functional implications for exosome biogenesis. *Immunol. Cell Biol.* 88, 851–856 (2010).
210. Baietti, M. F. et al. Syndecan–syntenin–ALIX regulates the biogenesis of exosomes. *Nat. Cell Biol.* 14, 677–685 (2012).

211. Pols, M. S. & Klumperman, J. Trafficking and function of the tetraspanin CD63. *Exp. Cell Res.* 315, 1584–1592 (2009).
212. L veill , C., AL-Daccak, R. & Mourad, W. CD20 is physically and functionally coupled to MHC class II and CD40 on human B cell lines. *Eur. J. Immunol.* 29, 65–74 (1999).
213. Polyak, M. J., Li, H., Shariat, N. & Deans, J. P. CD20 homo-oligomers physically associate with the B cell antigen receptor. Dissociation upon receptor engagement and recruitment of phosphoproteins and calmodulin-binding proteins. *J. Biol. Chem.* 283, 18545–18552 (2008).
214. Bubien, J. K., Zhou, L. J., Bell, P. D., Frizzell, R. A. & Tedder, T. F. Transfection of the CD20 cell surface molecule into ectopic cell types generates a Ca²⁺ conductance found constitutively in B lymphocytes. *J. Cell Biol.* 121, 1121–1132 (1993).
215. Clayton, A. et al. Analysis of antigen presenting cell derived exosomes, based on immunomagnetic isolation and flow cytometry. *J. Immunol. Methods* 247, 163–174 (2001).
216. Clayton, A., Turkes, A., Navabi, H., Mason, M. D. & Tabi, Z. Induction of heat shock proteins in B-cell exosomes. *J. Cell Sci.* 118, 3631–3638 (2005).
217. Clayton, A. et al. Adhesion and signaling by B cell-derived exosomes: the role of integrins. *FASEB J. Off. Publ. Fed. Am. Soc. Exp. Biol.* 18, 977–979 (2004).
218. Arita, S. et al. B cell activation regulates exosomal HLA production. *Eur. J. Immunol.* 38, 1423–1434 (2008).
219. Saunderson, S. C. et al. Induction of Exosome Release in Primary B Cells Stimulated via CD40 and the IL-4 Receptor. *J. Immunol.* 180, 8146–8152 (2008).
220. Riolland, P., Lankar, D., Raposo, G., Bonnerot, C. & Hubert, P. BCR-bound antigen is targeted to exosomes in human follicular lymphoma B-cells. *Biol. Cell* 98, 491–501 (2006).

221. Momen-Heravi, F., Bala, S., Bukong, T. & Szabo, G. Exosome-mediated delivery of functionally active miRNA-155 inhibitor to macrophages. *Nanomedicine Nanotechnol. Biol. Med.* 10, 1517–1527 (2014).
222. Liao, T.-L. et al. Rituximab May Cause Increased Hepatitis C Virus Viremia in Rheumatoid Arthritis Patients Through Declining Exosomal MicroRNA-155. *Arthritis Rheumatol. Hoboken NJ* 70, 1209–1219 (2018).
223. Yang, Z. et al. Plasma cells shape the mesenchymal identity of ovarian cancers through transfer of exosome-derived microRNAs. *Sci. Adv.* 7, eabb0737 (2021).
224. Saunderson, S. C., Dunn, A. C., Crocker, P. R. & McLellan, A. D. CD169 mediates the capture of exosomes in spleen and lymph node. *Blood* 123, 208–216 (2014).
225. Saunderson, S. C. & McLellan, A. D. Role of Lymphocyte Subsets in the Immune Response to Primary B Cell–Derived Exosomes. *J. Immunol.* 199, 2225–2235 (2017).
226. Denzer, K. et al. Follicular Dendritic Cells Carry MHC Class II-Expressing Microvesicles at Their Surface. *J. Immunol.* 165, 1259–1265 (2000).
227. Zumaquero, E. et al. Exosomes from human lymphoblastoid B cells express enzymatically active CD38 that is associated with signaling complexes containing CD81, Hsc-70 and Lyn. *Exp. Cell Res.* 316, 2692–2706 (2010).
228. Zhang, F. et al. Specific Decrease in B-Cell-Derived Extracellular Vesicles Enhances Post-Chemotherapeutic CD8⁺ T Cell Responses. *Immunity* 50, 738–750.e7 (2019).
229. Lundy, S. K., Klinker, M. W. & Fox, D. A. Killer B Lymphocytes and Their Fas Ligand Positive Exosomes as Inducers of Immune Tolerance. *Front. Immunol.* 6, 122 (2015).
230. Papp, K. et al. B lymphocytes and macrophages release cell membrane deposited C3-fragments on exosomes with T cell response-enhancing capacity. *Mol. Immunol.* 45, 2343–2351 (2008).

231. Mensah, F. F. K. et al. CD24 Expression and B Cell Maturation Shows a Novel Link With Energy Metabolism: Potential Implications for Patients With Myalgic Encephalomyelitis/Chronic Fatigue Syndrome. *Front. Immunol.* 9, 1–14 (2018).
232. Springer, T., Galfrè, G., Secher, D. S. & Milstein, C. Monoclonal xenogeneic antibodies to murine cell surface antigens: identification of novel leukocyte differentiation antigens. *Eur. J. Immunol.* 8, 539–551 (1978).
233. Alterman, L. A., Crispe, I. N. & Kinnon, C. Characterization of the murine heat-stable antigen: An hematolymphoid differentiation antigen defined by the J11d, M1/69 and B2A2 antibodies. *Eur. J. Immunol.* 20, 1597–1602 (1990).
234. Tan, Y., Zhao, M., Xiang, B., Chang, C. & Lu, Q. CD24: from a Hematopoietic Differentiation Antigen to a Genetic Risk Factor for Multiple Autoimmune Diseases. *Clin. Rev. Allergy Immunol.* 50, 70–83 (2016).
235. Huang, L., Lv, W. & Zhao, X. CD24 as a Molecular Marker in Ovarian Cancer: A Literature Review. *Cancer Transl. Med.* 2, 29 (2016).
236. Fang, X., Zheng, P., Tang, J. & Liu, Y. CD24: from A to Z. *Cell. Mol. Immunol.* 7, 100–103 (2010).
237. Daniel T., G., Vishal, M., Niko P., B. & Jan, P. The CD24 surface antigen in neural development and disease. *Neurobiol. Dis.* 99, 133–144 (2017).
238. Ayre, D. C. et al. Analysis of the structure, evolution, and expression of CD24, an important regulator of cell fate. *Gene* 590, 324–337 (2016).
239. Ayre, D. C. & Christian, S. L. CD24: A Rheostat That Modulates Cell Surface Receptor Signaling of Diverse Receptors. *Front. Cell Dev. Biol.* 4, 1–6 (2016).
240. Chen, G.-Y., Tang, J., Zheng, P. & Liu, Y. CD24 and Siglec-10 Selectively Repress Tissue Damage–Induced Immune Responses. *Science* 323, 1722–1725 (2009).

241. Liu, Y., Chen, G.-Y. & Zheng, P. CD24-Siglec G/10 discriminates danger- from pathogen-associated molecular patterns. *Trends Immunol.* 30, 557–561 (2009).
242. Ayre, D. C. et al. Dynamic regulation of CD24 expression and release of CD24-containing microvesicles in immature B cells in response to CD24 engagement. *Immunology* 146, 217–233 (2015).
243. Israel, E. et al. Expression of CD24 on CD19- CD79a+ early B-cell progenitors in human bone marrow. *Cell. Immunol.* 236, 171–178 (2005).
244. Hough, M. R. et al. Reduction of early B lymphocyte precursors in transgenic mice overexpressing the murine heat-stable antigen. *J. Immunol. Baltim. Md 1950* 156, 479–488 (1996).
245. Yin, S.-S. & Gao, F.-H. Molecular Mechanism of Tumor Cell Immune Escape Mediated by CD24/Siglec-10. *Front. Immunol.* 11, 1324 (2020).
246. Daoud, G., Rassart, É., Masse, A. & Lafond, J. Src family kinases play multiple roles in differentiation of trophoblasts from human term placenta. *J. Physiol.* 571, 537–553 (2006).
247. Sammar, M., Gulbins, E., Hilbert, K., Lang, F. & Altevogt, P. Mouse CD24 as a Signaling Molecule for Integrin-Mediated Cell Binding: Functional and Physical Association with src-Kinases. *Biochem. Biophys. Res. Commun.* 234, 330–334 (1997).
248. Zarn, J. A., Zimmermann, S. M., Pass, M. K., Waibel, R. & Stahel, R. A. Association of CD24 with the Kinase c-fgr in a Small Cell Lung Cancer Cell Line and with the Kinase lyn in an Erythroleukemia Cell Line. *Biochem. Biophys. Res. Commun.* 225, 384–391 (1996).
249. Suzuki, T. et al. CD24 Induces Apoptosis in Human B Cells Via the Glycolipid-Enriched Membrane Domains/Rafts-Mediated Signaling System. *J. Immunol.* 166, 5567–5577 (2001).

250. Baumann, P. et al. CD24 interacts with and promotes the activity of c-src within lipid rafts in breast cancer cells, thereby increasing integrin-dependent adhesion. *Cell. Mol. Life Sci.* 69, 435–448 (2012).
251. Huang, J. L., Oshi, M., Endo, I. & Takabe, K. Clinical relevance of stem cell surface markers CD133, CD24, and CD44 in colorectal cancer. *Am. J. Cancer Res.* 11, 5141–5154 (2021).
252. Fokra, A. et al. CD24 Induces the Activation of β -Catenin in Intestinal Tumorigenesis. *J. Cancer Sci Ther* 8, 135–142 (2016).
253. Wang, R. et al. Notch and Wnt/ β -catenin signaling pathway play important roles in activating liver cancer stem cells. *Oncotarget* 7, 5754–5768 (2016).
254. Pannuti, A. et al. Targeting Notch to target cancer stem cells. *Clin. Cancer Res. Off. J. Am. Assoc. Cancer Res.* 16, 3141–3152 (2010).
255. Harrison, H. et al. Regulation of breast cancer stem cell activity by signaling through the Notch4 receptor. *Cancer Res.* 70, 709–718 (2010).
256. Wan, X. et al. CD24 promotes HCC progression via triggering Notch-related EMT and modulation of tumor microenvironment. *Tumour Biol. J. Int. Soc. Oncodevelopmental Biol. Med.* 37, 6073–6084 (2016).
257. Lim, J., Lee, K., Shim, J. & Shin, I. CD24 regulates stemness and the epithelial to mesenchymal transition through modulation of Notch1 mRNA stability by p38MAPK. *Arch. Biochem. Biophys.* 558, 120–126 (2014).
258. Agrawal, S. et al. CD24 expression is an independent prognostic marker in cholangiocarcinoma. *J. Gastrointest. Surg. Off. J. Soc. Surg. Aliment. Tract* 11, 445–451 (2007).

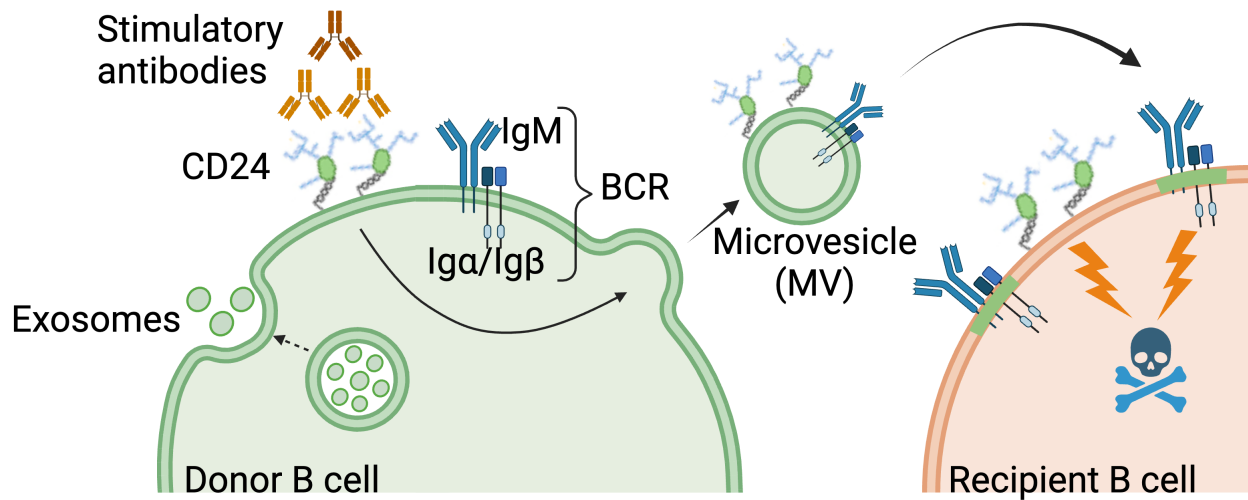
259. Wang, W. et al. CD24-dependent MAPK pathway activation is required for colorectal cancer cell proliferation. *Cancer Sci.* 101, 112–119 (2010).
260. Nakamura, K. et al. CD24 expression is a marker for predicting clinical outcome and regulates the epithelial-mesenchymal transition in ovarian cancer via both the Akt and ERK pathways. *Oncol. Rep.* 37, 3189–3200 (2017).
261. Chen, J. et al. PI3K/Akt/mTOR pathway dual inhibitor BEZ235 suppresses the stemness of colon cancer stem cells. *Clin. Exp. Pharmacol. Physiol.* 42, 1317–1326 (2015).
262. Bretz, N. P. et al. CD24 controls Src/STAT3 activity in human tumors. *Cell. Mol. Life Sci. CMLS* 69, 3863–3879 (2012).
263. Chappel, M. S. et al. Cross-linking the murine heat-stable antigen induces apoptosis in B cell precursors and suppresses the anti-CD40-induced proliferation of mature resting B lymphocytes. *J. Exp. Med.* 184, 1639–1649 (1996).
264. Taguchi, T. et al. Pre-B Cell Antigen Receptor-Mediated Signal Inhibits CD24-Induced Apoptosis in Human Pre-B Cells¹. *J. Immunol.* 170, 252–260 (2003).
265. Fischer, G. F., Majdic, O., Gadd, S. & Knapp, W. Signal transduction in lymphocytic and myeloid cells via CD24, a new member of phosphoinositol-anchored membrane molecules. *J. Immunol. Baltim. Md* 1950 144, 638–641 (1990).
266. Ayre, D. C. et al. CD24 induces changes to the surface receptors of B cell microvesicles with variable effects on their RNA and protein cargo. *Sci. Rep.* 7, 8642 (2017).

Chapter 2: CD24 and IgM stimulation of B cells triggers transfer of functional B cell receptor to B cell recipients via extracellular vesicles

2.1. Abstract

Extracellular vesicles (EVs) are membrane-encapsulated nanoparticles that carry bioactive cargo, including proteins, lipids, and nucleic acids. Once taken up by target cells, EVs can modify the physiology of the recipient cells. In past studies, we reported that engagement of the glycosphosphatidylinositol-anchored receptor CD24 on B lymphocytes (B cells) causes the release of EVs. However, a potential function for these EVs was not clear. Thus, we investigated whether EVs derived from CD24 or IgM-stimulated donor WEHI-231 murine B cells can transfer functional cargo to recipient cells. We employed a model system where donor cells expressing palmitoylated GFP (WEHI-231-GFP) were co-cultured, after stimulation, with recipient cells lacking either IgM (WEHI-303 murine B cells) or CD24 (CD24 knock-out (CD24KO) mouse bone marrow B cells). Uptake of lipid associated GFP, IgM, or CD24 by labeled recipient cells was analyzed by flow cytometry. We found that stimulation of either CD24 or IgM on the donor cells caused the transfer of lipids, CD24, and IgM to recipient cells. Importantly, we found that the transferred receptors are functional in recipient cells, thus endowing recipient cells with a second BCR or sensitivity to anti-CD24-induced apoptosis. In the case of the BCR, we found that EVs were conclusively involved in this transfer, while in the case in the CD24 the involvement of EVs is suggested. Overall, these data show that extracellular signals received by one cell can change the sensitivity of neighboring cells to the same or different stimuli, which may impact B cell development or activation.

2.2. Graphical abstract



CD24 stimulation on donor B cells caused the transfer of extracellular vesicles carrying lipids and functional receptors to B cell recipients, thus endowing recipient cells with a second BCR or sensitivity to anti-CD24-induced apoptosis. Created with BioRender.com.

2.3. Introduction

Extracellular vesicles (EVs) are released from all mammalian cells that have been examined¹. These vesicles are a heterogeneous group of phospholipid bilayer-enclosed particles that are classified based on their release pathway and size². Exosomes are the smallest EVs at 30 to 150 nm in diameter and are released through exocytosis from multivesicular bodies³⁻⁵. Slightly larger than exosomes, microvesicles (MVs) or ectosomes are formed by outward budding from the cell's plasma membrane and are 100 nm to 1 μ m in size^{6,7}. The largest type of EVs are apoptotic bodies that are generated by cells undergoing the final stages of apoptosis and can range from 1 μ m to 5 μ m⁸. According to a new study, apoptotic exosome-like vesicles, or ApoExos, are similar in size to exosomes but are produced by different biogenesis processes and have different markers. ApoExos lack traditional exosome markers such tetraspanins (CD9, CD63, and CD81), but expressing others like syntenin and TCTP⁴.

EVs are critical mediators of cell-to-cell communication during normal physiological and pathological processes⁹. EVs contain cargo that reflect the cell of origin and which can be transferred to recipient cells¹⁰⁻¹². These cargoes include lipids, proteins, and genetic material such as mRNA, miRNA, and DNA. Once taken up by recipient cells, EVs can alter the biological functions of target cells¹³. For example, the first report of EVs found that B lymphocytes release EVs carrying peptide-MHCII complexes that can directly activate CD4+ T cells¹¹. Apoptotic bodies have a powerful effect on recipient cells, which are both professional phagocytes and nonprofessional neighboring cells, just like MVs and exosomes do. However, the target cells of apoptotic bodies are less diverse than those of MVs and exosomes¹⁴.

The visualization of EVs is essential for understanding EV biology. EVs can be visualized directly via fluorescent chemical labelling using lipophilic dyes such as PKH26 or PKH67, which label cell membranes by the insertion of their aliphatic chains into the lipid bilayer. Fluorescence

microscopy and flow cytometry can then be used to detect EV uptake, as has been done for breast cancer cells, macrophages, dendritic cells, endothelial and myocardial cells¹⁵. However, PKH-labelled EVs may be degraded and/or recycled in vivo. In addition, PKH dyes can form micellar structures identical in size to EVs and can be retained in association with other lipid entities for long periods. Therefore, inaccurate spatiotemporal assessment of EV fate can be inferred based on the use of these dyes¹⁶. In contrast, fluorescent proteins such as GFP and tandem dimer Tomato (tdTomato) that are fused to a palmitoylation signal (palm-GFP and palm-tdTomato) have been reported to label all membrane-enclosed vesicles, including EVs¹⁷. This specific labeling allows tracking of EVs in culture for long periods of time in a more accurate manner than lipophilic dyes.

B lymphocytes (B cells) are critical components of the immune system. B cells are generated in the bone marrow from multi-potent hematopoietic stem cells that undergo maturation in discrete stages¹⁸. At each stage of B cell development, different cell surface receptors are used to identify each stage using either the Hardy fraction designators^{19,20} or established independent markers²¹. The primary driver of this maturation is the generation of the BCR, which is composed of the membrane-bound immunoglobulin IgM and two accessory molecules, Ig α and Ig β (CD79a and CD79b, respectively).

Of particular relevance for this study is CD24, also called heat stable antigen (HSA), which is highly expressed at the pro and pre-B cell stages²². CD24 is a lipid raft-localized glycosylphosphatidylinositol (GPI)-anchored membrane protein of 27 amino acids with extensive, but variable, N- and O-linked glycosylation^{23,24}. Several ligands have been identified for CD24, including P-, L-, and E-selectin, Sialic-acid-binding immunoglobulin-like lectin-G or Siglec 10, TAG-1, contactin, L1 cell adhesion molecule, and Neural cell adhesion molecule²⁵. However, the relevant CD24 ligand for bone marrow B cells is not known. Engaging CD24 on

pro- or pre- B cells with anti-CD24 antibodies leads to apoptosis and CD24 engagement in mature splenic B cells blocks CD40-induced proliferation^{26,27}. We have also found that antibody-mediated engagement of CD24 induces apoptosis in the immature murine WEHI-231 B cell line, demonstrating that this cell line models the CD24-mediated effects on developing B cells²⁸. Importantly, we found that engagement of CD24 increases the release of EVs into the extracellular environment^{28,29}. In addition, CD24-mediated stimulation promoted changes in the membrane protein composition of the secreted EVs²⁹.

Here, we tested the hypothesis that EVs released from anti-CD24- or anti-IgM- stimulated B cells can transfer functional receptors to recipient cells. We analyzed EV transfer by using cells that express palmitoylated fluorescence markers, which allows us to track EVs released from both donor and recipient cells. We visualized lipid transfer by tracking the transfer of palm-GFP or palm-tdTomato from donor to recipient cells. We visualized protein transfer by tracking the transfer of IgM from BCR-positive cells (WEHI-231) to BCR-negative cells (WEHI-303) and the transfer of CD24 from WEHI-231 cells to primary B cells isolated from CD24 knock-out (CD24KO) mice. We found that stimulation of either CD24 or IgM on donor cells resulted in the transfer of both CD24 and IgM to recipient cells. We found that both IgM and GFP are packaged into isolated EVs indicating that the transfer of lipid with transmembrane protein is most likely via EVs secreted by donor cells. To determine if the transferred receptors were functional, we assessed output from the newly transferred receptor on the recipient cells. We found that the transferred CD24 and IgM on the recipient cells were functional receptors that could initiate signaling and apoptosis in the recipient cells. These data suggest that stimulation of B cells could alter the responses of bystander cells via release of EVs.

2.4. Materials and Methods

2.4.1. Animal care

The Institutional Animal Care committee at Memorial University of Newfoundland approved all animal procedures (protocol 17-01-SC). C57BL/6N Cd24^{atm1PjIn} homozygous mice (CD24KO)³⁰⁻³² were a gift from Dr. Yang Liu (Center for Cancer & Immunology Research, Children's National Medical Center, Washington, DC).

2.4.2. Cell culture and transfection

All materials for cell culture were obtained from Life Technologies (Carlsbad, CA) unless otherwise indicated. Isolated bone marrow-derived immature B cells and cell lines were maintained in RPMI-1640 medium supplemented with 10% heat-inactivated fetal bovine serum, 1% antibiotic/antimycotic, 1% sodium pyruvate and 0.1% mercaptoethanol (complete media) at 37°C in a humidified 5% CO₂ atmosphere. WEHI-231 cells (ATCC) and WEHI-303.1.5 (WEHI-303)³³ were transfected with palm-GFP (WEHI-231-GFP) or palm-tdTomato (WEHI-303-tdTomato) lentiviral plasmids, generous gifts from Charles Lai, Institute of Atomic and Molecular Sciences, Taiwan¹⁷. Briefly, these were co-transfected with pCMV-VSV-G-M5 and pCMV- δ R8.91 (from Dorothee von Laer, Medical University of Innsbruck, Austria) into HEK293T cells (ATCC). Virus particles were collected at 12 h and 36 h post transfection and added to 12-well plates containing WEHI-231 or WEHI-303 cells, which were then centrifuged at 2000 rpm (750 x g) for 1 h at 21°C. Cells were cultured 48 h before enrichment by fluorescence-activated cell sorting. Cells were re-sorted regularly with the Beckman Coulter MoFlo Astrios EQ (Medical Laboratory Services, Memorial University) to maintain >90% fluorescently labelled cells (Supplemental Figure 2.1A).

2.4.3. Primary bone marrow B cell isolation

Femurs were removed from euthanized six to eight-week-old male or female CD24KO mice and bone marrow was flushed out with Quin saline (25mM NaHEPES, 125 mM NaCl, 5 mM KCl, 1 mM CaCl₂, 1mM Na₂HPO₄, 0.5 mM MgSO₄, 1 g/l glucose, 2 mM glutamine, 1 mM sodium pyruvate, 50 μM 2-mercaptoethanol, pH 7.2), using a 21-gauge needle. Cells were pooled from two mice and single-cell suspensions produced using a 100-μm nylon mesh. The EasySep Mouse B cell isolation kit (cat. no. 19854, StemCell Technologies) was used to enrich bone marrow isolates following the manufacturer's protocol. Primary bone marrow B cell purity was confirmed by flow cytometry to be > 80% B cells using anti-mouse CD19-Per-CP-Cy-5.5 (cat. no. 45-0193-82, eBioscience), IgM-APC/Cy7 (cat. no. 406515, Biolegend), CD45R (B220)-PE-Cy7 (cat. no. 25-0452-82, eBioscience) and CD24-PE (cat. no. 12-0242-82, eBioscience) antibodies. All analysis by flow cytometry was performed on the FACS Aria (BD Biosciences; Cold-ocean Deep Water Facility, Memorial University).

2.4.4. Cell stimulation

WEHI-231-GFP donor cells (5×10^5 cells/ml in 500 μl) were treated with stimulating antibodies as follows:

For stimulation of CD24, 10 μg/ml of functional grade primary monoclonal M1/69 rat anti-mouse CD24 antibody (16-0242-85, eBioscience) or 10 μg/ml matching primary isotype antibody (16-4031-85, eBioscience) were pre-incubated with 5 μg/ml goat anti-rat secondary antibody (112-005-003, Jackson ImmunoResearch) at a 2:1 ratio to ensure efficient cross-linking of primary antibody and that no excess secondary antibody was present. We have confirmed that isotype pre-incubated with second antibody does not bind to cells²⁸. After stimulation for 15 min at 37°C in complete media, donor cells were centrifuged at 400 x g for 5 min to remove antibody-

containing media and then resuspended in complete media followed by co-culture with recipient cells, WEHI-303-tdTomato (5×10^5 cells in 500 μ l), giving a final density of 10^6 cells/ml in 1 ml, at 37°C in a humidified incubator containing 5% CO₂ for a total of 24 h. The co-cultured cells were analysed by flow cytometry. Cleared supernatant (cSN) was collected from WEHI-231-GFP cells, stimulated as above for 1 h or 2 h, after centrifugation at 500 x g for 5 min, then 2,000 x g for 5 min. cSN was added to recipient cells as indicated.

When primary bone marrow B cells were used as recipients, they were pre-stained with proliferation dye eFluor 670 (cat. no. 65-0840, eBioscience) following the manufacturer's protocol and then co-cultured with WEHI-231-GFP cells as indicated. eFluor 670 positivity was determined by flow cytometry (Supplemental Figure 2.2G).

To assess anti-CD24-induced apoptosis in primary bone marrow B cells, WEHI-231-GFP and primary bone marrow B cells were plated at a density of 5×10^5 cells each in 500 μ L complete medium. The cultured cells were mixed 1:1, giving a final density of 10^6 cells/ml in 1 ml, and were treated with antibody as indicated for 24 h.

To stimulate IgM, WEHI-231-GFP cells were treated with 10 μ g/ml anti-mouse IgM (115-005-020, Jackson ImmunoResearch) or left untreated for 1 or 2 h, then centrifuged at 400 x g for 5 min to remove antibody-containing media and then resuspended in complete media followed by co-culture with recipient cells CD24KO B cells (5×10^5 cells in 500 μ l), giving a final density of 10^6 cells/ml in 1 ml, at 37°C in a humidified incubator containing 5% CO₂ for a total of 24 h. The co-cultured cells were analysed by flow cytometry.

To analyze anti-IgM-induced apoptosis of WEHI-303-tdTomato cells, WEHI-231-GFP and WEHI-303-tdTomato cells were plated at a density of 5×10^5 cells each in 500 μ L complete medium. The cultured cells were mixed 1:1, giving a final density of 10^6 cells/ml in 1 ml, and

were treated with 10 µg/ml anti-mouse IgM (115-005-020, Jackson ImmunoResearch) or left untreated for 24 h.

For stimulation of CD40, WEHI-231-GFP cells were treated with 10 µg/ml anti-mouse CD40 (16-0401-82, eBioscience) or 10 µg/ml isotype (16-4321-82, eBioscience) for 2 h, or left untreated, then centrifuged at 400 x g for 5 min to remove antibody-containing media and then resuspended in complete media followed by co-culture with recipient cells WEHI-303-tdTomato as above.

To stimulate CD48, WEHI-231-GFP were stimulated with 10 µg/ml anti-mouse CD48 (cat. no. 103402, Biolegend) or 10 µg/ml isotype (cat. no. 400902, Biolegend) for 1 h, or left untreated, followed by centrifuged at 400 x g for 5 min to remove antibody-containing media and then resuspended in complete media followed by co-culture with recipient cells WEHI-303-tdTomato as above.

2.4.5. EV isolation by size exclusion chromatography (SEC)

cSN was collected from WEHI-231-GFP cells as described above. Four millilitres of supernatant, from both 1 h stimulations (2 ml) and 2 h stimulations (2 ml), were loaded onto a qEV2/70nm SEC column (Izon Science, Medford, MA, USA) following the manufacturer's instructions. Fractions 7 to 12 were pooled and then concentrated to ~200 µL using Amicon ultra-15 centrifugal filter units (UFC901024, Millipore, Etobicoke, ON, Canada) at 3,000 x g for 50 min. The concentrated fraction was diluted in complete media and incubated with WEHI-303-tdTomato cells for 24 h at 37°C in a CO₂ incubator.

2.4.6. Nanoparticle tracking analysis

Isotype- and CD24-stimulated conditioned media were diluted 5-fold in sterile 0.1µm filtered 1X PBS if from cells cultured in EV-free media and left undiluted if from SEC. EV free media was prepared according to the previously established protocol³⁴; briefly, complete medium with 20% FBS was centrifuged at 100,000 x g at 4°C for 16 hours, passed through a 0.22µm filter, and then mixed with serum free RPMI in a 1:1 ratio. For each measurement, quintuplicate 1-minute videos were captured at a temperature of 25°C and syringe pump speed of 25 µl/s. Post capture, videos were analyzed to generate high resolution size and concentration data by the Nanosight NS300 software version 3.4 Build 3.4.003.

2.4.7. EV isolation by Vn96 peptide-based affinity isolation

One ml of conditioned media (CM) was incubated with 30 µg Vn96 peptide at 4°C, overnight on a rotator. The CM-Vn96 mix was then centrifuged at 17,000 x g for 15 mins and the supernatant removed. A second ml of CM was added to the pellet, followed by a brief vortex to disrupt the pellet and then incubation with rotation for 3 h at 4°C. Vn96-EVs were pelleted by centrifugation at 17,000 x g for 15 mins at 4°C, followed by three washes with 0.1 µm filtered 1X PBS supplemented with 1.2 mM PMSF.

2.4.8. Western blot

Vn96-EV pellets isolated as above were dissolved in 0.1µm filtered 1X PBS, mixed with Laemmli reducing sample buffer and 50% of the volume separated using 12% SDS-PAGE. Proteins were transferred onto nitrocellulose membranes, then blocked with 5% (w/v) skimmed milk in 0.1% Tween-20 Tris-buffered saline (TBST). Primary antibodies were diluted in 5%

(w/v) skimmed milk in TBST as follows: 1:1000 HSP90 α/β (SC-13119; Santa Cruz, Santa Cruz CA), 1:1000 CD81 (SC-166029; Santa Cruz, Santa Cruz CA), 1:1000 GFP (FL) (SC-8334, Santa Cruz, Santa Cruz CA). HSP90 and CD81 were detected using horseradish peroxidase-conjugated goat anti-mouse IgG (SC-13119; Santa Cruz, Santa Cruz CA). GFP was detected using HRP conjugated mouse anti-rabbit IgG (SC-2357). IgM was detected using goat anti-mouse IgM HRP (1:1000, SC-2064). All secondary antibodies were diluted 1:1000 in 5% (w/v) skimmed milk in TBST. Western chemiluminescent HRP substrate (Immobilon ECL Ultra Western HRP Substrate) was used for detection. Western blot images were acquired using chemidoc gel documentation system (Bio-Rad, Ca). Image manipulation involved adjustments to brightness and contrast only.

2.4.9. IgM and CD24 detection by flow cytometry

Cells were resuspended with FACS buffer (PBS 1x, pH 7.4, cat. no 10010-023, Life Technologies, containing 1% heat-inactivated fetal bovine serum) and stained with 0.5 μg of IgM-PE-Cy7 (25-5890, eBioscience) or with 0.25 μg of CD24-PE (12-0242-82, eBioscience) for 30 min at 4°C. Cells were then washed with FACS buffer and analysed by flow cytometry. See Supplemental Figures 1 and 2 for gating strategies.

2.4.10. Phospho-ERK detection by flow cytometry

After 24 h of co-culture, the cells were stimulated with 10 $\mu\text{g}/\text{ml}$ anti-mouse IgM (115-005-020, Jackson ImmunoResearch) for 5 min at 37°C, and the reaction stopped with 0.4 ml of cold 1x PBS containing 1 mM vanadate (13721-39-6, Sigma Aldrich). The cells were centrifuged at 400 x g for 5 min and then resuspended with 100 μl of pre-warmed fixation buffer (00-8222-49, eBioscience) for 35 min at room temperature (RT) followed by resuspension in 100 μl of permeabilization buffer (00-8333-56, eBioscience) and incubation with 1 μg of anti-phospho-

ERK1/2 conjugated with Alexa Fluor 647 (cat. no. 675503, BioLegend) for 35 min at 4°C in the dark. The reaction was stopped with 0.9 ml of permeabilization buffer before centrifugation at 400 x g for 5 min. The cell pellets were washed with FACS buffer and analysed by flow cytometry.

2.4.11. Apoptosis assay by flow cytometry

Cells were resuspended in Annexin V binding buffer (10 mM HEPES buffer, 140 mM NaCl, 2.5 mM CaCl₂, pH 7.4). Three microlitres of anti-annexin V conjugated with Alexa Fluor 647 (A23204, Invitrogen) or 5 µl of anti-annexin V conjugated with PE (640908, Biolegend) was added to 100 µl of cell suspension following the manufacturer's instructions. Cells were then washed with FACS buffer and analysed by flow cytometry.

2.4.12. Confocal microscopy

WEHI-303 cells were incubated with 5 µM CFSE (ThermoFisher) for 10 min at room temperature (RT) and then quenched with FBS following the manufacturer's instructions. WEHI-231 were stimulated with anti-CD24 for 15 min, washed, and then co-cultured with WEHI-303 for 24 h at 37°C, as above. Cells were incubated with coverslips pre-coated with 1 µg/ml anti-MHC II (MABF33, Millipore) overnight at 4°C. Cells were fixed in 4% paraformaldehyde for 10 min at RT. After washing 3 times with PBS, slides were blocked with 2% bovine serum albumin (BSA) in 1X PBS for 30 min at RT. Coverslips were incubated for 1 h at RT with Alexa Fluor 647-conjugated goat anti-mouse IgM (112-545-175, Jackson ImmunoResearch) in 2% BSA/PBS, washed in PBS and then mounted using Prolong Diamond (ThermoFisher) mounting media. Cells were imaged with spinning disk confocal microscopy using a Quorum Technologies system based on a Zeiss Axiovert 200 M microscope with a 100× NA 1.45 oil objective and a QuantEM

512SC Photometrics camera for image acquisition. Z-stacks were acquired in 0.5 μm increments. Images were assembled using ImageJ after export of 16-bit TIFF using Slidebook v6.0.4 software (3i Inc., Denver, CO).

2.4.13. Statistical analysis

Prism software (version 8.4.3; GraphPad) was utilized to generate graphs and for statistical analyses. One-way ANOVA was performed for comparing more than 2 conditions, followed by Sidak's multiple comparisons post-hoc test. Differences were considered to be significant when P values were smaller than 0.05. The number of repetitions is indicated in each figure legend.

2.5. Results

2.5.1. EV trafficking of lipid and membrane proteins between murine B lymphoma cells in response to CD24 stimulation.

The WEHI-231 murine B cell lymphoma cell line is used extensively as a model for B cell responses to receptor engagement. This cell line has surface receptor characteristics of immature B cells that undergo growth arrest and apoptosis in response to BCR crosslinking³⁵. To analyze the transfer of lipid and protein due to the action of EVs, we took advantage of the WEHI-231 variant, WEHI-303, which lacks membrane IgM (Supplementary Figure 2.1B)³³.

To test the hypothesis that lipids and proteins can be transferred between murine B cells in response to CD24 stimulation, we used a co-culture model to capture the maximum amount of exchange in this dynamic system. After antibody-mediated stimulation of CD24 on WEHI-231-GFP cells, excess antibody was washed out to ensure that the recipient WEHI-303-tdTomato cells were not exposed to stimulating antibody. Equal numbers of anti-CD24-stimulated or control antibody-stimulated (isotype) WEHI-231-GFP cells were then co-cultured with recipient WEHI-

303-tdTomato cells (Figure 2.1A). We found a statistically significant increase in GFP⁺tdTomato⁺ cells in response to CD24 engagement showing exchange of lipid between cells (Figure 2.1B-C). These data could represent WEHI-303-tdTomato cells that have taken up GFP from WEHI-231-GFP cells or vice versa. To determine the direction of the transfer more precisely, we made the assumption that tdTomato⁺ cells with lower levels of GFP are most likely WEHI-303-tdTomato cells that have incorporated GFP⁺ EVs and GFP⁺ cells with lower levels of tdTomato are most likely WEHI-231-GFP that have incorporated tdTomato EVs. Analysis of low, mid, or high levels of GFP in tdTomato⁺ cells revealed a statistically significant increase of GFP events in the low and mid-range but not in the high range (Figure 2.1D and Supplemental Figure 2.1D). These data suggest that the increase in double-positive events is most likely due incorporation of EVs into tdTomato cells and not a cellular fusion event, which would have high levels of both fluorophores. We also observed an increase in GFP⁺ cells that were tdTomato⁺, with statistically significant increases at the low and mid-tdTomato levels with the largest increase in the mid-range (Figure 2.1E and Supplemental Figure 2.1C-E). Thus, there is a bi-directional EV exchange between cells that is increased when CD24 is stimulated on the donor cells. It is not clear if the transfer of tdTomato⁺ from the WEHI-303-tdTomato 303 cells to the WEHI-231-GFP donor cells reflects an increase in the uptake of EVs by the WEHI-231-GFP cells or an increase in the release of EVs by WEHI-303-tdTomato cells in response to the acquisition of CD24 that has been clustered by anti-CD24 antibodies.

To determine if membrane proteins are also transferred in response to CD24 stimulation we analyzed the acquisition of IgM by WEHI-303-tdTomato cells. After co-culture with anti-CD24-treated WEHI-231-GFP cells, we found a significant and substantial increase in the number of cells expressing cell surface IgM as well as an increase in the level of IgM on WEHI-303-tdTomato cells, albeit at a lower level than WEHI-231 cells, (Figure 2.1F-G and

Supplemental Figure 2.1F). Neither the percent positive nor the level of IgM was changed in WEHI-231-GFP after stimulation (Figure 2.1G and Supplemental Figure 2.1G-H), indicating that the transfer of IgM to recipient cells did not substantially deplete IgM from the surface of the donor cells.

We then used confocal microscopy to visualize IgM transfer to WEHI-303 cells that had been labeled with CFSE since tdTomato fluorescence is destroyed upon fixation. We found that WEHI-303 cells displayed patches of IgM on their cell surface and that the size of these patches appeared to be greater when the donor WEHI-231-GFP cells had been co-cultured with anti-CD24 as opposed to an isotype-matched control antibody (Figure 2.1H).

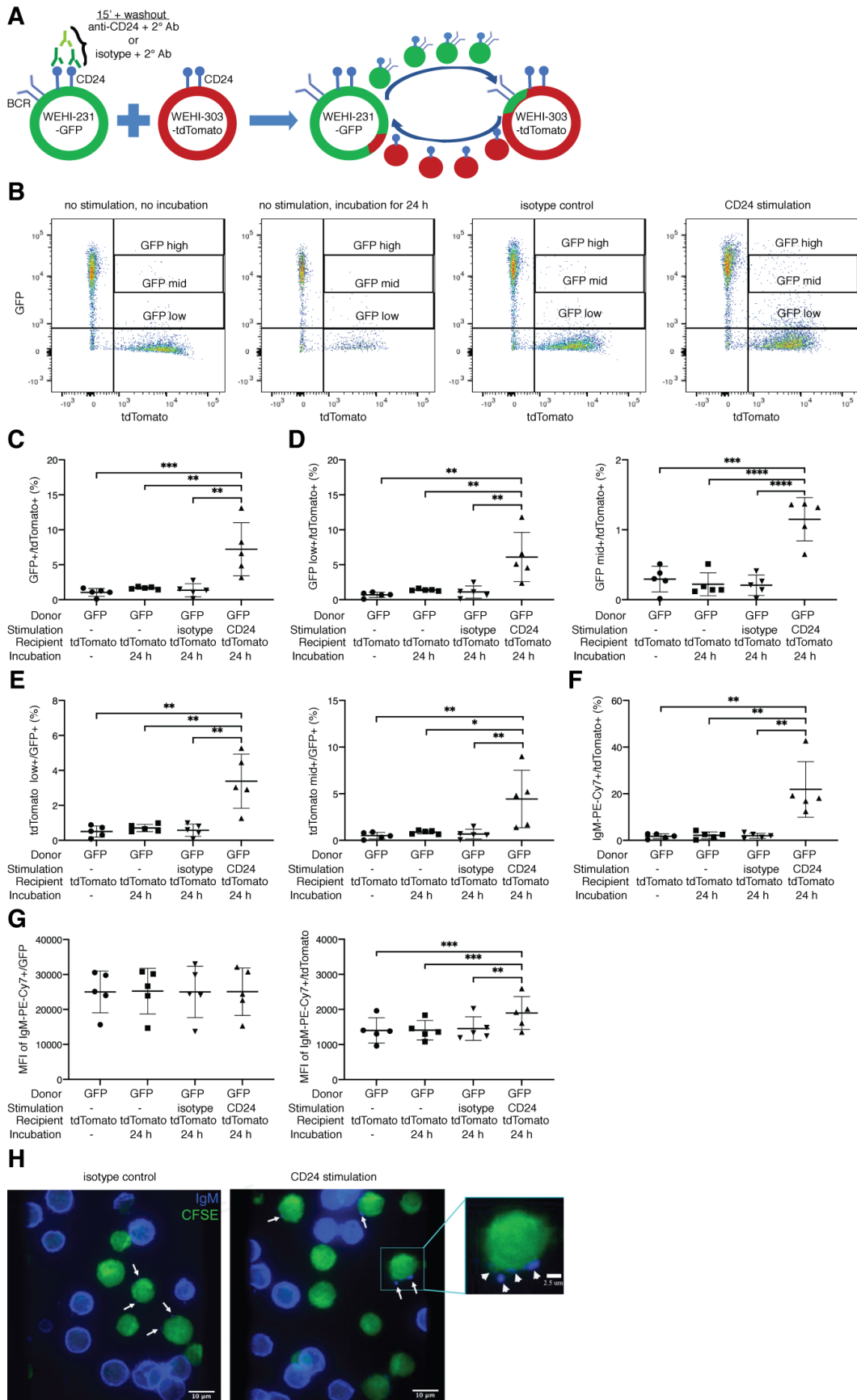


Figure 2.1. CD24 stimulation of donor cells causes transfer of GFP-labeled membrane and

IgM to recipient cells. (A) Schematic of experimental design using WEHI-231-palmitoylated

GFP (WEHI-231-GFP) and WEHI-303-palmitoylated tdTomato (WEHI-303-tdTomato) cells.

WEHI-231-GFP were stimulated with anti-CD24 or control (isotype) for 15 min, or left untreated, followed by washout and then a 24 h co-culture with WEHI-303-tdTomato.

Individually cultured, untreated cells were mixed immediately before the last centrifugation step.

(B) Representative dotplots of tdTomato⁺ cells with low, mid or high GFP signal. (C) Percent

GFP and tdTomato double-positive cells. (D) Percent tdTomato⁺ cells with low or mid-level GFP

fluorescence (see representative dot plots for gating strategy in Supplemental Fig. 1C) (E)

Percent GFP⁺ cells with low or mid tdTomato signal. (F) Percent IgM and tdTomato double-

positive cells. (G) Mean fluorescence intensity (MFI) of IgM on GFP⁺ (left) and tdTomato⁺

(right) cells. (n=5 as shown by individual symbols). Significance was determined by a one-way

ANOVA followed by the Sidak's multiple comparison test **P<0.01 ***P<0.005. (H)

Representative images of WEHI-303 cells (CFSE- green) and WEHI-231 cells showing IgM-

positive cells (blue) and patches (indicated by arrows) after co-incubation for 24 h. Scale bar = 10

µm or 2.5 µm for inset (n=3).

To further support our hypothesis that EVs mediate the transfer of lipids and proteins from donor to recipient cells, we used low speed centrifugation to generate a cell-free cSN from WEHI-231-GFP cells that had been stimulated with anti-CD24 antibodies, and then incubated the recipient cells with this cSN. Due to their small size, EVs would remain in the cSN, as much greater centrifugal forces are required to pellet them. When donor cSN isolated from an equal number of cells was added (1:1 ratio), there was no difference in the number recipient cells gaining GFP between CD24 and control stimulation (Figure 2.2A-B). However, when we used cSN at a 4:1 ratio we found a clear and statistically significant increase in the number of GFP+ tdTomato+ cells when the WEHI-303-tdTomato cells were cultured with the cSN of anti-CD24-treated WEHI-231-GFP cells, compared to when the WEHI-303 cells were exposed to cSN from isotype control-treated donor cells (Figure 2.2B). Interestingly, with both a 1:1 and a 4:1 ratio, we found a significant increase in the percent of recipient cells that acquired IgM after being cultured with cSN from CD24-stimulated donor cells (Figure 2.2C). However, the amount of IgM acquired was substantially greater when a 4:1 cSN ratio was used, as indicated by the significantly higher level of anti-IgM fluorescence associated with the cSN-treated WEHI-303-tdTomato cells (Figure 2.2D). Thus, there is a dose-dependent increase in the transfer of IgM.

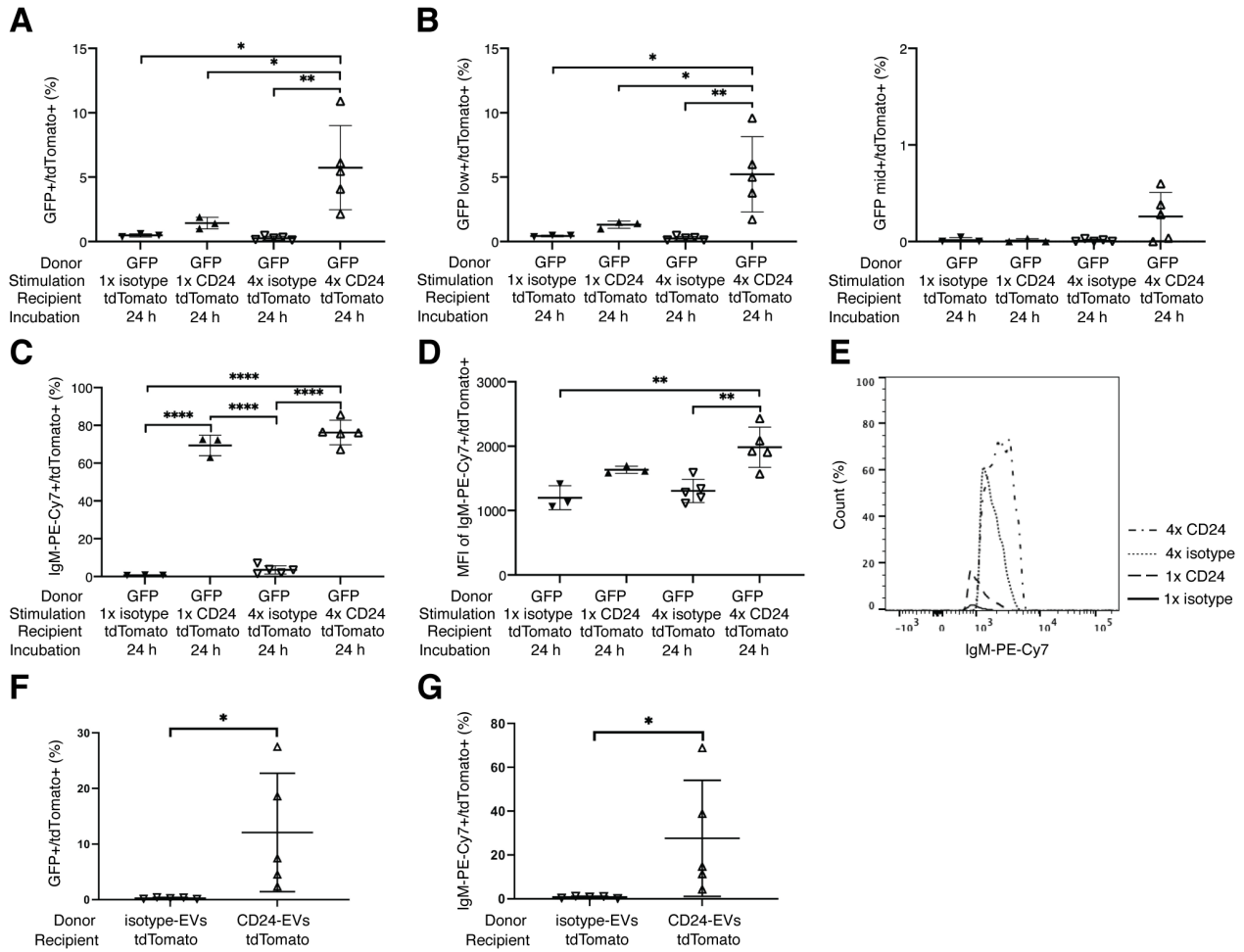


Figure 2.2. EV-dependent transfer of GFP and IgM by EVs. WEHI-231-GFP were stimulated with anti-CD24 or control (isotype) for 15 min followed by a washout then a 1 h or 2 h accumulation of EVs in the media. The supernatant was cleared of cell debris and incubated with WEHI-303-tdTomato for 24 h. (A) Percent GFP and tdTomato double-positive cells. (B) Percent tdTomato-positive cells with low or mid GFP fluorescence. (C) Percent IgM and tdTomato double-positive cells after 24 h incubation. (D-E) Mean fluorescence intensity of IgM in the presence of tdTomato (n=5), significance was determined by a one-way ANOVA followed by the Sidak's multiple comparison test *P<0.05 **P<0.01 ***P<0.005 ****P<0.001. (F) Percent GFP and tdTomato double-positive cells and (G) percent IgM and tdTomato double-positive cells after

24 h incubation of SEC-based isolated EVs for 24 h (n=5), significance was assessed using paired Wilcoxon test *P<0.05.

To further characterize the cSN, we analyzed the particles released following isotype or CD24 stimulation from WEHI-231-GFP cells cultured in EV-free media, using nanoparticle tracking analysis (NTA) (Supplemental Figure 2.3A). The mean EV size increased with 1 h CD24 stimulation, but not 24 h, (Supplemental Figure 2.3B left) whereas the concentration of released EVs was increased at 24 h but not 1 h (Supplemental Figure 2.3B right). These data are generally consistent with our previous work and showed EVs in the 100-200 nm size range²⁹. Next, we determined if both GFP and IgM are present in the EVs. EVs were isolated and characterized by western blot using the Vn96 peptide-based purification, which precipitates EVs based on interaction of the Vn96 peptide with heat-shock proteins, that we previously used for this purpose^{29,36}. We found that both GFP and IgM co-precipitated with the EV surface protein markers CD81 and Hsp90 showing the GFP and IgM are packaged in EVs (Supplemental Figure 2.3C). We also found GFP and IgM present in EVs isolated using size exclusion chromatography (SEC) (Supplemental Figure 2.3D). To determine if EVs were able to transfer IgM, we then isolated EVs from cSN using SEC followed by incubation with recipient cells for 24 h. The EVs isolated by SEC were slightly larger than the bulk EV population with no significant difference between isotype and CD24 stimulation (204±13 nm vs.181±15 nm, respectively). Similar to our results with cSN, stimulation of donor cells with CD24 resulted in a significant increase in GFP and IgM on recipient cells (Figure 2.2F-G). Thus, these results provide further evidence that GFP and IgM are transferred between B cells by EVs. Surprisingly, we did not observe transfer of CD24 when donor and recipient cells were co-cultured but separated by a filter with 0.4 µm pores in a Transwell system (Supplemental Figure 2.4A-B). This suggests that the exchange is likely dependent on close contact between cells.

Overall, we conclude that donor cells secrete EVs carrying lipids and membrane proteins that can be taken up by recipient cells. Consistent with our past work^{28,29}, and given that IgM is a

transmembrane cell surface receptor that we detect with an antibody directed against its extracellular domain, the simplest explanation for these data is that CD24 promotes the release of EVs from the plasma membrane that contain lipids and proteins, which are then incorporated into the plasma membrane of the recipient cells.

2.5.2. CD24 engagement on donor cells induces transfer of lipids and CD24 to recipient cells

We next asked if primary bone marrow B cells from CD24KO mice could also function as recipient cells. To do this, we labelled primary bone marrow cells with eFluor 670, which binds to cellular proteins in the cytoplasm, to track these as recipient cells. We found a statistically significant increase in GFP⁺eFluor 670⁺ cells in response to CD24 engagement on the donor cells, showing transfer of the lipid-associated palmGFP from donor to recipient cells (Figure 2.3A). Analysis of low and mid-levels of GFP in eFluor 670⁺ cells revealed statistically significant increases in GFP⁺ events in bone marrow B cells (Figure 2.3B). Over 95% of the cells that took up GFP were B cells based on expression of CD19 or B220 (Figure 2.3A-C). Conversely, there was also a CD24-mediated increase in GFP⁺ cells that acquired eFluor 670 fluorescence, with a statistically significant increase in the mid-range. Thus, this shows that cytoplasm was transferred from the eFluor 670⁺ CD24 KO bone marrow B cells to the anti-CD24-stimulated WEHI-231-GFP cells (Figure 2.3C). Thus, similar to when WEHI-303 are recipient cells, there is a bi-directional exchange between cells that is increased when CD24 is stimulated on the donor cell, either by increasing uptake by the donor cell or by causing recipient cells to release more EVs in response to the transferred receptor.

We next investigated CD24 transfer and found a significant increase in surface CD24 expression on the CD24KO primary B cells after they were co-cultured with CD24⁺ WEHI-231-GFP cells. Although this transfer of CD24 occurred in the absence of stimulating the WEHI-231-

GFP cells, we found enhanced transfer of CD24 to the bone marrow B cells after stimulation of CD24 on the donor cells (Figure 2.3D). In addition, we found that CD24 was transferred during the 4°C centrifugation step as indicated by the ~5% positive cells in the non-incubated control. (Figure 2.3D). Similar to the transfer of GFP, the vast majority of recipient cells (>89%) are primary B cells, indicating that contaminating cells are responsible for only a small percentage of uptake. Thus, CD24 is readily transferred to primary B cells and this transfer is increased when the donor cells are stimulated via CD24.

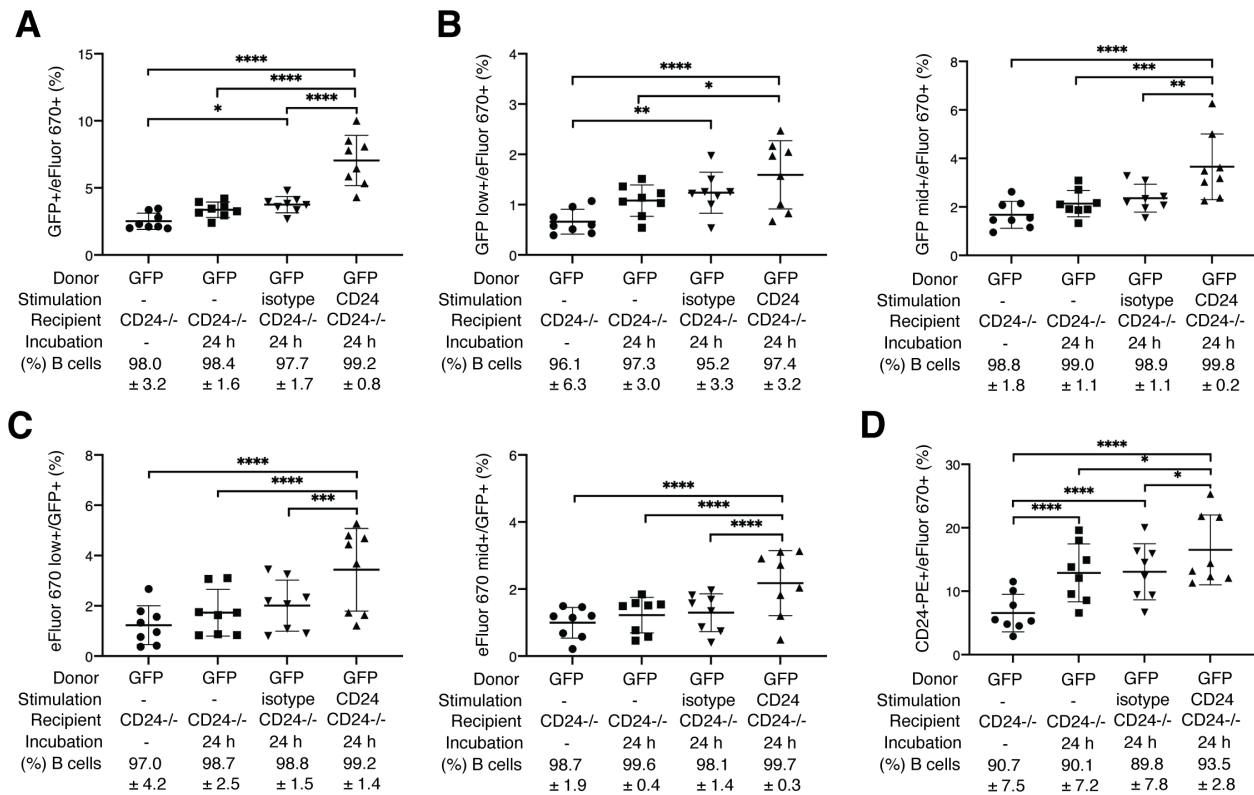


Figure 2.3. CD24 stimulation of donor cells causes transfer of GFP-labeled membrane and

CD24 to recipient cells. WEHI-231-GFP cells were stimulated with anti-CD24 or control

(isotype) for 15 min, or left untreated, followed by a washout and then a 24 h co-

culture with eFluor670-labeled primary bone marrow B cells from CD24KO mice. Individually

cultured, untreated cells were mixed immediately before the last centrifugation step. (A) Percent

GFP and eFluor670 double-positive cells. (B) Percent eFluor670⁺ cells with low or mid GFP

signal. (C) Percent GFP⁺ cells with low or mid eFluor670 signal. (D) Percent CD24 and

eFluor670 double-positive cells (n=8), significance was determined by a one-way ANOVA

followed by the Sidak's multiple comparison test *P<0.05, **P<0.01, ***P<0.005, ****P<0.001.

The percentage of B cells in a subset of replicates in each treatment group is shown (n=5). This

was found not to be significantly different between any groups by a one-way ANOVA.

2.5.3. CD24 engagement on donor cells induces transfer of signaling-competent IgM and CD24 to recipient cells.

We next asked if transferred receptors are functional in the recipient cells and can induce cellular responses. Antibody-mediated engagement of the BCR induces phosphorylation of ERK1/2 within minutes and we used this as a readout of BCR signaling³⁷. We confirmed that phospho-ERK1/2 is detected using intracellular flow cytometry upon IgM stimulation of WEHI-231-GFP but not the IgM-negative WEHI-303-tdTomato cells (Supplemental Figure 2.2E). Interestingly, we observed an increase in phospho-ERK cells in response to anti-IgM stimulation in WEHI-303-tdTomato cells that had been co-cultured with either isotype- or anti-CD24-stimulated donor cells (Figure 2.4A). To more carefully analyze the response of WEHI-303-tdTomato cells that were capable of responding to IgM stimulation, we analyzed only those WEHI-303-tdTomato cells that were GFP⁺, an indicator of cargo transfer from the donor WEHI-231-GFP cells. We found that anti-IgM treatment stimulated ERK phosphorylation in GFP⁺ WEHI-303-tdTomato cells that had been co-cultured with unstimulated WEHI-231-GFP donor cells and a larger percent of the WEHI-303-tdTomato cells exhibited increases in phospho-ERK if the donor WEHI-231-GFP cells had been stimulated through CD24 (Figure 2.4B). Therefore, the transferred IgM present on the surface of WEHI-303-tdTomato cells is functional, with a greater fraction of the cells acquiring IgM when donor cells were stimulated with CD24.

We next tested if engagement of CD24 on the donor cell can induce transfer of functional CD24 to recipient cells. Previously, we and others have shown that CD24 engagement can induce apoptosis in WEHI-231 and primary bone marrow B cells^{26,28}. When CD24KO B cells that had been co-cultured with anti-CD24-stimulated WEHI-231-GFP cells were exposed to anti-CD24 antibodies, we observed that the recipient cells (>95% B cells) that had acquired CD24 underwent apoptosis (Figure 2.4C). Focusing on GFP⁺ CD24KO B cells (i.e. evidence of cargo

transfer), we found an even more pronounced increase in CD24-induced apoptosis (Figure 2.4D). Therefore, CD24 that is transferred to CD24-negative primary B cells in response to CD24 stimulation of the donor cells retains its functionality.

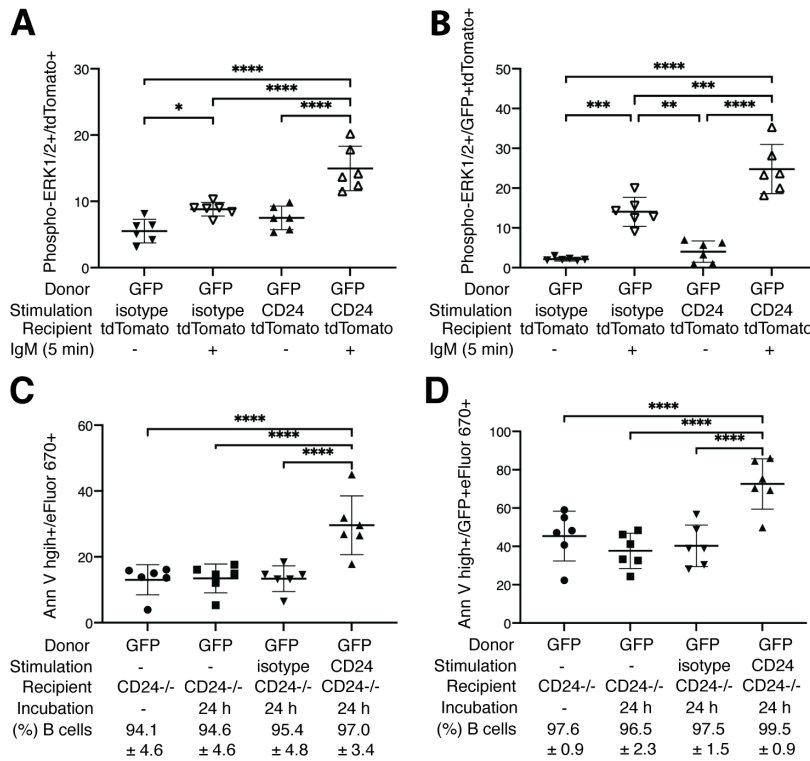


Figure 2.4. CD24 stimulation causes transfer of functional IgM and CD24 from donor to recipient cells. WEHI-231-GFP cells were either left untreated or treated with either primary rat anti-mouse CD24 antibody or primary isotype antibody, which had been pre-incubated with goat anti-rat secondary antibody, and then co-incubated with WEHI-303-tdTomato for 24 h. (A) Cells were then either untreated or stimulated with anti-IgM for 5 min, followed by phospho-ERK1/2 detection on WEHI-303-tdTomato cells or (B) on GFP-tdTomato-double positive cells. (C) Percent Annexin V-PE^{hi} and eFluor 670 double-positive apoptotic cells and (D) Percent Annexin V-PE^{hi} and GFP-eFluor 670-double positive cells. (Schematic of experimental design and representative dotplots can be found in Supplemental 2) (n=6) statistical significance was determined by a one-way ANOVA followed by the Sidak's multiple comparison test *P<0.05, **P<0.01, ***P<0.005, ****P<0.001. The percentage of B cells in a subset of replicates in each treatment group is shown (n=4). This was found not to be significantly different between any groups by a one-way ANOVA.

2.5.4. IgM stimulation of donor cells induces transfer of lipids and CD24 to recipient cells

Next, we set out to determine whether IgM stimulation of donor B cells can also induce transfer of lipids and proteins. To do this, we used WEHI-231-GFP cells as the donors and CD24KO primary cells as recipients, as in Figure 2.3. We found a statistically significant increase in GFP⁺eFluor 670⁺ recipient CD24KO cells (>95% B cells) when the donor WEHI-231 GFP cells had been stimulated with anti-IgM for 1-2 h, compared to when the recipient cells were co-cultured with untreated donor cells (Figure 2.5A-B). We also observed the donor cells had an increase in eFluor670 fluorescence, showing that anti-IgM stimulation of the donor cells increased the transfer of cytoplasm from the recipient cells (Figure 2.5C). To determine if surface proteins are transferred in response to IgM stimulation, we analyzed the acquisition of CD24 by CD24KO primary B cells. Although untreated or control isotype-treated donor cells were able to transfer CD24 to recipient cells (>90% B cells), stimulating the donor cells with anti-IgM for 1-2 h induced a statistically significant higher level of CD24 transfer to the CD24KO primary B cells (Figure 2.5D). Thus, IgM stimulation of the donor cells increased the percentage of recipient cells that gained CD24.

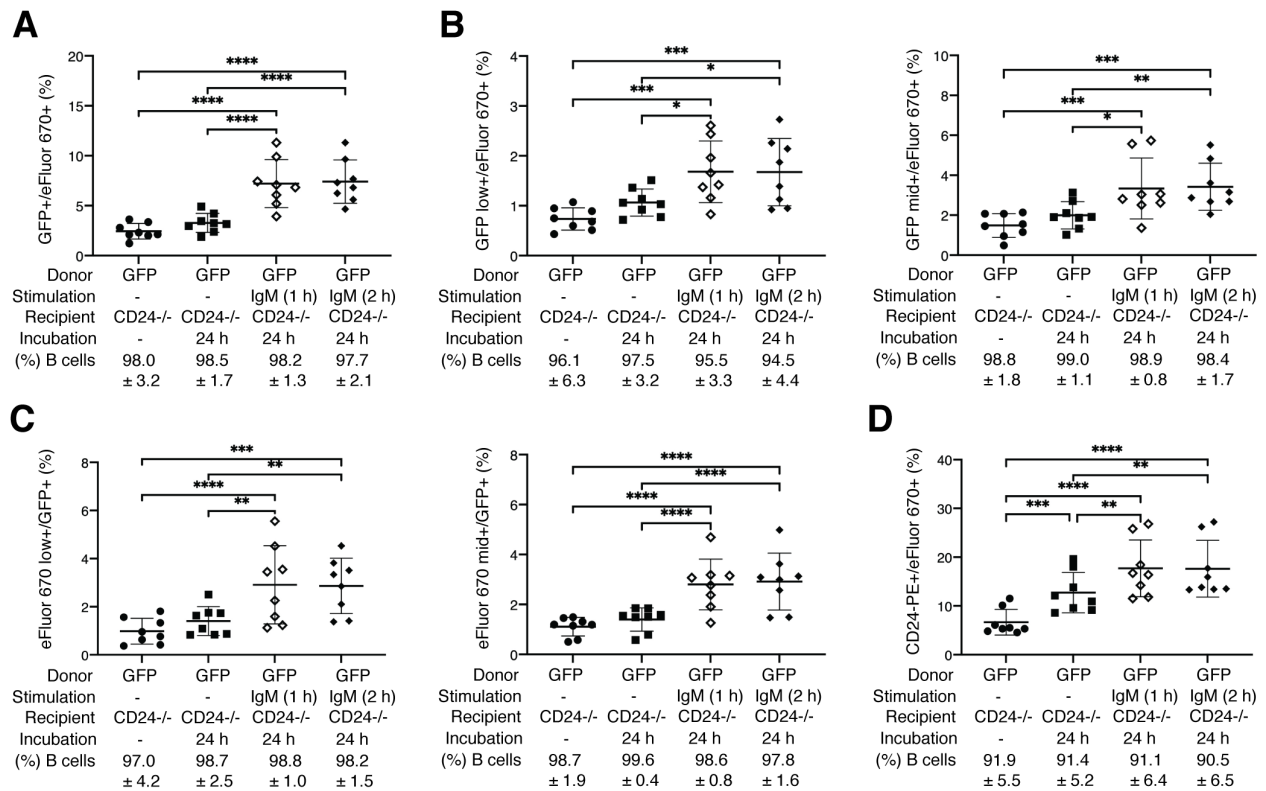


Figure 2.5. IgM stimulation of donor cells causes transfer of GFP-labeled membrane and CD24 to recipient cells. WEHI-231-GFP cells were left untreated or stimulated with anti-IgM antibody for 1 h or 2 h followed by washout and then co-cultured with eFluor 670-labeled primary bone marrow B cells from CD24KO mice for 24 h. Singly cultured, untreated cells were mixed immediately before the last centrifugation step. (A) Percent GFP and eFluor670 double-positive cells. (B) Percent eFluor670⁺ cells with low or mid GFP signal. (C) Percent GFP⁺ cells with low or mid eFluor670 signal. (D) Percent CD24 and eFluor670 double-positive cells (n=8), significance was determined by a one-way ANOVA followed by the Sidak's multiple comparison test *P<0.05, **P<0.01, ***P<0.001, ****P<0.0001. The percentage of B cells in a subset of replicates in each treatment group is shown (n=4). This was found not to be significantly different between any groups by a one-way ANOVA.

2.5.5. IgM stimulation of donor cells induces transfer of signaling-competent IgM to recipient cells

We then determined whether IgM stimulation of donor cells could induce the transfer of signaling competent IgM to recipient cells. Donor WEHI-231-GFP were mixed with WEHI-303-tdTomato recipient cells and stimulated with anti-IgM. In this case the stimulating antibody was not removed since the IgM-negative WEHI-303 cells do not undergo apoptosis in response to anti-IgM. As above, we found a statistically significant increase in GFP⁺tdTomato⁺ WEHI-303 cells after co-culture with anti-IgM-stimulated WEHI-231-GFP cells (Figure 2.6A) with a statistically significant increase of low and mid-range GFP⁺ cells, which are likely WEHI-303 cells that acquired GFP from the GFP^{hi} WEHI-231-GFP cells (Figure 2.6B). Similar to CD24 stimulation of donor cells, anti-IgM stimulation of the WEHI-231-GFP donor cells induced transfer of lipid from recipient cells to donor cells (Figure 2.6C).

Next, we analyzed IgM-mediated apoptosis, which allows us to detect transfer of functional BCRs to the WEHI-303 cells. We were not able to analyze IgM transfer to recipient cells in response to anti-IgM stimulation of donor cells because the stimulating anti-IgM antibody blocks all available epitopes for detecting transferred IgM on the surface of recipient cells. We found that anti-IgM-induced apoptosis of WEHI-303-tdTomato cells was significantly increased after they had been co-cultured cells with WEHI-231-GFP cells (Figure 2.6D). Not all of the WEHI-303-tdTomato cells that had acquired GFP from the donor cells became sensitive to anti-IgM induced apoptosis, perhaps because they did not also acquire IgM (Figure 2.6E). Thus, similar to CD24 signaling, BCR signaling is also able to induce the transfer of functional membrane proteins to recipient cells. Moreover, the transferred BCR is able to activate signaling pathways that initiate apoptosis, demonstrating that the transferred receptor can interact with host cellular machinery.

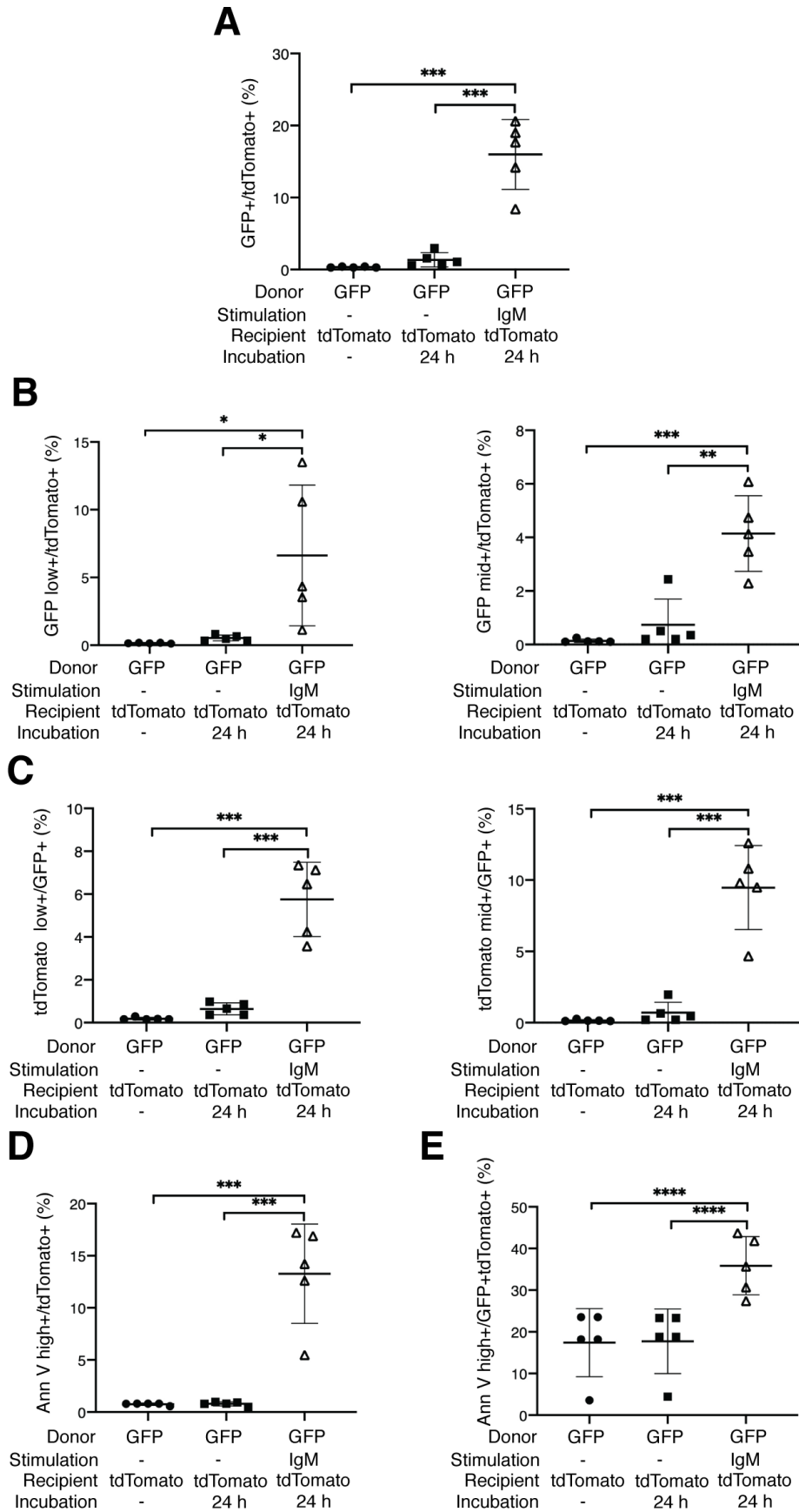


Figure 2.6. IgM stimulation of donor cells causes transfer of functional IgM to recipient cells. WEHI-231-GFP were co-cultured with WEHI-303-tdTomato for 24 h in the presence or absence of anti-IgM stimulating antibody. (A) Percent GFP and tdTomato double-positive cells. (B) Percent tdTomato⁺ cells with low or mid GFP signal. (C) Percent GFP⁺ cells with low or mid tdTomato signal. (D) Percent Annexin V-Alexa fluor 647^{hi} and tdTomato double-positive apoptotic cells. (E) Percent Annexin V-Alexa Fluor 647^{hi} and GFP-tdTomato-double positive cells (n=5), significance was determined by a one-way ANOVA followed by the Sidak's multiple comparison test *P<0.05, **P<0.01, ***P<0.005, ****P<0.001.

2.6. Discussion

In this study, we have demonstrated that stimulation of two receptors on B cells, which differ in structure, can both cause the release of EVs that can alter recipient cell responses by transferring functional membrane proteins. Transfer of membrane proteins was accompanied by a concurrent transfer of lipids to further support that the mechanism of transfer was via EVs. Furthermore, since cSN was able to transfer lipids and proteins, cell-cell contact was not necessary for this process. To the best of our knowledge, this is the first time that transfer of functional receptors by EVs has been shown to occur in B cells and the first time that stimulation of one receptor resulting in transfer of a second receptor has been shown in any cell type.

In these experiments, the number of cells that acquired lipids was consistently lower than the number that acquired either CD24 or IgM. This is most likely due to differences in the threshold of detection for the fluorophores combined with the limited packaging ability of palmGFP into EVs. The interior lumen of EVs that released in response to CD24 stimulation is estimated to be 20 to 90 nm³³⁸. GFP is a 28 kDa cylindrical protein that is 4.2 nm long by 2.4 nm wide (~19 nm³)³⁹. Therefore, we can estimate that there could be 1-4 GFP molecules inside one EV. In contrast, there could potentially be 10-fold more CD24 and IgM molecules on the surface of individual EVs⁴⁰, each with the potential to be bound by more than one detection antibody. Thus, the apparent difference in the uptake by recipient cells is most likely due to a limitation of this technique rather than a true difference in uptake of the lipids vs. membrane proteins by recipient cells and the amount of lipid transferred is likely underestimated.

Another limitation of this study is that we are using antibody-mediated engagement of CD24 to induce signalling. These conditions may not properly mimic endogenous activation of CD24 *in vivo*. The ligand for CD24 on bone marrow B cells has not been identified.

Identification of the relevant activating ligand would allow us to confirm that ligand-induced clustering of CD24 also stimulates EV release.

Interestingly, even though our data clearly show that EVs are responsible for transfer of lipids and IgM, we did not observe transfer when donor and recipient cells were separated by a membrane. Thus, close contact between cells is necessary for the EV-mediated transfer between cell populations. Our previous data showed that CD24 is exchanged between identical cellular populations²⁸, suggesting that autocrine uptake by the same cell type is likely contributing to the total amount of exchange in the co-culture. Thus, we are likely underestimating the extent of exchange mediated by EVs in our co-culture system as autocrine mechanisms likely account for a significant fraction of EV uptake.

Using western blot analysis, we were able clearly visualize GFP and IgM present in isolated EVs, as validated by Hsp90 and CD81 expression. However, we were unable to detect CD24 in a similar manner despite using multiple antibodies and conditions. We attempted to detect CD24 using 4 different antibodies using both reducing and non-reducing gels but were unsuccessful. We do not know if CD24 undergoes glycosylation, which can affect its migration on the gel and complicate detection, potentially leading to unexpected bands or a lack of detection. The glycosylation also can mask or alter the epitope, thus the antibodies may not be able to attach the protein effectively. However, in our previous work we were clearly able to show by flow cytometry that CD24 was present on sub-cellular size objects in the culture supernatant that also expressed phosphatidylserine as detected by Annexin-V⁴¹. Stimulation of CD24 increased the abundance of the CD24⁺AnnexinV⁺ particles⁴¹. In addition, we previously detected CD24 by flow cytometry using bead-based isolation of EVs⁴². We suspect that the lack of detection of CD24 in isolated EVs by western blot may be due to the reduced sensitivity of this technique because of the low levels of protein that are present in EVs. Thus, although we have

not conclusively shown that CD24 is also transferred via EVs here, the evidence thus far suggests that this is a likely mechanism for the transfer of CD24.

IgM is a transmembrane component of the BCR, which induces apoptosis in immature B cells⁴³⁻⁴⁵. CD24 is a GPI-anchored protein that induces apoptosis in vitro and during B cell development^{22,25-28}. CD24 is constitutively located in lipid rafts and the BCR translocates to lipid rafts after stimulation^{46,47}. Both can activate similar signaling pathways including those leading to apoptosis. For example, both activate the ERK signaling pathway and both activate the caspase-3 pathway^{28,46,48}. It is not known how CD24 or IgM regulate EV release, nor is it clear what specific properties of these receptors induce release of EVs. We found that stimulation of CD40, a lipid raft-resident TNF-receptor family member, that is a pro-proliferative co-stimulatory receptor for B cells^{49,50} did not induce a statistically significant amount of lipid transfer, potentially due to limitations in detecting GFP as discussed above, and only a minor amount of IgM transfer (Supplemental Figure 2.5A-C). Stimulation of CD48, a GPI-anchored lipid raft-resident, pro-adhesion and pro-proliferative co-stimulatory receptor of CD40⁵¹⁻⁵³ was able to induce a small but statistically significant transfer of lipids but not IgM (Supplemental Figure 2.5D-F). It is unclear if the small degree of transfer in either case is biologically meaningful. Together, these observations suggest that specific receptors can induce robust receptor-mediated EV release but that others do not. More work is needed to define the precise pathway(s) that regulate both EV release and EV uptake.

The data from this study and our previous studies suggests that the EVs induced by CD24 stimulation are MVs budded off the plasma membrane and not exosomes derived from multi-vesicular bodies^{28,29}. A number of stimuli have been shown to induce MV release from platelets and endothelial cells, including destabilization of the membrane by complement proteins, shear stress, and pro-apoptotic stimuli⁵⁴. Increased $[Ca^{2+}]_i$ can also cause lateral redistribution of

membrane components to promote membrane curvature^{55,56}. This physical alteration in membrane curvature, as well as protein crowding on the surface of cellular membranes, can directly contribute to MV formation⁵⁷. However, more work is needed to determine how MV release is regulated in response to stimulation of CD24 or IgM.

EV uptake can occur via EV internalization by phagocytosis or micropinocytosis⁵⁸, as well as theoretically by direct fusion between EVs and the plasma membrane. The lipid raft-like membrane composition of EVs is also known to contribute to fusion with recipient cell membranes⁵⁹. In addition, PS and P-selectin on the exterior of cells are necessary for fusion of tissue factor-expressing MVs with platelets, and PS is necessary for fusion of EVs with glioma cells⁶⁰⁻⁶². Interestingly, PS on EVs is increased upon stimulation of CD24, suggesting that PS-binding may be a mechanism by which the EVs that are released in response to CD24 stimulation bind to target cells²⁸. In this study, we observed the maintenance of the transmembrane orientation of both CD24 and the BCR by flow cytometry, the appearance of patches of BCR by confocal microscopy, and the transfer of cytosol from primary B cells to WEHI-231 cells, as assessed by the transfer of eFluor670. Recycling of the BCR to the plasma membrane from the cytosol would result in an inverted orientation of the BCR and CD24. Thus, the maintenance of the orientation of these receptors suggests that there is some fusion of the EVs with the plasma membrane. However, the precise mechanism responsible for EV uptake, and whether these EVs are targeted to recipient cells via specific receptors or PS, is not yet known.

During B cell development, the expression of the BCR is limited to one rearranged heavy chain and one light chain allele via allelic exclusion. This ensures that B cells can only be activated in response to one, or a closely related set of, antigenic determinants. The data that we present here suggests that B cells could acquire additional BCRs, with differing antigenic specificities, due to the action of EVs in response to stimulation of either CD24 or the BCR.

Furthermore, the newly acquired BCRs retain functionality in the recipient cells. Our data show that between 5% and 20% of cells in the bulk culture can acquire new receptors suggesting that a minority of cells in the population would acquire new receptors in this manner. We speculate that this may be a mechanism to maintain B cellular homeostasis. In this model, an increase in CD24⁺ cells, stimulation of CD24 by an unknown ligand, and/or stimulation of IgM, depending on the cellular compartment, would result in a concurrent increase in the release of EVs bearing CD24 and/or IgM. Uptake of these EVs by neighbouring cells would induce cell death in the presence of ligand or antigen. In the bone marrow, an increase in CD24⁺ pre-B cells could result in increased apoptosis in CD24⁻ B cells. An effect that is consistent with the leaky block in B cell development observed in CD24-transgenic mice²⁷. Overall, the paracrine effect of EVs could result in the appropriate reduction of cell number needed to maintain homeostasis. However, the presence of a second BCR with a different antigenic recognition could also result in the non-specific activation of B cells in the presence of co-stimulation. Future works is needed to determine the contribution of EVs to B cell development and activation.

Interestingly, the transfer of associated receptors in response to stimulation of a particular receptor (i.e. transfer of IgM by CD24 and vice versa) suggests that cells could transfer receptors with different functions than the activated receptor. The consequence of transferring different receptors would depend on the presence of the appropriate ligand for the transferred receptor. Nevertheless, this creates substantial potential for cross-activation of cells due to their acquisition of new functionalities.

Overall, our data demonstrate that both the BCR and CD24 can enable the transfer of functional receptors, via EVs in the case of BCR. This transfer allows recipient cells to become susceptible to novel antigenic or ligand stimulation. The effects of this acquisition are likely

localized in time and space during B cell development or activation in vivo. However, the impact of EV-mediated receptor transfer in vivo remains to be determined.

2.7. Acknowledgments

We would like to thank Nicole C. Smith at the Cold-ocean Deep-water Research Facility, Memorial University of Newfoundland, and Stephanie Tucker and Chris Corkum at the Medical Laboratory Facilities, Memorial University of Newfoundland, for expert assistance with flow cytometry. We thank the staff from Animal Care Services, Memorial University of Newfoundland, for their excellent assistance. The visual abstract was created in Biorender.com.

2.8. References

1. Yáñez-Mó, M. et al. Biological properties of extracellular vesicles and their physiological functions. *J. Extracell. Vesicles* 4, 27066 (2015).
2. Pegtel, D. M., Peferoen, L. & Amor, S. Extracellular vesicles as modulators of cell-to-cell communication in the healthy and diseased brain. *Philos. Trans. R. Soc. B Biol. Sci.* 369, 20130516 (2014).
3. Jeppesen, D. K., Zhang, Q., Franklin, J. L. & Coffey, R. J. Extracellular vesicles and nanoparticles: emerging complexities. *Trends Cell Biol.* 33, 667–681 (2023).
4. Brodeur, A. et al. Apoptotic exosome-like vesicles transfer specific and functional mRNAs to endothelial cells by phosphatidylserine-dependent macropinocytosis. *Cell Death Dis.* 14, 449 (2023).
5. Van Niel, G. et al. Challenges and directions in studying cell-cell communication by extracellular vesicles. *Nat. Rev. Mol. Cell Biol.* 23, 369–382 (2022).
6. Crompot, E. et al. Extracellular vesicles of bone marrow stromal cells rescue chronic lymphocytic leukemia B cells from apoptosis, enhance their migration and induce gene expression modifications. *Haematologica* 102, 1594–1604 (2017).
7. Witwer, K. W. et al. Standardization of sample collection, isolation and analysis methods in extracellular vesicle research. *J. Extracell. Vesicles* 2, 20360 (2013).
8. Kubo, H. Extracellular Vesicles in Lung Disease. *Chest* 153, 210–216 (2018).
9. Robbins, P. D. & Morelli, A. E. Regulation of immune responses by extracellular vesicles. *Nat. Rev. Immunol.* 14, 195–208 (2014).
10. Tkach, M. & Théry, C. Communication by Extracellular Vesicles: Where We Are and Where We Need to Go. *Cell* 164, 1226–1232 (2016).

11. Raposo, G. et al. B lymphocytes secrete antigen-presenting vesicles. *J. Exp. Med.* 183, 1161–72 (1996).
12. Teo, B. H. D. & Wong, S. H. MHC class II-associated invariant chain (Ii) modulates dendritic cells-derived microvesicles (DCMV)-mediated activation of microglia. *Biochem. Biophys. Res. Commun.* 400, 673–678 (2010).
13. Longjohn, M. N. et al. Deciphering the messages carried by extracellular vesicles in hematological malignancies. *Blood Rev.* 46, 100734 (2021).
14. Wen, J., Creaven, D., Luan, X. & Wang, J. Comparison of immunotherapy mediated by apoptotic bodies, microvesicles and exosomes: apoptotic bodies' unique anti-inflammatory potential. *J. Transl. Med.* 21, 478 (2023).
15. Pužar Dominkuš, P. et al. PKH26 labeling of extracellular vesicles: Characterization and cellular internalization of contaminating PKH26 nanoparticles. *Biochim. Biophys. Acta BBA - Biomembr.* 1860, 1350–1361 (2018).
16. Lai, C. P. et al. Dynamic Biodistribution of Extracellular Vesicles in Vivo Using a Multimodal Imaging Reporter. *ACS Nano* 8, 483–494 (2014).
17. Lai, C. P. et al. Visualization and tracking of tumour extracellular vesicle delivery and RNA translation using multiplexed reporters. *Nat. Commun.* 6, 1–12 (2015).
18. Pieper, K., Grimbacher, B. & Eibel, H. B-cell biology and development. *J. Allergy Clin. Immunol.* 131, 959–71 (2013).
19. Hardy, R. R., Carmack, C. E., Shinton, S. A., Kemp, J. D. & Hayakawa, K. Resolution and characterization of pro-B and pre-pro-B cell stages in normal mouse bone marrow. *J. Exp. Med.* 173, 1213–1225 (1991).
20. Hardy, R. R. et al. B-cell commitment, development and selection. *Immunol. Rev.* 175, 23–32 (2000).

21. Rolink, A. & Melchers, F. B-cell development in the mouse. *Immunol. Lett.* 54, 157–161 (1996).
22. Fang, X., Zheng, P., Tang, J. & Liu, Y. CD24: from A to Z. *Cell. Mol. Immunol.* 7, 100–103 (2010).
23. Kristiansen, G., Sammar, M. & Altevogt, P. Tumour Biological Aspects of CD24, A Mucin-Like Adhesion Molecule. *J. Mol. Histol.* 35, 255–262 (2003).
24. Kay, R., Rosten, P. M. & Humphries, R. K. CD24, a signal transducer modulating B cell activation responses, is a very short peptide with a glycosyl phosphatidylinositol membrane anchor. *J. Immunol.* 147, 1412–6 (1991).
25. Ayre, D. C. & Christian, S. L. CD24: A Rheostat That Modulates Cell Surface Receptor Signaling of Diverse Receptors. *Front. Cell Dev. Biol.* 4, 1–6 (2016).
26. Chappel, M. S. et al. Cross-linking the murine heat-stable antigen induces apoptosis in B cell precursors and suppresses the anti-CD40-induced proliferation of mature resting B lymphocytes. *J. Exp. Med.* 184, 1639–1649 (1996).
27. Hough, M. R. et al. Reduction of early B lymphocyte precursors in transgenic mice overexpressing the murine heat-stable antigen. *J Immunol* 156, 479–488 (1996).
28. Ayre, D. C. C. et al. Dynamic regulation of CD24 expression and release of CD24-containing microvesicles in immature B cells in response to CD24 engagement. *Immunology* 146, 217–233 (2015).
29. Ayre, D. C. C. et al. CD24 induces changes to the surface receptors of B cell microvesicles with variable effects on their RNA and protein cargo. *Sci. Rep.* 7, 8642 (2017).
30. Nielsen, P. J. et al. Altered Erythrocytes and a Leaky Block in B-Cell Development in CD24/HSA-Deficient Mice. *Blood* 89, 1058–1067 (1997).

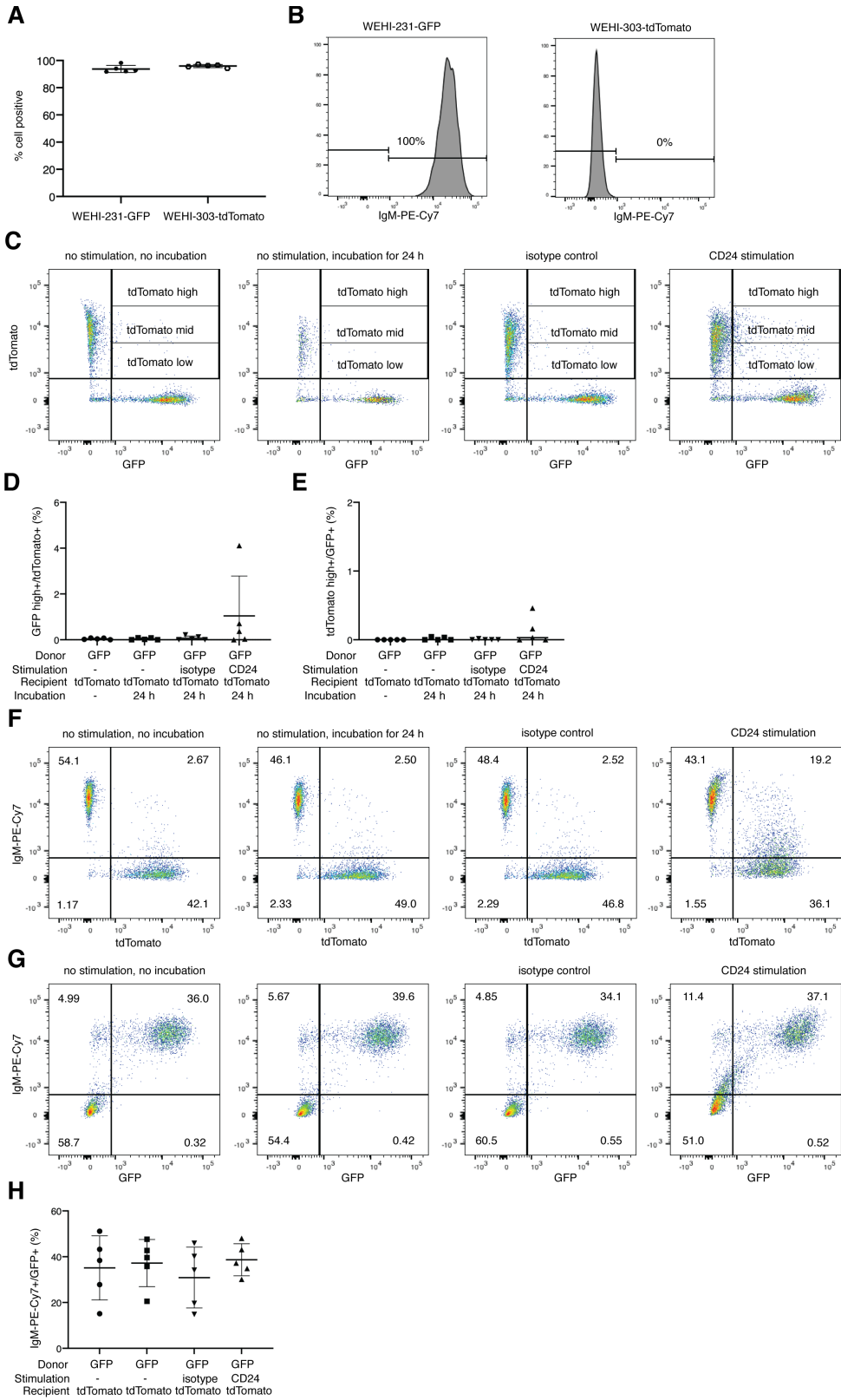
31. Chen, G.-Y., Tang, J., Zheng, P. & Liu, Y. CD24 and Siglec-10 Selectively Repress Tissue Damage-Induced Immune Responses. *Science* 323, 1722–1725 (2009).
32. Fairbridge, N. A. et al. Loss of CD24 in Mice Leads to Metabolic Dysfunctions and a Reduction in White Adipocyte Tissue. *PLOS ONE* 10, e0141966 (2015).
33. Condon, C., Hourihane, S. L., Dang-Lawson, M., Escribano, J. & Matsuuchi, L. Aberrant Trafficking of the B Cell Receptor Ig- $\alpha\beta$ Subunit in a B Lymphoma Cell Line. *J. Immunol.* 165, 1427–1437 (2000).
34. Théry, C., Amigorena, S., Raposo, G. & Clayton, A. Isolation and Characterization of Exosomes from Cell Culture Supernatants and Biological Fluids. *Curr. Protoc. Cell Biol.* 30, 3.22.1-3.22.29 (2006).
35. Grandoch, M. et al. B cell receptor-induced growth arrest and apoptosis in WEHI-231 immature B lymphoma cells involve cyclic AMP and Epac proteins. *Cell. Signal.* 21, 609–621 (2009).
36. Ghosh, A. et al. Rapid Isolation of Extracellular Vesicles from Cell Culture and Biological Fluids Using a Synthetic Peptide with Specific Affinity for Heat Shock Proteins. *PLoS ONE* 9, e110443 (2014).
37. Ten Hacken, E. et al. Functional Differences between IgM and IgD Signaling in Chronic Lymphocytic Leukemia. *J. Immunol.* 197, 2522–2531 (2016).
38. Ung, T. H., Madsen, H. J., Hellwinkel, J. E., Lencioni, A. M. & Graner, M. W. Exosome proteomics reveals transcriptional regulator proteins with potential to mediate downstream pathways. *Cancer Sci.* 105, 1384–1392 (2014).
39. Hink, M. A. et al. Structural dynamics of green fluorescent protein alone and fused with a single chain Fv protein. *J. Biol. Chem.* 275, 17556–17560 (2000).

40. Maas, S. L. N., Breakefield, X. O. & Weaver, A. M. Extracellular Vesicles: Unique Intercellular Delivery Vehicles. *Trends in Cell Biology* vol. 27 172–188 Preprint at <https://doi.org/10.1016/j.tcb.2016.11.003> (2017).
41. Ayre, D. C. et al. Dynamic regulation of CD24 expression and release of CD24-containing microvesicles in immature B cells in response to CD24 engagement. *Immunology* 146, 217–33 (2015).
42. Ayre, D. C. et al. CD24 induces changes to the surface receptors of B cell microvesicles with variable effects on their RNA and protein cargo. *Sci. Rep.* 7, 8642 (2017).
43. Hasbold, J. & Klaus, G. G. B. Anti-immunoglobulin antibodies induce apoptosis in immature B cell lymphomas. *Eur. J. Immunol.* 20, 1685–1690 (1990).
44. Benhamou, L. E., Cazenave, P. -a & Sarthou, P. Anti-immunoglobulins induce death by apoptosis in WEHI-231 B lymphoma cells. *Eur. J. Immunol.* 20, 1405–1407 (1990).
45. Page, D. M. & DeFranco, A. L. Antigen receptor-induced cell cycle arrest in WEHI-231 B lymphoma cells depends on the duration of signaling before the G1 phase restriction point. *Mol. Cell. Biol.* 10, 3003–3012 (1990).
46. Suzuki, T. et al. CD24 induces apoptosis in human B cells via the glycolipid-enriched membrane domains/rafts-mediated signaling system. *J Immunol* 166, 5567–5577 (2001).
47. Cheng, P. C., Dykstra, M. L., Mitchell, R. N. & Pierce, S. K. A role for lipid rafts in B cell antigen receptor signaling and antigen targeting. *J. Exp. Med.* 190, 1549–1560 (1999).
48. Eeva, J. & Pelkonen, J. Mechanisms of B Cell Receptor Induced Apoptosis. *Apoptosis* vol. 9 525–531 (Springer, 2004).
49. Nadiri, A. et al. CD40 translocation to lipid rafts: Signaling requirements and downstream biological events. *Eur. J. Immunol.* 41, 2358–2367 (2011).

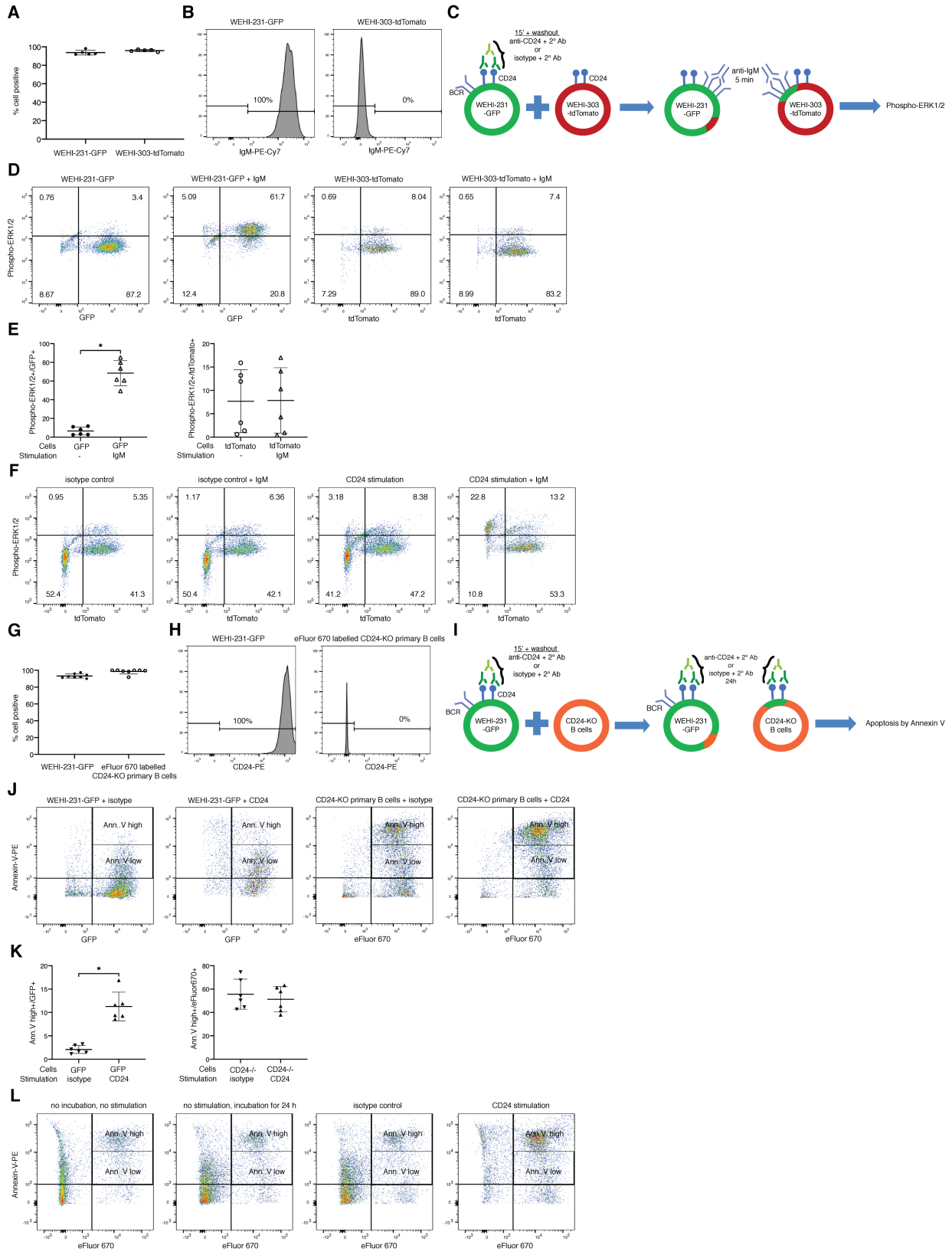
50. Tsubata, T., Wu, J. & Honjo, T. B-cell apoptosis induced by antigen receptor crosslinking is blocked by a T-cell signal through CD40. *Nature* 364, 645–648 (1993).
51. Klyushnenkova, E. N., Li, L., Armitage, R. J. & Choi, Y. S. CD48 delivers an accessory signal for CD40-mediated activation of human B cells. *Cell. Immunol.* 174, 90–98 (1996).
52. Elishmereni, M. & Levi-Schaffer, F. CD48: A co-stimulatory receptor of immunity. *International Journal of Biochemistry and Cell Biology* vol. 43 25–28 Preprint at <https://doi.org/10.1016/j.biocel.2010.09.001> (2011).
53. Garnett, D. & Williams, A. F. Homotypic adhesion of rat B cells, but not T cells, in response to cross-linking of CD48. *Immunology* 81, 103–110 (1994).
54. Simak, J. & Gelderman, M. P. Cell membrane microparticles in blood and blood products: Potentially pathogenic agents and diagnostic markers. *Transfus. Med. Rev.* 20, 1–26 (2006).
55. Pasquet, J.-M., Dachary-Prigent, J. & Nurden, A. T. Calcium Influx is a Determining Factor of Calpain Activation and Microparticle Formation in Platelets. *Eur. J. Biochem.* 239, 647–654 (1996).
56. Allolio, C. & Harries, D. Calcium ions promote membrane fusion by forming negative-curvature inducing clusters on specific anionic lipids. *bioRxiv* 2020.04.29.068221 (2020) [doi:10.1101/2020.04.29.068221](https://doi.org/10.1101/2020.04.29.068221).
57. Stachowiak, J. C. et al. Membrane bending by protein–protein crowding. *Nat. Cell Biol.* 14, 944–949 (2012).
58. Mulcahy, L. A., Pink, R. C. & Carter, D. R. F. Routes and mechanisms of extracellular vesicle uptake. *J. Extracell. Vesicles* 3, 24641 (2014).
59. Valapala, M. & Vishwanatha, J. K. Lipid raft endocytosis and exosomal transport facilitate extracellular trafficking of annexin A2. *J. Biol. Chem.* 286, 30911–30925 (2011).

60. Al-Nedawi, K. et al. Intercellular transfer of the oncogenic receptor EGFRvIII by microvesicles derived from tumour cells. *Nat. Cell Biol.* 10, 619–624 (2008).
61. Del Conde, I., Shrimpton, C. N., Thiagarajan, P. & López, J. A. Tissue-factor-bearing microvesicles arise from lipid rafts and fuse with activated platelets to initiate coagulation. *Blood* 106, 1604–1611 (2005).
62. Falati, S. et al. Accumulation of tissue factor into developing thrombi in vivo is dependent upon microparticle P-selectin glycoprotein ligand 1 and platelet P-selectin. *J. Exp. Med.* 197, 1585–1598 (2003).

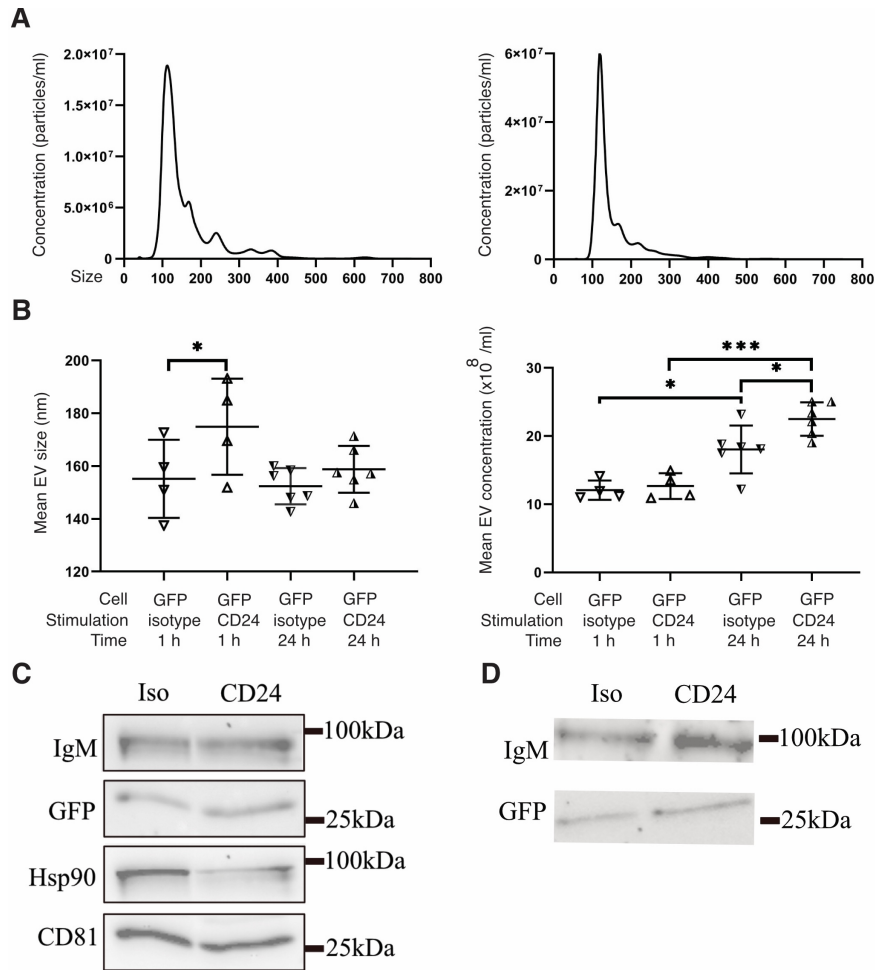
2.9. Supplemental figures



Supplemental Figure 2.1. Cell characterization and gating strategies. CD24 was stimulated and cells co-cultured as in figure 2.1. (A) The percentage of cells positive for GFP and tdTomato. (B) WEHI-231-GFP are 100% IgM positive while WEHI-303-tdTomato do not express IgM on their cell membrane. (C) Representative dotplots of GFP-positive cells with low or mid or high tdTomato signal. (D) Percent tdTomato-positive cells with high GFP signal. (E) Percent GFP-positive cells with high tdTomato signal. (F) Representative dotplots of IgM on WEHI-303-tdTomato and (G) WEHI-231-GFP after stimulation and co-culture. (H) Percent IgM and GFP double-positive cells. Non-significant by one-way ANOVA.

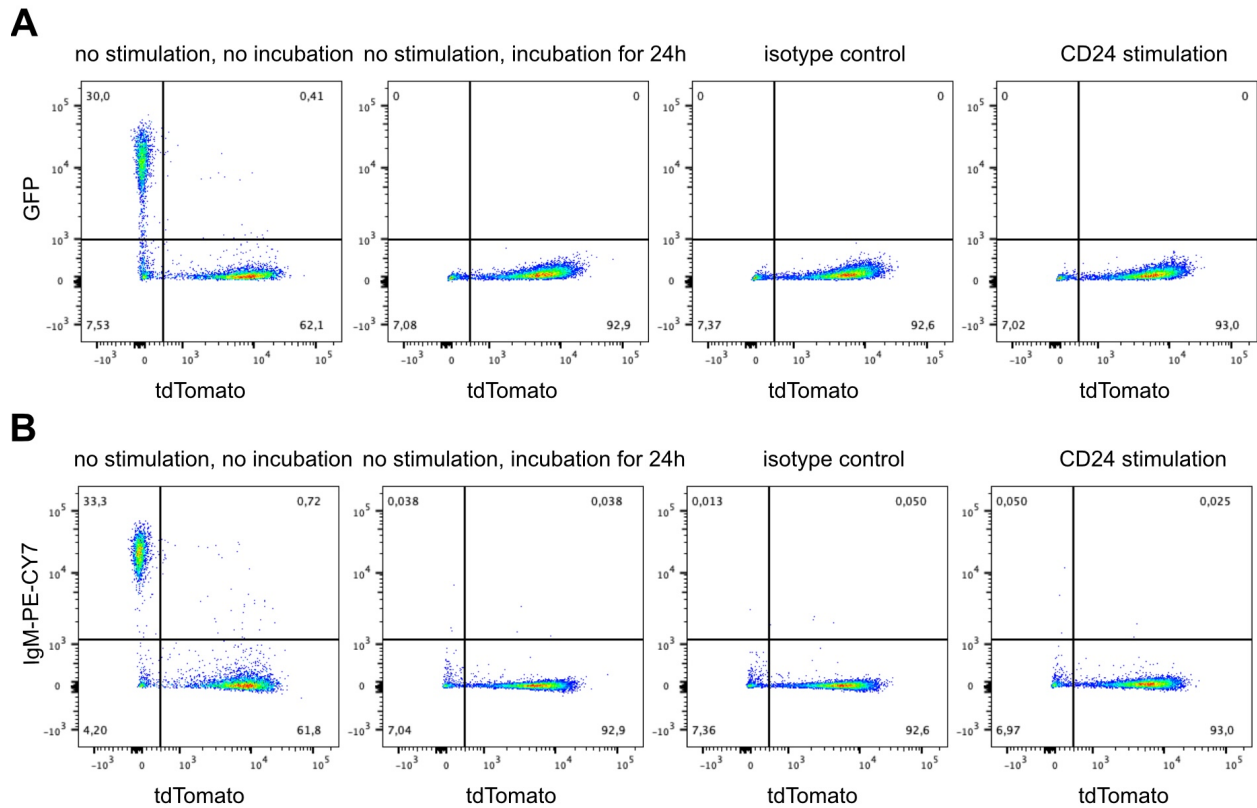


Supplemental Figure 2.2. CD24 stimulation causes transfer of functional IgM and CD24 from donor to recipient cells. Cells were treated as described in figure 2.4. (A) The percentage of cells positive for GFP and tdTomato. (B) WEHI-231-GFP are 100% IgM positive while WEHI-303-tdTomato do not express IgM on their cell membrane. (C) Schematic of experimental design for panels D – F. (D) Representative dotplots and (E) graphical analysis of phospho-ERK1/2 levels on WEHI-231-GFP due to IgM stimulation with no response in WEHI-303-tdTomato cells. (F) Representative dotplots of phospho-ERK1/2 levels in control and co-culture experiments. (G) Percentage of cells positive for GFP and eFluor 670. (H) CD24 is expressed on WEHI-231-GFP but not eFluor 670-labeled primary bone marrow B cells from CD24KO mice. (I) Schematic of experimental design for panels J – L. (J) Representative dotplots and (K) graphical analysis of apoptosis on WEHI-231-GFP due to CD24 stimulation with no response in primary CD24KO B cells. (L) Representative dotplots of annexin-V-positive cells in co-culture experiments (n = 6), significance was determined by Wilcoxon matched pairs test *P<0.05.

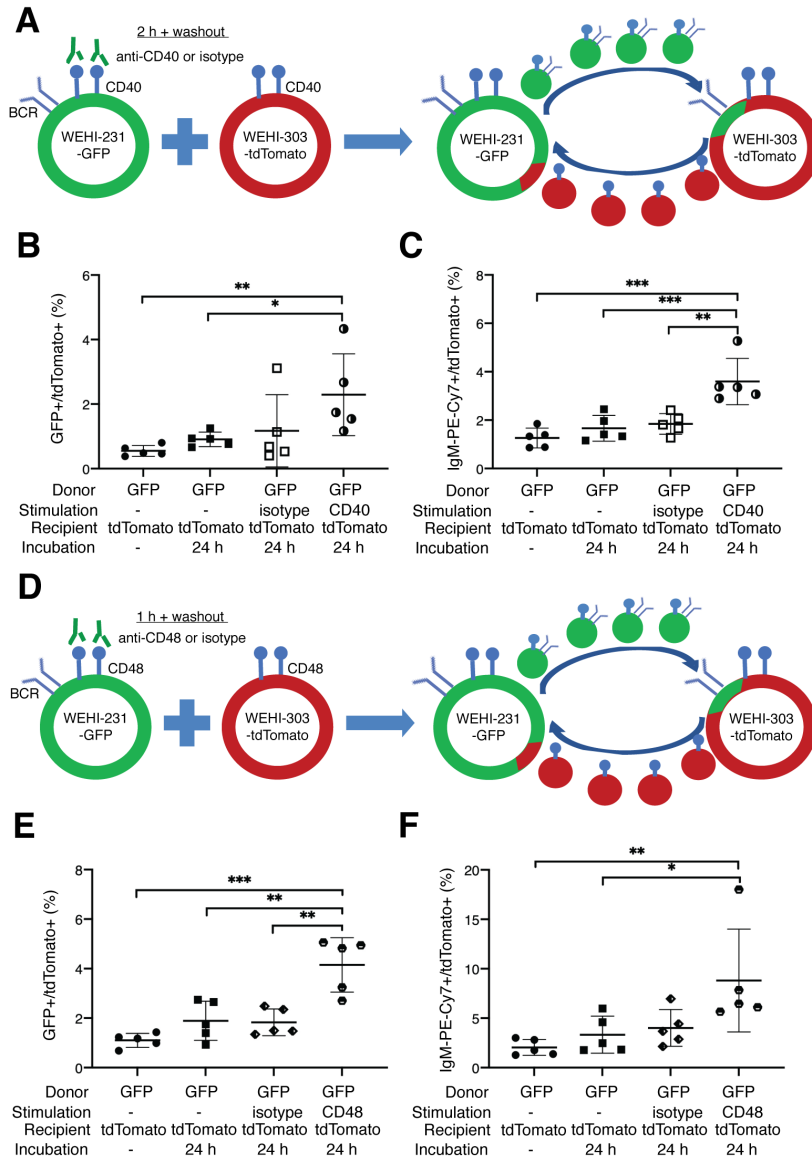


Supplemental Figure 2.3. Characterization of EVs isolated from cell culture. (A)

Representative nanoparticle tracking (NTA) plots of particle sizes and concentrations in supernatants from WEHI-231-GFP cells stimulated with either isotype (right) or CD24 (left) antibody for 24 h in EV-free media. (B) The mean size (left) and concentration (right) of particles from supernatants with either isotype or CD24 stimulation after 1 h (n=4) and 24 h (n=6). Significance was determined by a one-way ANOVA followed by the Sidak's multiple comparison test *P<0.05, ***P<0.005. (C-D) Western blot identified proteins enriched in EVs originating from isotype and CD24 stimulated WEHI-231-GFP cells and isolation by Vn96 peptide-based pull-down (C) and size exclusion chromatography (D), respectively. The position of the molecular weight markers is shown on the right (n=3).



Supplemental Figure 2.4. CD24 stimulation of donor cells did not induce GFP or BCR transfer to recipient cells through a transwell system. WEHI-231-GFP were stimulated with anti-CD24 or control (isotype) for 15 min, or left untreated, followed by washout and then incubated in the upper well, whereas WEHI-303-tdTomato incubated in the bottom well of a transwell system. Individually cultured, untreated cells were mixed immediately before the last centrifugation step. (A) Representative dot plots of percent GFP and tdTomato double-positive cells. (B) Representative dot plots of percent IgM and tdTomato double-positive cells.



Supplemental Figure 2.5. CD40 induces transfer of IgM but not lipid while CD48 induces transfer of lipid but not IgM. (A) Schematic of experimental design for panels B – C. WEHI-231-GFP were stimulated with anti-CD40 (10 μ g/ml) or control (isotype) for 2 h, or left untreated, followed by washout and then a 24 h co-culture with WEHI-303-tdTomato. Singly cultured, untreated cells were mixed immediately before the last centrifugation step. (B) Percent GFP and tdTomato double-positive cells. (C) Percent IgM and tdTomato double-positive cells (n=5). (D) Schematic of experimental design for panels E – F. WEHI-231-pGFP were stimulated

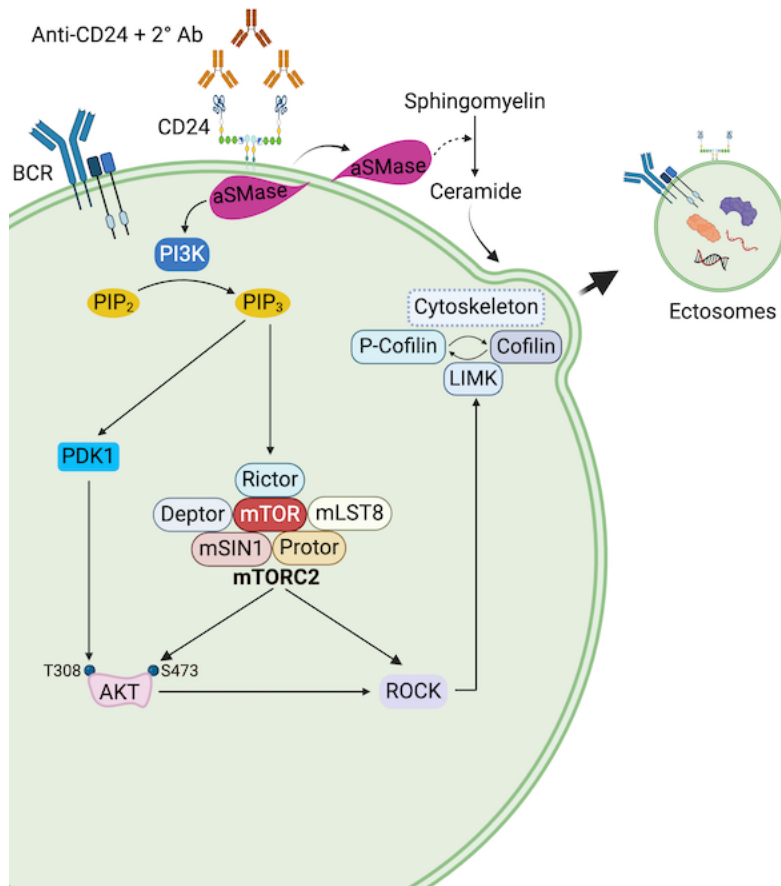
with anti-CD48 (10 $\mu\text{g/ml}$) or control (isotype) for 1 h, or left untreated, followed by washout and then a 24 h co-culture with WEHI-303-tdTomato. Singly cultured, untreated cells were mixed immediately before the last centrifugation step. (E) Percent GFP and tdTomato double-positive cells. (F) Percent IgM and tdTomato double-positive cells (n=5). Significance was determined by a one-way ANOVA followed by the Sidak's multiple comparison test * $P < 0.05$, ** $P < 0.01$, *** $P < 0.005$.

Chapter 3: CD24 regulates extracellular vesicle release via an aSMase/PI3K/mTORC2/ROCK/actin pathway in B lymphocytes

3.1. Abstract

CD24 is a glycosphosphatidylinositol-linked protein that regulates B cell development. We previously reported that stimulation of CD24 on donor B cells promotes the transport of functional receptors to recipient B cells via extracellular vesicles (EVs). However, the mechanisms regulating EV formation in response to CD24 are unknown. Using bioinformatics, we found a connection between CD24 and the PI3K/AKT and mTOR signaling pathways. To determine if PI3K or mTOR regulates EV release, we made use of our co-culture model, whereby donor B cells carrying the B cell receptor (BCR, IgM) that release EVs labeled with palmitoylated GFP upon CD24 stimulation are incubated with recipient B cells that lack IgM and express palmitoylated tdTomato. Using flow cytometry, we followed the transfer of EVs carrying lipid-associated GFP and surface IgM from donor to recipient cells. Using chemical and genetic inhibition, we found that a PI3K/mTORC2/ROCK/actin pathway regulates EV release. We also found that acid sphingomyelinase (aSMase) activates PI3K to induce EV release. Lastly, through live cell imaging, we found that ROCK is required for inducing the membrane dynamics associated with EV release. Overall, our data suggest that these EVs are ectosomes budded from the plasma membrane and not intracellularly derived exosomes. Importantly, we have uncovered a novel pathway regulating ectosome release.

3.2. Graphical abstract



CD24 activation triggers aSMase, which in turn activates the PI3K/AKT and mTORC2 signaling pathways, leading to the local disassembly of the cytoskeletal elements favoring ectosome release. Created with BioRender.com.

3.3. Introduction

Extracellular vesicles (EVs) are a heterogeneous group of small lipid bilayer-bound particles released by all cells tested to date¹. There are two primary kinds of EVs described, exosomes and ectosomes, the latter which includes microvesicles, that are distinguished based on their biogenesis². Exosomes originate from intraluminal vesicles (ILVs) that form through the inward budding of the endosomal membrane, resulting in the formation of multivesicular bodies (MVB). This is followed by secretion upon fusion of the MVB with the cell plasma membrane. Exosomes typically range in size from 30 to 150 nm³⁻⁵. Exosomes tend to be enriched in a number of proteins including chaperones (Hsp70 and Hsp90), cytoskeletal proteins (actin, myosin, and tubulin), endosomal sorting complex required for transport (ESCRT) proteins (TSG-101 and Alix), proteins involved in transport and fusion (Rab11, Rab7, Rab2, and Annexins), and tetraspanin proteins (CD9, CD63, CD81, and CD82)³⁻⁷. Ectosomes are generally considered to be 100-1000 nm in diameter and formed by direct outward budding from the surface of the plasma membrane. Ectosomes tend to be enriched in some proteins that differ from exosomes such as GTP-binding protein, ADP-ribosylation factor 6 (ARF6), matrix metalloproteinases (MMPs), glycoproteins (e.g., GPIb, GPIIb-IIIa), integrins, receptors (e.g., EGFRvIII), and cytoskeletal elements (e.g., β -actin and α -actinin-4)³⁻⁶.

Exosome release can be regulated by two distinct processes, namely the ESCRT and ESCRT-independent pathways that also participate in ILV formation. The ESCRTs are made up of four complexes (ESCRT-0, -I, -II, and -III) and the accessory Vps4 complex, each of which is made up of many subunits⁸. The primary job of ESCRT 0-II is to sort cargo on endosomal membranes into functional microdomains. In contrast, Vps4 assists ESCRT-III in completing the process of budding and scission of these domains to produce ILVs⁹. Recent evidence has revealed

that TSG101 and ALIX are often seen as exosome constituent proteins and are components of the ESCRT complex. The ESCRT accessory protein ALIX interacts with ESCRT-III subunits to promote intraluminal vesicle budding and abscission¹⁰. Moreover, Rab GTPases, the most prevalent family of proteins in the Ras superfamily of GTPases, are essential for exosome secretion and play a key role in intracellular vesicle transport, including endosome recycling and MVB trafficking to lysosomes¹¹. More research has revealed that many Rab proteins, including Rab27A/B, Rab7, Rab31, and Rab35, are involved in the control of exosome secretion¹². It has also been reported that Rab GTPases and SNARE proteins collaborate to cause the release of exosomes into the extracellular space by fusion of late endosomes with the plasma membrane^{11,13}. Although the ESCRT pathway is the critical driver of exosome synthesis, other studies have demonstrated exosomes can be released via an ESCRT-independent pathway. For instance, inhibition of the ESCRT-dependent pathway by depleting four ESCRTs did not eliminate MVB formation¹⁴. Another study reported that the release of exosomes is reduced after inhibition of neutral sphingomyelinase (nSMase), a protein responsible for the production of ceramide, suggesting that the budding of ILVs requires ceramide, an important component of lipid raft microdomains¹⁵. In addition, ApoE and tetraspanin CD63 are recruited for ILV formation and subsequent exosome release without the requirement of ESCRT or ceramide^{16,17}.

Ectosome release can be regulated via several pathways. For example, it has been shown that ectosome release can be stimulated through an increase in intracellular Ca^{2+} concentrations¹⁸. At steady state, the anionic phospholipids, phosphatidylserine (PS) and phosphatidylethanolamine (PE) localize to the inner leaflet of the plasma membrane, while phosphatidylcholine (PC) and sphingomyelin (SM) are found on the external membrane leaflet¹⁹. The physiological membrane asymmetry is maintained by five transmembrane enzymes: flippase, floppase, scramblase, translocase and calpain²⁰. The increase in cytoplasmic Ca^{2+} levels inhibits

the aminophospholipid translocase and activates lipid scramblase simultaneously^{21,22}. This process drives rearrangements in the asymmetry of the membrane phospholipids to expose PS from the inner leaflet to the cell surface. It then leads to the physical collapse of cell membrane asymmetry, which can promote ectosome release²³.

In addition to lipids, cytoskeletal elements and their regulators are required for ectosome formation²⁴. Reducing the levels of phosphatidylinositol 4,5-bisphosphate (PI(4,5)P₂), which participates in anchoring the membrane to the cortical cytoskeleton, can induce the disruption of the cortical cytoskeleton interaction with the plasma membrane^{25,26}, leading to increased ectosome biogenesis²⁷. Reduction of PI(4,5)P₂ can occur via activation of phospholipase C (PLC)- γ , phospholipase D (PLD), phosphoinositide 3-kinases (PI3Ks), or phosphatidylinositol phosphatases²⁸. Rab22a and ARF6, members of the Ras GTPase family, also have essential roles in ectosome generation. Rab22A is directly involved in ectosome formation as evidenced by its colocalization with budding vesicles and the fact that Rab22A knockdown prevents vesicle release²⁹. Importantly, ARF6 activity is required for subsequent phospholipase D activation, leading to localized myosin light chain kinase activity at the neck of budding vesicles³⁰. Furthermore, ARF6-mediated activation of RhoA and Rho-associated kinase (ROCK) signaling has been implicated in ectosome formation^{30,31}. An additional study has shown that the antagonistic interaction between Rab35 and ARF6 also controls ectosome biogenesis³². Furthermore, a key regulator in the formation of ectosomes, Ca²⁺ ions also contribute to the reorganization of the cytoskeleton through the activation of cytosolic calpain protease³³. Calpain cleaves several cytoskeletal components such as actin, ankyrin, protein 4.1 and spectrin^{34,35}. Calpain-mediated cleavage of the cytoskeleton further disrupts the cortical cytoskeleton protein

network, consequently, allowing membrane budding³⁶. Lastly, similar to exosomes, ceramide production can increase ectosome release³⁷.

CD24 (also known as heat stable antigen) is a glycoposphatidylinositol (GPI)-anchored glycoprotein, which is localized to lipid rafts on the plasma membrane³⁸. It contains 27 amino acids with extensive N-linked and O-linked glycosylation that can result in variable molecular weight products. CD24 is expressed on several cell types, including B cells, T cells, neutrophils, eosinophils, dendritic cells, macrophages, epithelial cells, and cancer cells. During B cell development in the bone marrow, CD24 is first expressed by pro-B cells (also called Fraction B) but is also highly expressed at the pre-B cell (Fraction C, C', and D) stages and in transitional B cells³⁹.

One of the most well-described effects of CD24-mediated signaling is its promotion of apoptosis in developing B cells⁴⁰. CD24 recruits Src family protein tyrosine kinases (PTKs) to activate signalling pathways via direct protein phosphorylation, intracellular calcium mobilization, and transcription factor activation³⁹. Moreover, existing evidence has demonstrated that multiple cancer related signaling pathways, such as Wnt/ β -catenin, mitogen activated protein kinase (MAPK), Src or PI3K/Akt, Notch, and Hedgehog, are activated downstream of CD24⁴¹.

We previously discovered that the engagement of CD24 enhances the release of EVs from ex vivo bone marrow-derived B cells and the mouse WEHI-231 B cell lymphoma cell lines⁴². We also found that the RNA cargo and the EV proteome are relatively stable, but the composition of the membrane proteins on the EVs is altered⁴³. Recently, we employed a model system where donor cells expressing palmitoylated GFP (WEHI-231-GFP cells) were co-cultured, after CD24 stimulation, with recipient cells lacking IgM and expressing palmitoylated tdTomato (WEHI-303-tdTomato cells) to study EV-mediated transfer of functional receptors. We found that EVs

trafficked lipid and membrane proteins between B lymphocytes in response to stimulation of CD24 on the donor cells. Notably, the transported receptors can induce apoptosis, which may affect B cell development in recipient bystander B cells during B cell development⁴⁴. The data from our previous studies suggest that the EVs induced by CD24 stimulation are ectosomes budded off the plasma membrane, not exosomes derived from MVBs. However, the underlying mechanisms that govern ectosome formation in response to engagement of CD24 have not been described.

To identify the relationship between CD24 gene expression and signaling pathways in B cells, we analyzed the expression of genes differentially expressed in the same manner as CD24 across B cell development using a dataset from the Immunological Genome Project (ImmGen) database⁴⁵. Network analysis revealed that CD24 expression is associated with genes that are enriched in the PI3K/Akt/mTOR signaling pathway. Therefore, in this study, we addressed the hypothesis that CD24-mediated ectosome release is regulated by the PI3K/Akt/mTOR pathway. Using our co-culture model, we found that CD24 mediates ectosome release via the activation of acid sphingomyelinase (aSMase), which activates the PI3K/mTORC2/ROCK pathways followed by actin cytoskeletal rearrangement.

3.4. Materials and Methods

3.4.1. Cell culture

WEHI-231 cells (American Type Culture Collection (ATCC), Manassas, VA) and WEHI-303.1.5 (WEHI-303)⁴⁶ were transfected with a lentiviral plasmid encoding either palm-GFP (WEHI-231-GFP) or palm-tdTomato (WEHI-303-tdTomato) obtained from Charles Lai, Institute of Atomic and Molecular Sciences, Taiwan⁴⁷. Cells were cultured in RPMI-1640 medium (Gibco) containing 10% heat-inactivated fetal bovine serum (FBS) (Gibco), 1.0 mM sodium pyruvate

(Gibco), 50 mM 2-mercaptoethanol (Sigma) and 100 U/ml penicillin, 100 µg/ml streptomycin (Invitrogen). For knockdown experiments, WEHI-231-GFP cells (2×10^5) were transiently transfected with 2 mM siRNA with the Neon Transfection Kit (MPK1025B, Invitrogen) using the Neon Electroporation system according to the manufacturer's instructions. The siRNAs used were control non-targeting siRNA-A (Santa Cruz Biotechnology, SC-37007), PI 3-kinase p110 δ siRNA (Santa Cruz Biotechnology, SC-39132), and Rock-1 siRNA (Santa Cruz Biotechnology, SC-36432). Cells were pulsed once with a voltage of 1700 and a width of 20. Transfected cells were cultured for 55 h before use.

3.4.2. Bioinformatics

ImmGen data (accession number GSE15907), containing gene expression data for B cells in the Fraction (Fr) A-F stages of development, was identified. The microarray gene expression data files for Fr A, Fr B/C, Fr C', Fr D, and Fr F were background corrected, and robust multi-array average (RMA) normalized using the Oligo, Biobase, and pd.mogene.1.0.st.v1 Bioconductor packages in R version 4.0.0. A list of differentially expressed genes with similar expression patterns to Cd24a was then compiled using the Limma and Affycoretools Bioconductor packages. Fr A B cells (pre-pro B cells) was used as the negative control for the differential expression analysis.

Differential expression analysis produced a list of 1838 genes expressed in a similar manner as Cd24a. The gene transcript cluster ID list was annotated with the corresponding gene names using the NetAffx analysis batch query and merged with the R expression data to create a median linkage hierarchical cluster in Genesis version 1.8.1. A clade of 44 genes whose expression patterns were most similar to that of Cd24a was identified (Figure 1A). Of the 44

genes in the clade, 41 were annotated. These 41 genes were used to generate pathway networks in Cytoscape version 3.8.0 using the ClueGO plugin version 2.5.7. The analysis used pathway network data from the KEGG, REACTOME Pathways, and WikiPathways databases to compile a network of signaling pathways associated with the 41 gene list.

3.4.3. Phosphatidylinositol (3,4,5)-trisphosphate (PIP₃) Quantification

WEHI-231-GFP cells (0.5×10^6) were pre-treated with the PI3K inhibitor, 10 μ M LY294002 (9901, Cell Signaling Technology), 10 μ M imipramine (J63723.06, Alfa Aesar), or with an equal volume of DMSO in a 37°C water bath for 15 min. Cells were then stimulated with 10 μ g/ml of functional grade primary monoclonal M1/69 rat anti-mouse CD24 antibody (16-0242085, eBioscience) or 10 μ g/ml matching primary isotype antibody (16-4031-85, eBioscience) that was pre-incubated with 5 μ g/ml goat anti-rat secondary antibody (112-005-003, Jackson ImmunoResearch) at RT for 15 min. After treatment, cells were centrifuged and phosphoinositides were extracted and measured using the PIP₃ ELISA kit (Creative Diagnostic, DEIA-XYZ6). All experiments were performed at least four times, each carried out in duplicate according to the manufacturer's instructions.

3.4.4. Analysis of cell surface IgM and lipid transfer by flow cytometry

WEHI-231-GFP cells (0.5×10^6) were pre-treated with either DMSO or inhibitor in a 37°C water bath for 15 min. The following inhibitors were used: 10 μ M LY294002^{48,49}, 0.25 μ M MK2206^{50,51} (S1078, Selleckchem), 0.25 μ M Torin 1^{52,53} (14379S, Cell Signaling Technology), 0.1 μ M rapamycin^{54,55} (A8167, APEX BIO), 0.1 μ M JR-AB2-011^{54,56} (HY-122022, MedChemExpress), 10 μ M Y27632^{57,58} (13624S, Cell Signaling Technology), 0.2 μ M

cytochalasin D⁵⁹ (PHZ1063, Gibco, ThermoFisher), 10 μ M imipramine⁶⁰, 20 μ M Arc39^{61,62} (1-aminodecylidene bis-phosphonic acid, 13583, Cayman Chemical), 20 μ M GW4869^{61,63,64} (D1692, Sigma Aldrich), 0.5 μ g/mL ionomycin⁶⁵ (I24222, Thermo Fisher) or 20 μ M BAPTA-AM⁶⁶ (B1205, Thermo Fisher). Flow cytometry was used as an orthogonal method to determine cell viability after treatment based on a dot plot of forward scatter versus side scatter. This analysis confirmed that the compounds did not result in toxicity at the concentrations we have chosen. Cells then were stimulated with anti-mouse CD24 antibody or isotype antibody as above followed by centrifugation to remove excess antibody. Cells were then co-cultured with the recipient WEHI-303-tdTomato cells (0.5×10^6) in the incubator at 37°C for 24 h. To assess cell surface IgM and lipid transfer, the mixed cells were resuspended in ice-cold FACS buffer (1x PBS, pH 7.4, containing 1% heat-inactivated FBS) and then stained on ice for 30 min with 0.5 mg of IgM-PE-Cy7 (25-5890, eBioscience) to detect IgM. Cells were then washed with FACS buffer and analyzed by flow cytometry. Flow cytometry was performed using a CytoFLEX (Beckman Coulter) counting at least 10,000 events and data were analyzed using FlowJo software version 10.4.1.

3.4.5. Immunoblotting

Cell extracts were separated on 8% to 15% SDS-PAGE gels and transferred to nitrocellulose membranes, which were blocked with either 5% milk powder or 5% BSA in 0.1% Tween-20-Tris-buffered saline (TBST) for 1 h at room temperature. The membranes were incubated with primary antibody in TBST overnight at 4°C: phospho-Akt (Ser473) antibody (Cell Signaling Technology, #9271, 1:1000), Akt (Cell Signaling Technology, #9272, 1:1000), phospho-cofilin (Cell Signaling Technology, #3313; 1:1000), cofilin (Cell Signaling Technology,

#3318, 1:1000), Rock-1 antibody (G-6) (Santa Cruz Biotechnology, SC-17794, 1:500), PI3K p110 δ antibody (A-8) (Santa Cruz Biotechnology, SC-55589, 1:1000), GAPDH (G-9) (Santa Cruz Biotechnology, SC-365062, 1:1000). The membrane was washed and incubated with a horseradish peroxidase (HRP)-conjugated goat anti-rabbit IgG (H+L) (Bio Rad, #1706515) or goat anti-mouse IgG (H+L) (Bio Rad, #1721011). Immunoreactive bands were visualized on a Chemidoc gel system (BioRad) using an ECL substrate (WBULS0100, Millipore). Image manipulation involved adjustments to brightness and contrast only. Protein detection was performed using ImageLab (BioRad). The protein density of each band was assessed using ImageJ 1.53q software (National Institutes of Health).

3.4.6. Live cell imaging

Glass coverslips measuring 35 mm were cleaned thrice with 1x PBS and incubated with 1 mg/mL of anti-MHC class II antibody (Sigma, MABF33) overnight at 4°C. Then, 0.5×10^6 WEHI-231-GFP cells were seeded onto the glass coverslips for 30 min at 4°C. The cells were washed with PBS and visualized with a Carl Zeiss LSM 880 laser scanning microscope system with a 63x oil immersion lens with numerical aperture (NA) of 1.4 objective under environment at 37°C and 5% CO₂. Laser excitation light was provided at a wavelength of 488 nm, and fluorescent emissions were collected at wavelengths above 515 nm. For image acquisition, an exposure time of 0.8 second was adopted with a binning of 2 x 2 yielding a pixel size of 0.68 μ m. Individual cells within a single field of view were captured with an Airyscan detector over a 5-min period for 250 cycles, with a 1.2-second shuttered interval between each image. Raw Airyscan images were processed using the Zeiss Zen Blue analysis software. Subsequent image

processing was conducted in ImageJ to create a video with 25 frames per second for a 10-second length.

3.4.7. Statistical analysis

Prism software (version 10.1.1; GraphPad) was utilized to generate graphs and for statistical analyses. One-way ANOVA was performed for comparing more than 2 groups or for investigating the level of PIP₃, followed by Sidak's multiple comparisons post-hoc test. Two-way ANOVA was used to analyze lipid and protein transfer to the recipient cells in the presence of donor cells with inhibitor pre-treatment and antibody stimulation as independent variables, followed by Sidak's multiple comparisons post-hoc test. Differences were considered to be significant when P values were less than 0.05. The number of repetitions is indicated in each figure legend.

3.5. Results

Prior research from our lab showed that B cells release EVs in response to CD24 engagement⁴²⁻⁴⁴. As the first step in attempting to elucidate the pathway(s) responsible for CD24-mediated release of EVs, we performed a bioinformatics-based analysis to find potential signaling pathways linked to CD24 expression in developing B cells. We identified 44 genes in the clade that most closely resembled Cd24a (Figure 3.1A). Of these, 41 could be used to predict CD24-related signaling pathways. In the networks of connected pathway terms, seven of the nodes had terms related to PI3K/Akt/mTOR signalling (Figure 3.1B). Thus, we predicted that CD24 may activate PI3K signaling. To determine if engagement of CD24 activated PI3K, we analyzed the levels of PIP₃, the immediate product of PI3K activation. We found that PIP₃ levels were significantly increased in response to CD24 stimulation, but not with isotype-control

stimulated cells. In addition, we observed the increase of PIP₃ was inhibited in the presence of the PI3K inhibitor, 10 μM LY294002 (LY, Figure 3.1C). These results clearly demonstrate that CD24 triggers B cells to activate PI3K.

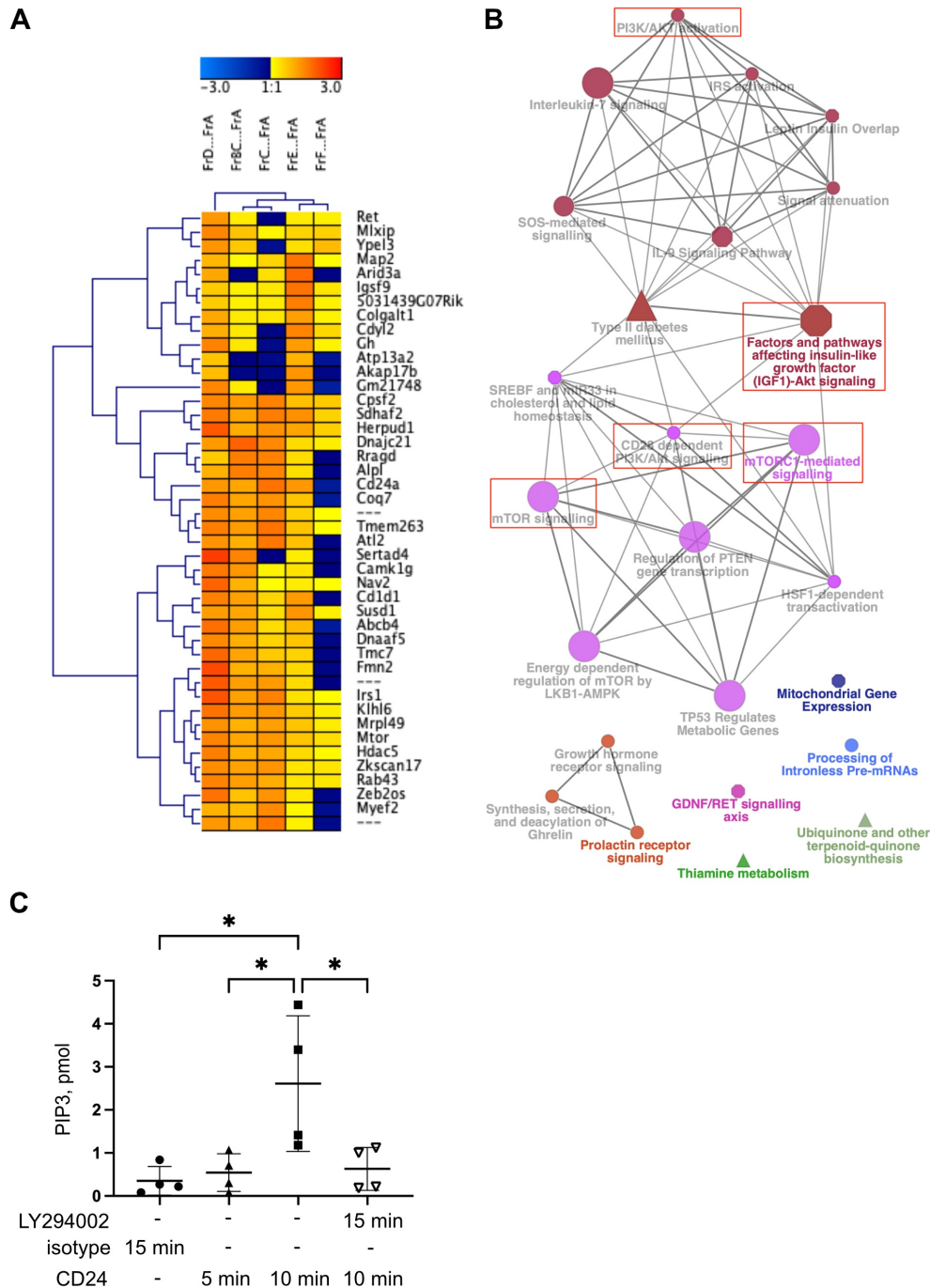


Figure 3.1. CD24 expression is associated with the PI3K-Akt signaling and mTOR pathways. (A) Hierarchical cluster analysis showing the clade of 44 genes (41 annotated) with similar differential gene expression patterns as CD24a. (B) Pathway network analysis generated from the differentially expressed 41-gene list identified the PI3K/Akt and mTOR signaling

pathway as being associated with CD24 expression in developing B cells. The red boxes indicate nodes with terms related to PI3K-Akt or mTOR signaling. (C) WEHI-231-GFP cells were pre-treated with LY294002 or DMSO (vehicle control) for 15 min then cells were stimulated with isotype antibody or anti-CD24 stimulating antibody for the times indicated. PIP₃ levels were analyzed by ELISA, n=4, significance was determined by a one-way ANOVA followed by the Sidak's multiple comparison test *P<0.05.

To determine if the PI3K signaling pathway regulates EV release in response to CD24 stimulation, we used our model system to track EV transfer (Supplemental Figure 3.1A-C). Transfer of EVs, as shown previously⁴⁴, can be evaluated by the uptake of GFP and IgM in the recipient tdTomato-positive cells. We found a significant increase in lipid transfer between the CD24-stimulated and the isotype-stimulated group in either the absence or presence of the inhibitor. However, the amount of lipid transferred in response to CD24 was significantly reduced in the presence of LY (Figure 3.2A and Supplemental Figure 3.1D). Parallel investigations into protein transfer revealed a similar pattern. There was a significant increase in protein transfer between the CD24-stimulated and the isotype-stimulated group in the presence or absence of LY with significantly less transfer in the CD24-stimulated group in the presence of LY (Figure 3.2B and Supplemental Figure 3.1E). To verify inhibition of the PI3K pathway, we analyzed Akt phosphorylation. We found that the level of phosphorylated Akt increased in response to CD24 stimulation, while it was markedly lower in cells pre-treated with LY for 15 min compared with those that received DMSO, particularly at the earliest timepoints of 5 and 10 min stimulation (Figure 3.2C). Thus, these data show that LY inhibits CD24-mediated PI3K signaling; however, some residual activation remains.

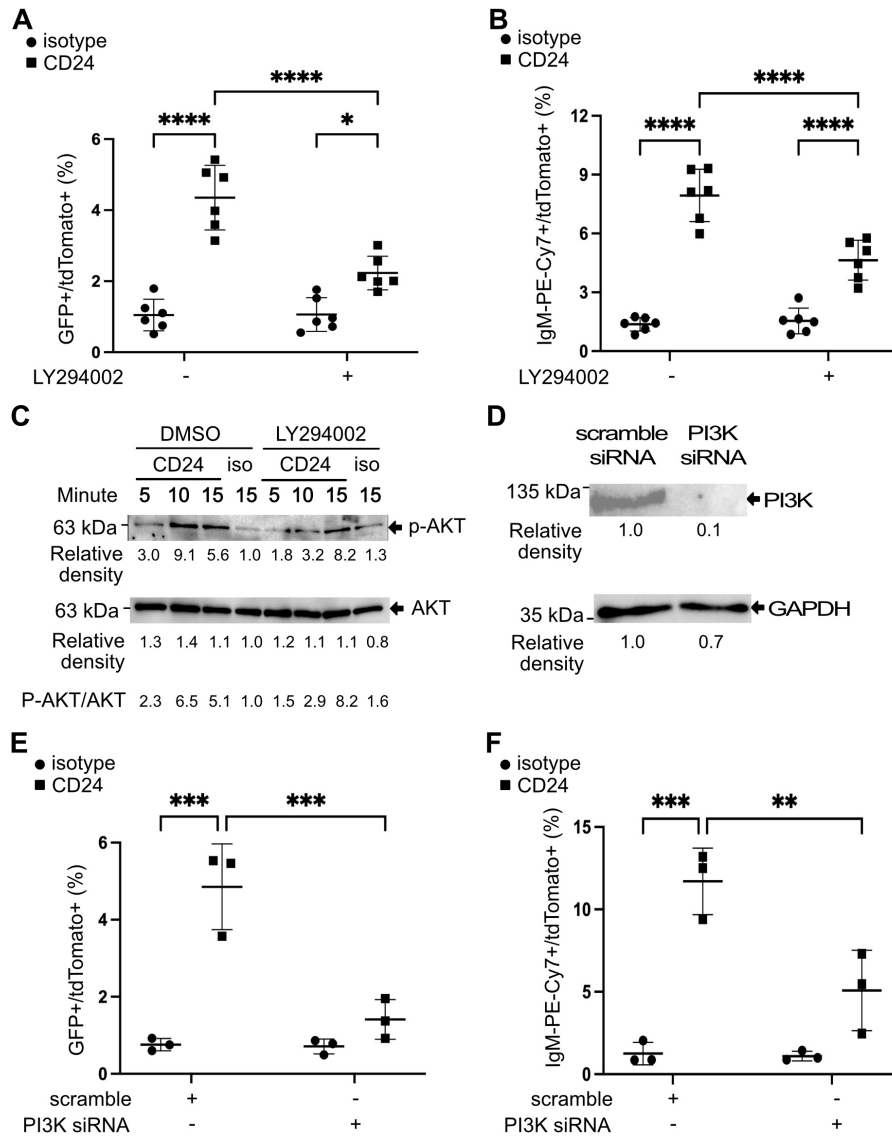


Figure 3.2. CD24-mediated EV release is regulated by PI3K. (A-B) WEHI-231-GFP cells were pre-treated with LY294002 or DMSO for 15 min, then stimulated with anti-CD24 (CD24) or isotype control (isotype, iso) for 15 min, followed by washout and then a 24 h co-culture with WEHI-303-tdTomato cells. (A) Percent GFP and tdTomato double-positive cells and (B) Percent IgM and tdTomato double-positive cells after 24 h incubation. n=6, statistical significance determined by a two-way ANOVA (interaction significant at P=0.0003 for A and P=0.0002 for B) followed by the Sidak's multiple comparison test *P<0.05, ****P<0.001. C) Total cell lysates from WEHI-231-GFP cells pre-treated with DMSO or LY2940002 for 15 min, then stimulated

with the above antibodies for different times indicated. Phosphorylated Akt and total Akt expression levels were determined by immunoblotting and a representative image from 4 replicates is shown. D) WEHI-231-GFP cells were transfected with scrambled control siRNA or PI3K siRNA, and PI3K and GAPDH levels determined by immunoblotting and a representative image from 3 replicates is shown. (E-F) WEHI-231-GFP cells with or without PI3K siRNA knock-down were stimulated with anti-CD24 or isotype for 15 min, followed by washout and then a 24 h co-culture with WEHI-303-tdTomato cells. (E) Percent GFP and tdTomato double-positive cells and (F) Percent IgM and tdTomato double-positive cells after 24 h incubation. n=3, statistical significance determined by a two-way ANOVA (interaction significant at P=0.0015 for E and P=0.0088 for F) followed by the Sidak's multiple comparison test **P<0.01, ***P<0.005.

Next, we sought to genetically validate the LY result using siRNA knock-down of PI3K in donor cells. The absence of PI3K expression in siRNA-transfected WEHI-231-GFP cells was confirmed by Western blot (Figure 3.2D). Analysis of lipid and protein transfer between the CD24-stimulated and isotype-stimulated groups revealed a significant increase in the scrambled control siRNA group, as expected. However, there was no transfer of lipid or protein in either the isotype-stimulated or CD24-stimulated groups when PI3K was knocked-down in the donor cells (Figure 3.2E-F). These findings strongly support a role for the PI3K signaling pathway in regulating CD24-mediated EV production.

We investigated further to see if proteins downstream of PI3K are involved in EV release in response to CD24. Akt is an important downstream kinase of PI3K, and it can be activated in response to phosphorylation by PI3K-mediated activation of the PDK1 and mTORC2 kinases^{67,68}. Phosphorylated Akt can activate multiple downstream signaling molecules, including TSC2, GSK3, and BAD, which drive cell growth, survival, and angiogenesis⁶⁹. After pre-treatment with the Akt inhibitor MK-2206, we found a significant decrease in CD24-mediated lipid and protein transfer to recipient cells (Figure 3.3A-B). Similar to PI3K inhibition, some residual EV transfer remained in the presence of the inhibitor.

Other signalling pathways downstream of PI3K are the mTOR signalling pathways. mTOR forms two structurally and functionally distinct complexes called mTORC1 and mTORC2⁷⁰. Therefore, we next determined if mTORC1 or mTORC2 regulates CD24-mediated EV release. To do this, we used Torin 1, an inhibitor of mTORC1/2, rapamycin, an inhibitor of mTORC1, and JR-AB2-011, an inhibitor of mTORC2⁷¹. As can be seen in Figure 3C and Figure 3D, there was a substantial statistical difference in lipid and protein transfer between the mTORC2 inhibition groups (Torin 1 and JR-AB2-011) and the control stimulated group, indicating that mTORC2 controls EV release in response to CD24.

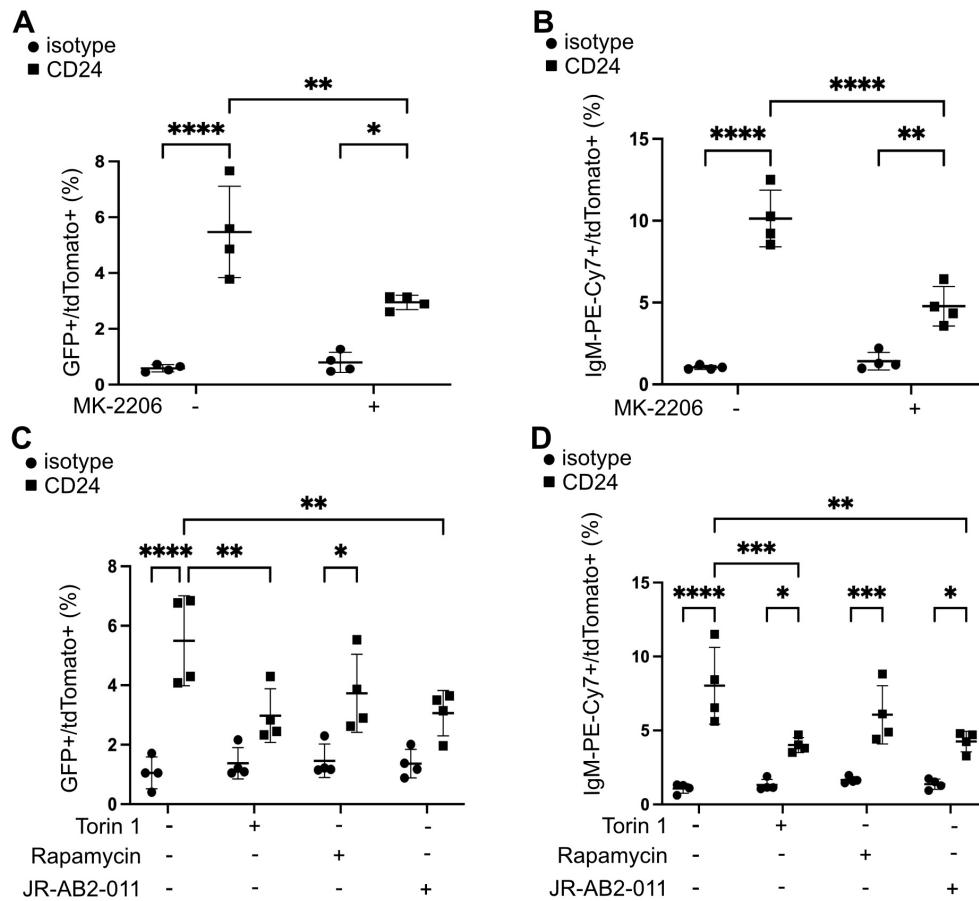


Figure 3.3. CD24-mediated EV release is dependent on Akt and mTOR signaling pathways.

(A-B) WEHI-231-GFP cells were pre-treated with MK-2206 or DMSO for 15 min, then stimulated with anti-CD24 or isotype control for 15 min, followed by washout and then a 24 h co-culture with WEHI-303-tdTomato cells. (A) Percent GFP and tdTomato double-positive cells and (B) Percent IgM and tdTomato double-positive cells after 24 h incubation. $n=4$, statistical significance determined by a two-way ANOVA (interaction significant at $P=0.0074$ for A and $P=0.0002$ for B) followed by the Sidak's multiple comparison test $*P<0.05$, $**P<0.01$, $****P<0.001$. (C-D) WEHI-231-GFP cells were pre-treated with Torin 1 or Rapamycin or JR-AB2-011 or DMSO for 15 min, then stimulated with anti-CD24 or isotype control for 15 min, followed by washout and then a 24 h co-culture with WEHI-303-tdTomato cells. (C) Percent GFP and tdTomato double-positive cells and (D) Percent IgM and tdTomato double-positive cells after

24 h incubation. n=4, statistical significance determined by a two-way ANOVA (interaction significant at P=0.0143 for C and P=0.0066 for D) followed by the Sidak's multiple comparison test *P<0.05, **P<0.01, ***P<0.005, ****P<0.001.

Rho-associated protein kinase (ROCK) is known to be regulated by the PI3K/mTORC2 signaling pathway⁷² and was identified by the bioinformatics analysis (Figure 3.1B). Therefore, we next asked whether CD24-mediated EV release was similarly regulated by the ROCK signaling pathway using the inhibitor Y27632⁷³. We found that, in comparison to EVs from the control group, the release of EVs from donor cells pre-treated with 10 μ M Y27632 for 15 min resulted in a significantly lower transfer of lipid and protein to recipient cells upon CD24 stimulation (Figure 3.4A-B). We found that there was a reduction but not a total block in phosphorylated cofilin, a downstream target of ROCK, suggesting that the inhibitor did not fully block ROCK activity (Figure 3.4C). Next, to genetically validate the Y27632 inhibitor result, we used siRNA to knock-down ROCK in donor cells (Figure 3.4D). We found that there was no transfer of lipids or proteins with CD24 stimulation when ROCK was knocked-down (Figure 3.4E-F). These data clearly demonstrate that CD24-mediated EV generation is regulated by ROCK.

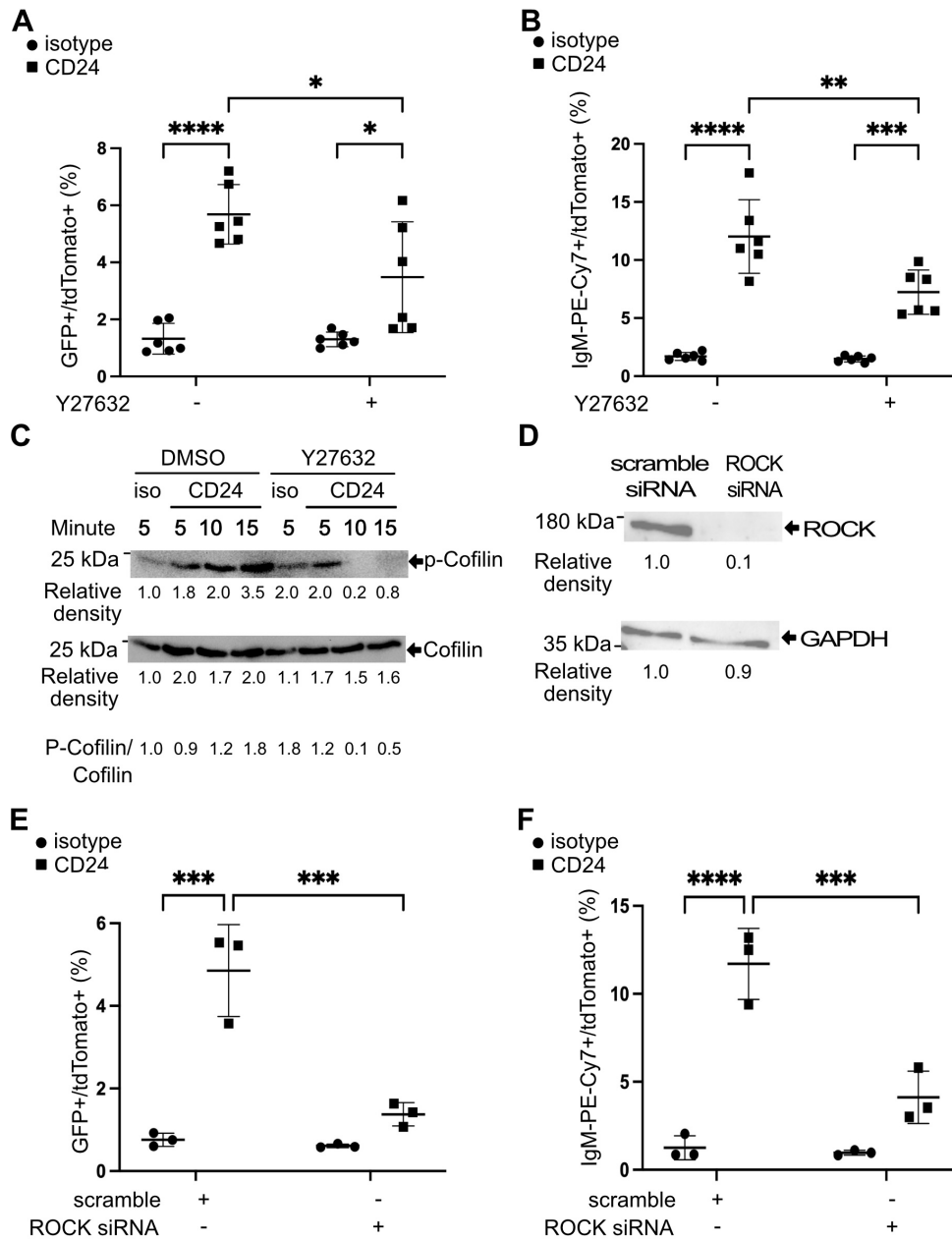


Figure 3.4. CD24-mediated EV secretion is dependent on ROCK. (A-B) WEHI-231-GFP cells were pre-treated with Y27632 or DMSO for 15 min, then stimulated with anti-CD24 (CD24) or isotype control (isotype, iso) for 15 min, followed by washout and then a 24 h co-culture with WEHI-303-tdTomato cells. (A) Percent GFP and tdTomato double-positive cells and (B) Percent IgM and tdTomato double-positive cells after 24 h incubation. n=6, statistical significance determined by a two-way ANOVA (interaction significant at P=0.03 for A and P=0.0069 for B)

followed by the Sidak's multiple comparison test * $P < 0.05$, ** $P < 0.01$, *** $P < 0.005$, **** $P < 0.001$.

C) Total cell lysates from WEHI-231-GFP cells pre-treated with DMSO or Y27632 for 15 min, then stimulated with the above antibodies for different times indicated. Phosphorylated Cofilin and total Cofilin expression levels were determined by immunoblotting and a representative image from 3 replicates is shown. D) WEHI-231-GFP cells were transfected with scrambled control siRNA or ROCK siRNA, and ROCK and GAPDH levels determined by immunoblotting and a representative image from 3 replicates is shown. (E-F) WEHI-231-GFP cells with or without ROCK siRNA knock-down were stimulated with anti-CD24 or isotype for 15 min, followed by washout and then a 24 h co-culture with WEHI-303-tdTomato cells. (E) Percent GFP and tdTomato double-positive cells and (F) Percent IgM and tdTomato double-positive cells after 24 h incubation. $n=3$, statistical significance determined by a two-way ANOVA (interaction significant at $P=0.0011$ for E and $P=0.0013$ for F) followed by the Sidak's multiple comparison test *** $P < 0.005$, **** $P < 0.001$.

We hypothesized that dynamic cytoskeletal reorganization downstream of ROCK that changes the shape of cell membrane will, in turn, promote EV release. Donor cells were thus pre-treated with cytochalasin D to prevent cytoskeleton rearrangement. The results showed that there was no increase in lipid and protein transfer in the cytochalasin D-treated CD24-stimulated group compared to the control stimulation (Figure 3.5A-B). Thus, actin cytoskeleton regulation plays a key role in regulating CD24-mediated EV release.

Sphingomyelin (SM), a phospholipid that localizes on the plasma membrane's outer leaflet and has a strong affinity for cholesterol, plays a significant role in determining the fluidity and structural integrity of the plasma membrane⁷⁴. nSMase and aSMase catalyze the hydrolysis of SM to ceramide, a process that is involved in both exosome and ectosome release⁷⁵. Exosome release has been previously shown to be regulated by nSMase, which can be blocked by GW4869¹², while a previous study has shown that imipramine blocked ectosome formation from glial cells by inhibiting aSMase³⁷. Thus, we treated donor cells with either GW4869, imipramine, or Arc39, a more specific inhibitor of aSMase to determine if nSMase or aSMase regulates CD24-mediated EV release. We found that there was no difference in lipid and protein transfer with GW4896 (Supplemental Figure 3.2A-B). In contrast, CD24-mediated lipid and protein transfer were significantly inhibited with imipramine and Arc39 treatment (Figure 3.6A-D). These findings show that aSMase, but not nSMase, regulates CD24-mediated EV release. These data are consistent with our previous studies that suggested that the EVs induced by CD24 stimulation are ectosomes budded off the plasma membrane and not exosomes derived from MVBS⁴²⁻⁴⁴.

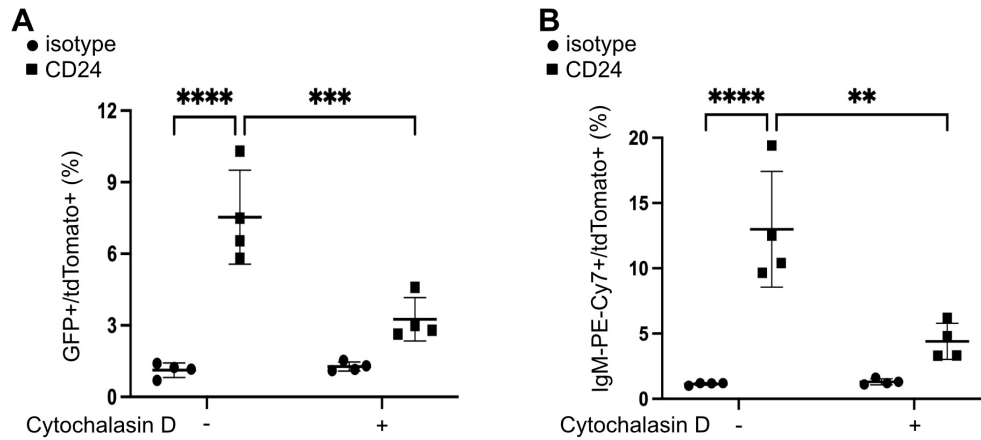


Figure 3.5. CD24-mediated EV release is controlled by actin cytoskeleton re-organization.

WEHI-231-GFP cells were pre-treated with cytochalasin D or DMSO for 15 min, then stimulated with anti-CD24 or isotype control for 15 min, followed by washout and then a 24 h co-culture with WEHI-303-tdTomato cells. (A) Percent GFP and tdTomato double-positive cells and (B) Percent IgM and tdTomato double-positive cells after 24 h incubation. n=4, statistical significance determined by a two-way ANOVA (interaction significant at P=0.0017 for A and P=0.0027 for B) followed by the Sidak's multiple comparison test **P<0.01, ***P<0.005, ****P<0.001.

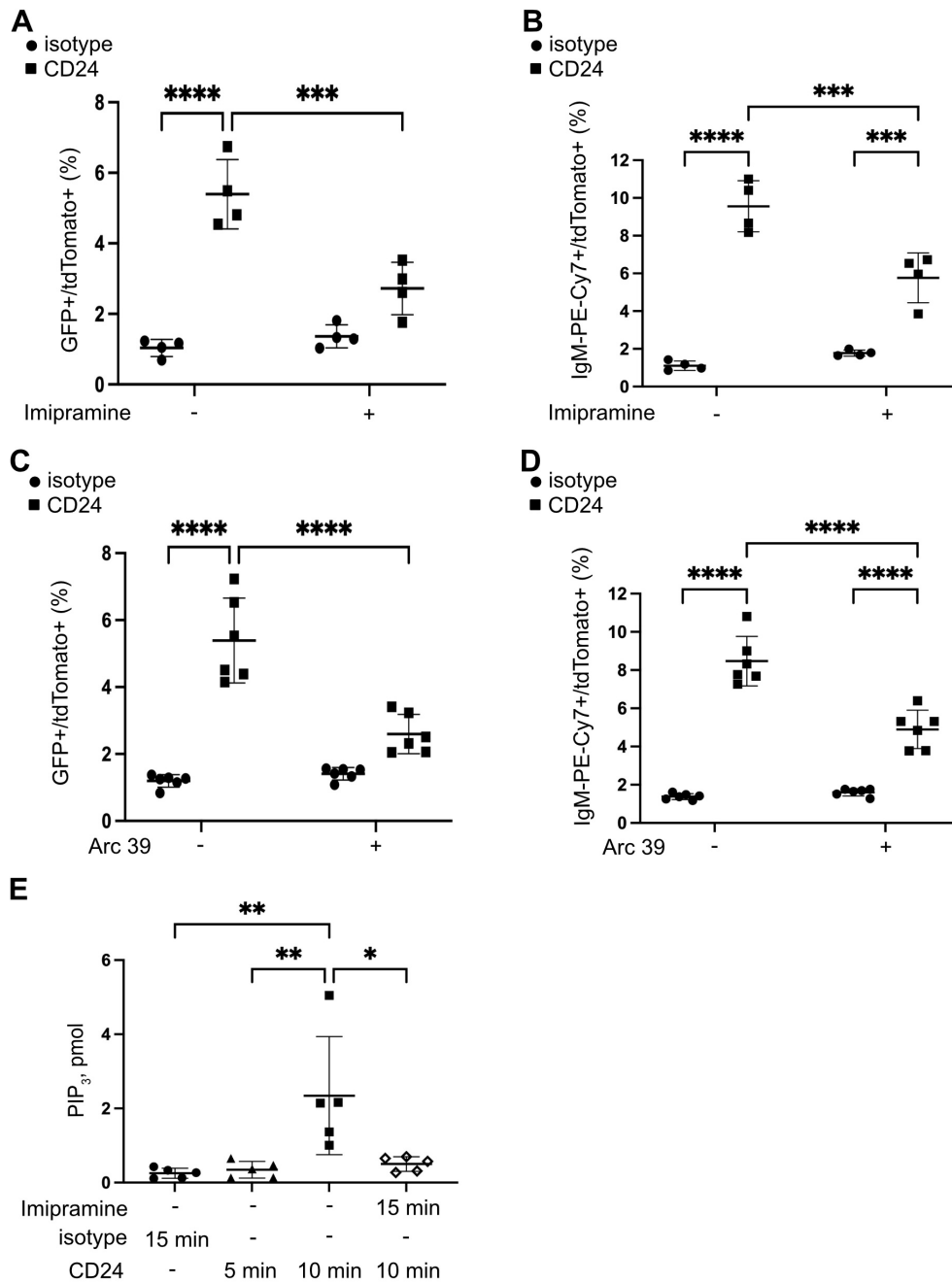


Figure 3.6. CD24-mediated EV release is controlled by aSMase activity. (A-B) WEHI-231-GFP cells were pre-treated with Imipramine or Arc39 or DMSO for 15 min, then stimulated with anti-CD24 or isotype control for 15 min, followed by washout and then a 24 h co-culture with WEHI-303-tdTomato cells. (A) Percent GFP and tdTomato double-positive cells and (B) Percent IgM and tdTomato double-positive cells after 24 h incubation. n=4, statistical significance

determined by a two-way ANOVA (interaction significant at $P=0.0006$ for A and $P=0.0006$ for B) followed by the Sidak's multiple comparison test $***P<0.005$, $****P<0.001$. (C-D) WEHI-231-GFP cells were pre-treated with Arc39 or DMSO for 15 min, then stimulated with anti-CD24 or isotype control for 15 min, followed by washout and then a 24 h co-culture with WEHI-303-tdTomato cells. (C) Percent GFP and tdTomato double-positive cells and (D) Percent IgM and tdTomato double-positive cells after 24 h incubation. $n=6$, statistical significance determined by a two-way ANOVA (interaction significant at $P<0.0001$ for C and $P<0.0001$ for D) followed by the Sidak's multiple comparison test $****P<0.001$. (E) WEHI-231-GFP cells were pre-treated with imipramine or DMSO (vehicle control) for 15 min then cells were stimulated with isotype antibody or anti-CD24 stimulating antibody for the times indicated. PIP_3 levels were analyzed by ELISA, $n=5$, significance was determined by a one-way ANOVA followed by the Sidak's multiple comparison test $*P<0.05$, $**P<0.01$.

We next determined if PI3K was upstream or downstream of aSMase by determining if inhibition of aSMase alters PIP₃ levels in response to CD24 stimulation. We found that the CD24-mediated increase of PIP₃ was significantly inhibited in the presence of imipramine (Figure 3.6E). Therefore, aSMase activation is upstream of PI3K.

Lastly, we performed live cell imaging to visualize EV release and membrane dynamics. We clearly saw green fluorescent punctae that were either intracellular, associated with cytoplasmic membranes, or embedded on and outside of GFP-labeled cell plasma membranes. The number of GFP membrane bound vesicles increased when cells were stimulated through CD24 (Figure 3.7A). In some cases, we were able to visualize EV-like structures budding from the plasma membrane with more apparent of these structures visible in CD24-stimulated cells; however, this was extremely difficult to quantify as the structures were very transient. We observed a reduction in membrane dynamics in the presence of PI3K and ROCK inhibitors during CD24 treatment when highly active cells were counted; however, only ROCK inhibition had a statistically significant effect (Figure 3.7B-C). These data suggest that the induction of membrane dynamics necessary for EV release requires ROCK activation.

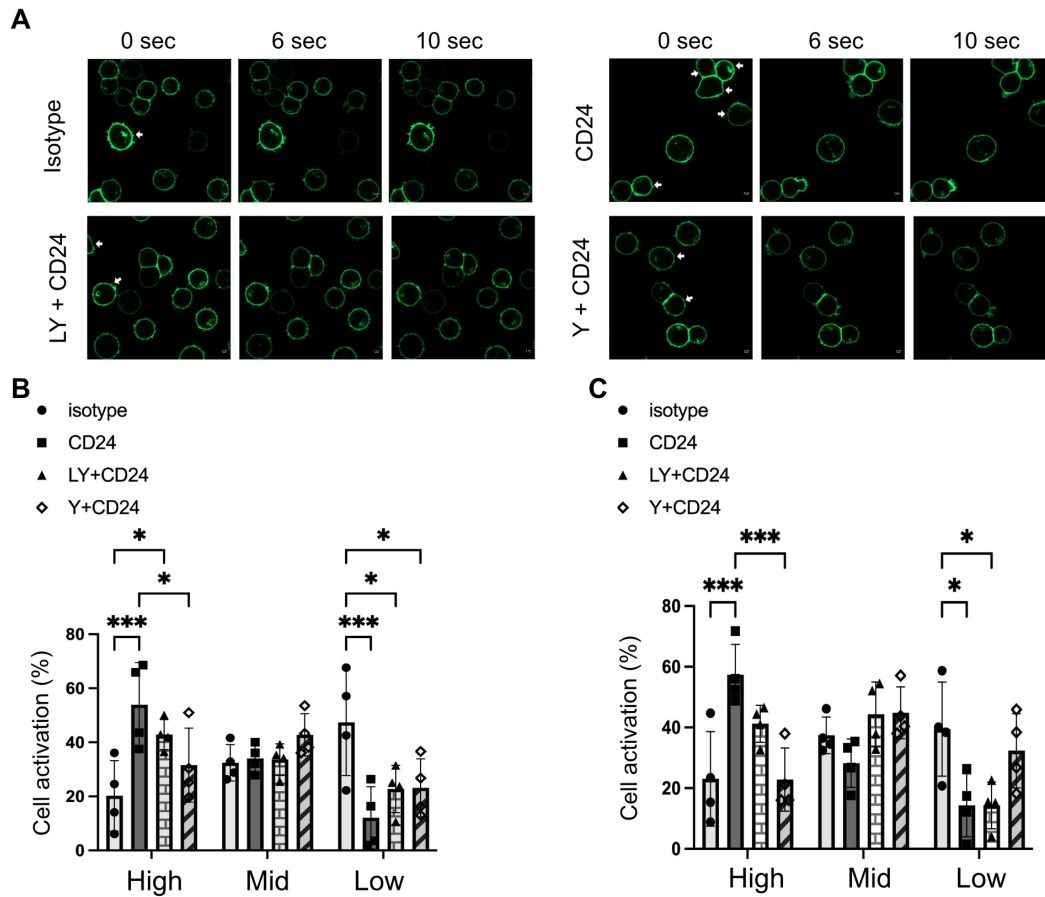


Figure 3.7. Representative images of WEHI-231-GFP cells show EV release and cell activation. WEHI-231-GFP cells were pre-treated with LY294002 or Y27632 or DMSO for 15 min, then stimulated with anti-CD24 or isotype control. (A) The cells were captured at 15 min after stimulation. White arrows indicate EV release. Scale bar = 2 mm. The analysis of cell activation was observed and marked at 3 levels of activation by 4 different individuals who were blinded to the treatments. Cell activation was determined at B) 15 min and C) 30 min after stimulation. $n=4$, statistical significance determined by a two-way ANOVA (interaction significant at $P<0.0001$ for B and $P<0.0001$ for C) followed by the Sidak's multiple comparison test $*P<0.05$, $***P<0.005$.

3.6. Discussion

We have identified a novel pathway regulating ectosome release, namely aSMase/PI3K/mTORC2/ROCK/actin pathway. By exploiting bioinformatics pathway analysis, we were able to identify PI3K and mTOR as potential nodes regulating CD24-mediated EV release. Further elucidation of potential regulators allowed us to determine that this pathway is initiated by aSMase which, through an unknown mechanism, activates PI3K to promote actin rearrangement downstream of the mTORC2/ROCK axis. To the best of our knowledge, this is the first time that CD24 has been linked to PI3K and to aSMase. In addition, this is the first report of PI3K regulating ectosome release. One previous publication linked PI3K to the generation of ABCG2-rich EVs in breast cancer cells; however, these EVs were most likely exosomes⁷⁶.

This study revealed a range of pharmacological agents that can effectively inhibit the release of ectosomes. The first inhibitor, LY294002, is an inhibitor of PI3K. Generation of PIP₃ from PI(4,5)P₂ by PI3K recruits protein kinase B (Akt), phosphoinositide-dependent kinase 1 (PDK1), and mTORC2 resulting in their colocalization. This permits PDK1 to phosphorylate Akt on threonine 308 and mTORC2 to phosphorylate serine 473^{67,68}. The second inhibitor, MK2206, is an inhibitor of Akt. PI3K/Akt signaling is implicated in various cellular processes, including differentiation, growth, proliferation, and intracellular trafficking, all of which are factors in B cell development and activation^{67,68}. mTOR is found in two complexes: mTORC1 (which contains mTOR, Raptor, and other proteins) and mTORC2 (which contains mTOR, Rictor, and other proteins)⁷⁷. mTORC1, called the rapamycin-sensitive mTOR complex, is a key regulator of cell proliferation and survival downstream of the PI3K/Akt pathway. It activates protein synthesis through modulation of the 40S ribosomal protein S6 kinase and the translational initiation factor eIF-4E binding protein 1⁷⁸. In contrast, the rapamycin-insensitive, rictor-containing complex (mTORC2) is assembled via binding of PIP₃ by the PH-domain containing protein mSIN1, and

thereby relieving its suppression on mTOR kinase activity⁷⁹. As mentioned, mTORC2 triggers Akt activation by phosphorylation on serine 473, as well as regulation of the actin cytoskeleton via RhoA and PKC α ⁸⁰. We used Torin1, rapamycin and JR-AB2-011 to determine if mTORC1 or mTORC2 is involved in the release of EVs. We found that mTORC2, but not mTORC1, is essential for CD24-mediated EV release. The sixth inhibitor, Y27632, is an inhibitor of ROCK. The two isoforms of ROCK, ROCK1 and ROCK2, are involved in multiple cellular processes such as cell growth, differentiation, and cytoskeleton regulation⁸¹. The seventh inhibitor tested, cytochalasin D, disrupts actin filaments of the cytoskeleton, particularly inhibiting actin polymerization. In addition, we provide evidence, by live cell imaging, that ROCK signaling regulates EV release in response to CD24 stimulation, likely by regulating actin anchorage to the plasma membrane. In addition, increases in PIP₃ can also regulate anchorage of the actin cytoskeleton by reducing the available PI(4,5)P₂^{25,26}. These findings expand our understanding of the molecular mechanisms governing CD24-mediated EV release and highlights the complexity of the signaling networks underlying this process (Supplemental Figure 3.3).

Contrary to the previous report^{18,36}, we did not find any involvement of intracellular calcium in the regulation of ectosome release. For instance, ionomycin was employed as an enhancer of [Ca²⁺]_i alone, which was insufficient to stimulate EV release, indicating that it is not a substantial regulator in the EV release observed (Supplemental Figure 3.4A-B). Moreover, it was an interesting finding that pre-treatment with BAPTA-AM, a calcium level inhibitor, did not suppress EV release in response to CD24 stimulation (Supplemental Figure 3.4C-D), but actually increased cellular exchange by inducing cell death and potentially apoptotic body formation (Supplemental Figure 3.4E).

Lipid rafts play a key role in the synthesis and function of EVs⁸². Ceramide-enriched lipid rafts have also been found in exosomal membranes⁸³. Herein, we report decreased levels of EV transfer in the presence of imipramine and Arc39, which prevent the activation of aSMase, and the subsequent increase in ceramide levels. Thus, in these cells, aSMase is likely inducing the formation of ceramide-enriched lipid rafts, which in turn promotes the membrane curvature needed for EV formation⁸⁴. The increase in local ceramide concentrations might displace cholesterol in the lipid rafts to alter their function and initiate signal transduction⁸⁵. However, alterations in lipid composition in lipid rafts in response to CD24 stimulation has yet to be determined.

Previous work has linked CD24 to the recruitment of PTEN, a negative regulator of PI3K signaling, to the plasma membrane to induce autophagy by inhibition of downstream proteins Akt and mTORC1⁸⁶. However, this is opposite to what we found, which was an activation of PI3K by CD24. CD24 has been found to mediate signal transduction by recruiting Src family protein tyrosine kinases, including Fgr, Lyn, and Lck to lipid rafts^{40,41}. Specifically, Lyn is activated by CD24 in B cells⁴⁰. Lyn activates PI3K in colorectal cancer cells and myeloma cells^{87,88}. In endometrial cells, Lyn has been shown to be activated by long chain glucosylceramide and in neutrophils by lactosylceramide^{89,90}. Therefore, activation of Lyn by re-organization of lipid raft components due to the increase in ceramide, as discussed above, may promote the activation of PI3K downstream of CD24.

Sphingolipids are an essential class of bioactive lipids. Ceramide is the principal sphingolipid metabolite that is produced through three main synthesis pathways, including the de novo pathway in the endoplasmic reticulum, the salvage pathway in the lysosome, and sphingomyelinase (SMase) both in lysosome and plasma membranes⁹¹. There are three types of SMase: nSMase, aSMase, and alkaline SMase named based on their pH optima⁹². aSMase is

further divided into lysosomal and secreted forms. Secretory aSMase translocates onto the cell surface from intracellular vesicles⁹³. At the outer leaflet of the plasma membrane, aSMase hydrolyzes sphingomyelin into ceramide⁹⁴, generating ceramide-enriched lipid rafts that induce membrane curvature⁹⁵ and facilitate membrane blebbing and shedding⁷⁵. It was reported that aSMase and ceramide are involved in ectosome release from glial cells, which requires p38 MAPK activation³⁷. Our findings that aSMase, and not nSMase, induces EV release supports our earlier research suggesting that the EVs generated by CD24 stimulation are not exosomes derived from multivesicular bodies, but rather ectosomes that have budded off the plasma membrane⁴²⁻⁴⁴. Future work will be needed to understand the mechanism that regulates CD24 activation of aSMase.

In sphingolipid metabolism, ceramide can be broken down by ceramidases to produce sphingosine⁹⁶. Ceramide and sphingosine both work by activating PKC δ and protein phosphatase 2A to suppress Akt activity, thereby inducing cell cycle arrest and promoting apoptosis⁶⁹. On the other hand, ceramide can be metabolized to ceramide-1-phosphate (C1P) by ceramide kinase. C1P can be converted back to ceramide by lipid phosphate phosphatases⁹⁷. Alternatively, sphingosine can be phosphorylated by sphingosine kinase to produce sphingosine-1-phosphate (S1P)⁹⁷. It is reported that both C1P and S1P activate PI3K, consequently contributing to cell survival and cell proliferation⁹⁸⁻¹⁰⁰. However, the appropriate balance between the amounts of these two metabolites for cell and tissue homeostasis is unknown. Here, we show that aSMase activates PI3K. However, whether this activation is via increases in ceramide or C1P levels has yet to be determined.

In summary, here we provide compelling evidence that CD24 activates an aSMase/PI3K/mTORC2/ROCK/actin signaling pathway to induce ectosome formation.

Importantly, these findings provide a new avenue for research into the regulation of ectosome generation.

3.7. References

1. Buzas, E. I. The roles of extracellular vesicles in the immune system. *Nat. Rev. Immunol.* 23, 236–250 (2023).
2. Van Niel, G., D'Angelo, G. & Raposo, G. Shedding light on the cell biology of extracellular vesicles. *Nat. Rev. Mol. Cell Biol.* 19, 213–228 (2018).
3. Jeppesen, D. K., Zhang, Q., Franklin, J. L. & Coffey, R. J. Extracellular vesicles and nanoparticles: emerging complexities. *Trends Cell Biol.* 33, 667–681 (2023).
4. Brodeur, A. et al. Apoptotic exosome-like vesicles transfer specific and functional mRNAs to endothelial cells by phosphatidylserine-dependent macropinocytosis. *Cell Death Dis.* 14, 449 (2023).
5. Van Niel, G. et al. Challenges and directions in studying cell-cell communication by extracellular vesicles. *Nat. Rev. Mol. Cell Biol.* 23, 369–382 (2022).
6. Maas, S. L. N., Breakefield, X. O. & Weaver, A. M. Extracellular Vesicles: Unique Intercellular Delivery Vehicles. *Trends Cell Biol.* 27, 172–188 (2017).
7. Colombo, M. et al. Analysis of ESCRT functions in exosome biogenesis, composition and secretion highlights the heterogeneity of extracellular vesicles. *J. Cell Sci.* 126, 5553–5565 (2013).
8. Henne, W. M., Buchkovich, N. J. & Emr, S. D. The ESCRT Pathway. *Dev. Cell* 21, 77–91 (2011).
9. Henne, W. M., Stenmark, H. & Emr, S. D. Molecular Mechanisms of the Membrane Sculpting ESCRT Pathway. *Cold Spring Harb. Perspect. Biol.* 5, a016766 (2013).
10. Zhang, Y., Liu, Y., Liu, H. & Tang, W. H. Exosomes: biogenesis, biologic function and clinical potential. *Cell Biosci.* 9, 19 (2019).

11. Blanc, L. & Vidal, M. New insights into the function of Rab GTPases in the context of exosomal secretion. *Small GTPases* 9, 95–106 (2017).
12. Jin, Y. et al. Extracellular signals regulate the biogenesis of extracellular vesicles. *Biol. Res.* 55, 35 (2022).
13. Liu, C. et al. Identification of the SNARE complex that mediates the fusion of multivesicular bodies with the plasma membrane in exosome secretion. *J. Extracell. Vesicles* 12, 12356 (2023).
14. Stuffers, S., Sem Wegner, C., Stenmark, H. & Brech, A. Multivesicular endosome biogenesis in the absence of ESCRTs. *Traffic Cph. Den.* 10, 925–937 (2009).
15. Trajkovic, K. et al. Ceramide triggers budding of exosome vesicles into multivesicular endosomes. *Science* 319, 1244–1247 (2008).
16. Van Niel, G. et al. Apolipoprotein E Regulates Amyloid Formation within Endosomes of Pigment Cells. *Cell Rep.* 13, 43–51 (2015).
17. Van Niel, G. et al. The tetraspanin CD63 regulates ESCRT-independent and dependent endosomal sorting during melanogenesis. *Dev. Cell* 21, 708–721 (2011).
18. Bucki, R., Bachelot-Loza, C., Zachowski, A., Giraud, F. & Sulpice, J. C. Calcium induces phospholipid redistribution and microvesicle release in human erythrocyte membranes by independent pathways. *Biochemistry* 37, 15383–15391 (1998).
19. Bretscher, M. S. Asymmetrical lipid bilayer structure for biological membranes. *Nature. New Biol.* 236, 11–12 (1972).
20. Piccin, A., Murphy, W. G. & Smith, O. P. Circulating microparticles: pathophysiology and clinical implications. *Blood Rev.* 21, 157–171 (2007).
21. Comfurius, P. et al. Loss of membrane phospholipid asymmetry in platelets and red cells may be associated with calcium-induced shedding of plasma membrane and inhibition of

- aminophospholipid translocase. *Biochim. Biophys. Acta BBA - Biomembr.* 1026, 153–160 (1990).
22. Hankins, H. M., Baldrige, R. D., Xu, P. & Graham, T. R. Role of flippases, scramblases, and transfer proteins in phosphatidylserine subcellular distribution. *Traffic Cph. Den.* 16, 35–47 (2015).
23. Gonzalez, L. J. et al. The influence of membrane physical properties on microvesicle release in human erythrocytes. *PMC Biophys.* 2, 7 (2009).
24. Pap, E., Pállinger, E., Pásztói, M. & Falus, A. Highlights of a new type of intercellular communication: microvesicle-based information transfer. *Inflamm. Res. Off. J. Eur. Histamine Res. Soc. A1* 58, 1–8 (2009).
25. Raucher, D. et al. Phosphatidylinositol 4,5-Bisphosphate Functions as a Second Messenger that Regulates Cytoskeleton–Plasma Membrane Adhesion. *Cell* 100, 221–228 (2000).
26. Niebuhr, K. et al. Conversion of PtdIns(4,5)P₂ into PtdIns(5)P by the *S. flexneri* effector IpgD reorganizes host cell morphology. *EMBO J.* 21, 5069–5078 (2002).
27. Flaumenhaft, R. Formation and fate of platelet microparticles. *Blood Cells. Mol. Dis.* 36, 182–187 (2006).
28. Nebl, T., Oh, S. W. & Luna, E. J. Membrane cytoskeleton: PIP₂ pulls the strings. *Curr. Biol.* 10, R351–R354 (2000).
29. Wang, T. et al. Hypoxia-inducible factors and RAB22A mediate formation of microvesicles that stimulate breast cancer invasion and metastasis. *Proc. Natl. Acad. Sci. U. S. A.* 111, E3234–E3242 (2014).
30. Muralidharan-Chari, V. et al. ARF6-regulated shedding of tumor cell-derived plasma membrane microvesicles. *Curr. Biol. CB* 19, 1875–1885 (2009).

31. Sedgwick, A. E., Clancy, J. W., Olivia Balmert, M. & D'Souza-Schorey, C. Extracellular microvesicles and invadopodia mediate non-overlapping modes of tumor cell invasion. *Sci. Rep.* 5, 14748 (2015).
32. Li, B., Antonyak, M. A., Zhang, J. & Cerione, R. A. RhoA triggers a specific signaling pathway that generates transforming microvesicles in cancer cells. *Oncogene* 31, 4740–4749 (2012).
33. Taylor, J., Azimi, I., Monteith, G. & Bebawy, M. Ca²⁺ mediates extracellular vesicle biogenesis through alternate pathways in malignancy. *J. Extracell. Vesicles* 9, 1734326 (2020).
34. Perrin, B. J., Amann, K. J. & Huttenlocher, A. Proteolysis of cortactin by calpain regulates membrane protrusion during cell migration. *Mol. Biol. Cell* 17, 239–250 (2006).
35. Storr, S. J., Carragher, N. O., Frame, M. C., Parr, T. & Martin, S. G. The calpain system and cancer. *Nat. Rev. Cancer* 11, 364–374 (2011).
36. Roseblade, A., Luk, F., Ung, A. & Bebawy, M. Targeting microparticle biogenesis: a novel approach to the circumvention of cancer multidrug resistance. *Curr. Cancer Drug Targets* 15, 205–214 (2015).
37. Bianco, F. et al. Acid sphingomyelinase activity triggers microparticle release from glial cells. *EMBO J.* 28, 1043–1054 (2009).
38. Kay, R., Rosten, P. M. & Humphries, R. K. CD24, a signal transducer modulating B cell activation responses, is a very short peptide with a glycosyl phosphatidylinositol membrane anchor. *J. Immunol. Baltim. Md* 150, 1412–1416 (1993).
39. Fang, X., Zheng, P., Tang, J. & Liu, Y. CD24: from A to Z. *Cell. Mol. Immunol.* 7, 100–103 (2010).

40. Suzuki, T. et al. CD24 Induces Apoptosis in Human B Cells Via the Glycolipid-Enriched Membrane Domains/Rafts-Mediated Signaling System. *J. Immunol.* 166, 5567–5577 (2001).
41. Yang, Y., Zhu, G., Yang, L. & Yang, Y. Targeting CD24 as a novel immunotherapy for solid cancers. *Cell Commun. Signal.* 21, 312 (2023).
42. Ayre, D. C. et al. Dynamic regulation of CD24 expression and release of CD24-containing microvesicles in immature B cells in response to CD24 engagement. *Immunology* 146, 217–233 (2015).
43. Ayre, D. C. et al. CD24 induces changes to the surface receptors of B cell microvesicles with variable effects on their RNA and protein cargo. *Sci. Rep.* 7, 8642 (2017).
44. Phan, H.-D. et al. CD24 and IgM Stimulation of B Cells Triggers Transfer of Functional B Cell Receptor to B Cell Recipients Via Extracellular Vesicles. *J. Immunol. Baltim. Md* 1950 207, 3004–3015 (2021).
45. Heng, T. S. P. et al. The Immunological Genome Project: networks of gene expression in immune cells. *Nat. Immunol.* 9, 1091–1094 (2008).
46. Page, D. M., Gold, M. R., Fahey, K. A., Matsuuchi, L. & DeFranco, A. L. Mutational analysis of antigen receptor regulation of B lymphocyte growth. Evidence for involvement of the phosphoinositide signaling pathway. *J. Biol. Chem.* 266, 5563–5574 (1991).
47. Lai, C. P. et al. Visualization and tracking of tumour extracellular vesicle delivery and RNA translation using multiplexed reporters. *Nat. Commun.* 6, 7029 (2015).
48. Duarte, A., Gobbi, G. G. G., Soave, D. F., Costa, J. P. O. & Silva, A. R. The Role of the LY294002 - A Non-Selective Inhibitor of Phosphatidylinositol 3-Kinase (PI3K) Pathway- in Cell Survival and Proliferation in Cell Line SCC-25. *Asian Pac. J. Cancer Prev. APJCP* 20, 3377 (2019).

49. Mallawaarachy, D. M., Mactier, S., Kaufman, K. L., Blomfield, K. & Christopherson, R. I. The phosphoinositide 3-kinase inhibitor LY294002, decreases aminoacyl-tRNA synthetases, chaperones and glycolytic enzymes in human HT-29 colorectal cancer cells. *J. Proteomics* 75, 1590–1599 (2012).
50. Richter, A. et al. Combined Application of Pan-AKT Inhibitor MK-2206 and BCL-2 Antagonist Venetoclax in B-Cell Precursor Acute Lymphoblastic Leukemia. *Int. J. Mol. Sci.* 22, 2771 (2021).
51. Wilson, J. M., Kunnimalaiyaan, S., Kunnimalaiyaan, M. & Gamblin, T. C. Inhibition of the AKT pathway in cholangiocarcinoma by MK2206 reduces cellular viability via induction of apoptosis. *Cancer Cell Int.* 15, 13 (2015).
52. Wang, Y. et al. mTOR contributes to endothelium-dependent vasorelaxation by promoting eNOS expression and preventing eNOS uncoupling. *Commun. Biol.* 5, 1–14 (2022).
53. Najafov, A. et al. RIPK1 Promotes Energy Sensing by the mTORC1 Pathway. *Mol. Cell* 81, 370-385.e7 (2021).
54. Ma, C. et al. mTOR hypoactivity leads to trophectoderm cell failure by enhancing lysosomal activation and disrupting the cytoskeleton in preimplantation embryo. *Cell Biosci.* 13, 219 (2023).
55. Kim, R. & Kim, J. H. Engineered Extracellular Vesicles with Compound-Induced Cargo Delivery to Solid Tumors. *Int. J. Mol. Sci.* 24, 9368 (2023).
56. Kořánová, T., Dvořáček, L., Grebeňová, D. & Kuželová, K. JR-AB2-011 induces fast metabolic changes independent of mTOR complex 2 inhibition in human leukemia cells. *Pharmacol. Rep. PR* (2024) doi:10.1007/s43440-024-00649-7.

57. Tramontano, A. F. et al. Statin decreases endothelial microparticle release from human coronary artery endothelial cells: implication for the Rho-kinase pathway. *Biochem. Biophys. Res. Commun.* 320, 34–38 (2004).
58. Kim, K., Min, S., Kim, D., Kim, H. & Roh, S. A Rho Kinase (ROCK) Inhibitor, Y-27632, Inhibits the Dissociation-Induced Cell Death of Salivary Gland Stem Cells. *Molecules* 26, 2658 (2021).
59. Shoji, K., Ohashi, K., Sampei, K., Oikawa, M. & Mizuno, K. Cytochalasin D acts as an inhibitor of the actin–cofilin interaction. *Biochem. Biophys. Res. Commun.* 424, 52–57 (2012).
60. Deng, L. et al. Imipramine Protects against Bone Loss by Inhibition of Osteoblast-Derived Microvesicles. *Int. J. Mol. Sci.* 18, 1013 (2017).
61. Quadri, Z. et al. Ceramide-mediated orchestration of oxidative stress response through filopodia-derived small extracellular vesicles. *J. Extracell. Vesicles* 13, e12477 (2024).
62. Naser, E. et al. Characterization of the small molecule ARC39, a direct and specific inhibitor of acid sphingomyelinase in vitro. *J. Lipid Res.* 61, 896 (2020).
63. Essandoh, K. et al. Blockade of Exosome Generation with GW4869 Dampens the Sepsis-Induced Inflammation and Cardiac Dysfunction. *Biochim. Biophys. Acta* 1852, 2362 (2015).
64. Pericoli, G. et al. Inhibition of exosome biogenesis affects cell motility in heterogeneous subpopulations of paediatric-type diffuse high-grade gliomas. *Cell Biosci.* 13, 207 (2023).
65. Zhang, C., Wu, Y.-L. & Boxer, L. M. Impaired Proliferation and Survival of Activated B Cells in Transgenic Mice That Express a Dominant-negative cAMP-response Element-binding Protein Transcription Factor in B Cells *. *J. Biol. Chem.* 277, 48359–48365 (2002).

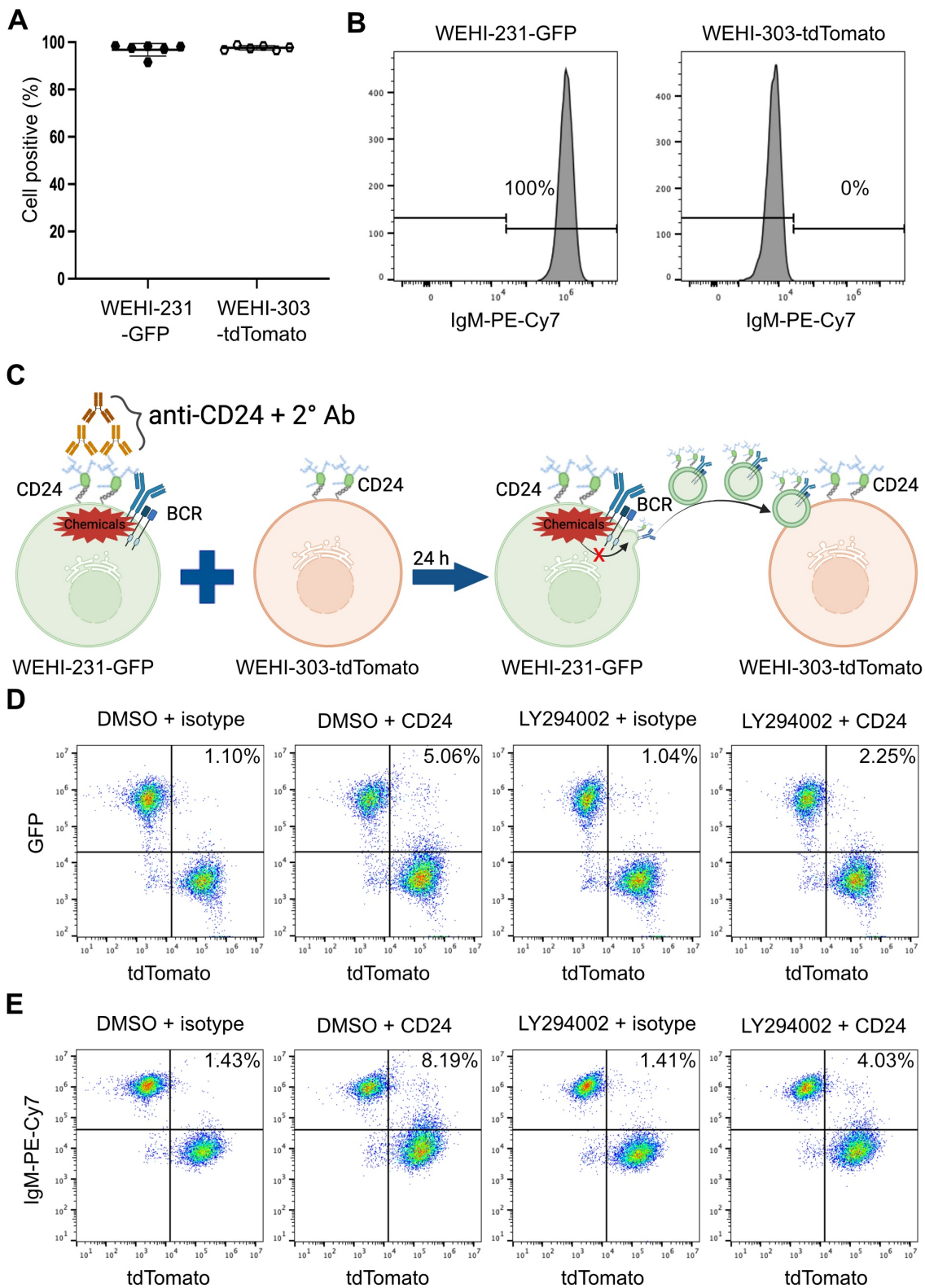
66. Kang, K. et al. BAPTA, a calcium chelator, neuroprotects injured neurons in vitro and promotes motor recovery after spinal cord transection in vivo. *CNS Neurosci. Ther.* 27, 919 (2021).
67. Jellusova, J. & Rickert, R. C. The PI3K Pathway in B Cell Metabolism. *Crit. Rev. Biochem. Mol. Biol.* 51, 359–378 (2016).
68. Limon, J. J. & Fruman, D. A. Akt and mTOR in B Cell Activation and Differentiation. *Front. Immunol.* 3, 1–12 (2012).
69. Yu, L., Wei, J. & Liu, P. Attacking the PI3K/Akt/mTOR signaling pathway for targeted therapeutic treatment in human cancer. *Semin. Cancer Biol.* 85, 69–94 (2022).
70. Panwar, V. et al. Multifaceted role of mTOR (mammalian target of rapamycin) signaling pathway in human health and disease. *Signal Transduct. Target. Ther.* 8, 1–25 (2023).
71. Zhou, H., Luo, Y. & Huang, S. Updates of mTOR inhibitors. *Anticancer Agents Med. Chem.* 10, 571–581 (2010).
72. Dai, H. & Thomson, A. W. The “other” mTOR complex: new insights into mTORC2 immunobiology and their implications. *Am. J. Transplant. Off. J. Am. Soc. Transplant. Am. Soc. Transpl. Surg.* 19, 1614–1621 (2019).
73. Catalano, M. & O’Driscoll, L. Inhibiting extracellular vesicles formation and release: a review of EV inhibitors. *J. Extracell. Vesicles* 9, 1703244 (2020).
74. Simons, K. & Ikonen, E. Functional rafts in cell membranes. *Nature* 387, 569–572 (1997).
75. Verderio, C., Gabrielli, M. & Giussani, P. Role of sphingolipids in the biogenesis and biological activity of extracellular vesicles. *J. Lipid Res.* 59, 1325–1340 (2018).
76. Goler-Baron, V., Sladkevich, I. & Assaraf, Y. G. Inhibition of the PI3K-Akt signaling pathway disrupts ABCG2-rich extracellular vesicles and overcomes multidrug resistance in breast cancer cells. *Biochem. Pharmacol.* 83, 1340–1348 (2012).

77. Guertin, D. A. & Sabatini, D. M. Defining the role of mTOR in cancer. *Cancer Cell* 12, 9–22 (2007).
78. Meric-Bernstam, F. & Gonzalez-Angulo, A. M. Targeting the mTOR signaling network for cancer therapy. *J. Clin. Oncol. Off. J. Am. Soc. Clin. Oncol.* 27, 2278–2287 (2009).
79. Liu, P. et al. PtdIns(3,4,5)P₃-Dependent Activation of the mTORC2 Kinase Complex. *Cancer Discov.* 5, 1194–1209 (2015).
80. Liu, L., Das, S., Wolfgang, L. & Carole, P. mTORC2 regulates neutrophil chemotaxis in a cAMP- and RhoA-dependent fashion. *Dev. Cell* 19, 845–857 (2010).
81. Shimokawa, H., Sunamura, S. & Satoh, K. RhoA/Rho-Kinase in the Cardiovascular System. *Circ. Res.* 118, 352–366 (2016).
82. Sapoń, K., Mańka, R., Janas, T. & Janas, T. The role of lipid rafts in vesicle formation. *J. Cell Sci.* 136, jcs260887 (2023).
83. Elsherbini, A. & Bieberich, E. Ceramide and exosomes: a novel target in cancer biology and therapy. *Adv. Cancer Res.* 140, 121–154 (2018).
84. López-Montero, I. et al. Rapid Transbilayer Movement of Ceramides in Phospholipid Vesicles and in Human Erythrocytes *. *J. Biol. Chem.* 280, 25811–25819 (2005).
85. Megha & London, E. Ceramide selectively displaces cholesterol from ordered lipid domains (rafts): implications for lipid raft structure and function. *J. Biol. Chem.* 279, 9997–10004 (2004).
86. Sun, J. et al. CD24 blunts the sensitivity of retinoblastoma to vincristine by modulating autophagy. *Mol. Oncol.* 14, 1740–1759 (2020).
87. Iqbal, M. S., Tsuyama, N., Obata, M. & Ishikawa, H. A novel signaling pathway associated with Lyn, PI 3-kinase and Akt supports the proliferation of myeloma cells. *Biochem. Biophys. Res. Commun.* 392, 415–420 (2010).

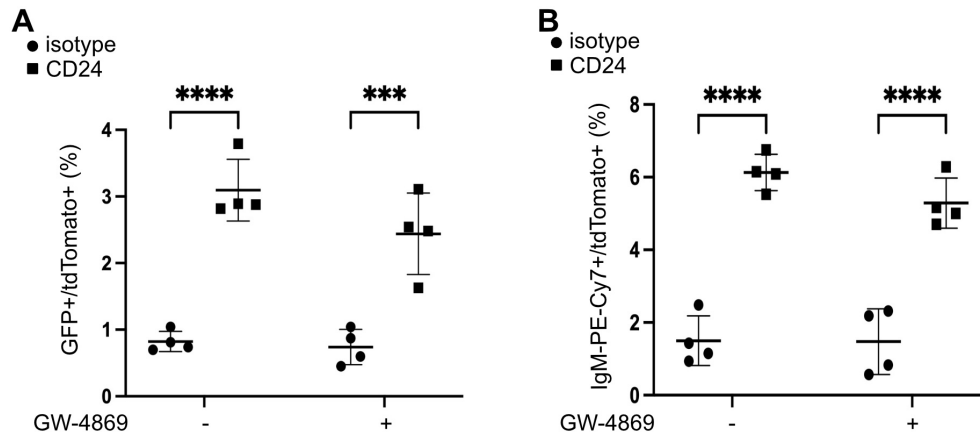
88. Su, N. et al. Lyn is involved in CD24-induced ERK1/2 activation in colorectal cancer. *Mol. Cancer* 11, 43 (2012).
89. Wimalachandra, D. et al. Long-chain glucosylceramides crosstalk with LYN mediates endometrial cell migration. *Biochim. Biophys. Acta BBA - Mol. Cell Biol. Lipids* 1863, 71–80 (2018).
90. Sonnino, S. et al. Role of very long fatty acid-containing glycosphingolipids in membrane organization and cell signaling: the model of lactosylceramide in neutrophils. *Glycoconj. J.* 26, 615–621 (2009).
91. Horbay, R. et al. Role of Ceramides and Lysosomes in Extracellular Vesicle Biogenesis, Cargo Sorting and Release. *Int. J. Mol. Sci.* 23, 15317 (2022).
92. Kolesnick, R. The therapeutic potential of modulating the ceramide/sphingomyelin pathway. *J. Clin. Invest.* 110, 3–8 (2002).
93. Stancevic, B. & Kolesnick, R. Ceramide-rich platforms in transmembrane signaling. *FEBS Lett.* 584, 1728–1740 (2010).
94. Marchesini, N. & Hannun, Y. A. Acid and neutral sphingomyelinases: roles and mechanisms of regulation. *Biochem. Cell Biol.* 82, 27–44 (2004).
95. Ira & Johnston, L. J. Sphingomyelinase generation of ceramide promotes clustering of nanoscale domains in supported bilayer membranes. *Biochim. Biophys. Acta BBA - Biomembr.* 1778, 185–197 (2008).
96. Gómez-Muñoz, A. Modulation of cell signalling by ceramides. *Biochim. Biophys. Acta BBA - Lipids Lipid Metab.* 1391, 92–109 (1998).
97. Gómez-Muñoz, A. Ceramide 1-phosphate/ceramide, a switch between life and death. *Biochim. Biophys. Acta BBA - Biomembr.* 1758, 2049–2056 (2006).

98. Gómez-Muñoz, A. et al. Ceramide-1-phosphate promotes cell survival through activation of the phosphatidylinositol 3-kinase/protein kinase B pathway. *FEBS Lett.* 579, 3744–3750 (2005).
99. Wang, H., Huang, H. & Ding, S.-F. Sphingosine-1-phosphate promotes the proliferation and attenuates apoptosis of Endothelial progenitor cells via S1PR1/S1PR3/PI3K/Akt pathway. *Cell Biol. Int.* 42, 1492–1502 (2018).
100. Xiao, S., Peng, K., Li, C., Long, Y. & Yu, Q. The role of sphingosine-1-phosphate in autophagy and related disorders. *Cell Death Discov.* 9, 1–14 (2023).

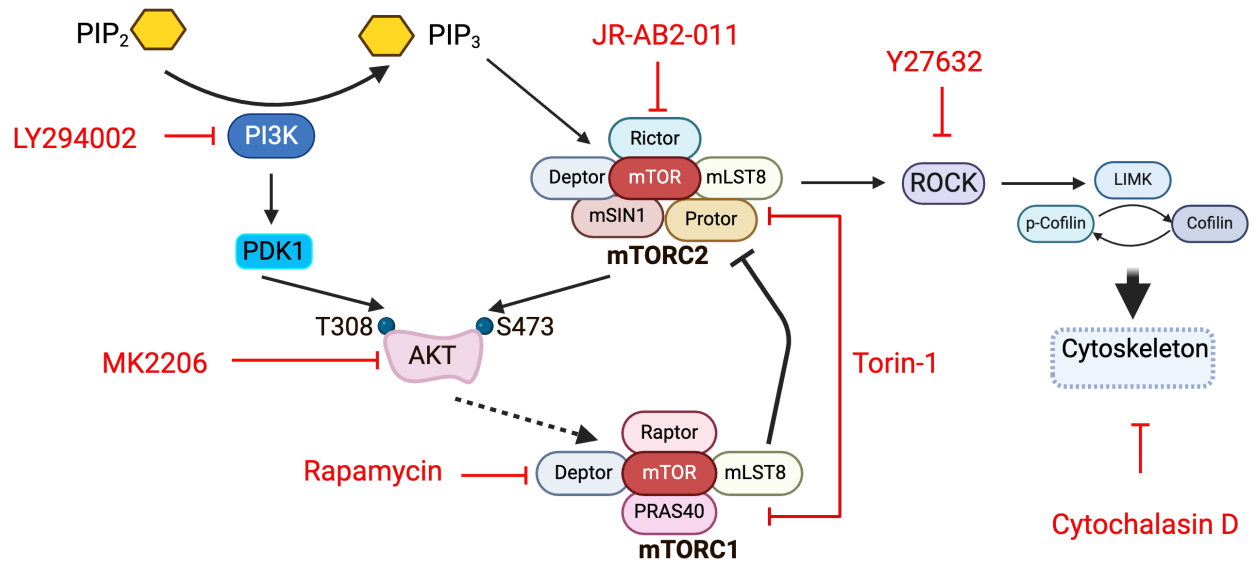
3.8. Supplemental figures



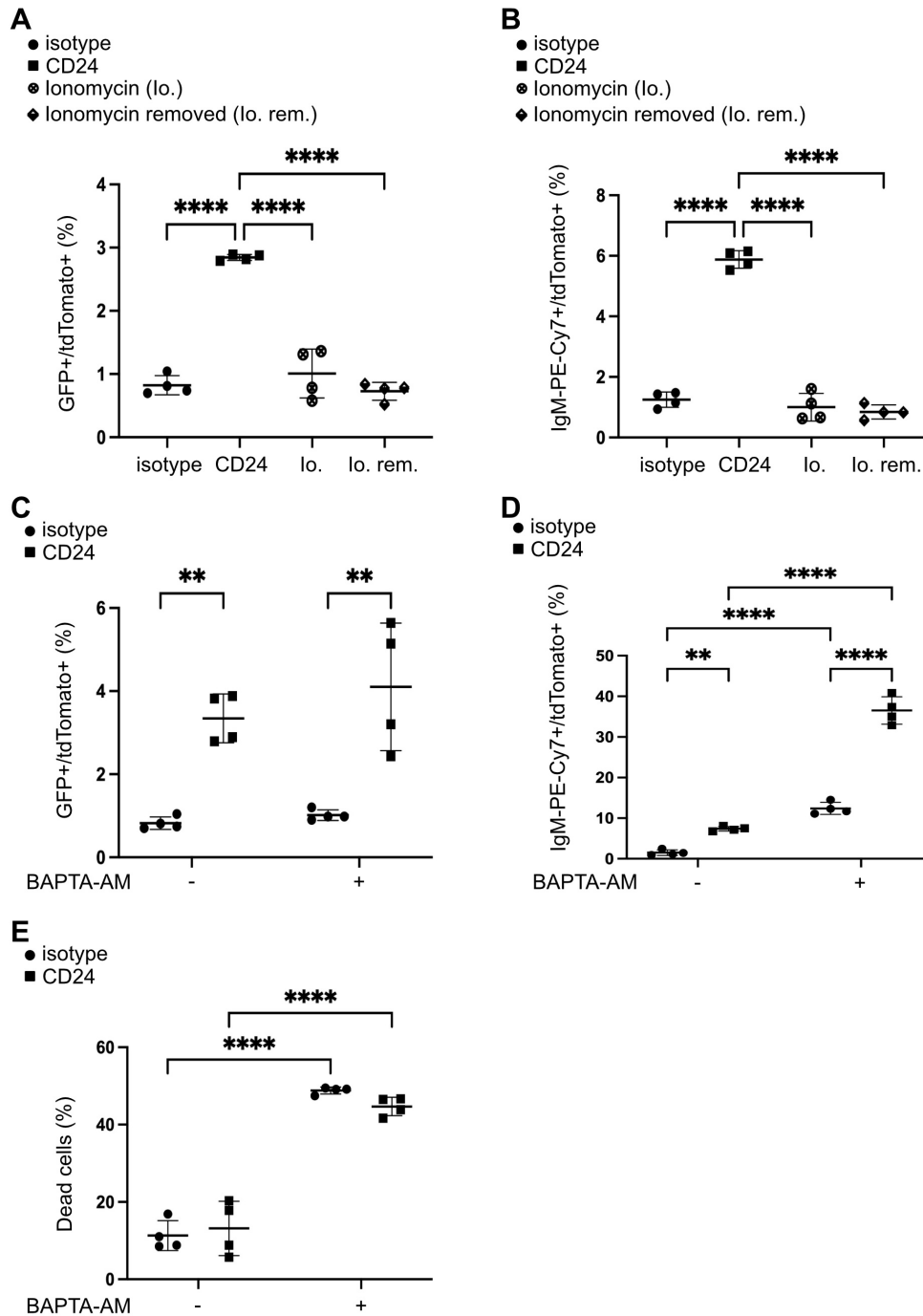
Supplemental Figure 3.1. Pre-treatment with inhibitor on donor WEHI-231-GFP cells inhibits the transfer of GFP and IgM from donor to recipient cells in response to CD24. (A) The percentage of cells positive for GFP and tdTomato. (B) WEHI-231-GFP are 100% IgM positive while WEHI-303-tdTomato cells do not express IgM on their cell membrane. (C) Schematic of experimental design of model system. WEHI-231-GFP cells were pre-treated with a chemical, for example, LY294002 or DMSO, for 15 min, then stimulated with isotype control or anti-CD24 for 15 min, followed by washout and then a 24 h co-culture with WEHI-303-tdTomato cells. Representative dotplots of GFP-positive (D) and IgM-positive (E) on WEHI-303-tdTomato cells after co-culture with stimulated donor WEHI-231-GFP cells.



Supplemental Figure 3.2. nSMase has no effect on EV release regulation. WEHI-231-GFP cells were pre-treated with GW4869 or DMSO for 15 min, then stimulated with anti-CD24 or isotype control for 15 min, followed by washout and then a 24 h co-culture with WEHI-303-tdTomato cells. (A) Percent GFP and tdTomato double-positive cells and (B) Percent IgM and tdTomato double-positive cells after 24 h incubation. n=4, statistical significance determined by a two-way ANOVA (interaction significant at P=0.2669 for A and P=0.4195 for B) followed by the Sidak's multiple comparison test ***P<0.005, ****P<0.001.



Supplemental Figure 3.3. Inhibition of CD24-mediated EV release by PI3K/Akt/mTORC2/ROCK signaling pathways. The enzyme PI3K and the downstream AKT protein were initially identified by their activity associated with various oncoproteins, growth factor receptors, and events associated with the cell cycle. LY294002 is a chemical compound that is a potent inhibitor of numerous proteins and a strong inhibitor of PI3Ks. MK-2206 is a selective allosteric inhibitor of AKT. The two complexes of mTOR, mTORC1 and mTORC2, are involved in cell growth and proliferation. Torin-1 is a potent and selective inhibitor of the mechanistic target of mTOR subtypes mTORC1 and mTORC2. Rapamycin is a specific inhibitor of mTORC1, whereas JB-AB2-011 is a potent and selective inhibitor of mTORC2 kinase activity. Rho-associated protein kinases (ROCK) are serine-threonine kinases involved in cytoskeleton re-organisation. Y27632 is a competitive inhibitor of both ROCK1 and ROCK2. Cytochalasin D is a potent inhibitor of actin polymerization. Created with BioRender.com.



Supplemental Figure 3.4. Calcium has no influence on the regulating of EV release. (A-B)

WEHI-231-GFP cells were stimulated with isotype control, anti-CD24, ionomycin or ionomycin removed after 15 min, followed by 24 h co-culture with WEHI-303-tdTomato cells. (A) Percent GFP and tdTomato double-positive cells. (B) Percent IgM and tdTomato double-positive cells

after 24 h incubation. n=4, statistical significance was determined by a one-way ANOVA followed by the Sidak's multiple comparison test ****P<0.001. (C-D) WEHI-231-GFP cells were pre-treated with BAPTA-AM or DMSO for 15 min, then stimulated with anti-CD24 or isotype control for 15 min, followed by washout and then a 24 h co-culture with WEHI-303-tdTomato cells. (C) Percent GFP and tdTomato double-positive cells and (D) Percent IgM and tdTomato double-positive cells after 24 h incubation. n=4, statistical significance determined by a two-way ANOVA (interaction significant at P=0.5072 for C and P<0.0001 for D) followed by the Sidak's multiple comparison test **P<0.01, ****P<0.001. (E) Percent dead cells determined from the non-gated population based on the BAPTA-AM experiment. n=4, statistical significance determined by a two-way ANOVA (interaction significant at P=0.1799) followed by the Sidak's multiple comparison test ****P<0.001.

4. Chapter 4: Discussion

4.1. Summary of results

Extracellular vesicles (EVs) can impact several biological processes by directly activating cell surface receptors and transporting molecular effectors into target cells¹⁻³. Prior research has documented that B cells produce more EVs in the engagement of CD24 stimulation⁴.

Consequently, I focused on EV-mediated cellular communication between B cells in order to confirm that EVs derived from donor B cells strongly modulate the activity of recipient B cells. In this work, I used multiple approaches to validate that donor B cell-derived EVs transferred lipids and surface proteins (CD24 and IgM) to recipient B cells in response to CD24 and IgM stimulation. For instance, CD24 and IgM challenge increased the number of EVs carrying GFP-associated lipid and surface proteins transferred to the recipient cells, when recipient cells were either co-cultured with treated donor cells in the same layer or cultured only with SEC-isolated EVs originated from treated donor cells. EV-specific proteins in the purified EV samples were identified using Western blotting with anti-CD81, anti-Hsp90, anti-IgM, and GFP antibodies, similar to EV markers described in other studies⁵⁻⁷. The number of EVs secreted from donor cells treated with surface proteins was substantially higher than those released from isotype treated cells. This data is generally consistent with earlier work and showed EVs in the 100-200 nm size range⁵. Moreover, EV carrying IgM membrane proteins was visualized in the recipient cells. To determine whether the surface membrane proteins (CD24 and BCR) were taken up by the recipient cells and if they triggered the cellular response in the recipient cells, different controls were used. EVs from donor B cells alone did not induce phosphorylation of ERK1/2 or apoptosis in the recipient cells, even when the donor cells were stimulated with isotype, indicating that only CD24 and IgM stimuli, were transferred via EVs to the recipient cells. These data provided

further evidence that in response to receptor engagement, donor cells can actively alter the behavior of neighboring cells by EV transfer of functional cargo.

Furthermore, using bioinformatics analysis suggested that the PI3K, AKT and mTOR signaling pathways may be relevant with the mechanism of action of CD24. I generated the hypothesis that CD24-mediated EV release is regulated by these pathways. Using chemical and genetic inhibition, I subsequently confirmed this theory by demonstrating that suppressing downstream targets, the PI3K-AKT signaling and regulation of actin cytoskeleton, inhibits the transfer of lipids and proteins to recipient cells in response to CD24. The data from this work and previous studies suggests that the EVs induced by CD24 stimulation are ectosomes budded off the plasma membrane, not exosomes derived from multivesicular bodies. Overall, this work provides a new insight into regulating ectosome generation.

4.2. Discussion and Question Arising

The work in this thesis identified a novel pathway regulating ectosome release into the extracellular microenvironment, which allowed them to alter the physiological state of the recipient cells. However, there is much about CD24-mediated ectosomes derived from B cells that remain unknown. There are several areas of future research that can be derived from this work: examining whether ectosomes derived from CD24-stimulated B cells may affect different bone marrow cell types and cause a biological reaction, investigating whether ectosomes produced from B cells activated by CD24 can be taken up by secondary cells *in vivo*, investigating how ectosomes uptake in recipient cells, investigating whether CD24 requires co-receptor binding for intracellular signal transduction, investigating how CD24 triggers aSMase on lipid rafts, as well as the mechanism of CD24 activation that drives the metabolism of ceramide/sphingosine and its antagonistic molecule to maintain regular cell activity.

Chapter 2 of this thesis identified that the release of ectosomes transferred lipid and functional surface proteins between neighboring B cells, and imparted functional consequence was extensive in recipient cells. However, to investigate the potential transfer of functional ectosomes in other cell types in the bone marrow environment is required. For instance, bone marrow mesenchymal stromal cells (BMSCs) are plastic adherent non-hematopoietic progenitor cells that can stimulate bone tissue repair and regeneration⁸. CD24 is initially presented at a small level of expression on the surface of BMSCs at the first day of osteogenic differentiation and reaches a maximal level after 7-10 days of osteogenic differentiation, suggesting that CD24 could serve as a surface marker for a subpopulation of BMSCs with increased osteoblastic potential⁹. An emerging question is whether CD24 expression on BMSCs comes from B cells during osteogenic differentiation of BMSCs. Additionally, EVs derived from BMSCs of leukemia patients rescue leukemic B cells from apoptosis and enhance their migration capacity¹⁰. However, there is limited knowledge on the effect of secreted EVs upon interactions with B cells originating from the BM, where BMSCs are resident. Further work should investigate the bidirectional transfer between B cells and BMSCs, and their functional consequences.

The work in Chapter 2 proved that ectosomes derived from CD24-stimulated immature B cells delivered functional proteins and activated apoptosis in CD24KO B cells, thereby increasing speculation about possible roles of EVs in B cell development. However, an emerging question is whether this transfer can observe *in vivo*. EVs are challenging to track *in vivo* because they are small size, quickly dispersed in body fluids, and have a similar composition to body cells¹¹. Recently, more refined techniques for EV imaging have made their way into the field which are slowly changing about the labeling and tracking of EVs, including fluorescent imaging, bioluminescent imaging, radio-labeling-assisted imaging, and nanoparticle-based imaging¹².

Further work should evaluate EV tracking, GFP and CD24 transportation, and subcellular localization following transfer using bioluminescent imaging, fluorescent signal, antibody immunofluorescence staining, and/or confocal microscopy.

Many studies have demonstrated that EVs can affect the physiological state of target cells through various uptake mechanism, including endocytosis, receptor-ligand interactions, fusion membrane^{6,7,13}. It is also known that the lipid raft-like membrane composition of EVs facilitates in fusing with the recipient cell membranes¹⁴. In addition, PS and P-selectin on the exterior of cells are necessary for fusion of tissue factor-expressing MVs with platelets, and PS is necessary for fusion of EVs with glioma cells¹⁵⁻¹⁷. Interestingly, PS on EVs is increased upon stimulation of CD24, suggesting that PS-binding may be a mechanism by which the EVs that are released in response to CD24 stimulation bind to target cells¹⁸. When EVs fuse with the target cells, they can transfer their parent cytosolic content and translocate cell membrane attached and spanning proteins¹⁹. In this study, I discovered that both CD24 and the BCR maintained their transmembrane orientation. Additionally, the appearance of patches of BCR was revealed under the confocal microscopy, and the transfer of cytosol from primary B cells to immature B cell lines, as assessed by the transfer of eFluor670. Only the addition of anti-IgM or anti-CD24, the functional transported proteins could induce intracellular signal transduction in recipient cells. Thus, the maintenance of the orientation of these receptors and the activation of intracellular signaling pathways by the transferred receptors suggest that there is some fusion of the EVs with the plasma membrane. Nevertheless, it is currently unknown what exact mechanism drives EV uptake and whether these EVs are directed towards recipient cells through specific receptors or PS. Therefore, further work should determine how ectosomes are uptaken up in recipient cells.

Chapter 3 of this thesis clarified, for the first time, that CD24 triggers the activation of the aSMase/PI3K/AKT/mTOR/ROCK signaling pathway in B cells to induce ectosome release. The

overexpression of CD24 in tumor cells has been linked to multiple signaling pathways, including Wnt/ β -catenin, mitogen activated kinase (MAPK), PI3K/AKT kinase, and Notch and Hedgehog pathway²⁰. However, it is notable that CD24 cannot directly signal into the host cell because it lacks intracellular transmembrane domains or cytoplasmic domains²¹. The extracellular domain of CD24 has varying numbers of N-linked and O-linked glycosylation sites, which interact with a range of cell surface receptors in glycolipid-enriched membrane domains in order to transduce intracellular signaling through engaging in cis (same cell) or trans (adjacent cells) interactions^{22,23}. Among the most studied ligands that bind CD24 are P-, L-, and E-selectin, the sialic acid binding immunoglobulin-like lectin (Siglec) 10, Siglec 15, the L1 cell adhesion molecule (LICAM), and transient axonal glycoprotein (TAG)-1^{24,25}. There are two siglecs expressed on the surface of B cells, named CD22 (Siglec-2) and Siglec-G or Siglec 10, which are known to bind CD24 to perform a variety of activities²⁶. CD22 binds α 2,6-linked sialic acids²⁷, while Siglec-G can bind both α 2,6- and α 2,3-linked sialic acids²⁸. CD22 and Siglec-G carry immunoreceptor tyrosine-based inhibitory motifs (ITIMs) within their cytoplasmic tail and recruit the tyrosine phosphate SHP-1 that inhibits BCR-mediated signaling²⁹. Siglec 2 has been shown to contribute to regulating B cell signalling, cell survival, proliferation, and antibody production^{30,31}. In addition, CD24/Siglec-G can activate SHP-1 and SHP-2 phosphates linked to ITIMs, inhibiting TLR-mediated inflammation and macrophage engulfment of cells³². The CD24/Siglec-G pathway engages danger-associated molecular patterns (DAMPs) while it is not affected by pathogen-associated molecular patterns (PAMPs) in response to signals of injury³³. Therefore, further work should determine if Siglec-G or CD22 is expressed on the B cell surface as a co-receptor for CD24 in controlling B cell development in the bone marrow.

The work in Chapter 3 demonstrated the functional role of aSMase, which triggers the PI3K signaling pathway in response to CD24 stimulation. As mentioned above, CD24 lacks intrinsic enzymatic activity; it interacts with other signal transducers to induce intracellular signaling through glycolipid-enriched membrane (GEM) domains, also called lipid rafts^{22,23}. The GEM domain is considered an important platform for signaling molecules, such as the Src family tyrosine kinases (SFK) and G-proteins^{34,35}. Several reports have shown that GPI-linked CD24 protein was shown to be associated with the Src family tyrosine kinases (SFK), which consist of nine members, including Blk, Fgr, Fyn, Hck, Lck, Lyn, Src, Yes, and Yrk^{35,36}. Cross-linking of CD24 enhances the interaction between CD24 and Lyn, which in turn regulates the increased activity of Lyn and the activation of mitogen-activated protein kinases (MAPK) that leads to B cell apoptosis³⁷. In addition, aSMase is required to distribute palmitoylated proteins, such as SNAP23 and Lyn, from the Golgi to the plasma membrane³⁸. The SFK activation initiates the recruitment of the PI3K^{39,40}. However, the interaction between Src family and aSMase is unknown, although these proteins are associated with CD24 activity. Thus, an emerging question is how CD24 triggers aSMase on lipid rafts.

Finally, one mystery that keeps coming up is how CD24 activation is involved in cell proliferation and apoptosis. As a well-established function, CD24 mediates intracellular signal transduction that leads to B cell apoptosis^{4,37,41}. However, my current work found that CD24 activation triggers aSMase, which in turn activates the PI3K, mTORC2 and Akt signaling pathways, which are more well-known for their role in B cell proliferation and survival⁴². aSMase hydrolyzes sphingomyelin to produce the biologically active lipid ceramide³⁸. Ceramide has long been recognized to cause necrosis or apoptosis in a variety of cell types, but more recent research shows that ceramide and its metabolites have a significant impact on cellular metabolism⁴³. In the process of sphingolipid metabolism, ceramide can be broken down to

generate sphingosine by ceramidases⁴⁴. Ceramide and sphingosine both function by stimulating protein phosphatase 2A and PKC δ , which in turn inhibits Akt activity and induces cell cycle arrest and apoptosis⁴⁵. It is reported that ceramide can become ceramide-1-phosphate (C1P) by the action of ceramide kinase. C1P can be converted back to ceramide by lipid phosphate phosphatases⁴⁶. Alternatively, sphingosine-1-phosphate (S1P) can be generated by phosphorylating sphingosine by the action of sphingosine kinase⁴⁶. Evidence showed that C1P and S1P activate PI3K, which supports cell survival and proliferation⁴⁷⁻⁴⁹. More research will be required to determine if the mechanisms of CD24 activation induce enzymes involved in ceramide/sphingosine and its antagonistic molecule to maintain regular cell activity.

4.3. Conclusion

The current study significantly adds to our knowledge of the role of EVs, especially ectosomes, as important mediators in cell-to-cell communication. Evidence showed that CD24 and IgM stimulation of B cells triggers transfer of surface receptors between B cells through ectosomes to induce functional changes in recipient cells. In addition, I identified a novel pathway regulating ectosome release that has not been reported in any cell types. The research topic enhances understanding the expression of CD24 on B cells during B cell development. It offers great opportunities into the diverse function of CD24 as well as increasing biomedical application of EVs, particularly in B cells.

4.4. References

1. Ratajczak, J. et al. Embryonic stem cell-derived microvesicles reprogram hematopoietic progenitors: evidence for horizontal transfer of mRNA and protein delivery. *Leukemia* 20, 847–856 (2006).
2. Valadi, H. et al. Exosome-mediated transfer of mRNAs and microRNAs is a novel mechanism of genetic exchange between cells. *Nat. Cell Biol.* 9, 654–659 (2007).
3. Camussi, G. et al. Exosome/microvesicle-mediated epigenetic reprogramming of cells. *Am. J. Cancer Res.* 1, 98 (2010).
4. Ayre, D. C. et al. Dynamic regulation of CD24 expression and release of CD24-containing microvesicles in immature B cells in response to CD24 engagement. *Immunology* 146, 217–233 (2015).
5. Ayre, D. C. C. et al. CD24 induces changes to the surface receptors of B cell microvesicles with variable effects on their RNA and protein cargo. *Sci. Rep.* 7, 8642 (2017).
6. Kwok, Z. H., Wang, C. & Jin, Y. Extracellular Vesicle Transportation and Uptake by Recipient Cells: A Critical Process to Regulate Human Diseases. *Process. Basel Switz.* 9, 273 (2021).
7. Liu, Y.-J. & Wang, C. A review of the regulatory mechanisms of extracellular vesicles-mediated intercellular communication. *Cell Commun. Signal.* 21, 77 (2023).
8. Lee, Y.-C., Chan, Y.-H., Hsieh, S.-C., Lew, W.-Z. & Feng, S.-W. Comparing the Osteogenic Potentials and Bone Regeneration Capacities of Bone Marrow and Dental Pulp Mesenchymal Stem Cells in a Rabbit Calvarial Bone Defect Model. *Int. J. Mol. Sci.* 20, 5015 (2019).

9. Van de Peppel, J. et al. Cell Surface Glycoprotein CD24 Marks Bone Marrow-Derived Human Mesenchymal Stem/Stromal Cells with Reduced Proliferative and Differentiation Capacity In Vitro. *Stem Cells Dev.* 30, 325–336 (2021).
10. Crompot, E. et al. Extracellular vesicles of bone marrow stromal cells rescue chronic lymphocytic leukemia B cells from apoptosis, enhance their migration and induce gene expression modifications. *Haematologica* 102, 1594–1604 (2017).
11. Jiang, A., Nie, W. & Xie, H. In Vivo Imaging for the Visualization of Extracellular Vesicle-Based Tumor Therapy. *ChemistryOpen* 11, e202200124 (2022).
12. Liu, Q., Huang, J., Xia, J., Liang, Y. & Li, G. Tracking tools of extracellular vesicles for biomedical research. *Front. Bioeng. Biotechnol.* 10, 943712 (2022).
13. Gurung, S., Perocheau, D., Touramanidou, L. & Baruteau, J. The exosome journey: from biogenesis to uptake and intracellular signalling. *Cell Commun. Signal. CCS* 19, 47 (2021).
14. Valapala, M. & Vishwanatha, J. K. Lipid Raft Endocytosis and Exosomal Transport Facilitate Extracellular Trafficking of Annexin A2. *J. Biol. Chem.* 286, 30911–30925 (2011).
15. Al-Nedawi, K. et al. Intercellular transfer of the oncogenic receptor EGFRvIII by microvesicles derived from tumour cells. *Nat. Cell Biol.* 10, 619–624 (2008).
16. Del Conde, I., Shrimpton, C. N., Thiagarajan, P. & López, J. A. Tissue-factor-bearing microvesicles arise from lipid rafts and fuse with activated platelets to initiate coagulation. *Blood* 106, 1604–1611 (2005).
17. Falati, S. et al. Accumulation of tissue factor into developing thrombi in vivo is dependent upon microparticle P-selectin glycoprotein ligand 1 and platelet P-selectin. *J. Exp. Med.* 197, 1585–1598 (2003).

18. Ayre, D. C. C. et al. Dynamic regulation of CD24 expression and release of CD24-containing microvesicles in immature B cells in response to CD24 engagement. *Immunology* 146, 217–233 (2015).
19. Cognasse, F. et al. The role of microparticles in inflammation and transfusion: A concise review. *Transfus. Apher. Sci.* 53, 159–167 (2015).
20. Yang, Y., Zhu, G., Yang, L. & Yang, Y. Targeting CD24 as a novel immunotherapy for solid cancers. *Cell Commun. Signal.* 21, 312 (2023).
21. Fang, X., Zheng, P., Tang, J. & Liu, Y. CD24: from A to Z. *Cell. Mol. Immunol.* 7, 100–103 (2010).
22. Daniel T., G., Vishal, M., Niko P., B. & Jan, P. The CD24 surface antigen in neural development and disease. *Neurobiol. Dis.* 99, 133–144 (2017).
23. Ayre, D. C. et al. Analysis of the structure, evolution, and expression of CD24, an important regulator of cell fate. *Gene* 590, 324–337 (2016).
24. Ayre, D. C. & Christian, S. L. CD24: A Rheostat That Modulates Cell Surface Receptor Signaling of Diverse Receptors. *Front. Cell Dev. Biol.* 4, 146 (2016).
25. Jiang, K.-Y., Qi, L.-L., Kang, F.-B. & Wang, L. The intriguing roles of Siglec family members in the tumor microenvironment. *Biomark. Res.* 10, 22 (2022).
26. Nitschke, L. CD22 and Siglec-G: B-cell inhibitory receptors with distinct functions. *Immunol. Rev.* 230, 128–143 (2009).
27. Engel, P., Wagner, N., Miller, A. S. & Tedder, T. F. Identification of the ligand-binding domains of CD22, a member of the immunoglobulin superfamily that uniquely binds a sialic acid-dependent ligand. *J. Exp. Med.* 181, 1581–1586 (1995).

28. Duong, B. H. et al. Decoration of T-independent antigen with ligands for CD22 and Siglec-G can suppress immunity and induce B cell tolerance in vivo. *J. Exp. Med.* 207, 173–187 (2010).
29. Jellusova, J. & Nitschke, L. Regulation of B Cell Functions by the Sialic Acid-Binding Receptors Siglec-G and CD22. *Front. Immunol.* 2, (2012).
30. Walker, J. A. & Smith, K. G. C. CD22: an inhibitory enigma. *Immunology* 123, 314 (2008).
31. Meyer, S. J., Linder, A. T., Brandl, C. & Nitschke, L. B Cell Siglecs—News on Signaling and Its Interplay With Ligand Binding. *Front. Immunol.* 9, 2820 (2018).
32. Li, X. et al. Targeting CD24/Siglec-10 signal pathway for cancer immunotherapy: recent advances and future directions. *Cancer Immunol. Immunother.* CII 73, 31 (2024).
33. Liu, Y., Chen, G.-Y. & Zheng, P. CD24-Siglec G/10 discriminates danger- from pathogen-associated molecular patterns. *Trends Immunol.* 30, 557–561 (2009).
34. Yin, S.-S. & Gao, F.-H. Molecular Mechanism of Tumor Cell Immune Escape Mediated by CD24/Siglec-10. *Front. Immunol.* 11, 1324 (2020).
35. Daoud, G., Rassart, É., Masse, A. & Lafond, J. Src family kinases play multiple roles in differentiation of trophoblasts from human term placenta. *J. Physiol.* 571, 537–553 (2006).
36. Sammar, M., Gulbins, E., Hilbert, K., Lang, F. & Altevogt, P. Mouse CD24 as a Signaling Molecule for Integrin-Mediated Cell Binding: Functional and Physical Association with src-Kinases. *Biochem. Biophys. Res. Commun.* 234, 330–334 (1997).
37. Suzuki, T. et al. CD24 induces apoptosis in human B cells via the glycolipid-enriched membrane domains/rafts-mediated signaling system. *J. Immunol. Baltim. Md* 1950 166, 5567–5577 (2001).
38. Xiong, X. et al. Acid sphingomyelinase regulates the localization and trafficking of palmitoylated proteins. *Biol. Open* 8, bio040311 (2019).

39. Iqbal, M. S., Tsuyama, N., Obata, M. & Ishikawa, H. A novel signaling pathway associated with Lyn, PI 3-kinase and Akt supports the proliferation of myeloma cells. *Biochem. Biophys. Res. Commun.* 392, 415–420 (2010).
40. Su, N. et al. Lyn is involved in CD24-induced ERK1/2 activation in colorectal cancer. *Mol. Cancer* 11, 43 (2012).
41. Phan, H.-D. et al. CD24 and IgM Stimulation of B Cells Triggers Transfer of Functional B Cell Receptor to B Cell Recipients Via Extracellular Vesicles. *J. Immunol. Baltim. Md* 1950 207, 3004–3015 (2021).
42. Limon, J. J. & Fruman, D. A. Akt and mTOR in B Cell Activation and Differentiation. *Front. Immunol.* 3, 1–12 (2012).
43. Guenther, G. G. & Edinger, A. L. A new take on ceramide: starving cells by cutting off the nutrient supply. *Cell Cycle Georget. Tex* 8, 1122–1126 (2009).
44. Gómez-Muñoz, A. Modulation of cell signalling by ceramides. *Biochim. Biophys. Acta BBA - Lipids Lipid Metab.* 1391, 92–109 (1998).
45. Yu, L., Wei, J. & Liu, P. Attacking the PI3K/Akt/mTOR signaling pathway for targeted therapeutic treatment in human cancer. *Semin. Cancer Biol.* 85, 69–94 (2022).
46. Gómez-Muñoz, A. Ceramide 1-phosphate/ceramide, a switch between life and death. *Biochim. Biophys. Acta BBA - Biomembr.* 1758, 2049–2056 (2006).
47. Gómez-Muñoz, A. et al. Ceramide-1-phosphate promotes cell survival through activation of the phosphatidylinositol 3-kinase/protein kinase B pathway. *FEBS Lett.* 579, 3744–3750 (2005).
48. Wang, H., Huang, H. & Ding, S.-F. Sphingosine-1-phosphate promotes the proliferation and attenuates apoptosis of Endothelial progenitor cells via S1PR1/S1PR3/PI3K/Akt pathway. *Cell Biol. Int.* 42, 1492–1502 (2018).

49. Xiao, S., Peng, K., Li, C., Long, Y. & Yu, Q. The role of sphingosine-1-phosphate in autophagy and related disorders. *Cell Death Discov.* 9, 1–14 (2023).

Appendix

1. Lentiviral transfection

1.1. Theoretical basis of the method

Retrovirus-based gene transfer to mammalian cells presented major advantages, due to producing stable transgene expression by interaction of their genome in the host cell chromosomes¹. In recent years, lentivirus vector development has received much interest because they have characteristics like their simple retrovirus counterparts, are devoid of viral protein, are free from replication-competent viruses, and can also transduce non-dividing cells². Lentivirus vectors bring more benefits than other transfected methods. For instance, lipofection, a non-viral vector, is low in cost and is non-pathogenic, but it has limited transfection efficiency³. Unlike adenoviral vectors, there are rarely neutralizing antibodies against lentiviral vectors⁴. Importantly, lentivirus has been modified to reduce biosafety risks, where the crucial genes are separated and packaged in several plasmids that form the viral glycoproteins⁵. In short brief, lentivector particles are generated by co-transfection of 3 plasmids in human embryonic kidney (HEK) 293T cells, including a packing plasmid, a transfer plasmid and an envelope-encoding plasmid⁶. Currently, there are four generations of lentiviral vectors provided⁷.

The scheme of a second-generation recombinant lentiviral vectors is shown in Figure 1.1. and schematic presentation of the production of lentivirus vector particles is shown in Figure 1.2.

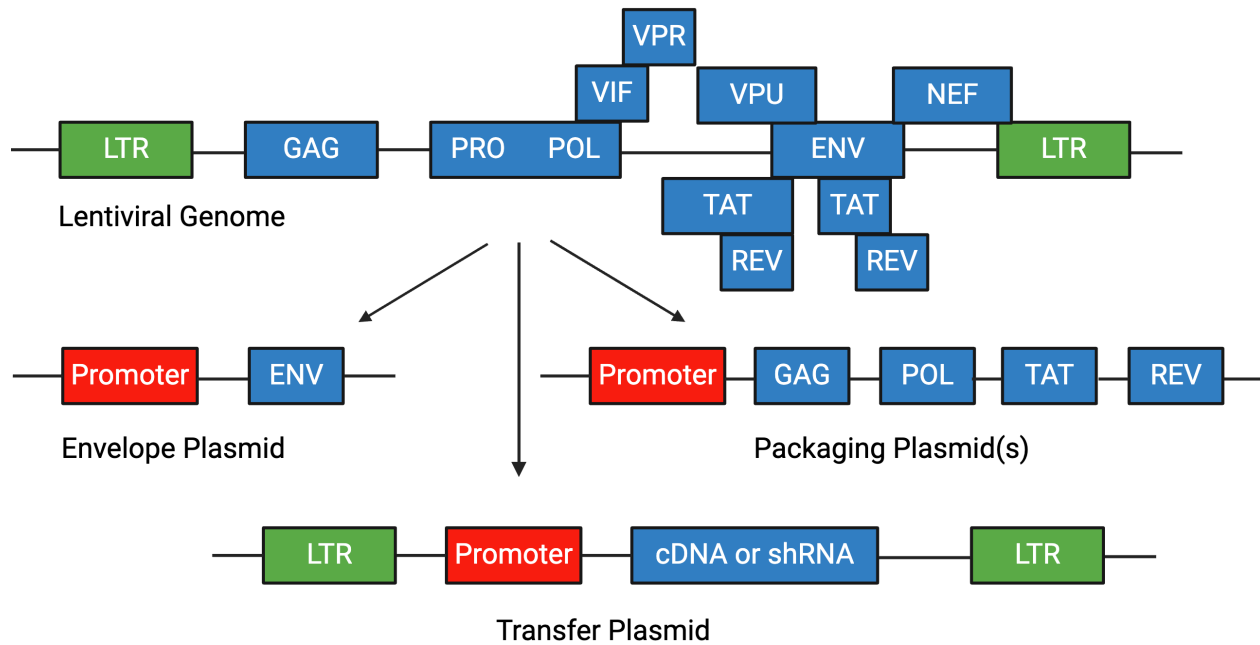


Figure 1.1. Scheme of a second-generation recombinant lentiviral vectors. The system contains three separate plasmids: a packaging plasmid, an envelope plasmid encoding the viral glycoprotein, and a transfer vector genome construct. The packaging plasmid express HIV Gag, Pol, and two regulatory genes for viral replication, Tat and Rev, under the control of a CMV promoter. The envelope plasmid expresses a viral glycoprotein such as VSV-G to provide the vector particles with a receptor binding protein. The transfer vector plasmid contains LTR that are require for viral gene expression, reverse transcription and transport of viral RNAs. Created with BioRender.com.

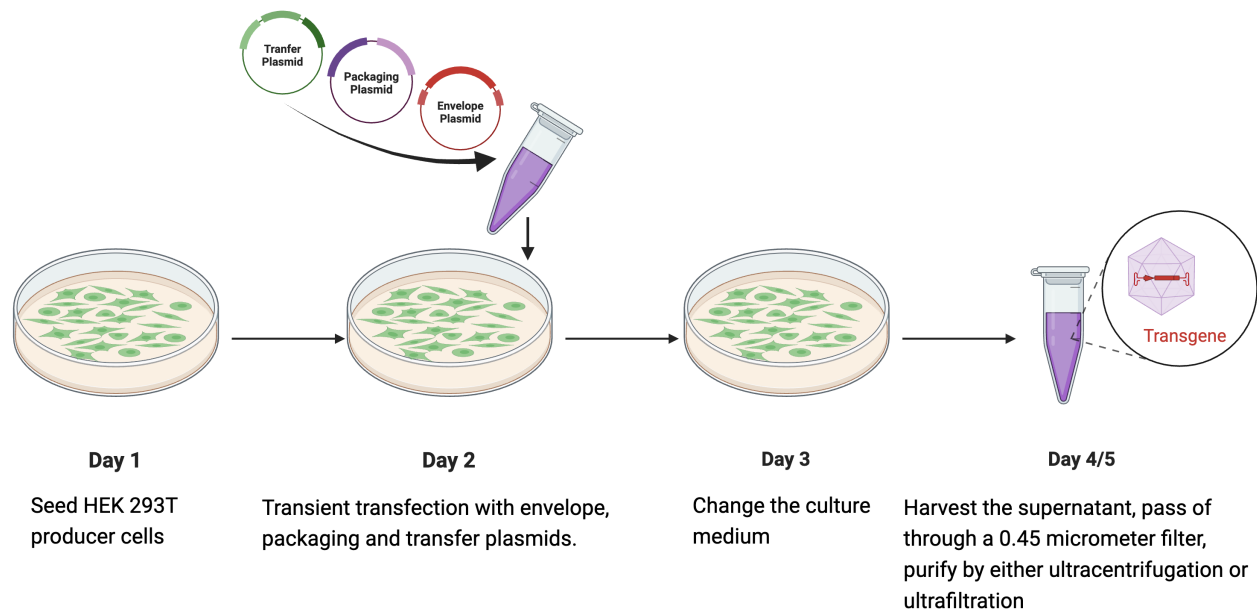


Figure 1.2. Schematic presentation of the production of lentivirus vector particles. The HEK 293T cells grow up to 90% confluency, followed by transfection using envelope, packaging and transfer plasmids. Virus particles were collected at 48 h and 36 h post transfection and subsequently filtered through a 0.45 μm filter. Post-transduction, cells expressing the target gene reporter were selectively identified using flow cytometry and/or other techniques. Created with BioRender.com.

1.2. Rationale for using this method

The pCMV-VSV-G-M5 is envelope plasmid that expresses the G glycoprotein of the vesicular stomatitis virus (VSV-G) under the control of the CMV immediated-early promoter. VSV-G is used in pseudotyping of Moloney murine leukemia virus (MMLV)-based retroviral vectors by mediating viral entry. VSV-G interacts with phospholipid components of the target cell membrane and fosters the fusion of viral and cellular membranes. VSV-G does not require a cell surface receptor and can serve as a surrogate viral envelope protein. The vector contains the ampicillin-resistance gene for propagation and antibiotic selection in bacteria.

The pCMV- δ R8.91 is a packing plasmid that contains Gag, Pol, Rev, and Tat. It can be used with the second and third generation transfer plasmids. Gag/Pol encodes structural proteins, and enzymes required for viral reproduction. Tat is necessary for high level expression of viral LTR, whereas Rev has the ability to transport mRNAs containing unsliced and singly spliced viral sequences from the nucleus to the cytoplasm. This vector also contains ampicillin-resistance gene.

The palmitoylation sequences (MLCCMRRTKQ) of growth cone-associated protein (GAP43) were genetically fused to the NH₂ terminus of GFP (PalmGFP) and tdTomato (PalmtdTomato) by PCR using Phusion high fidelity DNA polymerase. Plasmids pCAG-mGFP and pCSCMV-tdTomato were used as cDNA templates for GAP43, EGFP and tdTomato. PalmGFP and PalmtdTomato sequences were inserted into pCSCGW2 lentivector plasmid using NheI and XhoI sites⁸.

The lentiviral packaging plasmid pCMV- δ R8.91, and envelope plasmid pCMV-VSV-G-M5 were co-transfected with either the pCSCGW2-PalmGFP or pCSCGW2-PalmtdTomato lentiviral vector into HEK-293T cells. Lentiviral supernatant was harvested and subsequently filtered through a 0.45 μ m filter at 36 h post transfection, followed by adding it to 12-well plates

containing WEHI-231 or WEHI-303 cells. Cells were cultured 48 h before enrichment by fluorescence-activated cell sorting. WEHI-231-GFP and WEHI-303-tdTomato cells were re-sorted regularly with the Beckman Coulter MoFlo Astrios EQ (Medical Laboratory Services, Memorial University) to maintain >90% fluorescently labelled cells.

2. Vn96-based isolation

2.1. Theoretical basis of the method

Vn96 based isolation has been designed based on a series of peptides showing nucleotide-independent specific affinity for typical heat shock proteins. It has been demonstrated that Vn96 peptides can specifically and affinity capture HSP-containing EVs from cell culture growth media, plasma, and urine⁹. This technique is a more efficient isolation method than current methods based on physical characteristics (density and/or size separations) and multiple antibody affinity-based purifications. Vn96-isolated EVs have a cargo content similar to EVs isolated by the standard ultracentrifugation (UFC) purification method⁹. Moreover, Vn96 peptide can isolate EVs derived from cells under pathological conditions, such as cancer, infection, neurodegenerative, and metabolic diseases¹⁰. Thus, Vn96 peptide is an emerging technology for EV isolation because it provides a simple, efficient, and rapid method of EV enrichment and capture.

2.2. Rationale for using this method

There is no gold standard for isolation of EVs, however, UFC remains the most commonly used method¹¹. UFC takes a long time, requires specialized equipment, and cannot be used for diagnostic testing in a clinic. UFC separates and purifies EVs using centrifugal force. It does this by employing a high centrifugal speed long enough for individual EVs to travel the length of the

tube and form a pellet, although it is less effective at pelleting smaller or less dense particles. Although repeated centrifugation can reduce the amount of non-EV particles co-isolated with the EVs, it reduces particle yield due to lost and damaged EVs¹². A recent study showed that the size of EVs isolated with Vn96 is similar to UCF¹³. Therefore, in this study, Vn96 peptide was selected to isolate EVs in order to identify EV surface protein indicators such CD81, Hsp90, IgM, and GFP proteins because of its advantages, which include specificity, affinity, and less damaged EVs.

3. Inhibitors used

3.1. LY294002

LY294002 is a chemical compound that is a potent inhibitor of several proteins and a strong inhibitor of PI3Ks. It not only binds to class I PI3Ks and other PI3K-related kinases, but also to act on other lipid kinases and additional apparently unrelated to the PI3K family proteins. It is commonly used to investigate the role of the PI3K pathway in various biological processes, including cell growth, survival, and metabolism¹⁴.

Typically, LY294002 use concentrations range from 5 μ M to 50 μ M in cell culture studies. However, using 10 μ M LY294002 has shown a common choice in various studies^{15,16}. Although both 10 μ M and 50 μ M LY294002 pre-treatment were used, 10 μ M LY294002 was sufficient to inhibit signaling downstream of PI3K. Moreover, there was an emerging question if 50 μ M LY294002 concentration induced apoptosis, and thus the release of apoptotic bodies, this could have potentially increased the quantity of lipid and IgM transferred to the recipient cells compared to the 10 μ M LY294002 pre-treated group (Figure 3.1). Thus, 10 μ M LY294002 concentration was chosen in this study.

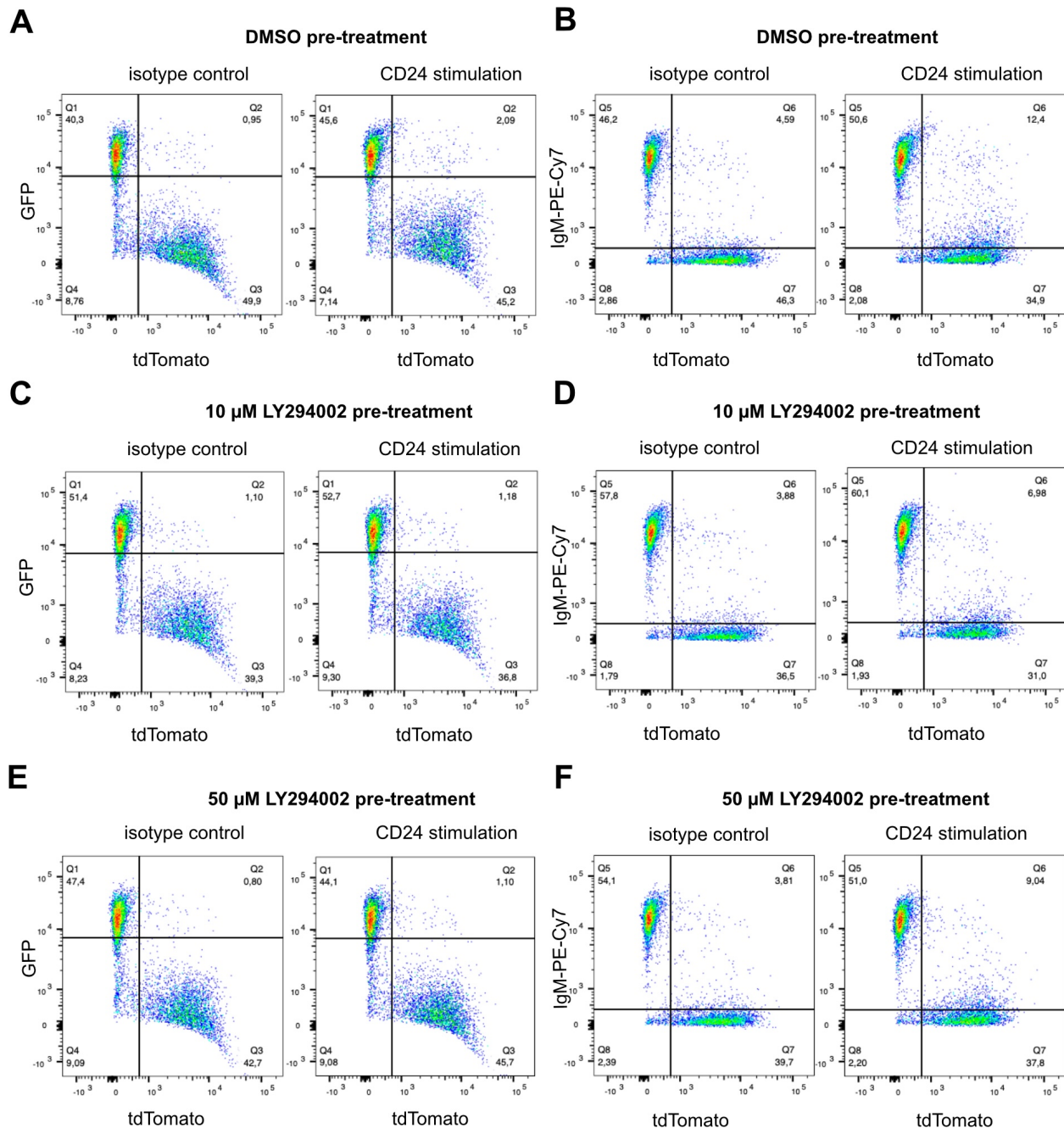


Figure 3.1. Representative dot plots showing the percent of GFP/ IgM-PE-CY7 and tdTomato in pre-treatment with LY294002 or DMSO for 15 min. WEHI-231-GFP cells were pre-treated with (A-B) DMSO for 15 min, or (C-D) 10 μ M LY294002 for 15 min or (E-F) 50 μ M LY294002 for 15 min, then stimulated with isotype control or anti-CD24 for 15 min, followed by washout and then a 24 h co-culture with WEHI-303-tdTomato cells. (A) Representative dot plots

of percent GFP and tdTomato double-positive cells indicating lipid transfer from WEHI-231-GFP to WEHI-303-tdTomato cells in Q2. (B) Representative dot plots of percent IgM and tdTomato double-positive cells indicating IgM transfer from WEHI-231-GFP to WEHI-303-tdTomato cells in Q6. (C) Representative dot plots of percent GFP and tdTomato double-positive cells indicating lipid transfer from WEHI-231-GFP to WEHI-303-tdTomato cells in Q2. (D) Representative dot plots of percent IgM and tdTomato double-positive cells indicating IgM transfer from WEHI-231-GFP to WEHI-303-tdTomato cells in Q6. (E) Representative dot plots of percent GFP and tdTomato double-positive cells indicating lipid transfer from WEHI-231-GFP to WEHI-303-tdTomato cells in Q2. (F) Representative dot plots of percent IgM and tdTomato double-positive cells indicating IgM transfer from WEHI-231-GFP to WEHI-303-tdTomato cells in Q6.

3.2. MK2206

MK2206 is a selective allosteric inhibitor of AKT. MK2206 has been demonstrated to inhibit auto-phosphorylation of both AKT at Threonine 308 and Serine 473 sites^{17,18}. It is recommended to use MK2206 at concentrations between 0.1 μM and 1.25 μM to inhibit AKT with minimal cytotoxicity¹⁹. Another study reported that cell viability reduced 30% upon cell types treated with 1 μM MK2206 for 48 h²⁰. In this study, both 0.25 μM and 0.5 μM MK2206 pre-treatment were sufficient to decrease the transfer of lipid and IgM to the recipient cells (Figure 3.2). However, there was an emerging question if the greater 0.5 μM MK2206 concentration induced apoptosis, and thus the release of apoptotic bodies, this might have led to a greater quantity of lipid and IgM being transferred to the recipient cells compared to the 0.25 μM MK2206 pre-treated group. Therefore, the concentration of 0.25 μM MK2206 was selected.

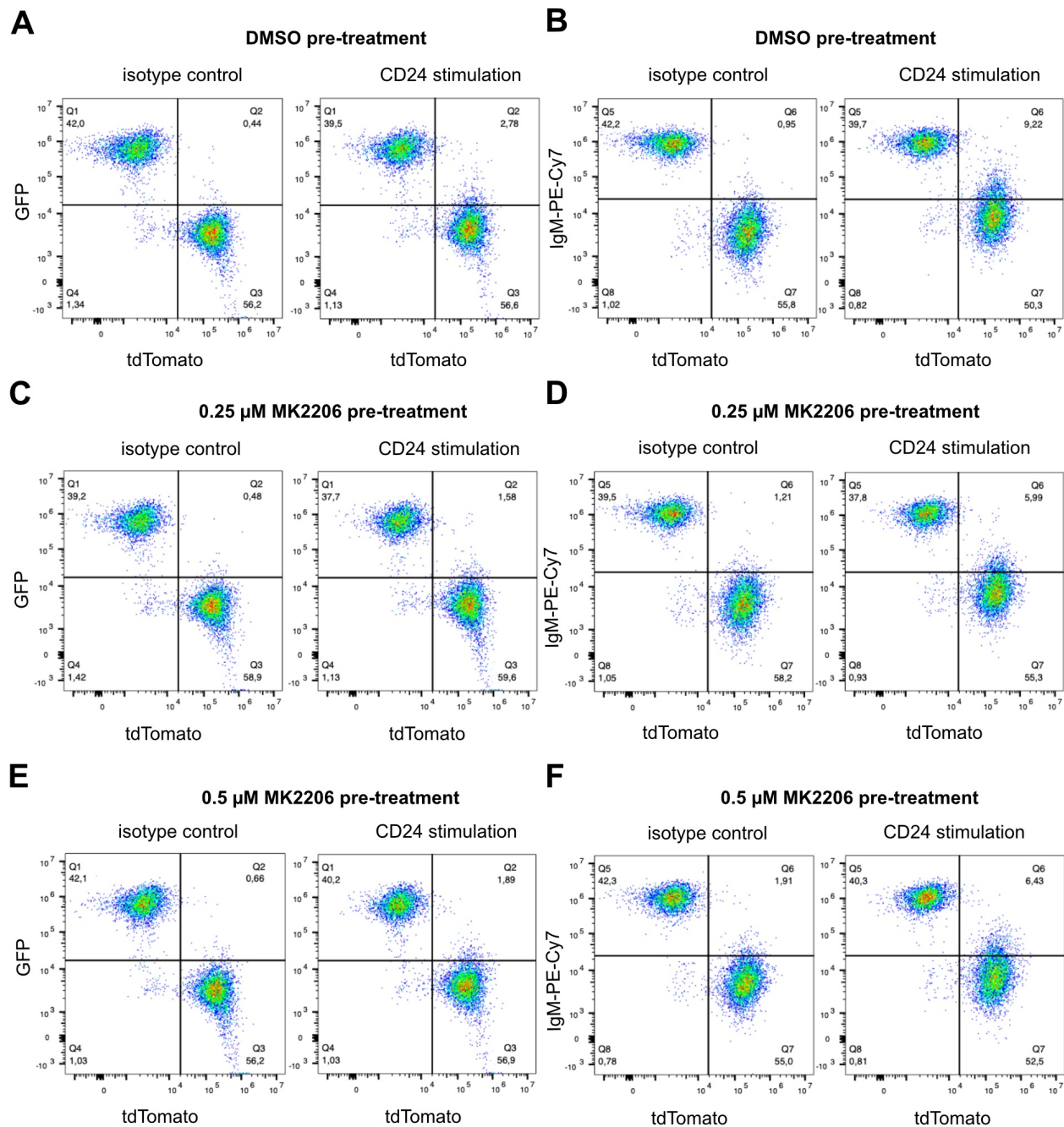


Figure 3.2. Representative dot plots showing the percent of GFP/ IgM-PE-CY7 and tdTomato in pre-treatment with MK2206 or DMSO for 15 min. WEHI-231-GFP cells were pre-treated with (A-B) DMSO for 15 min, or (C-D) 0.25 μ M MK2206 for 15 min or (E-F) 0.5 μ M MK2206 for 15 min, then stimulated with isotype control or anti-CD24 for 15 min, followed by washout and then a 24 h co-culture with WEHI-303-tdTomato cells. (A) Representative dot

plots of percent GFP and tdTomato double-positive cells indicating lipid transfer from WEHI-231-GFP to WEHI-303-tdTomato cells in Q2. (B) Representative dot plots of percent IgM and tdTomato double-positive cells indicating IgM transfer from WEHI-231-GFP to WEHI-303-tdTomato cells in Q6. (C) Representative dot plots of percent GFP and tdTomato double-positive cells indicating lipid transfer from WEHI-231-GFP to WEHI-303-tdTomato cells in Q2. (D) Representative dot plots of percent IgM and tdTomato double-positive cells indicating IgM transfer from WEHI-231-GFP to WEHI-303-tdTomato cells in Q6. (E) Representative dot plots of percent GFP and tdTomato double-positive cells indicating lipid transfer from WEHI-231-GFP to WEHI-303-tdTomato cells in Q2. (F) Representative dot plots of percent IgM and tdTomato double-positive cells indicating IgM transfer from WEHI-231-GFP to WEHI-303-tdTomato cells in Q6.

3.3. Torin-1

Torin-1 is a potent and selective inhibitor of both mTORC1 and mTORC2, relating to cell growth, proliferation, and metabolism^{21,22}. It has been reported to suppress mTOR activity with a concentration ranging from 0.25 μM to 2 μM ²³. Although both 0.25 μM and 0.5 μM Torin-1 pre-treatment were used, the pre-treatment of 0.25 μM Torin-1 was adequate to suppress the transfer of lipid and IgM to the recipient cells. Moreover, there was an emerging question if the greater 0.5 μM Torin-1 concentration induced apoptosis, and thus the release of apoptotic bodies, this could have potentially increased the quantity of lipid and IgM transferred to the recipient cells compared to the 0.25 μM Torin-1 pre-treated group (Figure 3.3). Therefore, a concentration of 0.25 μM Torin-1 was used.

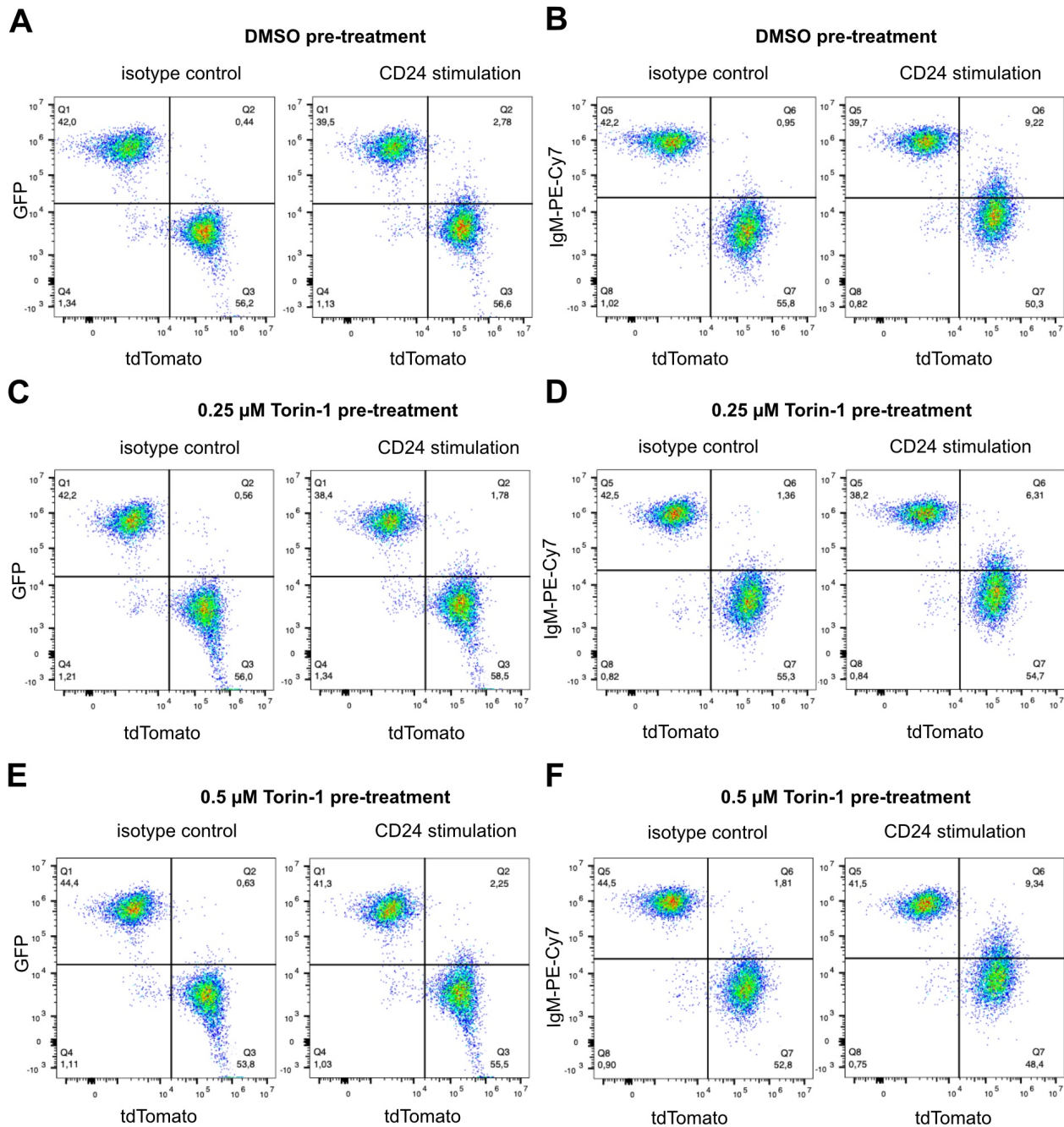


Figure 3.3. Representative dot plots showing the percent of GFP/ IgM-PE-CY7 and tdTomato in pre-treatment with Torin-1 or DMSO for 15 min. WEHI-231-GFP cells were pre-treated with (A-B) DMSO for 15 min, or (C-D) 0.25 μ M Torin-1 for 15 min or (E-F) 0.5 μ M Torin-1 for 15 min, then stimulated with isotype control or anti-CD24 for 15 min, followed by washout and then a 24 h co-culture with WEHI-303-tdTomato cells. (A) Representative dot plots

of percent GFP and tdTomato double-positive cells indicating lipid transfer from WEHI-231-GFP to WEHI-303-tdTomato cells in Q2. (B) Representative dot plots of percent IgM and tdTomato double-positive cells indicating IgM transfer from WEHI-231-GFP to WEHI-303-tdTomato cells in Q6. (C) Representative dot plots of percent GFP and tdTomato double-positive cells indicating lipid transfer from WEHI-231-GFP to WEHI-303-tdTomato cells in Q2. (D) Representative dot plots of percent IgM and tdTomato double-positive cells indicating IgM transfer from WEHI-231-GFP to WEHI-303-tdTomato cells in Q6. (E) Representative dot plots of percent GFP and tdTomato double-positive cells indicating lipid transfer from WEHI-231-GFP to WEHI-303-tdTomato cells in Q2. (F) Representative dot plots of percent IgM and tdTomato double-positive cells indicating IgM transfer from WEHI-231-GFP to WEHI-303-tdTomato cells in Q6.

3.4. Rapamycin

Rapamycin is a selective inhibitor of mTORC1, thus inhibits the proliferation and survival of cells^{24,25}. It has demonstrated that HK-2 cells did not undergo apoptosis when treated with rapamycin at a concentration of less than 5 μM for 24 hours²⁶. Another study found that treating SW1990 pancreatic cancer cells with rapamycin at concentrations below 200 nM had no effect on the cell viability²⁷. In this study, the transfer of lipid and IgM to the recipient cells decreased by pre-treatment with 0.1 μM and 1 μM rapamycin in donor cells (Figure 3.4). However, there was an emerging question if the pre-treatment of 1 μM rapamycin concentration caused apoptosis, and thus the release of apoptotic bodies, this might have led to a greater quantity of lipid and IgM being transferred to the recipient cells than the 0.1 μM rapamycin pre-treated group. Therefore, the concentration of 0.1 μM rapamycin was selected.

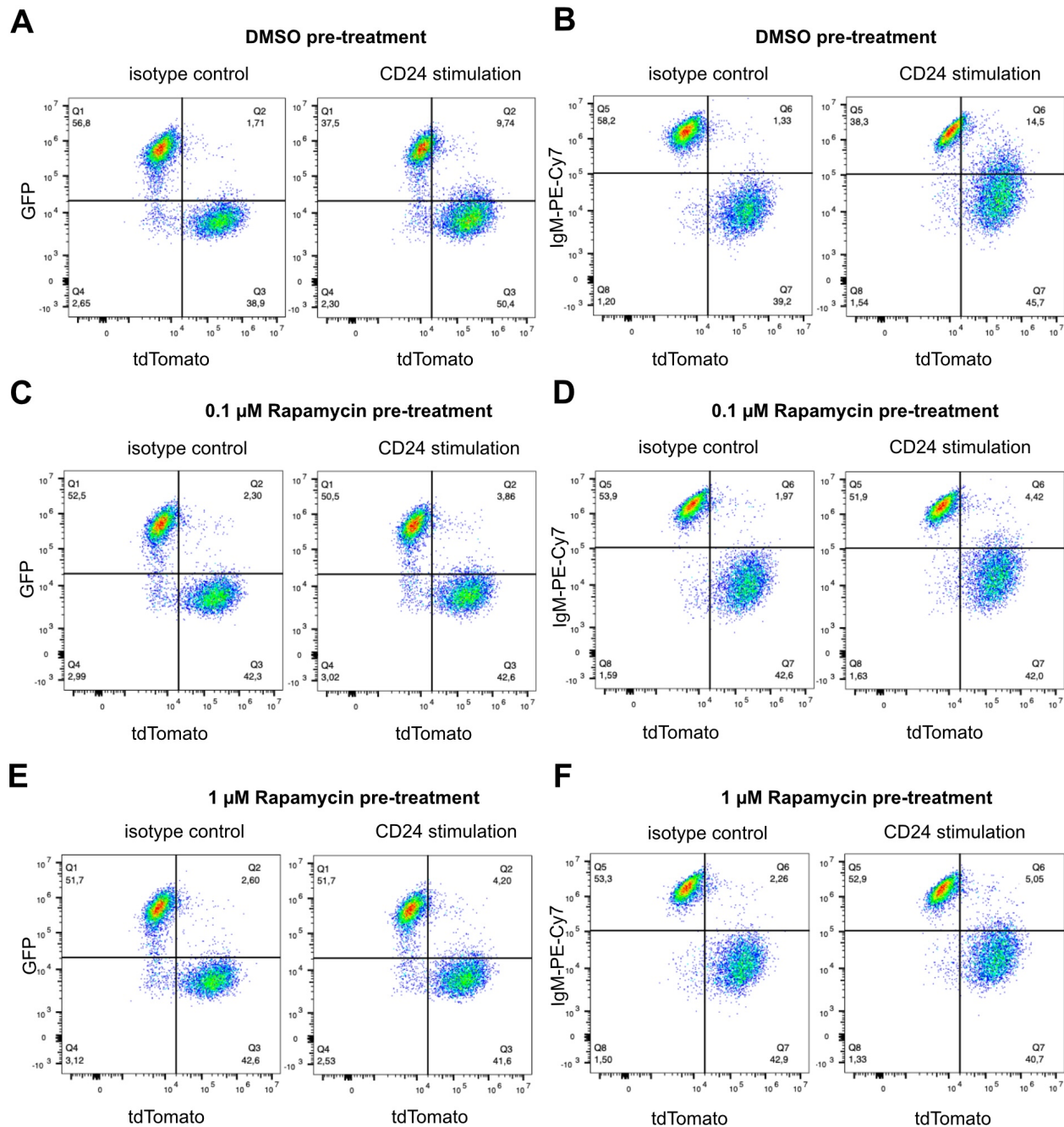


Figure 3.4. Representative dot plots showing the percent of GFP/ IgM-PE-CY7 and tdTomato in pre-treatment with Rapamycin or DMSO for 15 min. WEHI-231-GFP cells were pre-treated with (A-B) DMSO for 15 min, or (C-D) 0.1 μ M rapamycin for 15 min or (E-F) 1 μ M rapamycin for 15 min, then stimulated with isotype control or anti-CD24 for 15 min, followed by washout and then a 24 h co-culture with WEHI-303-tdTomato cells. (A) Representative dot plots

of percent GFP and tdTomato double-positive cells indicating lipid transfer from WEHI-231-GFP to WEHI-303-tdTomato cells in Q2. (B) Representative dot plots of percent IgM and tdTomato double-positive cells indicating IgM transfer from WEHI-231-GFP to WEHI-303-tdTomato cells in Q6. (C) Representative dot plots of percent GFP and tdTomato double-positive cells indicating lipid transfer from WEHI-231-GFP to WEHI-303-tdTomato cells in Q2. (D) Representative dot plots of percent IgM and tdTomato double-positive cells indicating IgM transfer from WEHI-231-GFP to WEHI-303-tdTomato cells in Q6. (E) Representative dot plots of percent GFP and tdTomato double-positive cells indicating lipid transfer from WEHI-231-GFP to WEHI-303-tdTomato cells in Q2. (F) Representative dot plots of percent IgM and tdTomato double-positive cells indicating IgM transfer from WEHI-231-GFP to WEHI-303-tdTomato cells in Q6.

3.5. JR-AB2-011

JR-AB2-011 is a selective inhibitor of mTORC2²⁴. A study reported that human melanoma cell lines had only little impact on the cell growth and viability up to 100 μ M JR-AB2-011 concentration for up to 48 h treatment²⁸. In this study, both 0.1 μ M and 1 μ M JR-AB2-011 pre-treatment were sufficient to decrease the transfer of lipid and IgM to the recipient cells (Figure 3.4). However, there was an emerging question if the greater 1 μ M JR-AB2-011 concentration caused apoptosis, and thus the release of apoptotic bodies, this might have led to a greater quantity of lipid and IgM being transferred to the recipient cells than the 0.1 μ M JR-AB2-011 pre-treated group. Therefore, the concentration of 0.1 μ M JR-AB2-011 was selected.

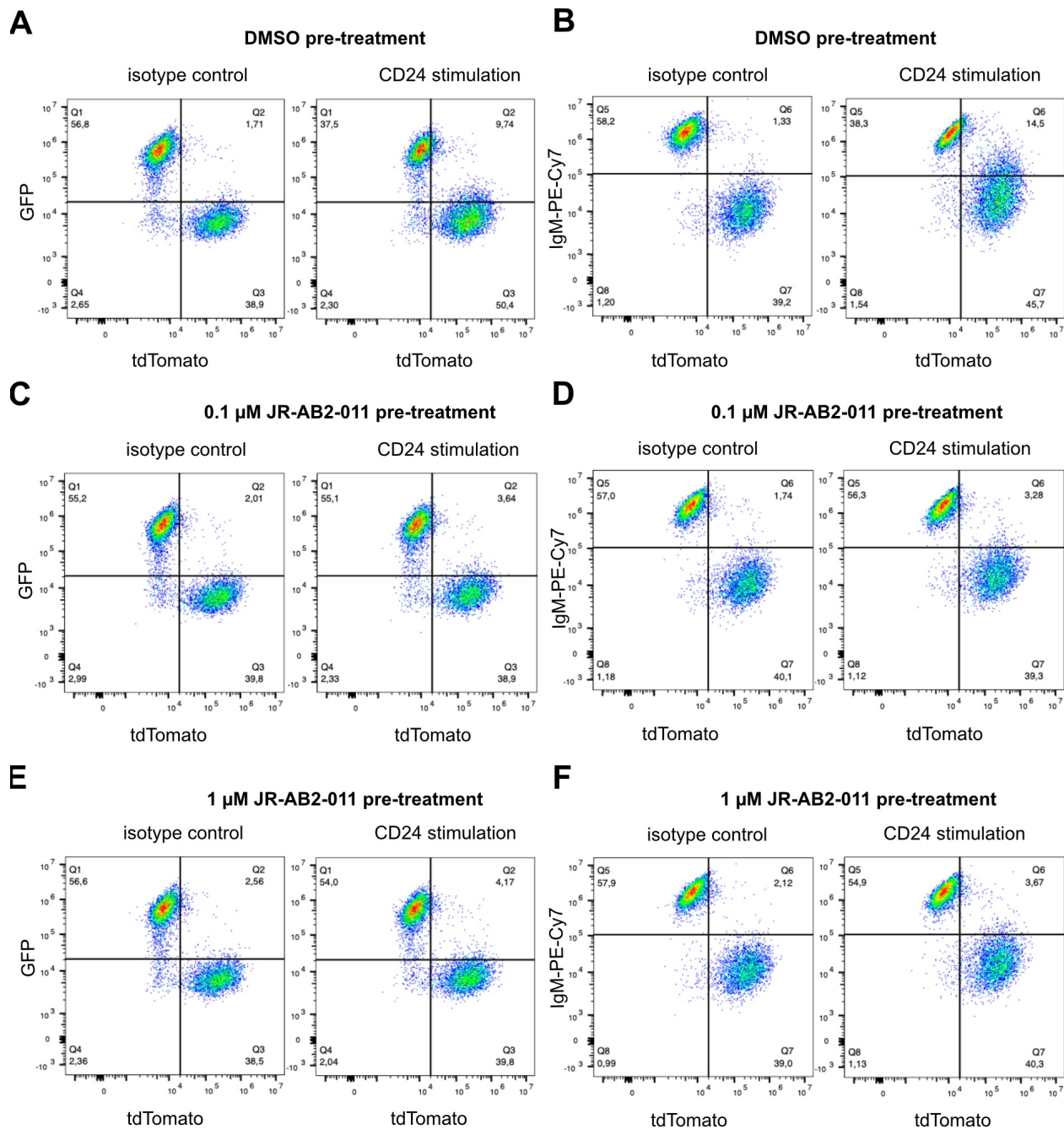


Figure 3.5. Representative dot plots showing the percent of GFP/ IgM-PE-CY7 and tdTomato in pre-treatment with JR-AB2-011 or DMSO for 15 min. WEHI-231-GFP cells were pre-treated with (A-B) DMSO for 15 min, or (C-D) 0.1 μM JR-AB2-011 for 15 min or (E-F) 1 μM JR-AB2-011 for 15 min, then stimulated with isotype control or anti-CD24 for 15 min, followed by washout and then a 24 h co-culture with WEHI-303-tdTomato cells. (A)

Representative dot plots of percent GFP and tdTomato double-positive cells indicating lipid transfer from WEHI-231-GFP to WEHI-303-tdTomato cells in Q2. (B) Representative dot plots of percent IgM and tdTomato double-positive cells indicating IgM transfer from WEHI-231-GFP to WEHI-303-tdTomato cells in Q6. (C) Representative dot plots of percent GFP and tdTomato double-positive cells indicating lipid transfer from WEHI-231-GFP to WEHI-303-tdTomato cells in Q2. (D) Representative dot plots of percent IgM and tdTomato double-positive cells indicating IgM transfer from WEHI-231-GFP to WEHI-303-tdTomato cells in Q6. (E) Representative dot plots of percent GFP and tdTomato double-positive cells indicating lipid transfer from WEHI-231-GFP to WEHI-303-tdTomato cells in Q2. (F) Representative dot plots of percent IgM and tdTomato double-positive cells indicating IgM transfer from WEHI-231-GFP to WEHI-303-tdTomato cells in Q6.

3.6. Y27632

Y27632 is a chemical compound that used in research focusing on the ROCK pathway. It is a selective inhibitor of ROCK and is often used in various biological studies^{29,30}. Treatment with 10 μM Y27632 did not induce cytotoxicity³⁰. Although both 5 μM and 10 μM Y27632 pre-treatment were used, 10 μM Y27632 was only sufficient to decrease the transfer of lipid and protein to the recipient cells (Figure 3.6). Therefore, the concentration of 10 μM Y27632 was selected.

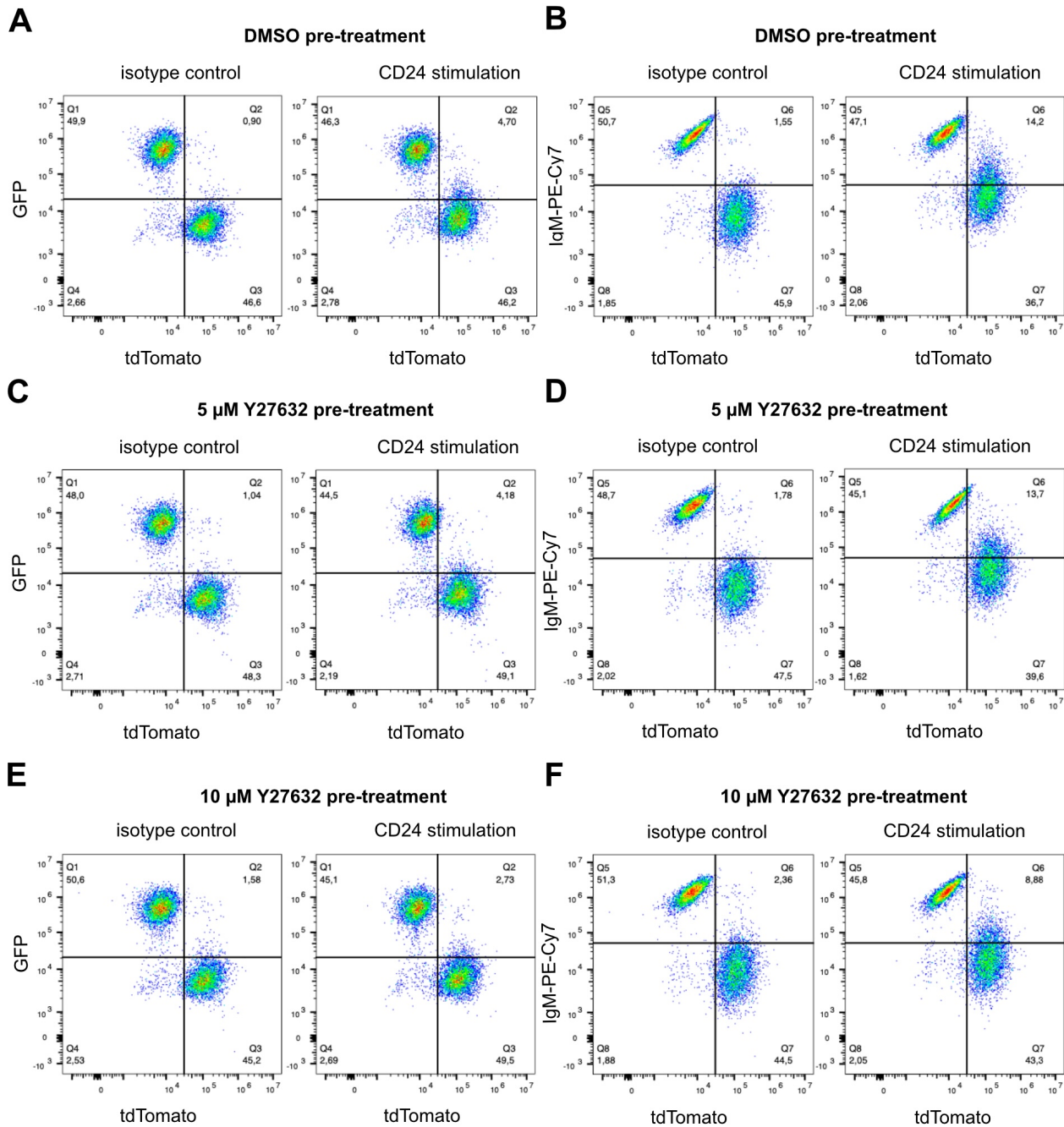


Figure 3.6. Representative dot plots showing the percent of GFP/ IgM-PE-CY7 and tdTomato in pre-treatment with Y27632 or DMSO for 15 min. WEHI-231-GFP cells were pre-treated with (A-B) DMSO for 15 min, or (C-D) 5 μ M Y27632 for 15 min or (E-F) 10 μ M Y27632 for 15 min, then stimulated with isotype control or anti-CD24 for 15 min, followed by washout and then a 24 h co-culture with WEHI-303-tdTomato cells. (A) Representative dot plots

of percent GFP and tdTomato double-positive cells indicating lipid transfer from WEHI-231-GFP to WEHI-303-tdTomato cells in Q2. (B) Representative dot plots of percent IgM and tdTomato double-positive cells indicating IgM transfer from WEHI-231-GFP to WEHI-303-tdTomato cells in Q6. (C) Representative dot plots of percent GFP and tdTomato double-positive cells indicating lipid transfer from WEHI-231-GFP to WEHI-303-tdTomato cells in Q2. (D) Representative dot plots of percent IgM and tdTomato double-positive cells indicating IgM transfer from WEHI-231-GFP to WEHI-303-tdTomato cells in Q6. (E) Representative dot plots of percent GFP and tdTomato double-positive cells indicating lipid transfer from WEHI-231-GFP to WEHI-303-tdTomato cells in Q2. (F) Representative dot plots of percent IgM and tdTomato double-positive cells indicating IgM transfer from WEHI-231-GFP to WEHI-303-tdTomato cells in Q6.

3.7. Cytochalasin D

Cytochalasin D is a cell-permeable inhibitor that prevents polymerization by binding actin filaments but not actin monomers³¹. Research reported that F-actin cytoskeleton organization started to affect at 0.2 μM cytochalasin D³². In this study, both 0.2 μM and 0.5 μM cytochalasin D pre-treatment of donor cells were shown to inhibit the transfer of lipid and IgM to the recipient cells (Figure 3.7). However, there was an emerging question if the greater 0.5 μM cytochalasin D pre-treatment included apoptosis, and thus the release of apoptosis bodies, this could have potentially increased the quantity of lipid and IgM transferred to the recipient cells compared to the 0.2 μM cytochalasin D pre-treatment group. Therefore, the pre-treatment of 0.2 μM cytochalasin D concentration was selected.

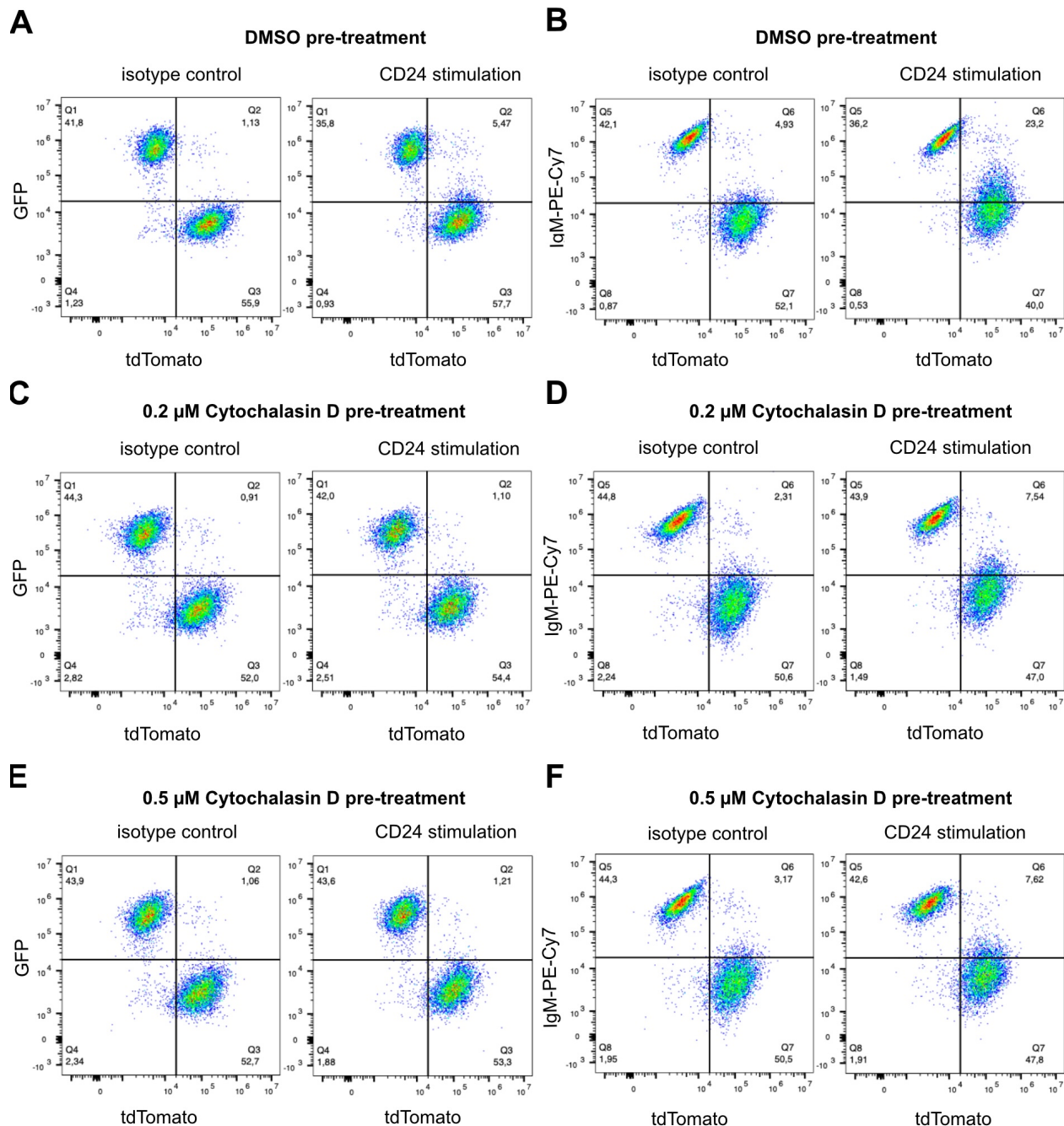


Figure 3.7. Representative dot plots showing the percent of GFP/ IgM-PE-CY7 and tdTomato in pre-treatment with Cytochalasin D or DMSO for 15 min. WEHI-231-GFP cells were pre-treated with (A-B) DMSO for 15 min, or (C-D) 0.2 μ M cytochalasin D for 15 min or (E-F) 0.5 μ M cytochalasin D for 15 min, then stimulated with isotype control or anti-CD24 for 15 min, followed by washout and then a 24 h co-culture with WEHI-303-tdTomato cells. (A)

Representative dot plots of percent GFP and tdTomato double-positive cells indicating lipid transfer from WEHI-231-GFP to WEHI-303-tdTomato cells in Q2. (B) Representative dot plots of percent IgM and tdTomato double-positive cells indicating IgM transfer from WEHI-231-GFP to WEHI-303-tdTomato cells in Q6. (C) Representative dot plots of percent GFP and tdTomato double-positive cells indicating lipid transfer from WEHI-231-GFP to WEHI-303-tdTomato cells in Q2. (D) Representative dot plots of percent IgM and tdTomato double-positive cells indicating IgM transfer from WEHI-231-GFP to WEHI-303-tdTomato cells in Q6. (E) Representative dot plots of percent GFP and tdTomato double-positive cells indicating lipid transfer from WEHI-231-GFP to WEHI-303-tdTomato cells in Q2. (F) Representative dot plots of percent IgM and tdTomato double-positive cells indicating IgM transfer from WEHI-231-GFP to WEHI-303-tdTomato cells in Q6.

3.8. Imipramine

Imipramine is introduced to prevent the activity of acid sphingomyelinase to catalyze sphingomyelin hydrolysis to ceramide³³. Treatment with imipramine at concentration of 30 μM imipramine reduced cell viability³⁴. Although both 5 μM and 10 μM imipramine pre-treatment were investigated, 10 μM imipramine was only sufficient to decrease the transfer of lipid and protein to the recipient cells (Figure 3.8). Therefore, the concentration of 10 μM imipramine was selected.

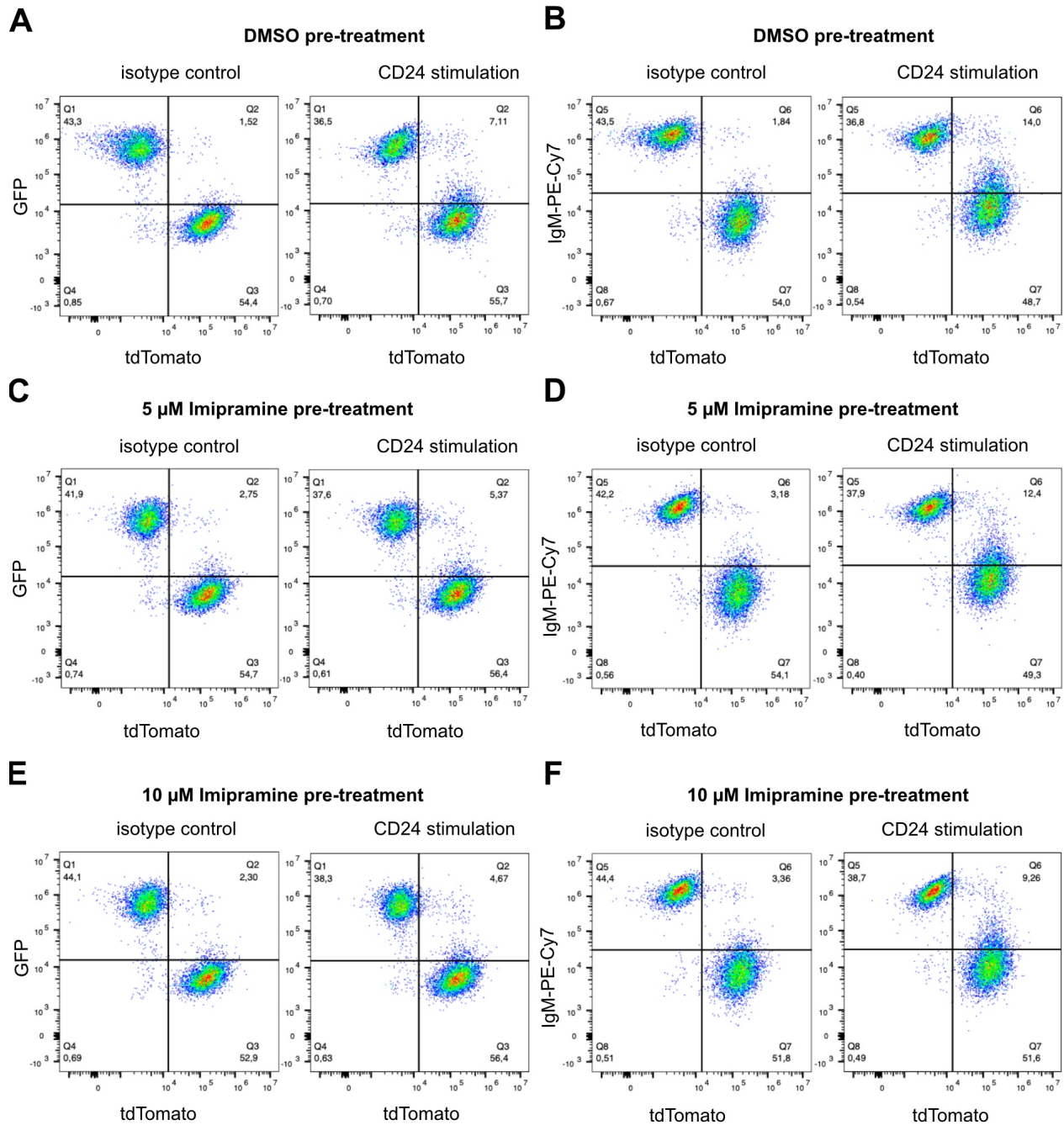


Figure 3.8. Representative dot plots showing the percent of GFP/ IgM-PE-CY7 and tdTomato in pre-treatment with Imipramine or DMSO for 15 min. WEHI-231-GFP cells were pre-treated with (A-B) DMSO for 15 min, or (C-D) 5 μ M imipramine for 15 min or (E-F) 10 μ M imipramine for 15 min, then stimulated with isotype control or anti-CD24 for 15 min, followed by washout and then a 24 h co-culture with WEHI-303-tdTomato cells. (A)

Representative dot plots of percent GFP and tdTomato double-positive cells indicating lipid transfer from WEHI-231-GFP to WEHI-303-tdTomato cells in Q2. (B) Representative dot plots of percent IgM and tdTomato double-positive cells indicating IgM transfer from WEHI-231-GFP to WEHI-303-tdTomato cells in Q6. (C) Representative dot plots of percent GFP and tdTomato double-positive cells indicating lipid transfer from WEHI-231-GFP to WEHI-303-tdTomato cells in Q2. (D) Representative dot plots of percent IgM and tdTomato double-positive cells indicating IgM transfer from WEHI-231-GFP to WEHI-303-tdTomato cells in Q6. (E) Representative dot plots of percent GFP and tdTomato double-positive cells indicating lipid transfer from WEHI-231-GFP to WEHI-303-tdTomato cells in Q2. (F) Representative dot plots of percent IgM and tdTomato double-positive cells indicating IgM transfer from WEHI-231-GFP to WEHI-303-tdTomato cells in Q6.

3.9. Arc39

Arc39 is a new inhibitor of ASM by inhibiting both lysosomal and secretory ASM³⁵. Since Arc39 is a relatively strong inhibitor, adding it directly to cell lysates results in an almost complete inhibition of ASM activity at a final dose of 0.3 to 0.5 μM in the experiment³⁶. In contrast, in living cells, ASM activity entirely inhibited by a dosage of 20 μM ³⁶. In this work, donor cells pre-treated with 20 μM Arc39 more effectively inhibited the transfer of lipid and protein to the recipient cells than those pre-treated with 10 μM Arc39 (Figure 3.9). Therefore, a concentration of 20 μM Arc39 was selected.

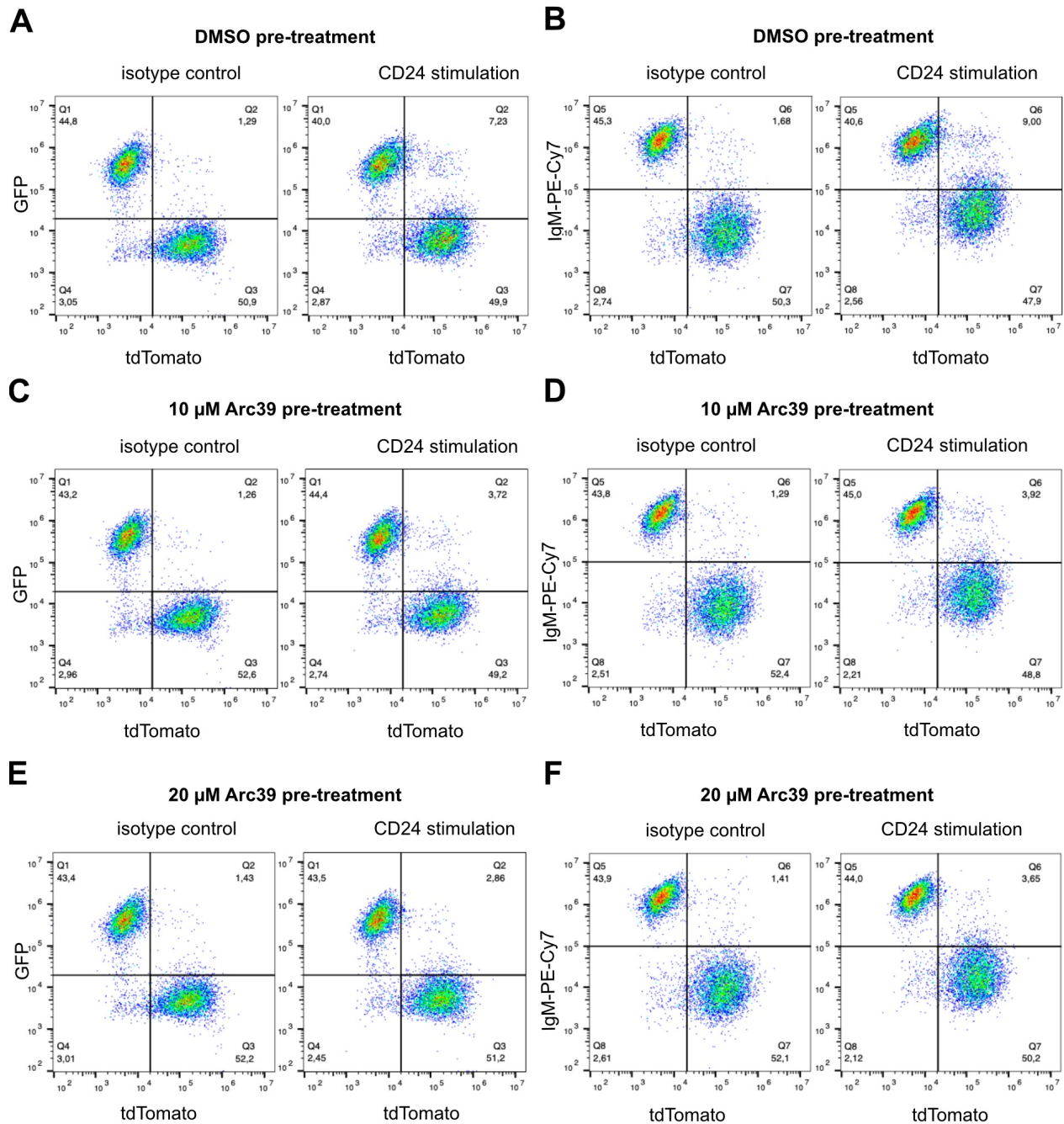


Figure 3.9. Representative dot plots showing the percent of GFP/ IgM-PE-CY7 and tdTomato in pre-treatment with Arc39 or DMSO for 15 min. WEHI-231-GFP cells were pre-treated with (A-B) DMSO for 15 min, or (C-D) 10 μ M Arc39 for 15 min or (E-F) 20 μ M Arc39 for 15 min, then stimulated with isotype control or anti-CD24 for 15 min, followed by washout and then a 24 h co-culture with WEHI-303-tdTomato cells. (A) Representative dot plots of

percent GFP and tdTomato double-positive cells indicating lipid transfer from WEHI-231-GFP to WEHI-303-tdTomato cells in Q2. (B) Representative dot plots of percent IgM and tdTomato double-positive cells indicating IgM transfer from WEHI-231-GFP to WEHI-303-tdTomato cells in Q6. (C) Representative dot plots of percent GFP and tdTomato double-positive cells indicating lipid transfer from WEHI-231-GFP to WEHI-303-tdTomato cells in Q2. (D) Representative dot plots of percent IgM and tdTomato double-positive cells indicating IgM transfer from WEHI-231-GFP to WEHI-303-tdTomato cells in Q6. (E) Representative dot plots of percent GFP and tdTomato double-positive cells indicating lipid transfer from WEHI-231-GFP to WEHI-303-tdTomato cells in Q2. (F) Representative dot plots of percent IgM and tdTomato double-positive cells indicating IgM transfer from WEHI-231-GFP to WEHI-303-tdTomato cells in Q6.

4. References

1. Cline, M. J. Perspectives for gene therapy: Inserting new genetic information into mammalian cells by physical techniques and viral vectors. *Pharmacol. Ther.* 29, 69–92 (1985).
2. Bukrinsky, M. I. et al. A nuclear localization signal within HIV-1 matrix protein that governs infection of non-dividing cells. *Nature* 365, 666 (1993).
3. Tilemann, L., Ishikawa, K., Weber, T. & Hajjar, R. J. Gene Therapy for Heart Failure. *Circ. Res.* 110, 777 (2012).
4. Kalidasan, V. et al. A guide in lentiviral vector production for hard-to-transfect cells, using cardiac-derived c-kit expressing cells as a model system. *Sci. Rep.* 11, 19265 (2021).
5. Thomas, C. E., Ehrhardt, A. & Kay, M. A. Progress and problems with the use of viral vectors for gene therapy. *Nat. Rev. Genet.* 4, 346–358 (2003).
6. Naldini, L., Blömer, U., Gage, F. H., Trono, D. & Verma, I. M. Efficient transfer, integration, and sustained long-term expression of the transgene in adult rat brains injected with a lentiviral vector. *Proc. Natl. Acad. Sci. U. S. A.* 93, 11382 (1996).
7. Tomás, H. A. et al. Lentiviral Gene Therapy Vectors: Challenges and Future Directions. in *Gene Therapy - Tools and Potential Applications* 287–317 (IntechOpen, 2013).
doi:10.5772/52534.
8. Lai, C. P. et al. Visualization and tracking of tumour extracellular vesicle delivery and RNA translation using multiplexed reporters. *Nat. Commun.* 6, 7029 (2015).
9. Ghosh, A. et al. Rapid Isolation of Extracellular Vesicles from Cell Culture and Biological Fluids Using a Synthetic Peptide with Specific Affinity for Heat Shock Proteins. *PLoS ONE* 9, e110443 (2014).

10. Maio, A. D. Extracellular heat shock proteins, cellular export vesicles, and the Stress Observation System: A form of communication during injury, infection, and cell damage: It is never known how far a controversial finding will go! Dedicated to Ferruccio Ritossa. *Cell Stress Chaperones* 16, 235 (2010).
11. Théry, C. et al. Minimal information for studies of extracellular vesicles 2018 (MISEV2018): a position statement of the International Society for Extracellular Vesicles and update of the MISEV2014 guidelines. *J. Extracell. Vesicles* 7, 1535750 (2018).
12. Helwa, I. et al. A Comparative Study of Serum Exosome Isolation Using Differential Ultracentrifugation and Three Commercial Reagents. *PloS One* 12, e0170628 (2017).
13. Roy, J. W. et al. A multiparametric extraction method for Vn96-isolated plasma extracellular vesicles and cell-free DNA that enables multi-omic profiling. *Sci. Rep.* 11, 8085 (2021).
14. Semba, S., Itoh, N., Ito, M., Harada, M. & Yamakawa, M. The in vitro and in vivo effects of 2-(4-morpholinyl)-8-phenyl-chromone (LY294002), a specific inhibitor of phosphatidylinositol 3'-kinase, in human colon cancer cells. *Clin. Cancer Res. Off. J. Am. Assoc. Cancer Res.* 8, 1957–1963 (2002).
15. Duarte, A., Gobbi, G. G. G., Soave, D. F., Costa, J. P. O. & Silva, A. R. The Role of the LY294002 - A Non-Selective Inhibitor of Phosphatidylinositol 3-Kinase (PI3K) Pathway- in Cell Survival and Proliferation in Cell Line SCC-25. *Asian Pac. J. Cancer Prev. APJCP* 20, 3377 (2019).
16. Mallawaarachy, D. M., Mactier, S., Kaufman, K. L., Blomfield, K. & Christopherson, R. I. The phosphoinositide 3-kinase inhibitor LY294002, decreases aminoacyl-tRNA synthetases, chaperones and glycolytic enzymes in human HT-29 colorectal cancer cells. *J. Proteomics* 75, 1590–1599 (2012).

17. Richter, A. et al. Combined Application of Pan-AKT Inhibitor MK-2206 and BCL-2 Antagonist Venetoclax in B-Cell Precursor Acute Lymphoblastic Leukemia. *Int. J. Mol. Sci.* 22, 2771 (2021).
18. Wilson, J. M., Kunnimalaiyaan, S., Kunnimalaiyaan, M. & Gamblin, T. C. Inhibition of the AKT pathway in cholangiocarcinoma by MK2206 reduces cellular viability via induction of apoptosis. *Cancer Cell Int.* 15, 13 (2015).
19. Chen, X. et al. AKT inhibitor MK-2206 sensitizes breast cancer cells to MLN4924, a first-in-class NEDD8-activating enzyme (NAE) inhibitor. *Cell Cycle* 17, 2069 (2018).
20. Li, Y.-L. et al. The Combination of MK-2206 and WZB117 Exerts a Synergistic Cytotoxic Effect Against Breast Cancer Cells. *Front. Pharmacol.* 10, 1311 (2019).
21. Wang, Y. et al. mTOR contributes to endothelium-dependent vasorelaxation by promoting eNOS expression and preventing eNOS uncoupling. *Commun. Biol.* 5, 1–14 (2022).
22. Najafov, A. et al. RIPK1 Promotes Energy Sensing by the mTORC1 Pathway. *Mol. Cell* 81, 370-385.e7 (2021).
23. Marin Zapata, P. A. et al. Time course decomposition of cell heterogeneity in TFEB signaling states reveals homeostatic mechanisms restricting the magnitude and duration of TFEB responses to mTOR activity modulation. *BMC Cancer* 16, 355 (2016).
24. Ma, C. et al. mTOR hypoactivity leads to trophectoderm cell failure by enhancing lysosomal activation and disrupting the cytoskeleton in preimplantation embryo. *Cell Biosci.* 13, 219 (2023).
25. Kim, R. & Kim, J. H. Engineered Extracellular Vesicles with Compound-Induced Cargo Delivery to Solid Tumors. *Int. J. Mol. Sci.* 24, 9368 (2023).

26. Wang, Y. et al. ADAR1 plays a protective role in proximal tubular cells under high glucose conditions by attenuating the PI3K/AKT/mTOR signaling pathway. *Open Med. Wars. Pol.* 19, 20241037 (2024).
27. Zhang, J.-W., Zhao, F. & Sun, Q. Metformin synergizes with rapamycin to inhibit the growth of pancreatic cancer in vitro and in vivo. *Oncol. Lett.* 15, 1811 (2017).
28. Guenzle, J. et al. Pharmacological Inhibition of mTORC2 Reduces Migration and Metastasis in Melanoma. *Int. J. Mol. Sci.* 22, 30 (2020).
29. Tramontano, A. F. et al. Statin decreases endothelial microparticle release from human coronary artery endothelial cells: implication for the Rho-kinase pathway. *Biochem. Biophys. Res. Commun.* 320, 34–38 (2004).
30. Kim, K., Min, S., Kim, D., Kim, H. & Roh, S. A Rho Kinase (ROCK) Inhibitor, Y-27632, Inhibits the Dissociation-Induced Cell Death of Salivary Gland Stem Cells. *Molecules* 26, 2658 (2021).
31. Shoji, K., Ohashi, K., Sampei, K., Oikawa, M. & Mizuno, K. Cytochalasin D acts as an inhibitor of the actin–cofilin interaction. *Biochem. Biophys. Res. Commun.* 424, 52–57 (2012).
32. Kitamura, E., Gribanova, Y. E. & Farber, D. B. Regulation of Retinoschisin Secretion in Weri-Rb1 Cells by the F-Actin and Microtubule Cytoskeleton. *PLoS ONE* 6, e20707 (2011).
33. Deng, L. et al. Imipramine Protects against Bone Loss by Inhibition of Osteoblast-Derived Microvesicles. *Int. J. Mol. Sci.* 18, 1013 (2017).
34. Sukma, M., Tohda, M. & Watanabe, H. Chronic Treatment With Imipramine Inhibits Cell Growth and Enhances Serotonin 2C Receptor mRNA Expression in NG 108-15 Cells. *J. Pharmacol. Sci.* 92, 433–436 (2003).

35. Roth, A. G. et al. Potent and selective inhibition of acid sphingomyelinase by bisphosphonates. *Angew. Chem. Int. Ed Engl.* 48, 7560–7563 (2009).
36. Naser, E. et al. Characterization of the small molecule ARC39, a direct and specific inhibitor of acid sphingomyelinase in vitro. *J. Lipid Res.* 61, 896 (2020).